APASL STC 2022

Asian Pacific Association for the Study of the Liver

3 - 5 JUNE · BEIJING · CHINA

www.apaslstc.com

Liver Fibrosis in the Era of Translational Medicine

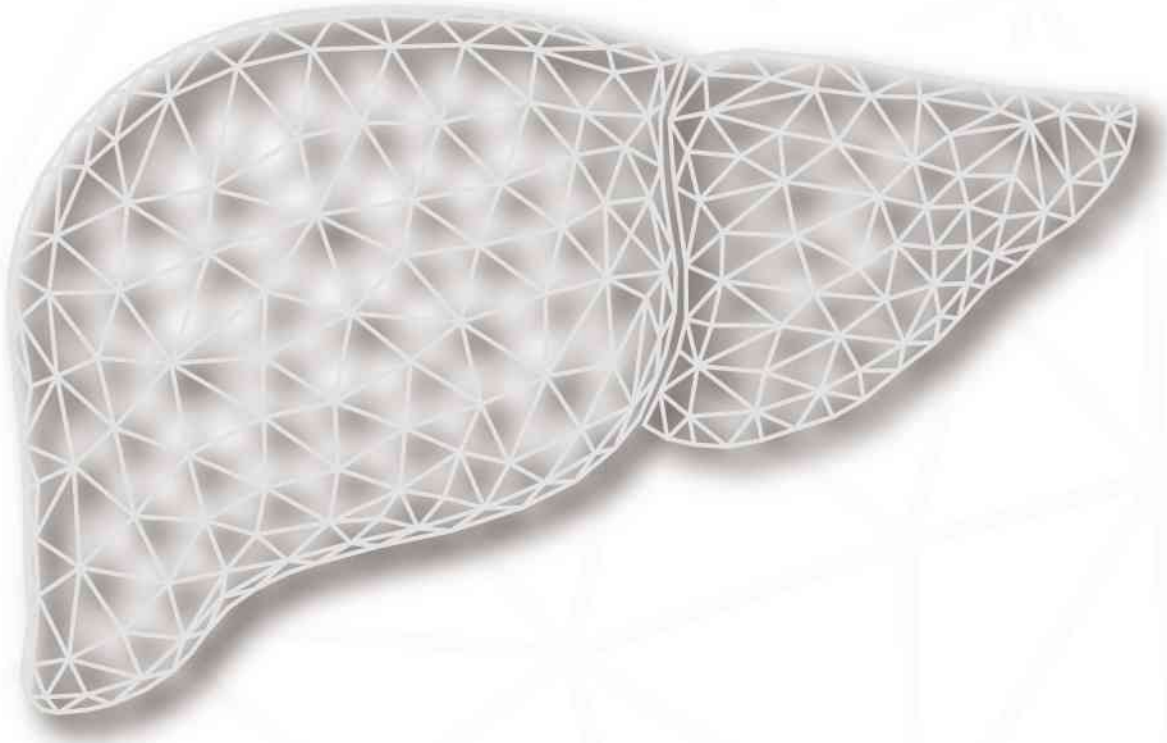

ABSTRACT BOOK

— 论 文 汇 编 —

Follow us on WeChat

Offical Minisite

Oral Presentation

Accepted Abstracts

❖ OP-001

Comparable role and crosstalk of lysyl oxidase and lysyl oxidase-like 1 in hepatic stellate cells

Wei Chen[1], *Wen Zhang*[1], *Ning Zhang*[1], *Xuzhen Yan*[1], *Aiting Yang*[1], *Hong You*[1]
[1]*No. 95 Yong'an road, Xicheng District, Beijing 100050, China.*

Background: Lysyl oxidase (LOX) family members (LOX and LOXL1 to 4) are important copper-dependent enzymes responsible for the cross-linking of collagens and elastin. Previous studies have revealed LOX and LOXL1 are the most dramatically dysregulated LOX isoforms during liver fibrosis. However, the crosstalk between them in hepatic stellate cells (HSCs) and their roles in HSC profibrotic behaviors remain unclear.

Method: Publicly available transcriptomic profiles and experimental liver fibrosis rodent models were used to measure the expression and location patterns of LOX and LOXL1. HSC profibrotic behaviors, extracellular matrix (ECM) remodeling, and biological functions mediated by LOX or LOXL1 intervention were detected, respectively, followed by the crosstalk between LOX and LOXL1.

Result:LOX and LOXL1 exhibited comparable expression and location patterns during liver fibrogenesis. Overexpression of LOX or LOXL1 could promote ECM remodeling and HSC activation, proliferation, migration and contraction; whereas inhibition of either of them could refrain ECM remodeling and HSC profibrotic behaviors. The NOTCH signaling and cell adhesion pathways were regulated by LOX or LOXL1 in HSCs. Perturbation of LOX or LOXL1 expression could affect their expression with each other, which could be partially explained by the physical interaction of LOX and LOXL1 in HSCs since their interplay delayed their protein degradation rates.

Conclusion: This study systematically explored the comparable roles of LOX and LOXL1 in HSC profibrotic behaviors and their crosstalk with each other, providing experimental evidence for LOX and LOXL1 as the therapeutic targets of liver fibrosis.

Table and Figure:

Figure 1. Comparable role and crosstalk of lysyl oxidase and lysyl oxidase-like 1 in hepatic stellate cells

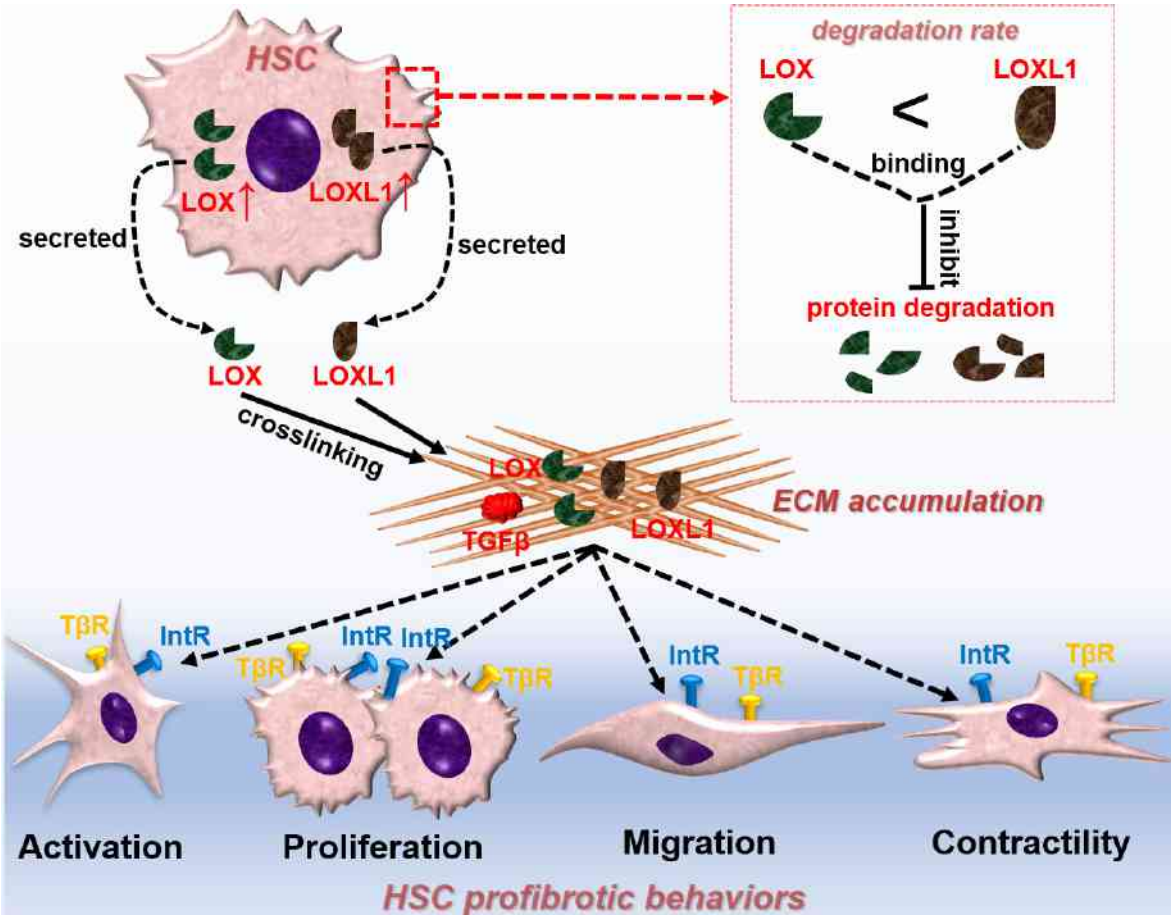

❖ OP-002

The m6A methyltransferase Mettl3 deficiency attenuates hepatic stellate cell activation and liver fibrosis

WITHDRAWAL

❖ OP-003

Caffeine Attenuates Nonalcoholic Steatohepatitis via Up Regulating Hepatic DUSP9 and Inhibiting Downstream ASK1 Activation

Xin Xin[1], Hu Yi-Yang[1], Feng Qin[1]
[1]Institute of Liver Diseases, Shuguang Hospital affiliated to Shanghai University of Traditional Chinese Medicine

Background: Coffee beverages and their functional extracts are recommended in clinical guidelines as potential interventions for the treatment of obesity and non-alcoholic steatohepatitis. The protective effect of caffeine, one of the main functional extracts of coffee, on non-alcoholic steatohepatitis is also gradually uncovered. However, the pharmacological mechanism of caffeine against NASH is still unclear. Therefore, the aim of this study was to investigate the pharmacodynamic effects and pharmacological mechanisms of caffeine on nonalcoholic steatohepatitis mice.

Method:C57BL/6J mice were fed normal chow or HFHC chow, and at the end of 24 weeks, mice on HFHC diet were divided into HFHC group, caffeine group and positive control drug, obeticholic acid group. HFHC group was gavaged with drinking water, and mice in caffeine and obeticholic acid groups were gavaged with caffeine (75 mg/kg) and obeticholic acid (10 mg/kg) for 6 weeks. We evaluated the effects of caffeine on glucolipid metabolism, liver inflammation and fibrosis. And the liver tissues of each group of mice were assessed transcriptomically and analyzed using the GSEA method to select the set of genes associated with the caffeine phenotype in the pathway with higher enrichment, and the top-ranked gene and its downstream indicators were selected based on the enrichment score for validation using PCR and immunoblotting. Subsequently, a liver knockout NASH mouse model was used to observe whether the effect of caffeine intervention on pharmacodynamic phenotype and pharmacological mechanism improvement changed.

Result: Pharmacodynamic results showed that caffeine significantly reduced the degree of disrupted glucolipid metabolism, inflammation and hepatic fibrosis under metabolic stress and was significantly superior to the positive control drug, obeticholic acid. In addition, GSEA analysis of liver tissue transcriptomics suggested that the key mechanism associated with the protective effect of caffeine may be MAPK pathway-dependent, and the DUSP9 gene had the highest enrichment score in this pathway. Validation results

showed that caffeine significantly upregulated DUSP9 mRNA and protein expression and dephosphorylated downstream kinases including ASK1, p38 and JNK. Gene editing studies showed that after knockdown of DUSP9 in liver tissues, the effect of caffeine to improve the degree of glucolipid metabolism disorder, inflammation and liver fibrosis in NASH mice was significantly attenuated, as was its inhibitory effect on downstream ASK1, p38 and JNK kinase phosphorylation.

Conclusion: Caffeine has a significant protective effect on the glucolipid metabolism disorder, inflammation and fibrosis in NASH mice under metabolic stress through upregulating DUSP9 and inhibiting downstream ASK1 activation in MAPK signaling pathway.

❖ OP-004

Prevalence and Characteristics of Metabolic Associated Fatty Liver Disease in the North China

Mengmeng Hou[1], Yuemin NAN[1], Xiwei Yuan[1]
[1]Department of Traditional and Western Medical Hepatology, Third Hospital of Hebei Medical University, shijiazhuang, China

Background: To compare the prevalence and characteristics of Metabolic associated fatty liver disease (MAFLD) and non-alcoholic fatty liver disease (NAFLD) and evaluate risk factors associated with liver fibrosis in MAFLD in Chinese population.

Method:12955 subjects were enrolled from a health examination population in Shijiazhuang, Hebei between 2019 to 2021. The diagnosis of MAFLD was based on the new international expert consensus, hepatic steatosis was estimated by ultrasound examination, significant fibrosis was defined by FIB-4 index ≥1.3. MAFLD were classified into three subgroups: obesity/overweight, diabetes and metabolic dysregulation. The prevalence of hepatic steatosis, MAFLD and NAFLD was investigated, clinical and biochemical characteristics were compared between subjects with MAFLD and NAFLD, as well as metabolic features in different MAFLD subtypes. Multivariate logistic regression was used to analyze the risk factors for significant fibrosis of MAFLD.

Result: The overall prevalence of hepatic steatosis, MAFLD and NAFLD in all participants was 29.51%, 26.21%, and 22.53%, respectively. Patients with MAFLD had a higher risk of metabolic disorders, worse liver and kidney function compared to participants with NAFLD. The estimated prevalence of significant fibrosis in MAFLD and NAFLD were 14.32% and 13.86%, respectively ($P < 0.05$). Furthermore, MAFLD with more diagnosis conditions tended to have significant fibrosis, diabetic MAFLD with significant fibrosis was significant than MAFLD diagnosed by overweight or metabolic dysregulation ($P < 0.05$).

Conclusion:MAFLD criteria identified a significant group of people with more comorbidities and significant fibrosis compared to NAFLD. Liver fibrosis in patients with MAFLD varies according to subgroup classification based on diabetes, body mass index, and metabolic risk factors.

❖ OP-005

Engineering vascular model reveals mechanism of hepatic vascular microenvironment response to hydrostatic pressure in liver fibrosis progression

Yi Long[1], Yan Zhang[1], Yudi Niu[1], Bingjie Wu[1], Liping Deng[1], Yanan Du[1]
[1]Tsinghua University

Background: In the process of liver fibrosis, the mechanical microenvironment changes significantly. On the one hand, the elasticity of the matrix increases. On the other hand, abnormal changes in hemodynamic forces are evident within the liver. Pathological mechanical parameters lead to vascular morphological changes, functional imbalance, increase of portal vein pressure in a vicious cycle and progression of liver fibrosis. Liver sinusoidal endothelial cells (LSECs) play an important regulatory role during the development of chronic liver disease, and their response to the hemodynamic parameters within hepatic sinusoidal vessels is the key factor to maintain physiological homeostasis. At present, it remains unclear about the mechanism of fibrosis progression regulated by LSECs dysfunction and sinusoidal remodeling under portal hypertension. In this investigation, biomimetic hepatic vascular models in vitro were used to explore the relationship between abnormal portal pressure and sinusoidal endothelial dysfunction at different stages of liver fibrosis.

Method:A hemodynamic monitor was applied to measure the changes of hepatic portal vascular pressure, flow velocity and intrahepatic vascular resistance during the progression of hepatic fibrosis. We also incorporated an intravital imaging technique to observe the morphological changes in blood vessels at different stages of fibrosis. A tow-dimensional pressure chamber with adjustable elasticity and a three-dimensional hepatic vascular model with resistance modules were further established to explore the effect of hydrostatic pressure on LSECs. Similarities of gene expression in LSECs between pathological conditions in vivo and within engineering vascular model in vitro are analyzed by RNA-sequencing.

Result: In vivo imaging of the liver depicted a decrease in the number of intrahepatic vessels at the late stage of fibrosis. LSECs cultured in a two-dimensional pressure chamber undergo apoptosis or necrosis after being subjected to high pressure. In the biomimetic engineering vascular model in vitro, cellular response towards different gradients of hydrostatic pressure corresponded to the LSECs in different stages of hepatic

fibrosis. Gene differential analysis reflected similarities between LSECs cultured in vitro and in vivo Increased pressure led to endothelial apoptosis at the late stage of liver fibrosis.

Conclusion: This work reveals that capillary rarefaction in the late stage of liver fibrosis is caused by pressure-driven endothelial dysfunction. High pressure at the late stage of fibrosis induces cellular apoptosis and necrosis. Membrane protein on LSECs may be a potential mechanical pressure sensor that participates in liver fibrosis progression. This mechanotransduction mechanism may provide precision intervention therapeutic strategies for the treatment of liver fibrosis.

Table and Figure:

Figure 1. Hepatic vascular degeneration during liver cirrhosis

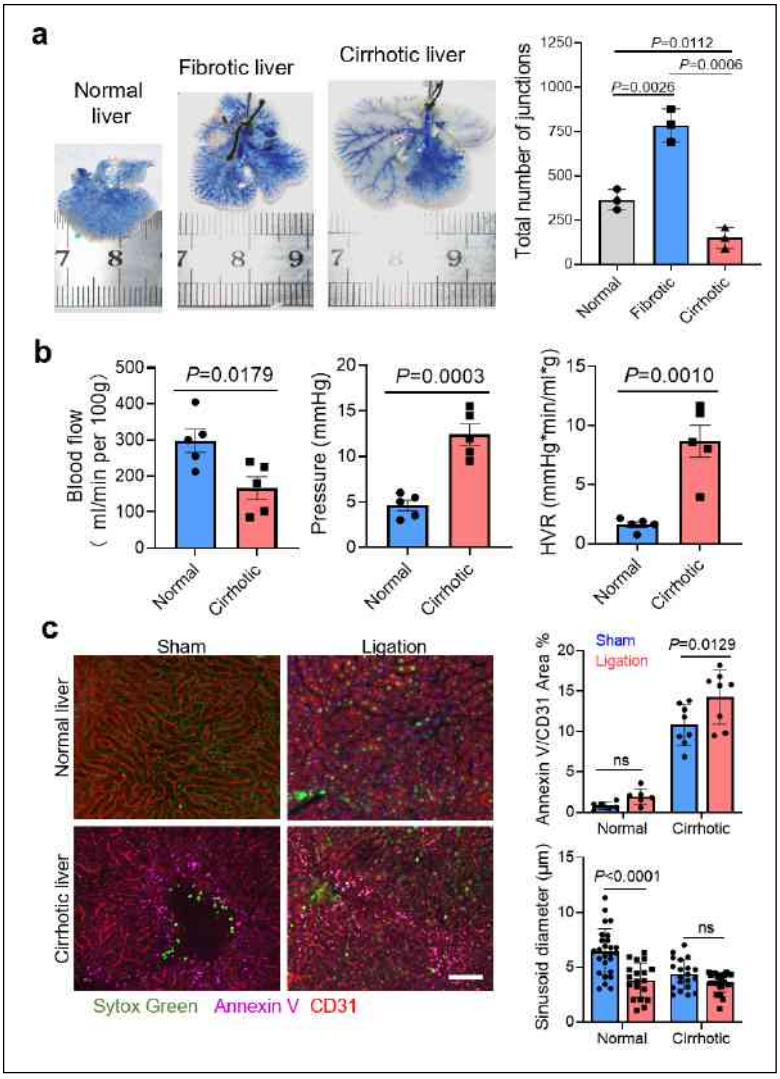

Figure 2.2D and 3D engineering vascular model reveals mechanism of hepatic vascular dysfunction induced by hydrostatic pressure in liver fibrosis progression

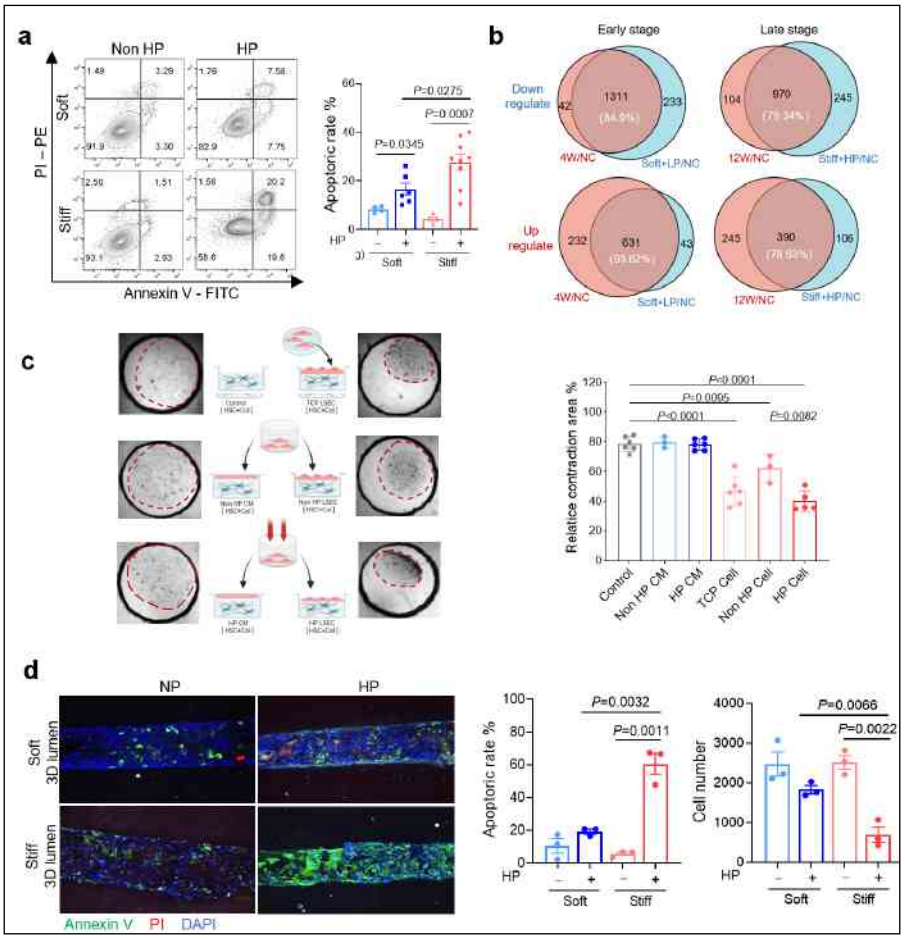

❖ OP-006

Evaluation of Amino Acids profile as non invasive Biomarkers of Hepatocellular Carcinoma among Egyptians

Samar Ebrahim Ghanem[1], Mohamed Abdel-Samiee[2], Hala El-Said[1], Eman Abdelsameea[2], Inas Maged Moaz[3], Sayed F Abdelwahab[4], Marwa Lotfy Helal[1]
[1]Department of Clinical Biochemistry and Molecular Diagnostics, National Liver Institute, Menoufia University, [2]Department of Hepatology and Gastroenterology, National Liver Institute, Menoufia University, [3]Department of Epidemiology and Preventive Medicine, National Liver Institute, Menoufia University, [4]Department of Pharmaceutics and Industrial Pharmacy, Taif College of Pharmacy, Taif University, PO Box11099, Taif 21944,

Background: The liver is the main organ where most metabolic processes occur like detoxification of blood, production of bile, glucose storage in the form of glycogen, and amino-acid precursor's synthesis. Hepatic cells, which constitute 85% of the liver, are responsible for the most of these metabolic processes. Hepatocellular carcinoma (HCC) is the most dangerous complication of chronic liver disease. It is a multifactorial complicated disease. Hepatitis C virus (HCV) and hepatitis B virus (HBV) represent the main causes of HCC in Egypt. Early diagnosis is very important to help early intervention. Aim of the study: To determine the metabolic role of different amino acids as non- invasive biomarkers in HCC course.

Method: This study was conducted on 302 participants, including 97 diagnosed untreated HCC patients, 81 chronic HCV patients, 56 chronic HBV patients, 18 co-infected patients, and a control group of50 normal individuals matched in age and gender. All participants were subjected to full history taking, complete clinical examination, abdominal ultrasonography and/or computed tomography, routine laboratory investigations, estimation of serum α-fetoprotein and determination of amino acid levels by ultra-performance liquid chromatography (UPLC MS-MS).

Result: This work revealed a decrease in branched chain amino acids (BCAA) and increase in aromatic amino acids (AAA) among studied groups (HCC, HBV, HCV, and co-infected patients) compared to control subjects and there was a significant difference in Fisher's and the BCAAs/tyrosine molar concentration ratios (BTR)between control and the other groups.

Conclusion: Different amino acids especially BCAA can be used as non-invasive markers in follow up of chronic viral hepatitis to predict HCC.

Table and Figure:

Figure 1. Fig 1: BCAA between HCC and control

Fig 1: BCAA between HCC and control

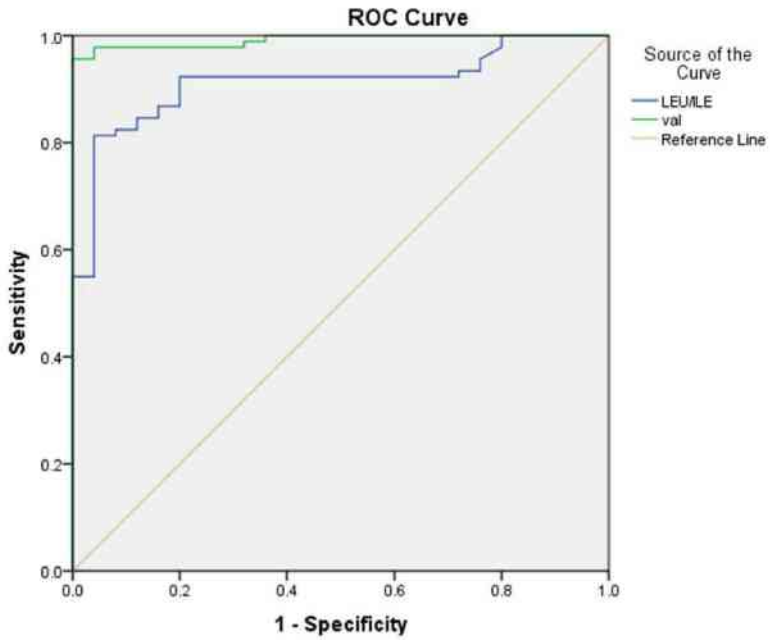

Diagonal segments are produced by ties.

Area Under the Curve

Test Result Variable(s)	Area	Std. Error[a]	Asymptotic Sig.[b]	Asymptotic 95% Confidence Interval	
				Lower Bound	Upper Bound
LEU/ILE	.912	.025	.000	.863	.961
Val	.992	.006	.000	.981	1.000

	Leu/iso	Valine
AUC(95%CI)	91.2 (86.3-96.1)%	99.2 (98.1-100.0)%
Cut off point	174.0	150.3
Sensitivity	87.0%	98.0%
Specificity	80.0%	88.0%
PPV	89.0%	94.0%
NPV	75.0%	96.0%
Accuracy	84.0%	95.0%

❖ OP-007

Liver fibrosis assessment by viewing sinusoidal capillarization: ultrasound molecular imaging versus two-dimensional shear-wave elastography in rats

Xiaoyan Miao[1], Tingting Sha[1], Wei Zhang[1], Huichao Zhou[1], Chen Qiu[1], Huan Deng[1], Yujia You[1], Jie Ren[1], Xinling Zhang[1], Rongqin Zheng[1], Tinghui Yin[1]
[1]Department of Ultrasound, Laboratory of Novel Optoacoustic (Ultrasonic) Imaging, The Third Affiliated Hospital of Sun Yat-sen University, Guangzhou 510630, China.

Background: Ultrasound elastography is a first-line assessment of liver fibrosis severity. However, its application is limited by its insufficient sensitivity in early-stage fibrosis detection, and its measurements are affected by inflammation. Ultrasound molecular imaging holds great potential in assessing liver fibrosis. Herein, the aims of our study are to assess the sensitivity of ultrasound molecular imaging in early-stage liver fibrosis detection and to determine whether ultrasound molecular imaging can specifically distinguish fibrosis regardless of inflammation when compared with two-dimensional shear-wave elastography.

Method: Ultrasound molecular imaging and two-dimensional shear-wave elastography were performed in 120 male Sprague–Dawley rats with varying degrees of liver fibrosis and acute hepatitis and control rats. Liver sinusoidal capillarization was viewed at CD34-targeted ultrasound molecular imaging and quantitatively analyzed by the normalized intensity difference. Data were compared by using a two-sided Student t-test or one-way analysis of variance. Linear correlation analyses were used to evaluate the relationships between collagen proportionate area values and normalized intensity difference and liver stiffness measurement values. Receiver operating characteristic curve were applied to assess the diagnostic performance in detecting liver fibrosis.

Result: Both normalized intensity difference and liver stiffness measurement values showed good linear correlations with collagen proportionate area values ($r = 0.91$ and 0.87, respectively). No difference was observed between the areas under the curve for detecting F0-1 between ultrasound molecular imaging and two-dimensional shear-wave elastography (0.97 vs. 0.91, $P = 0.20$). Ultrasound molecular imaging detected liver fibrosis at early-stage more accurately than two-dimensional shear-wave elastography (area under the curve 0.97 vs. 0.82, $P = 0.01$). Rats with hepatitis had higher liver stiffness values than controls (9.83 ± 0.79 kPa vs. 6.55 ± 0.38 kPa, $P < 0.001$), with no difference in the

normalized intensity difference values between controls and hepatitis rats (6.75% ± 1.43% vs. 6.74% ± 0.86%, P = 0.98).

Conclusion: Sinusoidal capillarization viewed at ultrasound molecular imaging helped to detecte early-stage liver fibrosis more accurately than two-dimensional shear-wave elastography and helped assess fibrosis regardless of inflammation.

Table and Figure:

Figure 1. Detection of early-stage liver fibrosis by ultrasound molecular imaging compared with two-dimensional shear wave elastography.

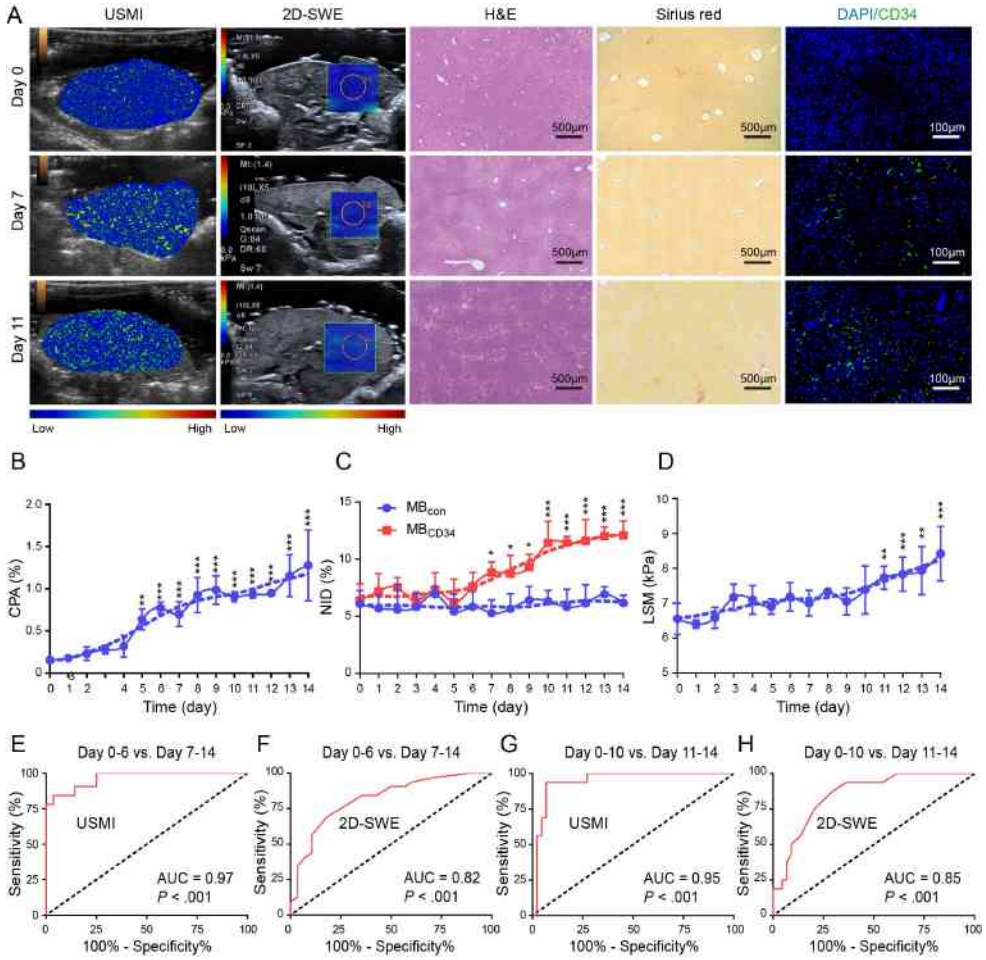

Figure 2. Distinguishing liver fibrosis from inflammation by ultrasound molecular imaging compared with two-dimensional shear wave elastography.

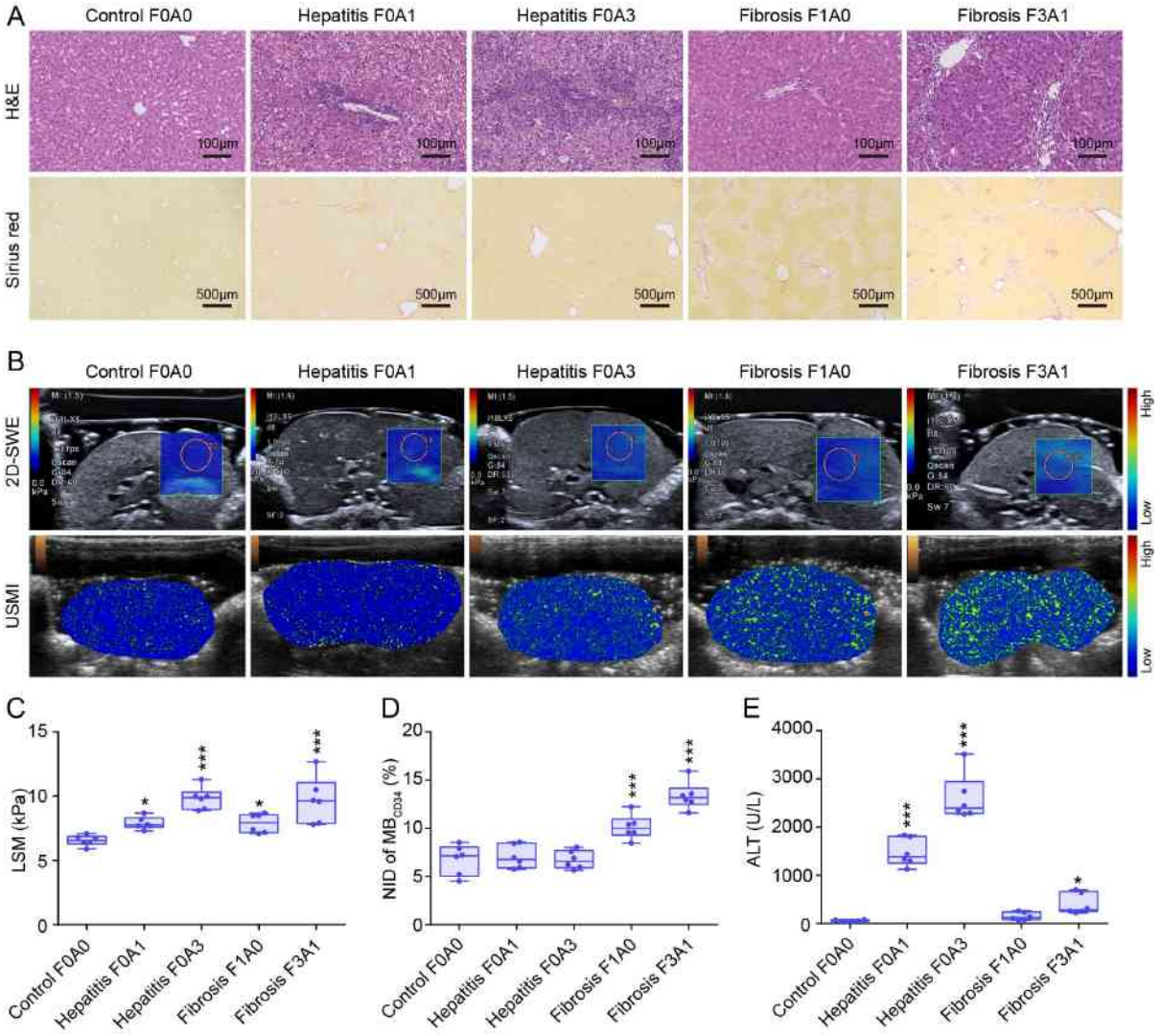

❖ OP-008

A novel role of glutathione S-transferase A3 in inhibiting hepatic stellate cell activation and rat hepatic fibrosis

WITHDRAWAL

❖ OP-009

The expression of Fmnl1 and Myh9 in monocyte-macrophage-DC cells system is associated with the progression of fibrosis in NASH

WITHDRAWAL

❖ OP-010

STING mediates hepatocyte pyroptosis via activating NLRP3 inflammasome during liver fibrosis

Jinhang Gao[1]
[1]Lab of Gastroenterology and Hepatology, West China Hospital, Sichuan University, Chengdu, China.

Background: Previous studies emphasized the crucial role of apoptosis and necrosis during liver cirrhosis; while recent evidence suggests that pyroptosis may also play a pivotal role in chronic liver diseases. The activation of stimulator of interferon genes (STING) and NOD-like receptors protein 3 (NLRP3) inflammasomes-mediates hepatocytes proptosis signaling pathways represent a central mechanism in several liver diseases. Whether blocking STING can prevent hepatocyte pyroptosis during liver fibrosis remains unknown and is the focus of this study.

Method: Liver cirrhosis was induced by thioacetamide (TAA), carbon tetrachloride (CCl4) administration, or bile duct ligation (BDL) in Sting knockout, hepatocyte-specific Nlrp3 deletion, and Gasdermin D (Gsdmd) knockout mice. RNA-sequence, ultra-high-performance liquid chromatography of metabonomics, and chromatin immunoprecipitation assays were applied in the liver and primary murine hepatocytes to verify the mechanism of NLRP3 regulation and NLRP3 inflammasomes-mediates hepatocytes proptosis.

Result:RNA-sequence in a CCl4-induced murine cirrhotic model indicated that cytosolic DNA-sensing and NLRP3 inflammasome signaling pathways were activated, and were verified in human and murine cirrhotic liver. However, RNA-sequence analysis showed that the active NLRP3 inflammasome signaling pathway way was significantly attenuated bySting knockout. Sting knockout ameliorated pyroptosis, hepatic inflammation, and liver fibrosis in the CCl4-induced murine cirrhotic model. In vitro, STING promoted NLRP3 transcription in primary murine hepatocytes by enhancing interferon regulatory transcription factor (IRF3) binding to the NLRP3 promoter. The STING-IRF3 signaling pathway also participates in the NLRP3 inflammasome-mediated hepatocyte pyroptosis. The RNA-sequence and metabonomics analysis in NLRP3 inhibitor MCC950-treated primary murine hepatocytes and livers of hepatocyte-specific Nlrp3deletion mice showed that metabolic signaling pathways might participate in hepatocyte pyroptosis. Moreover, hepatocyte-specific Nlrp3 deletion and downstream Gsdmd knockout

attenuated pyroptosis, hepatic inflammation, and liver fibrosis in TAA- and BDL-induced liver cirrhosis.

Conclusion: This study describes a novel mechanism by which the STING-IRF3-NLRP3 signaling pathway enhances hepatocyte pyroptosis and hepatic inflammation in liver cirrhosis. Inhibition of the STING-NLRP3-GSDMD signaling pathway protects hepatocytes from pyroptosis and attenuates hepatic inflammation and liver fibrosis. These results shed light on the anti-pyroptosis strategy as a potential therapeutic candidate for patients with liver cirrhosis.

❖ OP-011

JCAD Deficiency Attenuated Liver Fibrosis by Suppressing Hepatic Stellate Cell Activation in Mice with Bile Duct Ligation

Xie Li[1], Chen Hui[1], Zhang Li[1], Yang Yong Yu[1], Zhou Yuan[1], Wu Jian[1,2,3]
[1]Dept. of Medical Microbiology, Fudan University School of Basic Medical Sciences, Shanghai
[2]Dept. of Gastroenterology & Hepatology, Zhongshan Hospital of Fudan University, Shanghai
[3]Shanghai Institute of Liver Diseases, Fudan University Shanghai Medical College, Shanghai

Background:JCAD is a membrane conjunction protein, and is expressed in cholangiocytes. Our previous study reported that JCAD interacts with LATS2 in the Hippo signaling pathway and promotes the transition from NASH to HCC (Cancer Res 2017; 77: 5287–5300). The aim of this study was to investigate whether JCAD is involved in cholestasis-associated fibrosis in mice with bile duct ligation (BDL).

Method: Hepatic fibrosis was induced in JCAD knock-out (KO) or wild-type (WT) mice, and evaluated by histopathology, hydroxyproline quantitation and biochemical tests 2 weeks after BDL. Bile duct epithelial (BDE) proliferation and hepatic stellate cell (HSC) activation were determined by counter-staining of CK-19 with Ki67, smooth-muscle α-actin (α-SMA) expression and serum transforming growth factor-β1 (TGF-β1) level by ELISA.

Result: As evidenced by immunohistochemical staining, JCAD was significantly up-regulated in both cholangiocytes and activated HSCs in WT mice undergone BDL as well as in liver biopsy sections from patients with primary biliary cholangitis (PBC). JCAD deficiency remarkably ameliorated BDL-induced hepatic injury and fibrosis as documented by serum levels of ALT (260.0±59.5 vs. 479.4±64.3 U/L, $p<0.05$), AST (467.0±19.9 vs. 1384±155.7 U/L, $p<0.01$), bilirubin (174.9±29.8 vs. 349.2±40.2 μmol/L, $p=0.01$), bile acids (426.8±38.6 vs. 682.1±82.4 μmol/L, $p<0.05$), liver hydroxyproline content (280±50 vs. 460±60 ng/mg, $p<0.01$) when compared to WT mice. Collagen deposition was dramatically reduced in JCAD-KO compared to WT mice as visualized by Trichrome staining and semiquantitative score (2.6±0.2 vs. 5.7±0.7 %, $p<0.01$). Gene expression of α-SMA, fibronectin, and procollagen type-1(α1) was markedly enhanced in BDL mice; whereas they were suppressed in JCAD null mice. There was a significant decrease in serum TGF-β1 levels (66.6±2.5 vs. 87.8±2.3 ng/ml, $p<0.01$) in JCAD-KO compared to WT mice after BDL. Moreover, cytokeratin-19+/Ki67+ BDE and α-SMA+ HSC counts in JCAD-KO liver were much lower than those in WT mice.

Conclusion:JCAD inactivation effectively reversed biliary hyperplasia, hepatic injury, and fibrosis induced by BDL and the underlying mechanisms may be associated with suppressed Hippo signaling activity in both BDEs and HSCs. The elucidation of the critical role of JCAD in cholestatic fibrosis would facilitate to uncover the cross-talk between BDE and HSCs and to develop molecular intervention for cholestasis-associated fibrosis.

❖ OP-012

Identifying the Tipping Point with Its Driving Genes during Liver Fibrosis Progression by Dynamic Network Biomarker Analysis.

Jinsheng Guo[1], Luonan Chen[2]
[1]Zhongshan Hospital affiliated to Fu Dan University, [2]Shanghai Institute of Biochemistry and Cell Biology, Chinese Academy of Sciences, 320 Yue Yang Road, Shanghai 200031, China

Background: Liver fibrogenesis is a complex scar-forming process in the liver, which first responds to various chronic injuries with gradual changes, then reaches the critical state (tipping point) and ultimately results in advanced cirrhosis with a rapid transition. Here, we present a systems biology study to identify the tipping point and its driving genes during this process using dynamic network biomarker (DNB) with high-throughput data of liver transcriptomes.

Method: Mice model of liver fibrosis was induced by intraperitoneal injection of thioacetamide (TAA) and liver tissues were collected at different time points post TAA administration. Dynamic network biomarker (DNB) analysis were performed on the time series of liver transcriptomes. In addition, the functional impact of a top-ranking DNB on fibrogenic genes expression was further validated in vitro with an immortalized mouse HSC line JS1.

Result: By DNB analysis, the week 9 post TAA treatment (pathologically relevant to bridging fibrosis) was identified as a tipping point just before the significant fibrosis transition with 153 DNB genes, which were key factors for the critical transition. DNB genes were functionally enriched in fibrosis-associated pathways, in particular, Tgfb3 was ranked as the top DNB gene, which negatively regulated Mmp13 in the interaction path. Moreover, we found that Tgfb3 and Mmp13 formed a bistable switching system from a dynamical perspective. The upregulatory effects of Tgfb3 on fibrogenic genes (e.g., CTGF and collagen type 1) and down-regulatory effects on Mmp13 were further confirmed by both theoretical model and in vitro study with an immortalized mouse HSC line JS1, and in line with clinical expression profiles of these genes in patients with chronic liver diseases.

Conclusion: The critical transition during liver fibrogenesis is driven by key DNB genes, which marks not only the initiation of significant fibrogenesis but also the repression of the scar resolution.

❖ OP-013

Hydronidone for the treatment of liver fibrosis related to chronic hepatitis B: a Phase 2 randomized controlled trial

Xiaobo Cai[1], Xuehan Liu[2], Wen Xie[3], Anlin Ma[4], Youwen Tan[5], Jia Shang[6], Jimin Zhang[7], Chengwei CHEN[8], Yanyan Yu[9], Yin Qu[10], Lin Zhang[11], Yin Luo[11], Ping Yin[12], Jun Cheng[13], Lungen LU[10]
[1] Shanghai General Hospital, Shanghai Jiaotong University School of Medicine, [2] ShaDepartment of Epidemiology and Biostatistics, School of Public Health, Tongji Medical Collegenghai General Hospital, Shanghai Jiaotong University School of Medicine, [3],Institute of Infectious Diseases, Beijing Ditan Hospital, Capital Medical University, [4]Department of Infectious Diseases, China-Japan Friendship Hospital, [5]Department of Infectious Diseases, the Third People's Hospital of Zhenjiang, [6]Department of Infectious Diseases, Henan Provincial People's Hospital, [7]Department of Infectious Diseases, Huashan Hospital, Fudan University, [8]Center for Liver Diseases, 905th Hospital of PLA Navy, [9]Department of Infectious Diseases, Peking university first hospital, [10]Department of Gastroenterology, Shanghai General Hospital, Shanghai Jiaotong University School of Medicine, [11]Continent Pharmaceuticals, [12]School of Public Health, Tongji Medical College, Huazhong University of Science and Technology, [13]Institute of Infectious Diseases, Beijing Ditan Hospital, Capital Medical University

Background: Hepatitis B virus (HBV) infection frequently leads to liver fibrosis and is the leading cause of hepatocellular carcinoma (HCC) and cirrhosis in Asia Pacific. Pirfenidone is approved by FDA for treatment of idiopathic pulmonary fibrosis and Hydronidone is a novel structural modification of pirfenidone with the aim of reducing hepatoxicity. We aimed to investigate the safety and efficacy of hydronidone in patients with chronic hepatitis B (CHB) associated liver fibrosis.

Method: This was a 52-week multicenter, randomized, double-blind, placebo-controlled, phase 2 study at 8 centers in China. CHB patients with biopsied documented liver fibrosis were eligible and were randomly assigned into receiving daily placebo or hydronidone orally (180 mg/day ,270 mg/day or 360 mg/day). All enrolled subjects also received entecavir 0.5 mg/day. A second liver biopsy was performed at week 52. The primary endpoint was defined as fibrosis improvement (reduction of at least one Ishak score at week 52 of treatment).

Result: From June 25, 2015, to September 5, 2019, 168 CHB patients with liver fibrosis met the inclusion/exclusion criteria and were subsequently randomized, 43 in the placebo group and 125 in the hydronidone groups (42 in the 180mg group, 42 in the 270mg group, and 41 in the 360mg group). The fibrosis improvement endpoint was achieved by 11 (25.6%) patients in placebo group and 17 (40.5%) patients in the 180 mg group (p=0.12), 23 (54.8%)patients in the 270 mg group (p=0.006) and 18 (43.90%) patients in the 360 mg group (p=0.08). The improvement rate was 58/125 (46.4%) in the combined

hydronidone group (p=0.014). The overall safety profile and incidence of serious adverse events were similar among the groups.

Conclusion: Hydronidone plus entecavir showed clinically significant histological improvement of liver fibrosis in CHB patients and the dose of 270 mg showed best efficacy of fibrosis regression. Further studies are required to assess the long-term effectiveness of hydronidone in regression of hepatic fibrosis. ClinicalTrials.gov number, NCT02499562.

Table and Figure:

Figure 1. Patient flow diagram

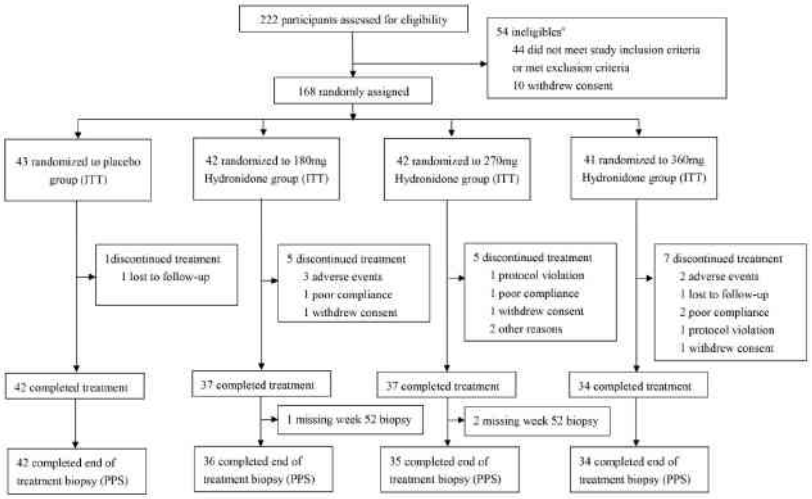

Figure 2. Treatment efficacy

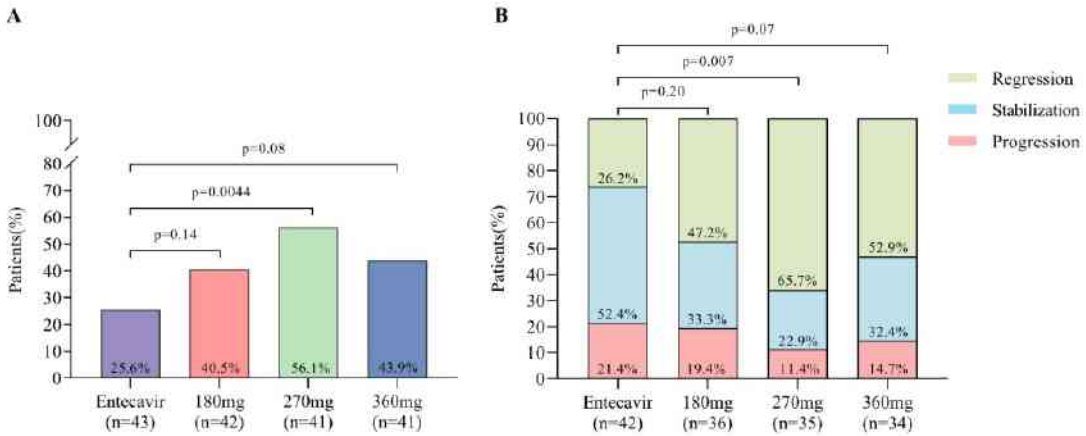

❖ OP-014

Fibrosis regression brings long-term clinical benefits in CHB patients with anti-HBV therapy

Yameng Sun[1], Shuyan Chen[1], Xiaoning Wu[1], Bingqiong Wang[1], Jialing Zhou[1], Tongtong Meng[1], Xinyan Zhao[1], Chen Shao[2], Xiaojuan Ou[1], Jidong Jia[1], Hong You[1]
[1]Liver Research Center, Beijing Friendship Hospital, Capital Medical University, [2]Department of Pathology, Beijing You-an Hospital, Capital Medical University

Background: Liver fibrosis could be regressed after successful anti-HBV therapy. However, the long-term clinical benefits of fibrosis regression have not been fully studied. In this study, we assessed associations between biopsy proved fibrosis regression with liver-related events in patients with chronic hepatitis B (CHB).

Method: Patients with post-treatment liver biopsy and significant fibrosis/cirrhosis (Ishak ≥ stage 3) due to CHB were enrolled in this study. The biopsy was performed after at least one year of anti-HBV treatment. Liver fibrosis was staged by Ishak score. Fibrosis regression was evaluated according to the PIR score of Beijing Classification. Cox regression was used to determine associations of fibrosis regression with liver-related clinical events.

Result:A total of 489 patients with significant fibrosis (Ishak stage 3/4, n=272, 56%) and cirrhosis (Ishak stage 5/6, n=217, 44%) by post-treatment liver biopsy were enrolled. According to PIR score, fibrosis regression, indeterminate and progression were observed in 162 (33%), 145 (30%) and 182 (37%) patients, respectively. During a median follow-up of 5 years after liver biopsy, 47 (12.5%) had liver-related events (decompensations, HCC or death); 25 (7.5%) patients were diagnosed with HCC, 21 (5.2%) patients had decompensations and 1 (0.2%) patient died. Fibrosis regression was associated with a lower risk of events versus non-regression (6.0% [7/162] vs. 15.3% [40/327]; HR, 2.63; 95% CI: 1.18-5.88 [P= 0.018]). Patients with fibrosis regression tended to be at higher risk of both decompensations (2.1% vs. 6.5%) and HCC (4.0% vs. 9.1%) than those with non-regression.

Conclusion: Regression of fibrosis after anti-HBV therapy is associated with a reduction in liver-related events in patients with CHB. These data support the use of histologic fibrosis regression and post-treatment PIR score as surrogate endpoints for clinical events of HBV-related fibrosis.

❖ OP-015

Causal relationships between metabolic associated fatty liver disease and iron status: a two-sample Mendelian randomization study

He He[1], Shenling Liao[1], Wanting Sun[1], Chuanmin Tao[1]
[1]West China Hospital, Sichuan University

Background: This study aimed to elucidate the causal effects of five iron metabolism markers (serum iron, ferritin, transferrin, transferrin saturation, and liver iron levels), regular iron supplementation, and the risk of metabolic-associated fatty liver disease (MAFLD) using a two-sample bidirectional Mendelian randomization (MR) analysis.

Method: Genetic summary statistics were obtained from open genome-wide association study (GWAS) databases. A two-sample MR was performed to estimate the causal effect between iron status and MAFLD, including the MR inverse variance-weighted (IVW), MR-Egger regression, and weighted median methods. The MR-PRESSO outlier test, Cochran's Q test, and MR-Egger regression were used to assess the outliers, heterogeneity, and pleiotropy, respectively.

Result: In the MR analysis for serum iron, ferritin, transferrin, transferrin saturation, liver iron, regular iron supplementation, and MAFLD risk, 4, 2, 10, 8, 4, 8, and 2 single nucleotide polymorphisms were used, respectively. No significant outliers, heterogeneity, or pleiotropy were detected, except for significant heterogeneity in the MR of MAFLD on liver iron. The MR IVW results showed that genetically predicted serum ferritin (odd ratio, OR = 1.42, 95%CI = 1.00, 2.02, P = 0.049) and liver iron (OR = 1.27, 95%CI = 1.07, 1.52, P = 0.008) were associated with an increased risk of MAFLD. There was no statistically significant causal effect of MAFLD risk on serum iron, ferritin, transferrin, transferrin saturation, or regular iron supplementation.

Conclusion: This study revealed the potential causal effect of serum ferritin and liver iron on the risk of MAFLD in European individuals. There is no evidence supporting the causal association between MAFLD and iron status.

Table and Figure:

Figure 1. The workflow of the study.

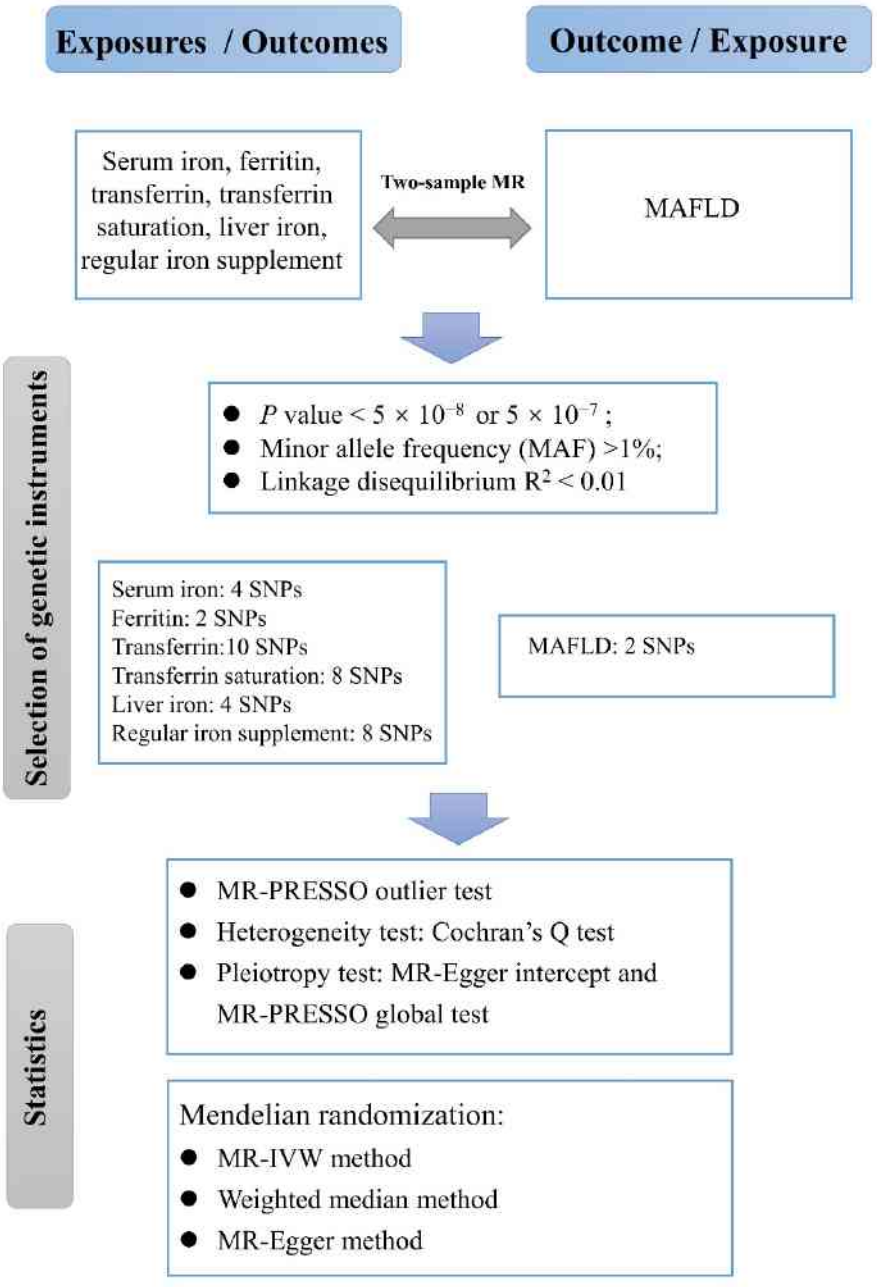

❖ OP-016

HOW STIGMA AND DISCRIMINATION AFFECTING THE ELIMINATION OF HBV? FINDINGS IN 5 ASIAN COUNTRIES

Inno Community Development Org, Dee Lee[1], Ice Huang[1], Anson Liu[1], Mahendra Singh[1], Letitia Xu[1], Zhengwei Huang[2]
[1]Inno Community Development Organisation, [2]Beijing University of Chinese Medicine

Background: In the last decade, the attention on stigma and discrimination against people living with hepatitis (PLWH) has been raised because of the staggering number of the stories told by the community around the world predominantly in Asia. The social friendliness for the PLWH has be been bettered through years of campaign however cases of stigma and discrimination are still existing among the community and the headlines of social tragedies. In the meantime, progress is being made toward a functional cure for chronic HBV. It is a most critical time for the disease and PLWH. Can the cure also be the cure for the stigma and discrimination? More importantly how stigma and discrimination will be affecting the elimination of the HBV even when the cure is available? The study is going to cultivate the issue to try giving suggestion to the new chapter of HBV sector.

Method: The study is going to conduct the survey in 5 Asian countries, China, India, Cambodia, Vietnam and Thailand where HBV is a high burden where Inno, as an action-taken agent to fight stigma and discrimination against PLWH, has her own team to deliver the outputs. The team will interview the PLWH in different types of gender and age groups. There will be totally 250 samples collected through our 8-year-long hotline platform and 25 in-depth face to face. Also a desktop research on the cases listed in the mainstream news in their own countries will also be the amendment for the study.

Result: In our early study, we found out that the stigma and discrimination against PLWH has been playing a role of barrier to cut off the linkage to care. Schools and workplace are the most significant places for the stigma and discrimination later in the family life. Also an early finding is that a high percentage of the interviewees have experienced depression or even have tendency to commit suicide. A low percentage of the interviewees show willingness to get cured or functional cure if they have to come out and listed in public health system or close relationship

Conclusion:A holistic approach to stigma and discrimination is mostly demanded to embrace the possible cure of HBV. They can be barriers but also an empirical leverage to help with the elimination of HBV. Law and regulation in education system and workplace

are and will be in place to prevent the damage of the explicit discrimination and stigma but more needs to be done like mental support, workplace hotline and other measures to micro manage them. Moreover a preparedness of reducing stigma and discrimination as barriers of the cure of HBV in the community are in great need to accelerate the treatment

❖ OP-017

Myeloid-derived suppressor cells ameliorate liver mitochondrial damage by releasing small extracellular vesicles in the treatment of autoimmune hepatitis

WITHDRAWAL

❖ OP-018

Presence of liver inflammation and fibrosis in Asian patients with chronic hepatitis B in the grey zone

WITHDRAWAL

❖ OP-019

Long-term outcomes of cirrhotic patients After HCV eradication with direct acting antivirals

Eman Abdelsameea[1], Nehad Darwish[2], Alyaa Sabry[3], Mostafa Elhelbawy[4], Asmaa Gomaa[1], Maha Elsabaawy[1], Mohsen Salama[1]

[1]Professor of hepatology and gastroenterology, National Liver Institute , Menoufia University, Egypt,
[2]Assistant lecturer of hepatology and gastroenterology, National Liver Institute , Menoufia University, Egypt,
[3]Assistant Professor of hepatology and gastroenterology, National Liver Institute , Menoufia University, Egypt,
[4]Lecturer of hepatology and gastroenterology, National Liver Institute , Menoufia University, Egypt

Background: In the past decade, treatment of chronic hepatitis C virus (HCV) infection has evolved from interferon (IFN)-based regimens to IFN-free oral direct-acting antiviral agents (DAAs). However, data on long-term outcomes in patients with HCV related liver cirrhosis treated by DAAs are contradictory and limited. This study aimed to determine long-term outcome in cirrhotic patients who achieved sustained virological response (SVR) after DAAs based regimens.

Method: This study was conducted on 193 post hepatitis C liver cirrhosis patients (Child Pugh score ≥ 5) who previously received DAAs and achieved SVR. Clinical, laboratory and radiological features, at 1 and 3-year follow-up after end of treatment were analyzed. Overall survival (OS) and development of liver decompensation and hepatocellular carcinoma (HCC) were determined at 5-year follow up.

Result: Male represented 68.4% with mean age of 54.8±7.7 years. Follow up at 1 and 3 year showed significant improvement of albumin (p= 0.001, p= 0.001), liver enzymes (p< 0.001, 0.001), alfa-fetoprotein (p< 0.001, p < 0.001), platelets (p< 0.001, p< 0.001), MELD score (p= 0.001 & 0.01), FIB4 and APRI scores (p < 0.001, p < 0.001). Liver stiffness (LS) also showed significant improvement (p=0.001, p= 0.001) respectively. At 5-year, the mean OS was 58.3 months, with 14.5% &17.6% of patients developed denovo HCC and decompensation, respectively. The cumulative rates of HCC development were 2.1%, 4.1%, 10.4% and 14.5% during 1year, 2 years, 3 years and 5 years follow up respectively. Mean OS at 5-year follow up was shorter for patients who developed HCC and for those with liver decompensation (p= 0.001). Diabetes, alfa-fetoprotein and LS were predictive factors for HCC development.

Conclusion: Despite of SVR, continuous surveillance of HCC is mandatory in patients with advanced liver disease.

❖ OP-020

Platelet count and MELD to discriminate high risk of decompensation in compensated HBV cirrhosis patients with esophageal varices during anti-HBV treatment.

Bingqiong Wang[1,2], Jialing Zhou[1,2], Xiaoning Wu[1,2], Yameng Sun[1,2], Shuyan Chen[1,2], Tongtong Meng[1,2], Xinyu Zhao[3,2], Xiaojuan Ou[1,2], Jidong Jia[1,2], Hong You[1,2]
[1]Liver Research Center, Beijing Friendship Hospital, Capital Medical University,
[2]National Clinical Research Center for Digestive Diseases,
[3]Clinical Epidemiology & EBM Unit, Beijing Friendship Hospital, Capital Medical University

Background: Antiviral therapy can reverse portal hypertension (PHT) and improve long-term prognosis in chronic hepatitis B patients. Whereas, the incidence of decompensation and risk factors associated with decompensation in cirrhotic patients with PHT after treatment were lack of evidence. Our aim was to identify predictors of clinical decompensation in HBV compensated cirrhotic with portal hypertension under well etiology control.

Method: Eligible patients had documented for receiving anti-HBV treatment at least 2 year and diagnosed with cirrhosis during antiviral therapy at the time of esophagogastroduodenoscopy. Patients were followed prospectively at the interval of every 6 months. Decompensation events (defined as the development of ascites, variceal hemorrhage [VH], or hepatic encephalopathy [HE]) or death were recorded during study. Univariate and multivariate Cox regression analysis were conducted to identify predictors enrolled in the final stratified strategy. Time dependent receiver operating characteristic (ROC) curve was used to identify the threshold of enrolled predictors. C index were used to evaluate diagnostic capacity of the new prediction model.

Result:A total of 269 on-treatment compensated cirrhosis patients with esophageal varices (EVs). After median follow-up time of 28.0 months (IQR, 23.0-37.0), thirty (11.2%) of those patients developed decompensation (Figure 1). Among them, 20 (80.0%) were ascites, 4 (13.3%) were VH, 2 (6.7%) were HE. In patients with mild varices, the 3-year cumulative incidence of decompensation was 5.9%, in which platelet (HR=0.970; 95% CI, 0.941-0.990) were independently associated with decompensation. In patients with moderate/severe varices, the 3-year cumulative incidence of decompensation was 29.8%, in which model of end-stage liver disease (MELD) (HR=1.374; 95% CI, 1.108-1.704) were selected as risk factor. Accordingly, in we developed a new stratified strategy including degree of EVs and platelet count, and MELD score using the cut off value of PLT at

85×109/L and MELD at 10 point, respectively. By this stratified analysis, the 3-year incidence of decompensation showed significant difference within the same degree of varices both in patients with mild varices (0.7% in low-risk and 17.3% in high-risk, P<0.001) and patients with moderate/severe varices (15.7% in low-risk and 62.1% in high-risk, P<0.001) (Figure 2).

Conclusion: Platelet count and MELD are independently associated with clinical decompensation in compensated cirrhotic patients with different degree of varices, especially helpful in discriminating patients with mild EVs who are at high risk of decompensation.

Table and Figure:

Figure 1. Flow chart

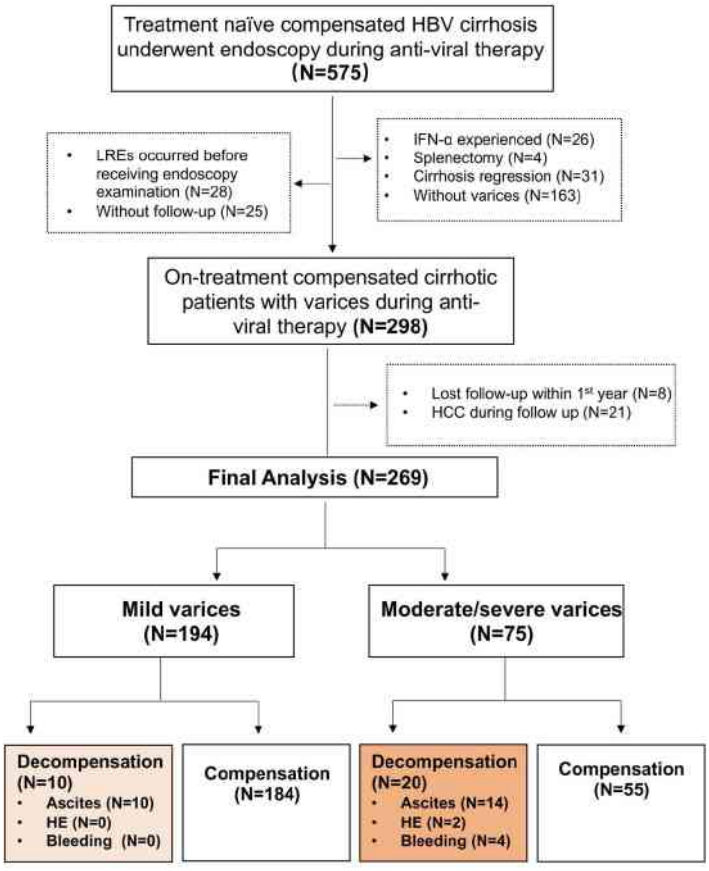

Figure 2. Comparation of cumulative incidence of decompensation according to different groups based on new proposed stratified strategy.

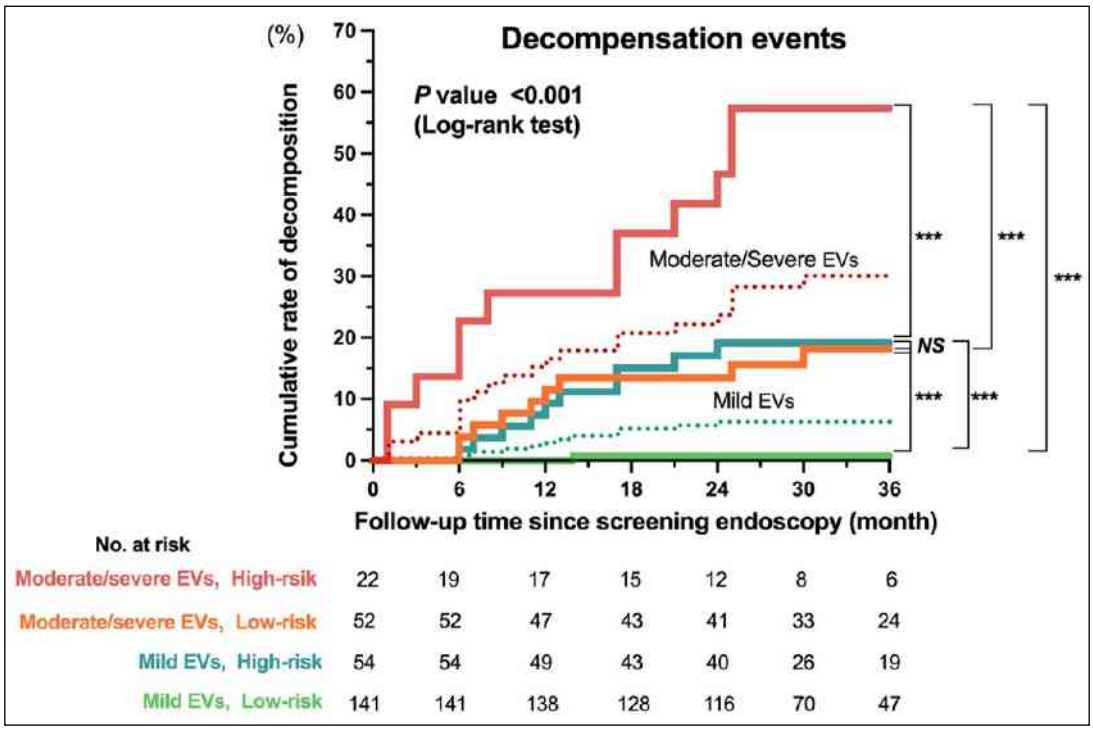

❖ AA-001

Hepatic stellate cells/fibroblast-specific LOXL1 deficiency attenuated hepatic inflammation, fibrosis, and ductal reaction in BDL and Mdr2-/- mice

Xuzhen Yan[1,2], Aitng Yang[2,3,4], Weiyu Li[1,2], Wei Chen[2,3,4], Hong You[1,2,4]
[1]Liver Research Center, Beijing Friendship Hospital, Capital Medical University, Beijing Key Laboratory of Translational Medicine on Liver Cirrhosis, National Clinical Research Center of Digestive Diseases, Beijing, P.R. China;, [2]National Clinical Research Center of Digestive Diseases, Beijing, P.R. China;, [3]Experimental and Translational Research Center, Beijing Friendship Hospital, Capital Medical University, Beijing, P.R. China;, [4]Beijing Clinical Medicine Institute, Beijing, P.R. China;

Background: Liver fibrosis, a manifestation of chronic liver disease, occurs as a result of long-term irritation from multiple etiologies. The activation of hepatic stellate cells (HSCs)/ myo-fibroblast results in massive deposition of extracellular matrix (ECM), especially collagen and elastin, which is the dominant mechanism of liver fibrosis. Lysyl oxidase (LOX) family is important in regulating ECM cross-linking, then affecting the stability and stiffness of ECM, especially Lysyl oxidase-like 1(LOXL1). However, the potential role of LOXL1 in the pathogenesis of bile duct ligation (BDL) and Mdr2-/- mice has not been previously studied.

Method: We constructed recombinant adeno-associated virus knockdown Loxl1 expression (rAAV2/6-shLoxl1) to selectively restrain the HSCs/fibroblast-derived Loxl1. rAAV2/6-shLoxl1, or its negative control (rAAV2/6-NC) was administrated intravenously to mice with Mdr2-/- and BDL model. We examined the Loxl1 suppression efficiency as well as degree of liver fibrosis, inflammation and ductal reaction profile in liver tissue.

Result:LOXL1 was decreased in Mdr2-/- and BDL mice (29% and 40% respectively in mRNA level) and LOXL1 showed a near-total absence in desmin-positive area after rAAV2/6-shLoxl1 injection. Compared to rAAV2/6-NC treatment, LOXL1 inhibition in HSCs/ fibroblast ameliorated Mdr2-/- and BDL induced fibrosis with reduced Sirius Red positive area (30% and 50% respectively), as well as pro-fibrogenic gene, such as Col1a1 (46% and 59% respectively), a-SMA (51% and 38% respectively) and Timp-1 (39% and 58% respectively). This was paralleled by pro-inflammation gene reduction, such as Mcp1 (62% and 64%), Tnfa (42% and 71%) and Il1b(39% and 52%). Furthermore, LOXL1 inhibition in HSCs/fibroblast could suppress cytokeratin 19 positive area (19% and 40%) and mRNA expression of Hnf1b (22% and 52%).

Conclusion: Our study demonstrated LOXL1 may contribute to fibrosis progression both in Mdr2-/- and BDL mice and HSCs/fibroblast-specific knockdown of LOXL1 attenuated liver fibrosis, inflammation and ductal reaction.

❖ AA-002

Inhibition of AEBP1 Decreases Hepatic Stellate Cells Proliferation by Targeting Toll Like Receptor Signaling Pathway

Wen Zhang[1,2], Yujia Li[3], Wei Chen[4,5], Ning Zhang[1,2], Xuzhen Yan[4,5], Aiting Yang[4,5], Hong You [1,2]
[1]Liver Research Center, Beijing Key Laboratory of Translational Medicine in Liver Cirrhosis, Beijing Friendship Hospital, Capital Medical University, Beijing, China , [2]National Clinical Research Center of Digestive Diseases, Beijing, China, [3]Emory University, Atlanta, USA, [4]Beijing Clinical Research Institute, Beijing, China, [5]Experimental and Translational Research Center, Beijing Friendship Hospital, Capital Medical University, Beijing, China

Background: Integrated bioinformatics analyses revealed that adipocyte enhancing binding protein 1 (AEBP1) was robustly elevated in fibrotic liver regardless of any etiology. AEBP1 expression could be as an index to distinct fibrotic from non-fibrotic livers. However, the potential mechanisms of AEBP1 involved in liver fibrosis remains unclear.

Method: Liver fibrosis and spontaneously regressive mouse models were induced by CCl4 intoxication and cessation. AEBP1 expression and location were determined by western blot and immunofluorescence. A publicly available single cell RNA sequencing (scRNA-seq) dataset was enrolled to investigate the cellular source for AEBP1 production. AEBP1 specific siRNA was transiently transfected into LX-2 cells, followed by MTT assay, Ki67 mRNA detection, bulk RNA sequencing and gene set enrichment analysis (GSEA).

Result: Aebp1 was significantly increased in CCl4-induced liver fibrosis mouse model but only decreased in the late regressive period after CCl4termination. In fibrotic liver Aebp1 was mainly located in the portal area, central vein, and perisinusoidal space but in the regressive liver Aebp1 was persistently expressed in the perisinusoidal space. scRNA-seq analysis highlighted that Aebp1 gene was primarily expressed in fibroblasts. Silence of Aebp1 evidently inhibited the proliferation of LX-2 cells. Bulk RNA sequencing analysis highlighted a significant change in LX-2 cells after Aebp1 inhibition since the principal component analysis (PCA) plot clearly separated the siRNA group and negative control group. Further GSEA analysis activity of toll-like receptor signaling pathway and key genes involved in this pathway were notably decreased.

Conclusion:AEBP1 silence inhibits proliferation of hepatic stellate cells probably by affecting toll-like receptor signaling pathway, which requires further investigation.

Table and Figure:

Figure 1.AEBP1 expression and location in liver fibrosis and spontaneously regressive mouse models.

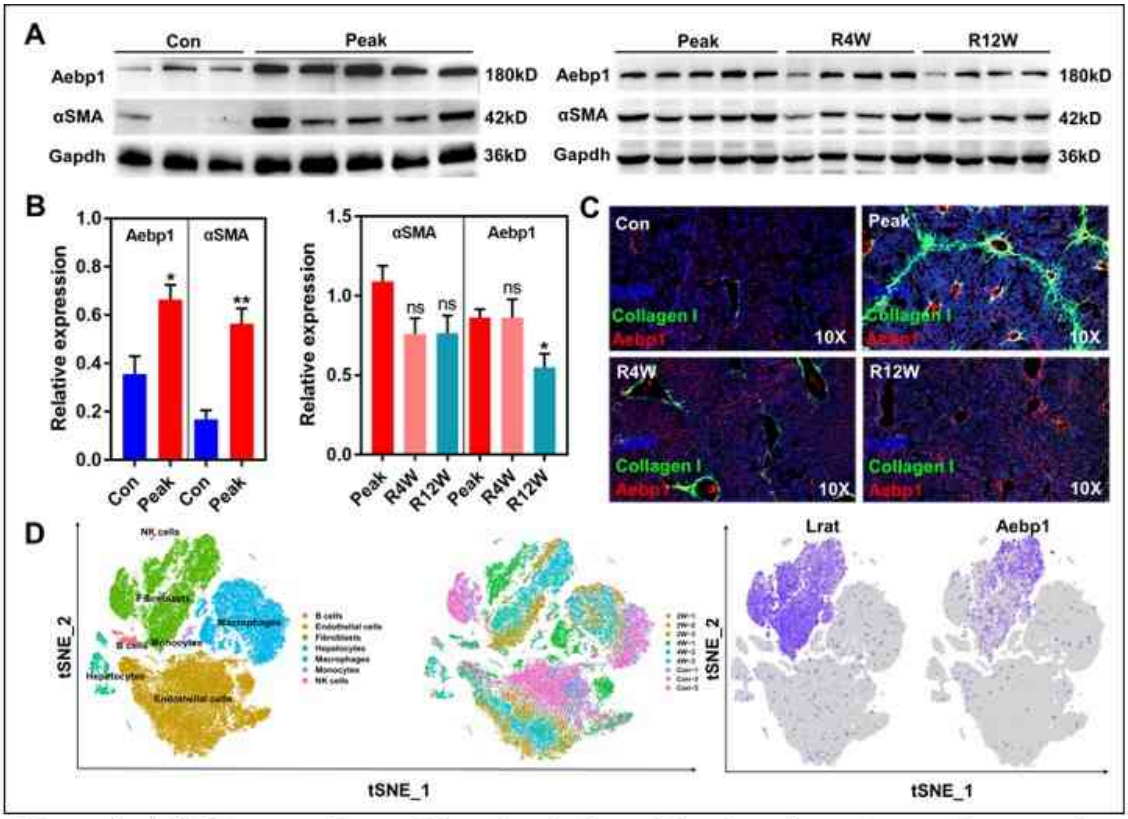

Figure 1. AEBP1 expression and location in liver fibrosis and spontaneously regressive mouse models. AEBP1 and aSMA protein detection in (**A**) CCl_4-induced liver fibrosis mouse models (CCl_4 injection: twice a week for up to 12 weeks [peak]) and (**B**) spontaneously regressive mouse models (CCl_4 cessation for 4 weeks [R4W] or 12 weeks [R12W]). (**C**) Immunofluorescence detection of AEBP1, collagen I and DAPI that were color coded. (**D**) tSNE plots of cell type, sample distribution and Lrat or Aebp1 expression by scRNA-seq analysis from GSE145086 dataset.

Figure 2.AEBP1 silence inhibited LX-2 cells proliferation probably by affecting toll-like receptor signaling pathway.

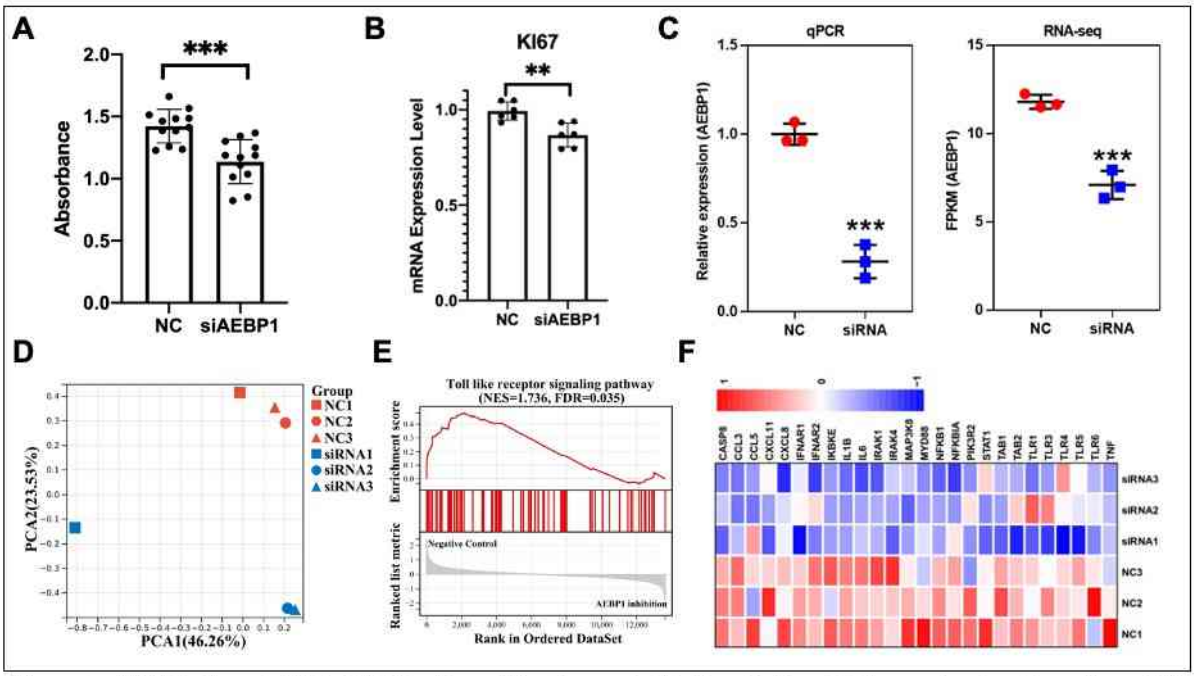

Figure 2. AEBP1 silence inhibited LX-2 cells proliferation probably by affecting toll-like receptor signaling pathway. (**A**) LX-2 cells proliferation was reduced after AEBP1 siRNA transfection under TGFβstimulation. (**B**) Ki67 gene expression was significantly decreased after AEBP1 silence under TGFβtreatment. (**C**) AEBP1 gene was significantly silenced after AEBP1 siRNA transfection under TGFβincubation. (**D**) PCA plot showed siRNA and negative control (NC) groups were cleared clustered when the differentially expressed genes were regarded as the observable variables. (**E**) GSEA plot of toll-like receptor signaling pathway and heatmap of the expression of key genes involved in this pathway.

❖ AA-003

YAP promoting liver sinusoidal endothelial cell mediated angiogenesis and hepatic fibrosis via Notch signaling

Junjun Wang[1], Weiming Dai[1], Zhenyang Shen[1], Hui Dong[1], Lungen Lu[1], Xiaobo Cai[1]
[1]Shanghai First People's Hospital

Background: Liver sinusoidal endothelial cells (LSECs) play an important role in liver angiogenesis and fibrogenesis. During persistent liver injury, LSECs undergo capillarization and acquire pro-vasoconstrictor, pro-inflammatory, pro-thrombotic, pro-angiogenic, and pro-fibrotic phenotypes, leading to increased hepatic angiogenesis. Previous studies have shown that activation of Notch signaling play a pivotal role in the capillarization and angiogenesis of LSCEs. Studies also showed that Yes-associated protein (YAP) can regulate endothelial cell proliferation, migration, survival, and vascular remodeling in other organs. However, the role of YAP in LSECs mediated angiogenesis during liver fibrosis is still unclear.

Method: The expression of YAP in LSECs was detected in choline-deficient, ethionine-supplemented (CDE) and 3,5-diethoxycarbonyl 1,4-dihydrocollidine (DDC) diet-induced liver injury mice. Immortalized LSECs was transfected with siYAP and overexpression plasmid, siGATA6 and their negative control, respectively. Western blot and qRT-PCR were used to detect expression of YAP, GATA6 and Notch signaling molecules. EDU, transwell migration and Matrigel tube-forming assays were used to detect the abilities of the proliferation, migration and angiogenesis of LSECs. In the DDC diet-induced hepatic fibrosis mice, Hyaluronic acid-polyethyleneimine/siYAP (HA-PEI/siYAP) were injected into the tail vein to specifically inhibit the expression of YAP in LSECs.

Result: Increased expression of YAP in LSECs and hepatic angiogenesis was demonstrated in mice with CDE and DDC diet-induced chronic liver injury. Vascular endothelial growth factor (VEGF) increased the nuclear expression of YAP, GATA6, and Notch intracellular domain (NICD). Overexpression of YAP promoted the abilities of proliferation, migration and angiogenesis of LSECs, Notch signaling activation, and also enhance the expression of GATA6. Inhibition of YAP and GATA6 expression decreased the abilities of proliferation, migration and angiogenesis of LSECs, and the activation of Notch signaling. Moreover, YAP could directly bind to the NICD, while also indirectly regulate Notch signal by binging to GATA6 to influence the angiogenesis of LSECs. VEGF could

promote the combination of YAP with NICD and GATA6 (Figure 1). In vivo that HA-PEI/siYAP could target YAP in LSECs effectively and inhibit the expression of YAP and its downstream genes. The biochemical parameters such as ALT, AST, ALP, and TBIL decreased in the DDC+HA-PEI/siYAP group. The decrease of YAP in LSECs inhibited the expression of CD31 and Vegfr2, macrophage aggregation and alleviated liver fibrosis (Figure 2).

Conclusion:YAP can regulate Notch signaling by directing binging to the NICD or GATA6, and promote LSECs mediated hepatic angiogenesis during liver injury. YAP in LSECs may be a potential therapeutic target for chronic liver disease and hepatic fibrosis.

Table and Figure:

Figure 1. Figure1: YAP regulate Notch signaling by directing binging to the NICD or GATA6.

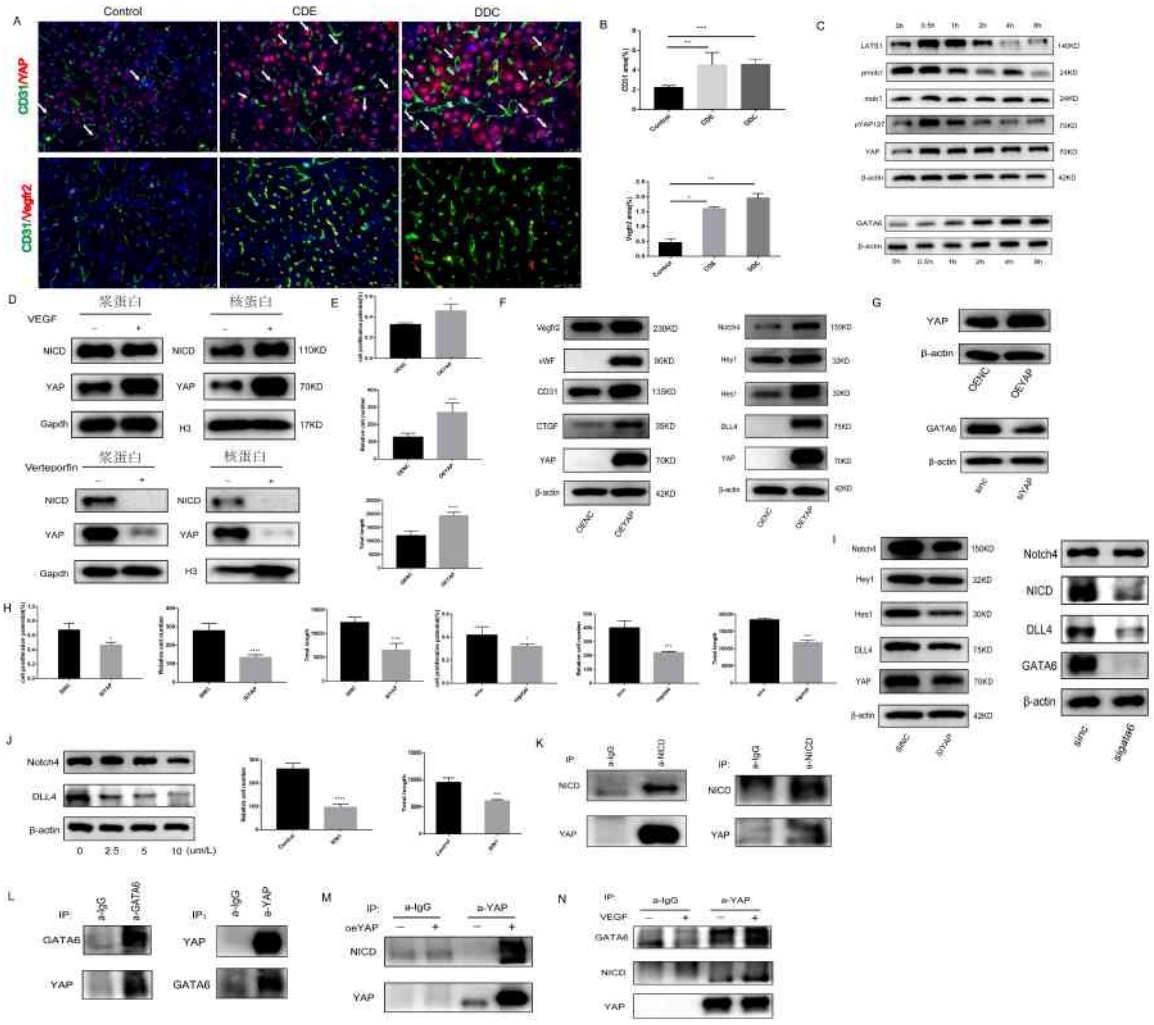

Figure 2. Figure2:Inhabiting YAP in LSECs can decrease hepatic angiogenesis, liver inflammatory, and mitigate liver fibrosis.

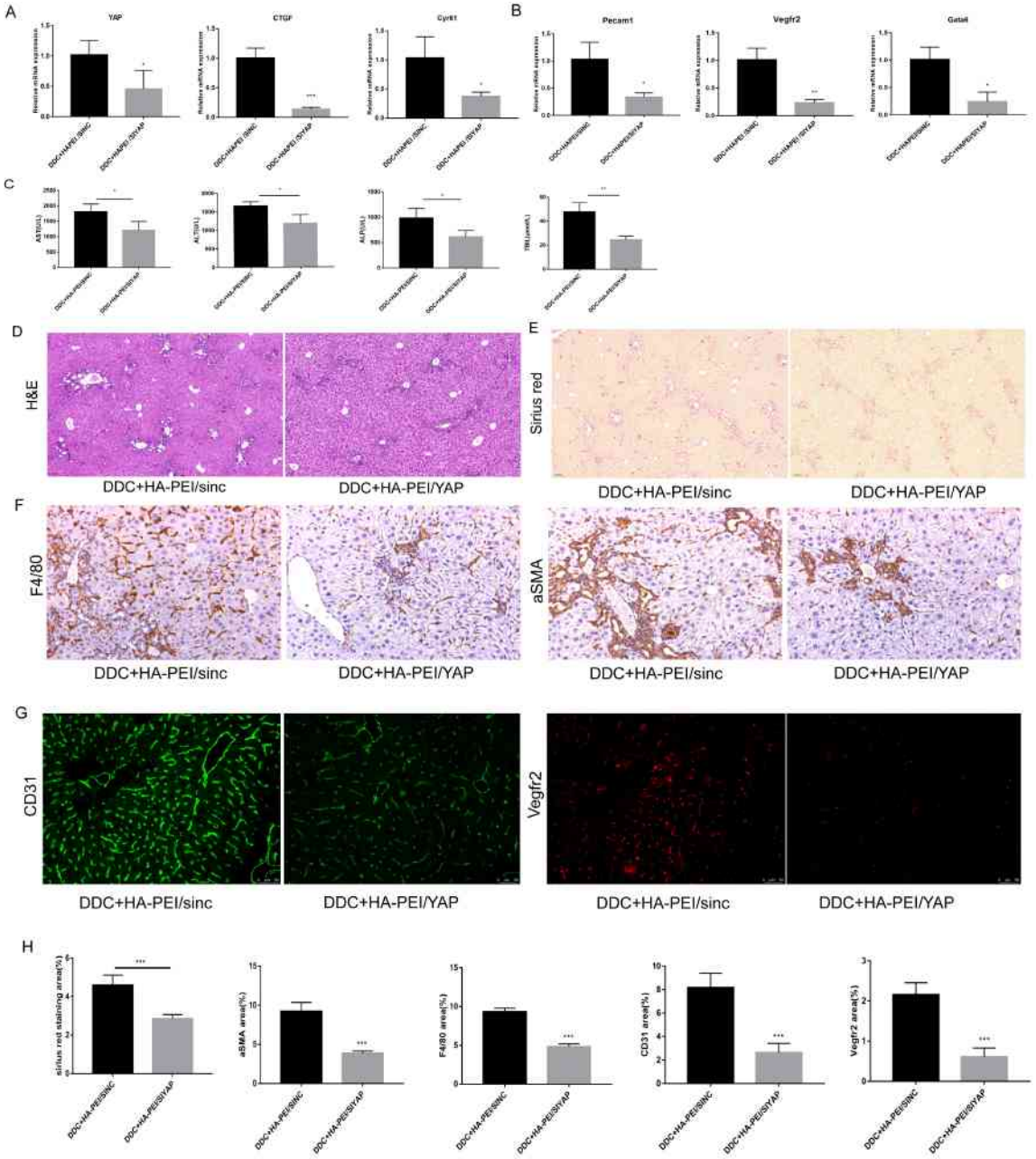

❖ AA-004

Tyrosine Kinase receptor B (TrkB) attenuates liver fibrosis via inhibiting TGFβ/SMAD signaling

Yu Song[1,2], Jiayi Wei[1,2], Rong Li[3], Ruifeng Fu[4], Guangcong Zhang[1,2], Shuyu Li[1,2], Sinuo Chen[1,2], Zhiyong Liu[1,2], Yicheng Zhao[1,2], Changfeng Zhu[1,2], Jimin Zhu[1,2], Taotao Liu[1,2], Ling Dong[1,2], Shuncai Zhang[1,2], Jian Wu[1,2,5], Hao Pei[6], Jiefei Cheng[7,8], Guangqi Song[1,9], Xizhong Shen[1,2], Qunyan Yao[1,2]

[1]Department of Gastroenterology and Hepatology, Zhongshan Hospital, Fudan University, Shanghai 200032, P.R. China, [2]Shanghai Institute of Liver Diseases, Shanghai 200032, P.R. China, [3]School of Life Sciences and Biotechnology, Shanghai Jiao Tong University, Shanghai, P.R. China. , [4]Department of Histology and Embryology, College of Basic Medicine, Second Military Medical University, Shanghai 200032, P.R. China, [5]Department of Medical Microbiology, Key Laboratory of Medical Molecular Virology, School of Basic Medical Sciences, Fudan University, Shanghai 200032, P. R. China, [6]Department Shanghai Key Laboratory of Green Chemistry and Chemical Processes School of Chemistry and Molecular Engineering, East China Normal University, Shanghai 201203, P. R. China, [7]Otsuka Shanghai Research Institute, Shanghai 201318, China, [8]Shanghai University of Traditional Chinese Medicine, Shanghai 201203, China, [9]Joint Laboratory of Biomaterials and Translational Medicine, Puheng Technology, Suzhou 215000, China

Background: Liver fibrosis is a main indicator for increased mortality and long-term comorbidity in nonalcoholic steatohepatitis (NASH); and activation of hepatic stellate cells (HSCs) and excessive deposition of extracellular matrix components are the hallmarks of liver fibrogenesis. Tropomyosin-related tyrosine kinase B (TrkB) is a multifunctional receptor participating in neurodegenerative disorders. However, paucity of literature is available about TrkB function in liver fibrosis. Herein, TrkB function and its regulatory network were explored in progression of hepatic fibrosis.

Method: Human LX-2 cells and constructed 3D liver spheroids were used to explore the role of TrkB in HSC proliferation and activation. The role of TrkB was assessed by examining the activity of TGFβ/SMAD signaling in HSCs, and investigated in fibrotic mouse models with its overexpression by adeno-associated virus vector (AAV6 and AAV8).

Result: Protein levels of TrkB were decreased in CDAHFD/CCl4-induced hepatic fibrosis mouse model. TrkB suppressed TGFβ-induced proliferation and activation in HSCs, and significantly repressed TGFβ/SMAD signaling pathway via directly interacting with SMAD2/3. Meanwhile, TGFβ-induced Nedd4 family interacting protein-1 (Ndfip1) expression promoted the ubiquitination and degradation of TrkB via E3 ligase Nedd4-2. Moreover, AAV-medicated TrkB overexpression attenuated the extent of liver fibrosis in mouse models.

Conclusion:TGFβ stimulated TrkB degradation through E3 ligase Nedd4-2 in HSCs. Meanwhile, TrkB overexpression inhibited the activation of TGFβ/SMAD signaling and alleviated hepatic fibrosis both in vitro and in vivo. These findings underscore that TrkB functions as a novel suppressor of hepatic fibrosis, and confers a novel therapeutic perspective in hepatic fibrosis.

Table and Figure:

Figure 1. Working model depicting how TrkB regulates the progression of liver fibrosis through TGFβ/SMADs pathway. TrkB inhibited TGFβ/SMADs pathway by directly interacted with SMADs proteins and repressed SMADs nuclear retention in HSCs. Meanwhile, TGFβ induced Ndfip1 promoted the ubiquitination and proteasomal degradation of TrkB during HSCs activation via E3 ligase Nedd4-2.

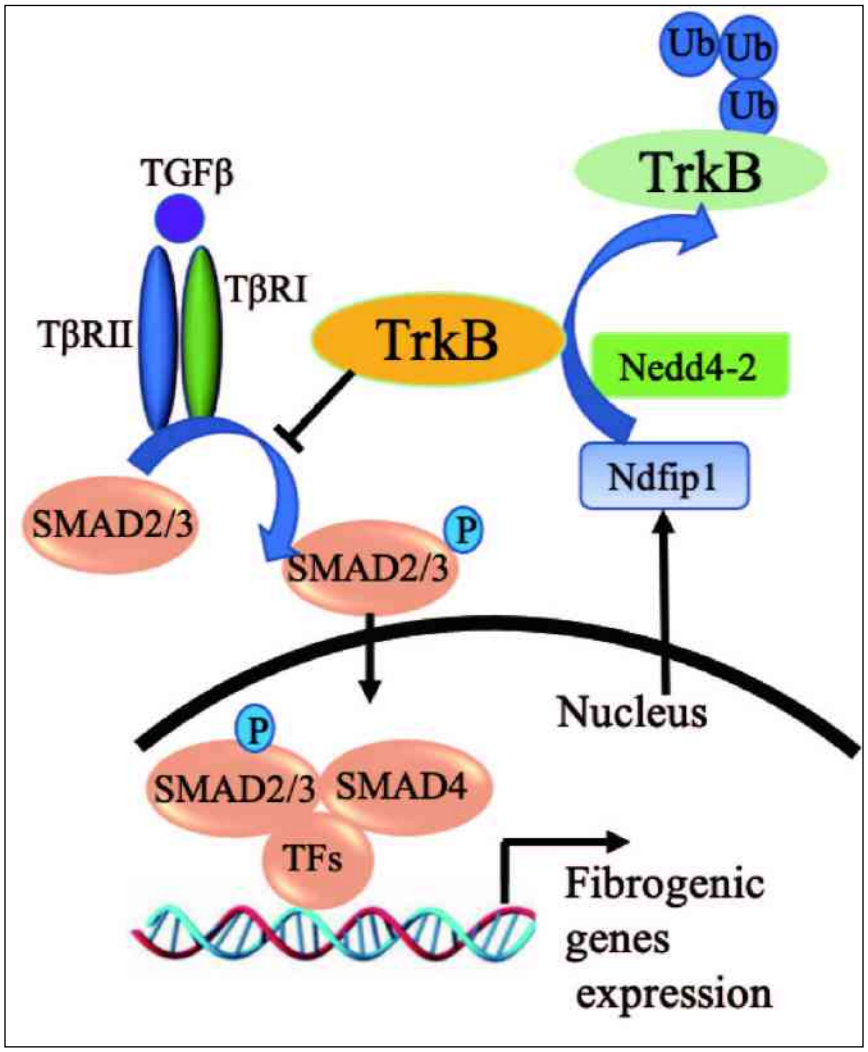

❖ AA-005

The loss of FAM172A gene prompts cell proliferation in liver regeneration

[1]Department of Gastroenterology, Beijing Ditan Hospital, Capital Medical University, Beijing, 100015, China., [2]Department of Gastroenterology, Peking University People's Hospital, Peking University, Beijing, 100044, China., [3]Clinical Center of Immune-Mediated Digestive Diseases, Peking University People's Hospital, Beijing, 100044, China. , [4]Beijing Key Laboratory of Emerging Infectious Diseases, Institute of Infectious Diseases, Beijing Ditan Hospital, Capital Medical University, Beijing 100015, China., [5]Beijing Institute of Infectious Diseases, Beijing, 100015, China., [6]National Center for Infectious Diseases, Beijing Ditan Hospital, Capital Medical University, Beijing 100015, P.R. China.

Background: Liver regeneration is a self-healing process to damage induced by various agents. The liver is the first line defense to external perturbations, such as surgical resection, ischemia, toxin damage, and pathogen infection. Nowadays, over one million people have died annually from chronic liver disease. Hence, targeted therapy for liver regeneration may be an effective treatment strategy for patients with acute and chronic liver disease.

Method: Experimental studies were performed in C57B/6J mice (FAM172A-/- and wild–type). Mice were then sacrificed at 0, 12, 24, 48, 72, and 168 hours after 70% partial hepatectomy (PH). And we also verified the results in vitro. Western blot and immunohistochemistry were performed.

Result: Firstly, we tested that FAM172A protein level increased significantly from 48 to 168 hours in the liver of wild-type (WT) mice after PH (Figure 1A). Our team had constructed the FAM172A gene knockout mice previously. Through immunohistochemistry (IHC) staining of FAM172A, the results showed that FAM172A was expressed in both hepatocytes and nonparenchymal liver cells in WT mice, no expression in FAM172A-/- mice (Figure 1B). Then we proceeded PH on WT and FAM172A-/- mice and compared liver weight / body weight (LW/BW) between two groups. There were significant differences except at 0 hour (Figure 1C). Proliferating cell nuclear antigen (PCNA) could more truly reflect in initiating cell proliferation in previous studies. The data showed that FAM172A-/- mice had higher PCNA level at 12, 24, 48, 72, and 168 hours (Figure 1D). Therefore, our results indicated that knocking out the FAM172A gene could promote liver proliferation in mice after PH. Although FAM172A gene knockdown promoted hepatocytes proliferation, its mechanism was still unclear. It had been reported that FAM172A silencing induced phosphorylated extracellular signal-regulated kinase (pERK)

increase, which ERK signaling pathway was involved in liver regeneration. So we examined the level of pERK. As shown in Figure 2A, FAM172A knockdown increased the levels of pERK and PCNA. It also had been reported that yes associated protein 1 (YAP1) was an ERK signal transduction target. As we expected, the pERK inhibitor- U0126 reversed the up-regulated effect of FAM172A knockdown on YAP1 (Figure 2B). More importantly, down-regulated YAP1 expression by YAP1 siRNA could inhibit cell proliferation by reducing the expression of PCNA, cyclin A, B1, D1 and E (Figure 2C). On the contrary, up-regulated FAM172A expression resulted in decreased PCNA through inhibiting ERK-YAP1-cyclin axis (Figure 2D). In vivo, we confirmed that FAM172A-/- mice after PH had higher levels of pERK, YAP1 and PCNA (Figure 2E). In summary, the above results indicate that the knockout of FAM172A gene promotes cell proliferation through the pERK-YAP1 axis.

Conclusion: In general, The loss of FAM172A gene facilitates cell proliferation during liver regeneration by high expression of YAP1 induced by ERK activation in FAM172A-/- hepatocytes.

Table and Figure:

Figure 1. Figure 1: The loss of FAM172A gene facilitated hepatocytes proliferation during liver regeneration.

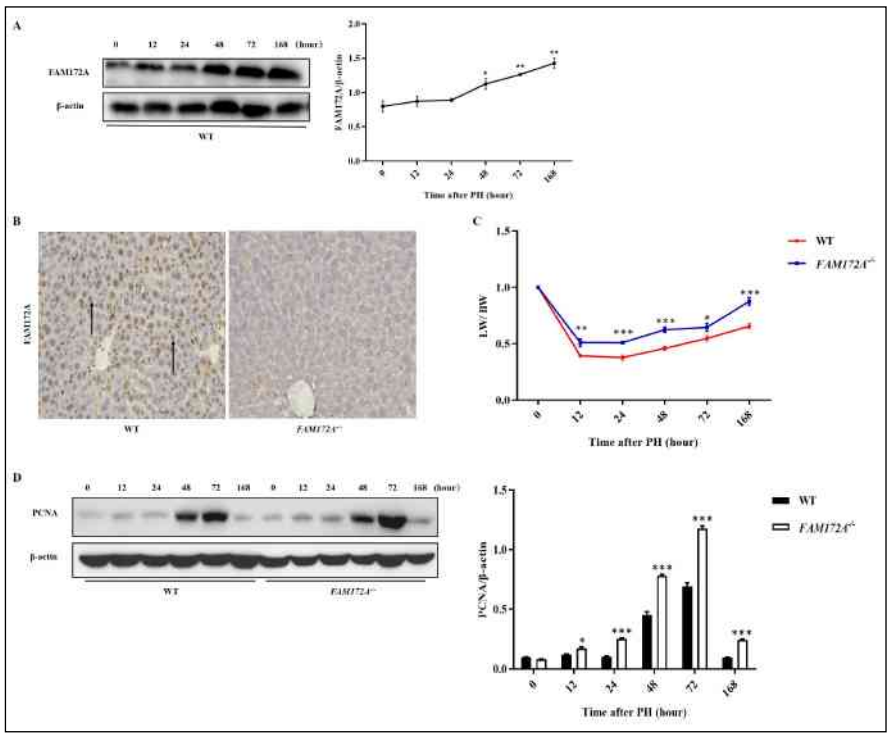

Figure 2. Figure 2: Loss of FAM172A gene prompted cell proliferation by regulating the pERK-YAP1 signaling.

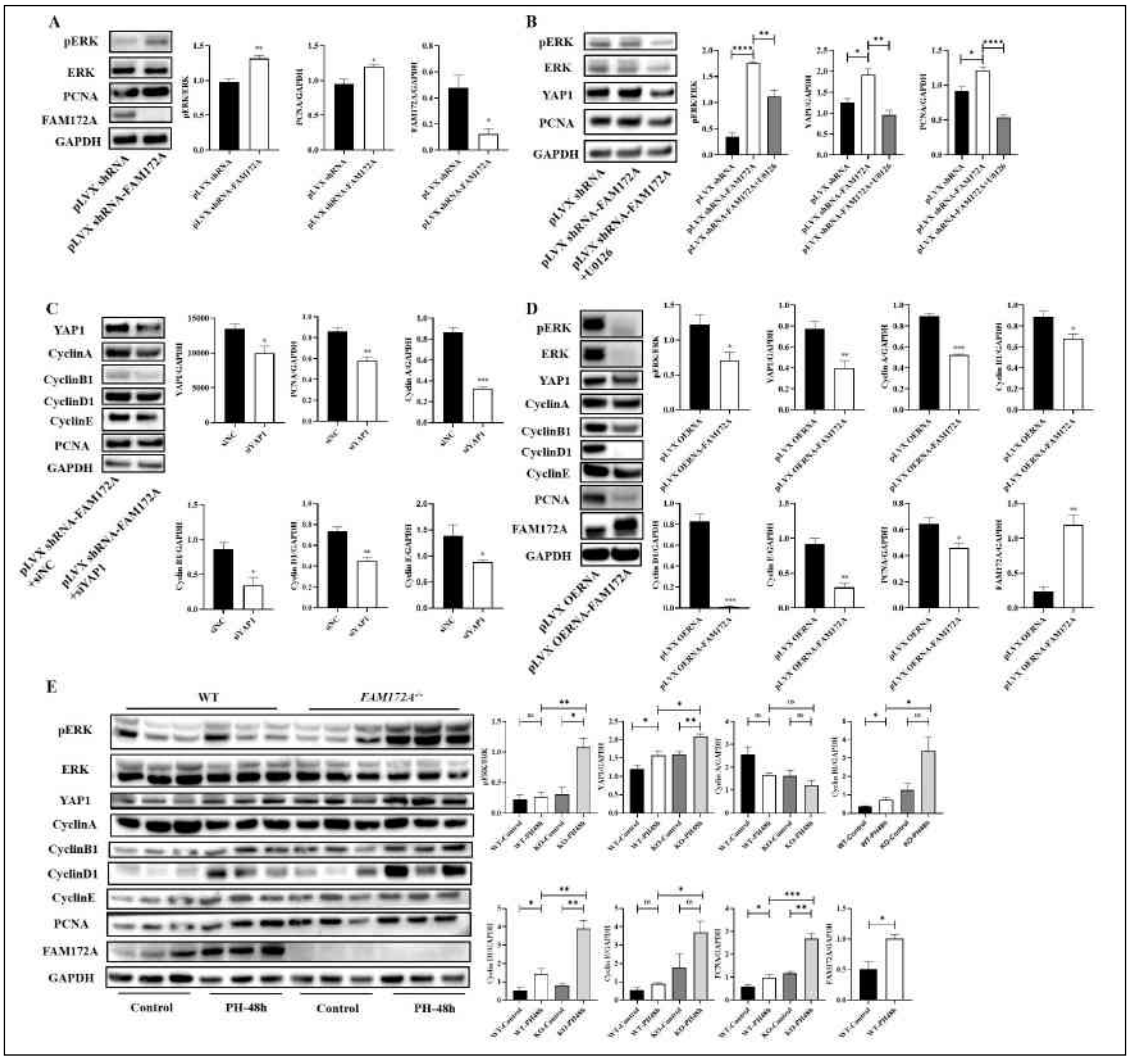

❖ AA-006

hMSCs-derived exosome circCDK13 inhibits liver fibrosis by regulating the expression of MFGE8 through miR-17-5p/KAT2B

Jing Ma[1]
[1]*Department of Infectious Disease, The Second Xiangya Hospital, Central South University*

Background: Liver fibrosis acts as a risk factor for liver cancer and activated hepatic stellate cells (HSCs) are responsible for the progressive course of liver cancer . Emerging evidence has reported that MSCs-derived exosomes may be considered as a novel therapeutic strategy for liver fibrosis because their advantages are superior to MSCs .A previous study revealed that circCDK13 was involved in the progressive disease of liver cancer . Hence, we speculated that whether circCDK13 could be transmitted to HSCs by hMSCs-Exo and play a role in liver fibrosis. MiR-17-5p has been reported to activate HSCs and get involved in the progressive course of liver fibrosis . It is also reported that circRNA could inhibit liver fibrosis through regulating miR-17-5p . KAT2B has been reported as a novel regulator of hepatic lipogenesis and is expressed in liver cells. StarBase found the binding site of circCDK13 and KAT2B to miR-17-5p. Hence, in this study, we first aimed to explore whether hMSCs-derived exo-circCDK13 could affect the progression of liver fibrosis by regulating miR-17-5p/KAT2B.

Method: Exosomes derived from hMSCs were extracted and identified by flow cytometry and osteogenic and adipogenic induction, and the expressions of marker proteins on the surface of exosomes were detected by Western blot. Cell proliferation was measured by CCK8 assay, the expression of active markers of HSCs by immunofluorescence, and the expressions of fibrosis-related factors by Western blot. A mouse model of liver fibrosis was established by intraperitoneal injection of thioacetamide (TAA). Fibrosis was detected by HE staining, Masson staining and Sirius red staining. Western blot was utilized to test the expressions of PI3K/AKT and NFκB pathway related proteins, dual-luciferase reporter assay and RIP assay to validate the binding between circCDK13 and miR-17-5p as well as between miR-17-5p and KAT2B, and ChIP to validate the effect of KAT2B on H3 acetylation and MFGE8 transcription.

Result:hMSCs derived exosomes inhibited liver fibrosis mainly through circCDK13. Dual luciferase reporter assay and RIP assay demonstrated the binding between circCDK13 and miR-17-5p as well as between miR-17-5p and KAT2B. Further experimental results

indicated that circCDK13 mediated liver fibrosis by regulating the miR-17-5p/KAT2B axis, and KAT2B promoted MFGE8 transcription by H3 acetylation. Exo-circCDK13 inhibited PI3K/AKT and NF-κB signaling pathways activation through regulating the miR-17-5p/KAT2B axis.

Conclusion:hMSCs-derived exosome circCDK13 inhibited liver fibrosis by regulating the expression of MFGE8 through miR-17-5p/KAT2B axis.

❖ AA-007

Interleukin-10 activates STAT3 to induce senescence of HSCs in rats with liver fibrosis

Jiabing Chen[1], Yuehong Huang[1], Yizhen Chen[1], Yixuan Huang[1]
[1]Department of Gastroenterology and Fujian Institute of Digestive Disease, Fujian Medical University Union Hospital, 29#Xinquan Road, Gulou District, Fuzhou, 350001, Fujian, China

Background: Hepatic fibrosis is a chronic pathological process characterized by abnormal activation of hepatic stellate cells (HSCs) and excessive accumulation of the extracellular matrix (ECM).Therefore, activated HSCs is the main target cells for improvement of liver fibrosis. Our previous studies have shown that interleukin 10 (IL-10) induces HSCs senescence through activating the signal transducer and activator of transcription 3(STAT3) and P53/P21 pathway to attenuate liver fibrosis. However, the precise mechanism of STAT3 on senescence of activated HSCs is unclear. The objective of this study is to explore the relationship between the activation of STAT3 and IL-10-induced senescence of HSCs.

Method: Firstly,STAT3 was transiently overexpressed or knock-down in immortality HSCs line(HSC-T6) and primary rat HSCs(pHSC) by using a recombinant adenovirus vector particle(Ad-STAT3) or a RNA interference for STAT3 (Si-STAT3) in the absence or presence of IL-10. SA-β-Gal and immunofluorescence staining, fluorescence quantification, western blot and flow cytometry analysis were used to detect the senescence phenotype, senescent related proteins, cell cycle arrest. In vivo, fibrotic rats treated with or without IL-10 gene were used to isolated fibrotic HSCs. The relationship between the activation of STAT3 and senescence- and cycle-associated proteins in fibrotic HSCs were detected by western blot. Lastly, fibrotic rats were treated with STAT3 specific inhibitor cryptotanshinone alone or in combination with IL-10.The activation of STAT3,senescence of HSCs and liver fibrosis were measured by histopathological staining and Western Blot analysis.

Result: In vitro, adenovirus infection-induced STAT3 overexpression induced senescence of HSCs by up-regulating the activity and expression of SA-β-Gal, and promoting the expression and nuclear translocation of P53, by inducing HSCs cell-cycle arrest at G1-S checkpoint and inhibiting the expression of CyclinD1 complex and pRb/Rb and proliferation of HSCs .STAT3 knockdown attenuates senescence of HSCs, as indicated by

inhibiting the expression of senescence proteins, reducing the nuclear translocation of P53, activating cell cycle and promoting cell proliferation. However, STAT3 knockdown-induced effect in HSCs was reversed by IL-10 treatment. In vivo, induced-senescence effect of IL-10 is associated with the activation of STAT3 and the increased expression of cell cycle and senescence protein in fibrotic HSCs. Moreover, cryptotanshinone treatment alone inhibited senescence of HSCs by suppressing the activation of STAT3; IL-10 pretreatment reversed the effects of cryptotanshinone.

Conclusion:IL-10 activates STAT3 to induce senescence of HSCs in fibrotic rats, and its mechanisms are associated with inhibiting the cell cycle and proliferation of HSCs.

Table and Figure:

Figure 1. IL-10 activates STAT3 to induce cellular senescence and cycle arrest in HSCs.

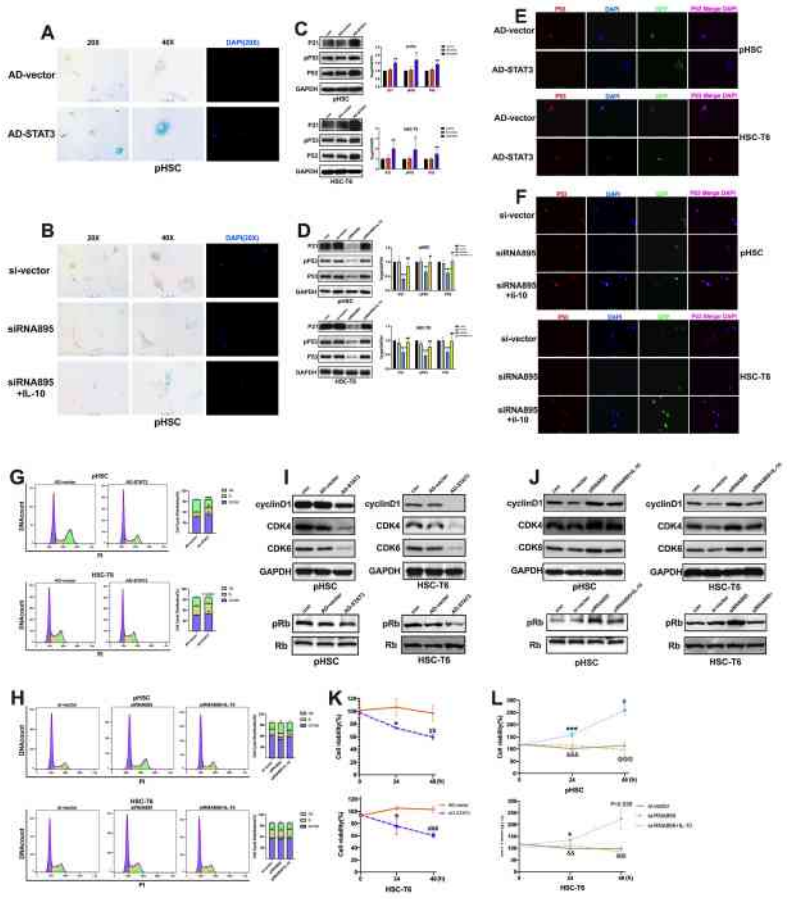

Figure1.IL-10 activates STAT3 to induce cellular senescence and cycle arrest in HSCs.
A-B： Senescence Associated β-Galactosidase activity Staining; C-D:Western Blot detected the expression of pP53,P53,P21; E-F: Immunofluorescence localization of p53; G-H: Cell cycle analysis by flow cytometry; I-J: Western Blot detected the expression of CyclinD1,CDK4,CDK6,pRb/Rb; K-L: CCK-8 detected cell proliferation. A,C,E,G,I,K: con,control; AD-vector/STAT3,infected with adenovirus AD-GFP or AD-STAT3 to over express STAT3. B,D,F,H,J,L: con,control; si-vector/siRNA895,infected with adenovirus si-vector or siRNA895 to knock down STAT3; siRNA895+IL-10, infected with adenovirus siRNA895 to knock down STAT3 and IL-10 treatment for 24h. Data are mean ± SEM, n = 3 experiments, each in triplicate. *p < 0.05, **p<0.01, ***p<0.001.

Figure 2.IL-10 induces senescence of HSCs in rats with liver fibrosis by activating STAT3.

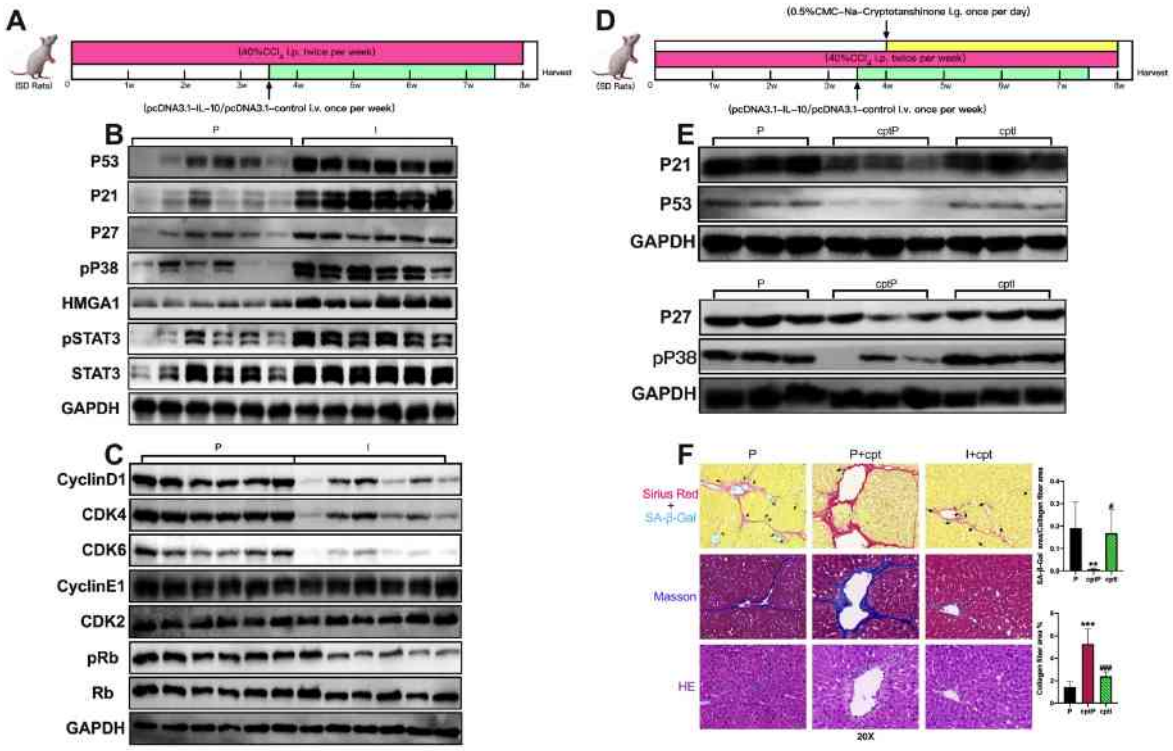

Figure2.IL-10 induces senescence of HSCs in rats with liver fibrosis by activating STAT3.
A: CCl4 i.p. into rats for 6 weeks to induce liver fibrosis(Group P), the expression of IL-10 in rat liver tissue was targeted by hydrodynamic method for 4 weeks(Group I); B,C: Western Blot detected the expression of protein; D: CCl4 i.p. into rats for 6 weeks to induce liver fibrosis(Group P). Inhibition of STAT3 phosphorylation in rats by cryptotanshinone I.g.(Group cptP), and the expression of IL-10 in rat liver tissue was targeted by hydrodynamic method for 4 weeks(Group cptI); E: Western Blot detected the expression of protein; F: Assessment of cell senescence and liver fibrosis by pathological staining.Data are mean ± SEM, n = 6, *p < 0.05, **p<0.01, ***p<0.001.

❖ AA-008

Change of liver volumes and histological features in different fibrotic stages

Tingting Zhu[1], Zhengxin Li[1,2], Kai Huang[1,3], Gaofeng Chen[1], Zhimin Zhao[1,3], Chenghai Liu[1,3]
[1] Institute of Liver Diseases, Shuguang Hospital, Shanghai University of Traditional Chinese Medicine, Shanghai, China, [2]Gongli Hospital of Shanghai Pudong New Area, Shanghai, China, [3]Shanghai Key Laboratory of Traditional Chinese Clinical Medicine, Shanghai, China

Background: Liver cirrhosis is the final pathological stage of different chronic liver diseases, which included the macroscopic manifestations such as liver volume reduction, imbalance between left and right lobes. Also it had pathological features as excessive collagen deposition, pseudolobular formation, and parenchymal extinction. This study try to observe the liver macroscopic volume and microscopic pathology in different fibrotic stages of chronic liver disease, in order to explore the relationship between liver macroscopic volumes and microscopic histology and potential mechanisms.

Method:A total of 53 patients with chronic liver disease of different etiologies were enrolled in this study. All patients underwent liver biopsy and abdominal magnetic resonance imaging. Based on the Ishak fibrosis classification, patients were divided into mild (F1-2) , moderate (F3-4) and severe fibrosis (F5-6) . Syngo.via VB10B software was used to measure the total liver volume , right hepatic lobe volume , left hepatic lobe volume , caudate lobe volume , spleen volume. The immunohistochemistry staining of CD31, Ki67, GS were used to reflect the changes of angiogenesis, hepatocyte regeneration and parenchymal extinction in the progressions of chronic liver disease, and TUNEL staining was used to observe the hepatocyte apoptosis. The correlation of macroscopic volume with microscopic pathology was assessed.

Result: The total liver volume and right hepatic lobe volume of 53 patients gradually decreased with the progressing of liver fibrosis ($p<0.05$), and the SV gradually increased ($p<0.05$). The expression of CD31 gradually increased with the progressing of liver fibrosis. CD31 positive rate show negatively correlated with right hepatic lobe volume ($r=-0.609$, $p=0.000$) and total liver volume ($r=-0.363$, $p=0.017$), but no significant correlation with SV($r=0.235$, $p=0.129$). The expression of Ki67 was significantly increased in the moderate fibrosis stage, and reduced in the advanced fibrosis stage. Ki67 positive rate was significantly positively correlated with the RV($r=0.423$, $p=0.018$). Apoptosis gradually increased with the progressing fibrosis, and the positive rates of apoptotic

cells was significantly negatively correlated with total liver volume (r=-0.860, p=0.000). Parenchymal extinctions mainly occurs in patients with advanced fibrosis stages which reflect by GS expressions, expression of GS was observed to be significantly upregulated in advanced fibrosis and positively correlated with RV(r=-0.440, p=0.002).

Conclusion: As the liver fibrosis progress, the entire and right hepatic lobe volume decrease, which may be associated with parenchymal extinction lesions, angiogenesis and the impairment of hepatocytes proliferation.

Table and Figure:

Figure 1. Table 1. Univariate analysis of magnetic resonance variables

Variables	mild fibrosis (n=20)	moderate fibrosis (n=21)	severe fibrosis (n=12)	*p* value
TLV（cm3）(mean ± SD)	1591.050 ±373.279	1469.420 ±355.774	1294.370 ±264.740*	0.022
RV（cm3）(mean ± SD)	1045.410±217.977	894.130±191.394△△	700.310±247.521**##	<0.01
LV（cm3）(median,IQR)	448.775(377.077,625.100)	479.850(355.850,742.19)	547.380(451.867,714.862)	0.554
CV（cm3）(median,IQR)	30.840(21.835,40.825)	27.490(18.420,40.390)	29.665(20.507,38.752)	0.976
SV（cm3）(median,IQR)	333.165(193.530,464.102)	392.940(261.865,514.285)	664.370(406.230,777.610)**##	<0.01
RV/TLV(mean ± SD)	0.670±0.104	0.630±0.131	0.540±0.125**##	<0.01
LV/TLV(mean ± SD)	0.310±0.099	0.370±0.109	0.440±0.119**##	<0.01
CV/RV(median,IQR)	0.025(0.021,0.039)	0.031(0.021,0.048)	0.045(0.026,0.058)	0.147
CV/LV(median,IQR)	0.066(0.047,0.081)	0.057(0.041,0.073)	0.055(0.043,0.065)	0.633
SV/TLV (median,IQR)	0.220(0.140,0.270)	0.260(0.195,0.370)	0.505(0.335,0.715)**##	<0.01
TLV/BMI (median,IQR)	65.384(56.607,86.448)	58.708(51.480,82.799)	55.973(45.063,64.934)*	0.047
SV/BMI(median,IQR)	13.435(9.387,20.910)	16.817(10.645,21.470)	26.805(16.505,39.687)**##	<0.01

Figure 2. Figure1. Pathological features of hepatic microvascular and hepatocyte in different fibrosis stages of chronic liver disease with various etiologies

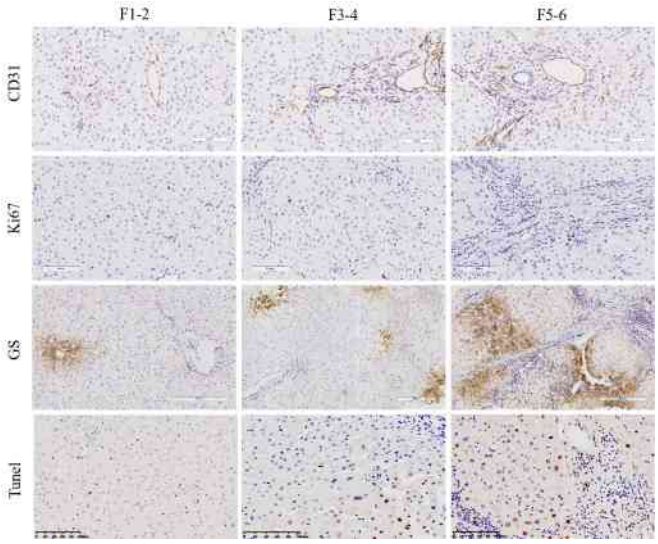

❖ AA-009

Transcriptome Analysis of Hepatic Stellate Cells and Liver Sinusoidal Endothelial Cells in Cirrhotic Patients

Xu Liu[1], Heming Ma[1], Yanhang Gao[1], Huan Wang[2], Guangyi Wang[3], Guoyue Lv[3], Junqi Niu[1,4]
[1]Department of Hepatology, The First Hospital of Jilin University, [2]Department of Infectious Diseases, Union Hospital, Tongji Medical College, Huazhong University of Science and Technology,
[3]Department of hepatopancreatobiliary surgery, The First Hospital of Jilin University, [4]Center of Infectious Diseases and Pathogen Biology, The First Hospital of Jilin University

Background: Liver cirrhosis is a significant global health burden. Intrahepatic non-parenchymal cells, including hepatic stellate cells (HSCs) and liver sinusoidal endothelial cells (LSECs), participate in fibrotic occurrence and reversion; however, the exact mechanisms remain unclear. We aimed to analyze the changes in the transcriptional patterns of patient-derived HSCs and LSECs, and to reveal their interactions in cirrhosis.

Method: Primary cells were isolated from human liver tissues by recirculating perfusion. Traditional RNA sequencing (RNA-seq) was performed to profile the mRNA expressions of HSCs by two comparative schemes [scheme A: Group_Cir (n=9)-Group_Noncir (n=6); scheme B: Group_Act (n=7)-Group_Fre (n=7)] and LSECs from 7 non-cirrhotic and 4 cirrhotic livers. Cells from 4 hepatitis B virus-related cirrhotic and 3 non-cirrhotic livers were obtained for single-cell RNA sequencing (scRNA-seq). The dysregulated mRNAs induced by cirrhosis were identified, and bioinformatics analyses were depicted. After searching for candidates, hub genes were verified by quantitative real time PCR. Finally, ligand-receptor interaction analyses in scRNA-seq were applied to predict the crosstalk between HSCs and LSECs.

Result: In the sequencing data of HSCs, we observed 3828 and 2262 differentially expressed genes (DEGs) in scheme A and B, respectively. The DEGs were significantly enriched in focal adhesion; retinol metabolism; and the formation, assembly, or degradation of collagen and the extracellular matrix. In the traditional RNA-seq of LSECs, 1987 DEGs were identified in cirrhotic group compared with non-cirrhotic group, and 103 common DEGs were reserved after combining the results with the scRNA-seq data. The DEGs participated in the biological function and impairment of LSECs. Thereafter, CAV1, ESR1, APP, SHC1, BCR, and LPL in HSCs, and FGF23, IL1RL1, CD9, GPR182, HSPA1B, and HSPA6 in LSECs were screened as hub genes. By scRNA-seq, we further demonstrated that the expression profiles of two cell lineages had similarities. They mediated the progression of cirrhosis through certain ligand-receptor pairs.

Conclusion: Our study offers multiple sequencing data from human liver tissues; reveals the changing characteristics of human HSCs and LSECs induced by cirrhosis; investigates potential targets associated with cirrhosis; and deciphers the close communication between two cells. It therefore provides information for the detection and treatment of liver cirrhosis.

Table and Figure:

Figure 1.figure

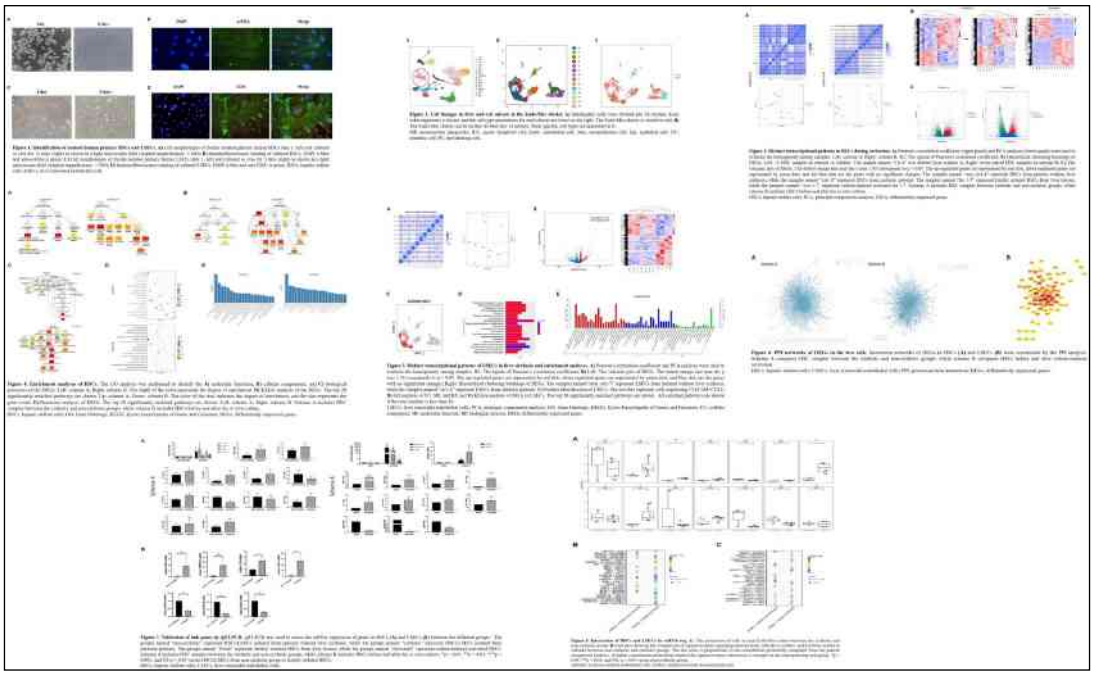

❖ AA-010

Diethyldithiocarbamate, a potential drug for non-alcoholic fatty liver disease

Tianhui Liu[1], Xiangyun Sun[1], Bilian Kang[1], Qinghong Yu[1]
[1]Liver Research Center, Beijing Friendship Hospital, Capital Medical University

Background: The prevalence of non-alcoholic fatty liver disease (NAFLD) is increasing annually worldwide. Up to now, no drugs are approved for NAFLD by regulatory agencies. We previously reported that Diethyldithiocarbamate (DDC) exhibits a protective function in methionine-choline deficient (MCD) diet-induced NAFLD in mice. In this study, we validated the therapeutic effect of DDC on western diet (WD) and choline-deficient, L-amino acid-defined (CDAA) diet-induced NAFLD in mice, and further explore the possible therapeutic mechanisms of DDC on NAFLD.

Method:C57BL/6 mice received WD diet for 20 weeks or CDAA diet for 9 weeks, 12 weeks and 15 weeks to establish the model of NAFLD with or without DDC treatment via daily gavage or drinking water, respectively. Sirius Red and haematoxylin and eosin (H&E) staining were performed to identify the severity of hepatic fibrosis, steatosis and inflammation. Microarray analyses were used to investigate the possible processes and pathways regulated by DDC.

Result: Compared with control group, the body wight increased in mice on WD diet, and significantly decreased after DDC treatment. Compared with control group, the serum levels of leptin increased in mice fed with both WD and CDAA diet, and were decreased by DDC treatment. Compared with NAFLD group, HE and Sirius Red staining revealed that the ballooning of hepatocytes, hepatic inflammation and perisinusoidal fibrosis were significantly decreased by DDC treatment regardless of feed, model severity and mode of DDC administration. Microarray data showed that DDC strongly regulated the genes related to the function of mitochondria. Compared with control group, the levels of oxidative phosphorylation (OXPHOS) complex proteins notably decreased in the liver of CDAA-diet induced mice, and increased upon DDC treatment.

Conclusion:DDC improves hepatic inflammation and fibrosis in mice models of NAFLD through inhibiting the secretion of leptin and improving the function of mitochondria. As a

drug for alcohol dependence with well-established pharmacokinetics, safety and tolerance at the US FDA-recommended dosage, DDC might be a potential drug for NAFLD.

❖ AA-011

Pharmacological Regulation of Tissue Fibrosis by Targeting the Mechanical Contraction of Myofibroblasts

Zhengquan He[1,2,3], Xuewei Yuan[1,2,3], Zongbao Lu[1,2,4], Yuhuan Li[1,5], Yufei Li[1,2,3], Xin Liu[1,2,4], Liu Wang[1,2,3], Ying Zhang[1,2,3], Qi Zhou[1,2,3], Wei Li[1,2,3]

[1]State Key Laboratory of Stem Cell and Reproductive Biology, Institute of Zoology, Chinese Academy of Sciences, Beijing 100101, China,

[2]Institute for Stem Cell and Regenerative Medicine, Chinese Academy of Sciences, Beijing 100101, China,

[3]Beijing Institute for Stem Cell and Regenerative Medicine, Chinese Academy of Sciences, Beijing 100101, China,

[4]University of Chinese Academy of Sciences, Beijing 100049, China, [5]The First Hospital of Jilin University, Xinmin Street No. 1, Changchun Jilin 130021, China

Background: Fibrosis can occur in almost all tissues and organs, and affects normal physiological function, which may have serious consequences, such as organ failure. However, there are currently no effective, broad-spectrum drugs suitable for clinical application. Revealing the process of fibrosis is an important prerequisite for the development of new therapeutic targets and drugs. Studies have shown that the limiting of myofibroblast activation or the promoting of their elimination can ameliorate fibrosis. However, it has not been reported whether a direct decrease in cell contraction can inhibit fibrosis in vivo.

Method: In this study, we evaluated the effects of the contractile inhibition of stress fibers using a non-muscle myosin II inhibitor, (-)-blebbistatin (Ble), on fibrosis in TGF-β1 induced myofibroblasts activation in vitro and in multiple chronic liver and lung injury models in vivo.

Result: We have shown that (-)-blebbistatin (Ble), a non-muscle myosin II inhibitor, displayed significant inhibition of liver fibrosis in different chronic injury mouse models in vivo. We found that Ble reduced the stiffness of fibrotic tissues from the early stage, which reduced the extent of myofibroblast activation induced by a stiffer ECM. Moreover, Ble also reduced the activation of myofibroblasts induced by TGF-β1, which is the most potent pro-fibrotic cytokine. Mechanistically, Ble reduced mechanical contraction, which inhibited the assembly of stress fibers, decreased the F/G-actin ratio, and led to the exnucleation of YAP1 and MRTF-A. Finally, we verified its broad-spectrum antifibrotic effect in multiple models of organ fibrosis. Our results highlighted the important role of mechanical contraction in myofibroblast activation and maintenance, rather than just a characteristic of

activation, suggesting that it may be a potential target to explore broad-spectrum drugs for the treatment of fibrotic diseases.

Conclusion: Our study highlights the important role of the mechanical contraction of myofibroblasts in their activation and maintenance, rather than acting only as an indicator of their activation. The pharmacological inhibition of mechanical contraction inhibited the activation of myofibroblasts by decreasing the nuclear accumulation of both YAP1 and MRTF-A and significantly relieving fibrosis in multiple organs in vivo. Therefore, the regulation of mechanical contraction regulation may be an important candidate for the development of broad-spectrum drugs for the treatment of fibrotic diseases.

Table and Figure:

Figure 1. Graphical Abstract

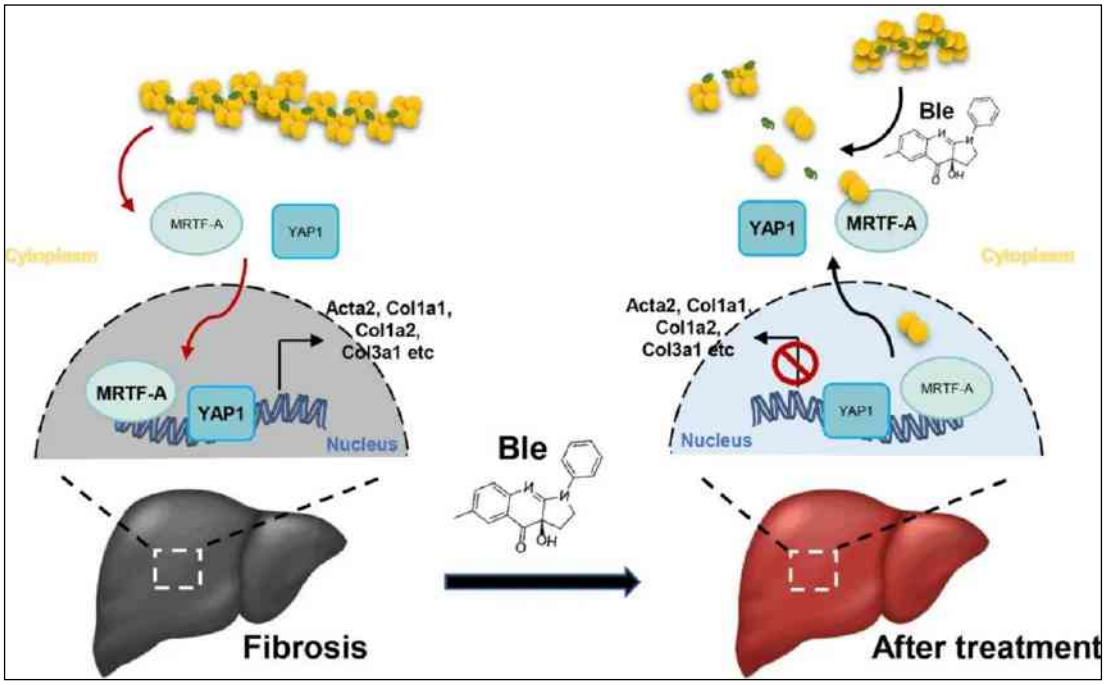

❖ AA-012

Interleukin 10 activates STAT3 to inhibit activation of HSCs and liver fibrogenesis

Yuehong Huang[1], Jiabing Chen[1], Yizhen Chen[1], Yixuan Huang[1]
[1]Fujian Medical University Union Hospital

Background: Hepatic fibrosis is a common pathological process in response to various chronic or iterative liver damage, characterized by a net accumulation of extracellular matrix(ECM) and activation of hepatic stellate cells (HSCs).Therefore, inhibition of ECM secretion is a crucial strategy for study of liver fibrosis. Our previous studies have shown that interleukin 10 (IL-10) activates the signal transducer and activator of transcription 3(STAT3) to induce HSCs senescence and cell cycle arrest to attenuate liver fibrosis. However, little is known about the role of STAT3 in IL-10 regulating HSCs activation and fibrogenesis. The aim of present study is to explore the relationship between activation of STAT3 and anti-fibrotic effect of IL-10.

Method: Firstly,STAT3 was transiently overexpressed or knock-down in immortality HSCs line(HSC-T6) and primary rat HSCs(pHSC) by using a recombinant adenovirus vector particle(Ad-STAT3) or a RNA interference for STAT3 (Si-STAT3) in the absence or presence of IL-10.The expression of α-smooth muscle actin(α-SMA),collagen type I(Col1A1), matrix metalloproteinases (MMP2, MMP9, MMP13) and tissue inhibitor of metalloproteinase1(TIMP1) were measured by Real-Time PCR and Western Blot to evaluate the role of STAT3 in the regulation of IL-10 on HSCs activation and fibrogenesis. Secondly, fibrotic rats were treated with or without IL-10 gene, the relationship among the expression of total and phosphorylated STAT3,α-SMA and ECM protein in fibrotic HSCs were detected by Western Blot to judge the role of activation of STAT3 in anti-fibrotic effect of IL-10.Lastly,Fibrotic rats were treated with STAT3 specific inhibitor cryptotanshinone alone or in combination with IL-10.The activation of STAT3 and HSCs and liver fibrosis were measured by histopathological staining and Western Blot analysis.

Result: In vitro, adenovirus infection-induced STAT3 overexpression repressed the activation of HSCs and fibrogenesis by decreasing α-SMA and Col1A1 mRNA and protein levels, and by promoting MMP2, MMP9 and MMP13 protein levels and by inhibiting TIMP1 expression.STAT3 knockdown up-regulated the expression of a-SMA, Col1A1 and TIMP1 and down-regulated the expression of MMP2, MMP9 and MMP13.STAT3 knockdown-induced effect in HSCs was reversed by IL-10 treatment. In vivo, anti-fibrotic effect of IL-10

is associated with the activation of STAT3 and the decreased expression of α-SMA and ECM protein in fibrotic HSCs. Likewise, cryptotanshinone treatment alone aggravated hepatic fibrosis by suppressing the activation of STAT3 while the effects were reversed by in combination with IL-10.

Conclusion:IL-10 activates STAT3 to inhibit HSCs activation and liver fibrogenesis, its mechanisms are associated with the decreased secretion and increased degradation of ECM.

Table and Figure:

Figure 1.IL-10 activates STAT3 to inhibit HSCs activation and promote ECM degradation.

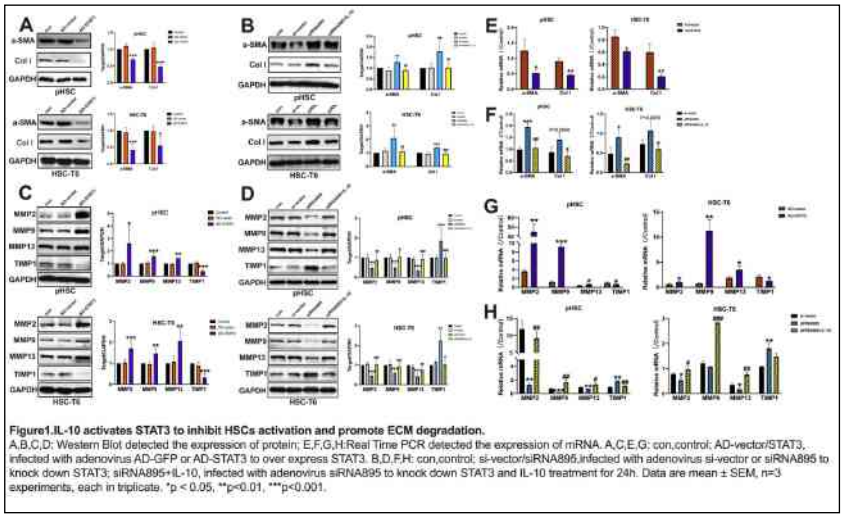

Figure1.IL-10 activates STAT3 to inhibit HSCs activation and promote ECM degradation.
A,B,C,D: Western Blot detected the expression of protein; E,F,G,H:Real Time PCR detected the expression of mRNA. A,C,E,G: con,control; AD-vector/STAT3, infected with adenovirus AD-GFP or AD-STAT3 to over express STAT3. B,D,F,H: con,control; si-vector/siRNA895,infected with adenovirus si-vector or siRNA895 to knock down STAT3; siRNA895+IL-10, infected with adenovirus siRNA895 to knock down STAT3 and IL-10 treatment for 24h. Data are mean ± SEM, n=3 experiments, each in triplicate. *p < 0.05, **p<0.01, ***p<0.001.

Figure 2. IL-10 alleviates rat liver fibrosis by activating STAT3

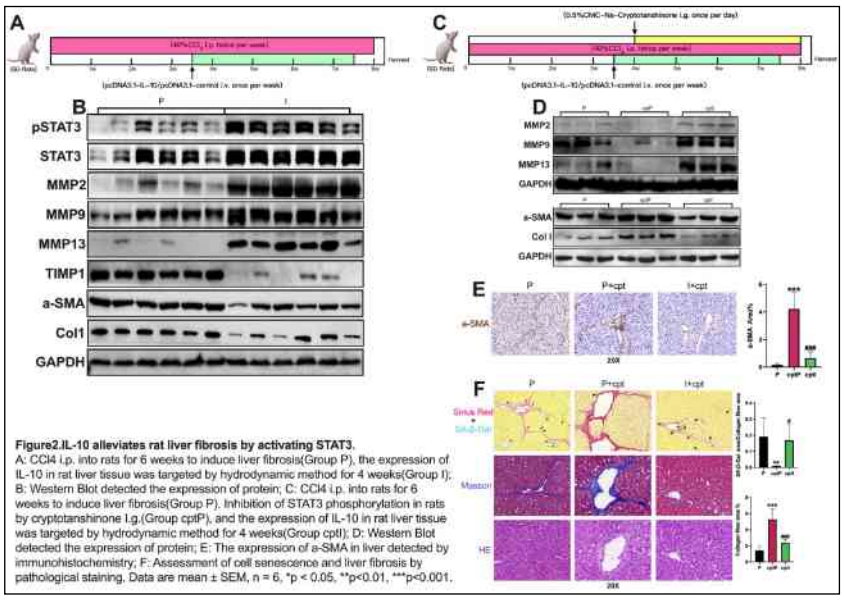

Figure2.IL-10 alleviates rat liver fibrosis by activating STAT3.
A: CCl4 i.p. into rats for 6 weeks to induce liver fibrosis(Group P), the expression of IL-10 in rat liver tissue was targeted by hydrodynamic method for 4 weeks(Group I); B: Western Blot detected the expression of protein; C: CCl4 i.p. into rats for 6 weeks to induce liver fibrosis(Group P). Inhibition of STAT3 phosphorylation in rats by cryptotanshinone I.g.(Group cptP), and the expression of IL-10 in rat liver tissue was targeted by hydrodynamic method for 4 weeks(Group cptI); D: Western Blot detected the expression of protein; E: The expression of α-SMA in liver detected by immunohistochemistry; F: Assessment of cell senescence and liver fibrosis by pathological staining. Data are mean ± SEM, n = 6, *p < 0.05, **p<0.01, ***p<0.001.

❖ AA-013

Salazosulfapyridine, a drug for ulcerative colitis, alleviates liver fibrosis by modulating gut microbiota

Hong Yan Xiang[1], De Juan Xiang[1], Shuang Xiao[1], Zong Yi Liu[1], Huan Yu Xiang[1], Jing Xiao[1], Wei Shen[1], Peng Hu[1], Hong Ren[1], Ming Li Peng[1]
[1]Key Laboratory of Molecular Biology for Infectious Diseases (Ministry of Education), Institute for Viral Hepatitis, Department of Infectious Diseases, The Second Affiliated Hospital, Chongqing Medical University, Chongqing 400010, China

Background: Cirrhosis and hepatocellular carcinoma caused by liver fibrosis are the major causes of mortality in patients with chronic liver disease. Currently, there are no effective anti-fibrotic drugs to meet clinical needs.This study aimed to discover new anti-fibrotic uses for old drugs by integrating data from Gene Expression Omnibus database (GEO) and Connectivity Map (Cmap) platform.

Method: Three datasets involving HBV, HCV, and NAFLD-induced liver fibrosis/cirrhosis were downloaded from GEO and differentially expressed genes (DEGs) were identified by R packages. Cmap LP100 platform was used to predict potential drugs against liver fibrosis. A carbon tetrachloride (CCl4)-induced rat liver fibrosis model was used to verify anti-hepatic fibrosis effects. 16S ribosomal DNA sequencing was applied for faecal microbiota composition. An ultra-performance liquid chromatography-tandem mass spectrometry (UPLC-MS/MS) analysis was used for serum and faecal bile acid profiles.

Result: Based on 46 common DEGs in 3 different etiological fibrosis/cirrhosis datasets, Cmap computationally predicted that drugs targeting cyclooxygenase (COX) were potential anti-fibrotic candidates, including celecoxib (CLE), aspirin (ASA), ibuprofen (IBP) and salazosulfapyridine (SASP) which are widely used in clinical practice. Among the above predicated drugs, we interestingly found SASP, a drug for the treatment of ulcerative colitis, exhibited the best safety profile and good anti-fibrotic efficacy in CCl4-induced rat liver fibrosis model, along with no mortality, lower transaminases levels, and lower hydroxyproline contents. Mechanistically, SASP significantly improved the intestinal environment by reversing the overgrowth of gut microbiota in genus Lachnospiraceae_UCG_010, Clostridium_sensu_stricto_1, Enterococcus, and Fusobacterium. However, faecal and serum bile acid profiles indicated that SASP treatment did not induce significant changes in bile acid profiles.

Conclusion: Salazosulfapyridine, an antibacterial and anti-inflammatory drug targeting the gut, exhibits good parenteral hepatoprotective and anti-fibrotic effects by modulating gut microbiota, which is different from traditional liver-targeted treatment strategies. It may serve as a new potential therapy for liver fibrosis.

Table and Figure:

Figure 1. Salazosulfapyridine improves liver fibrosis by modulating gut microbiota

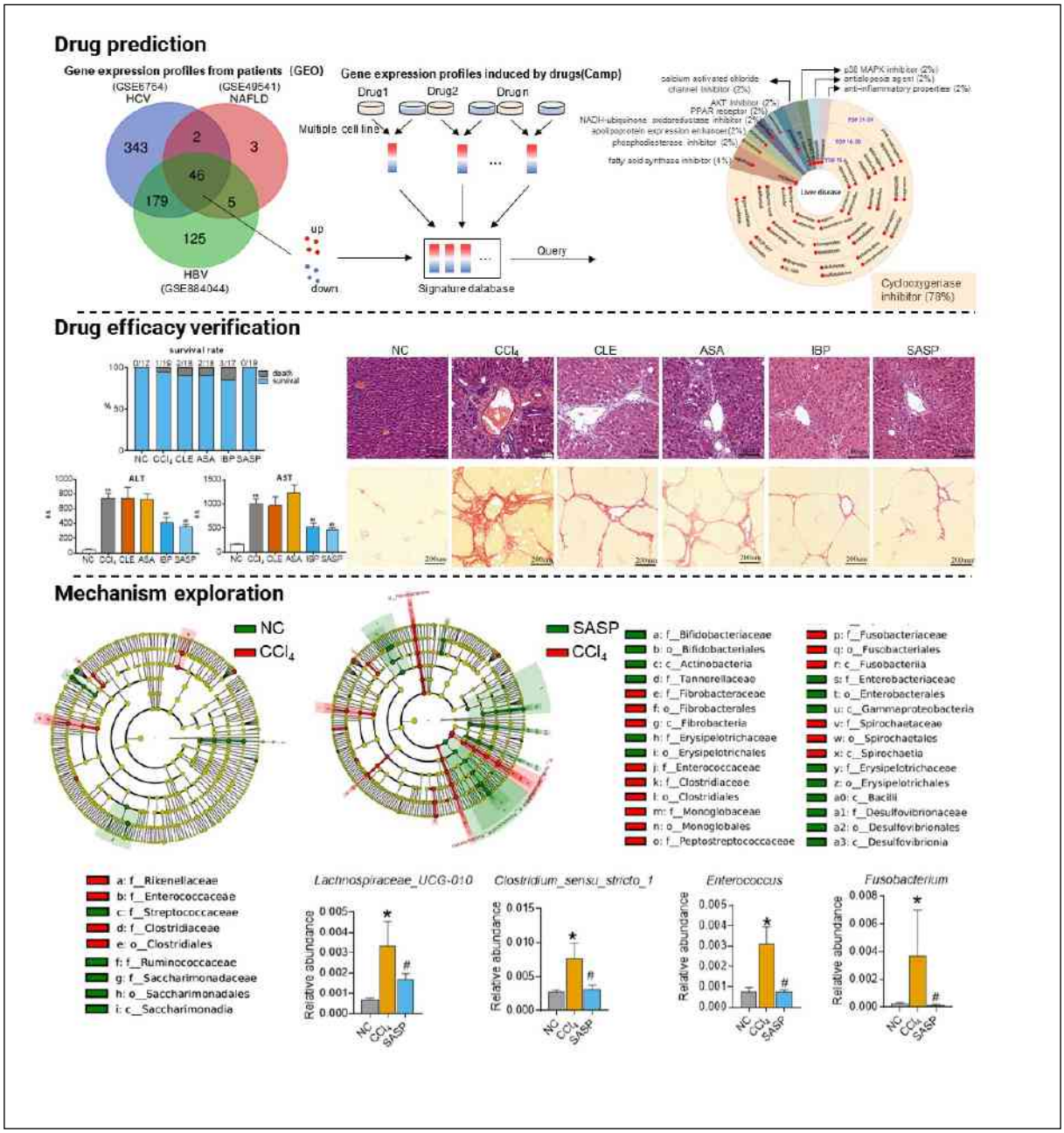

❖ AA-014

KLF14 Deficiency Promotes HSCs Activation and Liver Fibrosis by Downregulating PPARγ

Zhipeng Du[1], Mei Liu[1], Wei Yan[1], Limin Xia[1], Dean Tian[1]
[1]Department of Gastroenterology, Institute of Liver and Gastrointestinal Diseases, Tongji Hospital of Tongji Medical College, Huazhong University of Science and Technology

Background: Chronic liver diseases lead to liver fibrosis, through which activated hepatic stellate cells (HSCs) secrete extracellular matrix, and finally results in liver cirrhosis. Globally, liver cirrhosis causes 1.16 million deaths each year, and there is still no approved anti-fibrotic agent. Therefore, it is urgent to make further elucidation of liver fibrosis. The quiescent HSCs are featured by abundant cytoplasmic lipid droplets (LD). Once activated, the quiescent HSCs transdifferentiate to fibrogenic myofibroblasts, accompanied by rapid loss of LD. Recent studies reported that recovery of the LD content in activated HSCs could convert the activated HSCs to the quiescent phenotype and contribute to the regression of liver fibrosis. Recently, the transcription factor KLF14 has been emerged as a master regulator of lipid metabolism. However, the roles and mechanisms of KLF14 in the regulation of HSCs activation and LD remain unknown.

Method:KLF14 expression was detected in human fibrotic models and rat primary HSCs. The human HSCs (LX-2) were transfected with KLF14-expressing lentivirus (LV-KLF14), and the effects of KLF14 on LD accumulation and HSCs activation were assessed by RT-qPCR, Western blot and Oil red O staining assays. RT-qPCR and Western blot assays were applied to investigate the regulation of KLF14 on adipogenic transcription factors PPARγ, C/EBPs, LXRα, SREBP-1c. Luciferase reporter and chromatin immunoprecipitation assays were utilized to explore the transcriptional regulation of KLF14 on PPARγ expression. The PPARγ antagonist GW9662 and LV-shPPARγ were used to verify whether KLF14 exerts its roles through PPARγ. In vivo, KLF14-expressing adenovirus was injected via tail vein to thioacetamide (TAA)-treated rats, and GW9662 were administered intraperitoneally, to investigate the role of KLF14 in liver fibrosis.

Result:KLF14 expression was remarkably decreased in human fibrotic liver tissues and activated rat primary HSCs. Overexpression of KLF14 increased LD accumulation and inhibited HSCs activation. Mechanistically, KLF14 transactivated PPARγ promoter activity. Inhibition of PPARγ blocked the suppressive roles of KLF14 overexpression in HSCs. Adenovirus-

mediated KLF14 overexpression ameliorated TAA-induced rat liver fibrosis in PPARγ-dependent manner.

Conclusion:KLF14 exerts a critical anti-fibrotic role in liver fibrosis, and targeting the KLF14/PPARγ axis might be a novel therapeutic strategy for liver fibrosis

Table and Figure:

Figure 1.KLF14 is inversely correlated with liver fibrosis and HSCs activation, and it regulates lipid droplets content and HSCs activation through PPARγ.

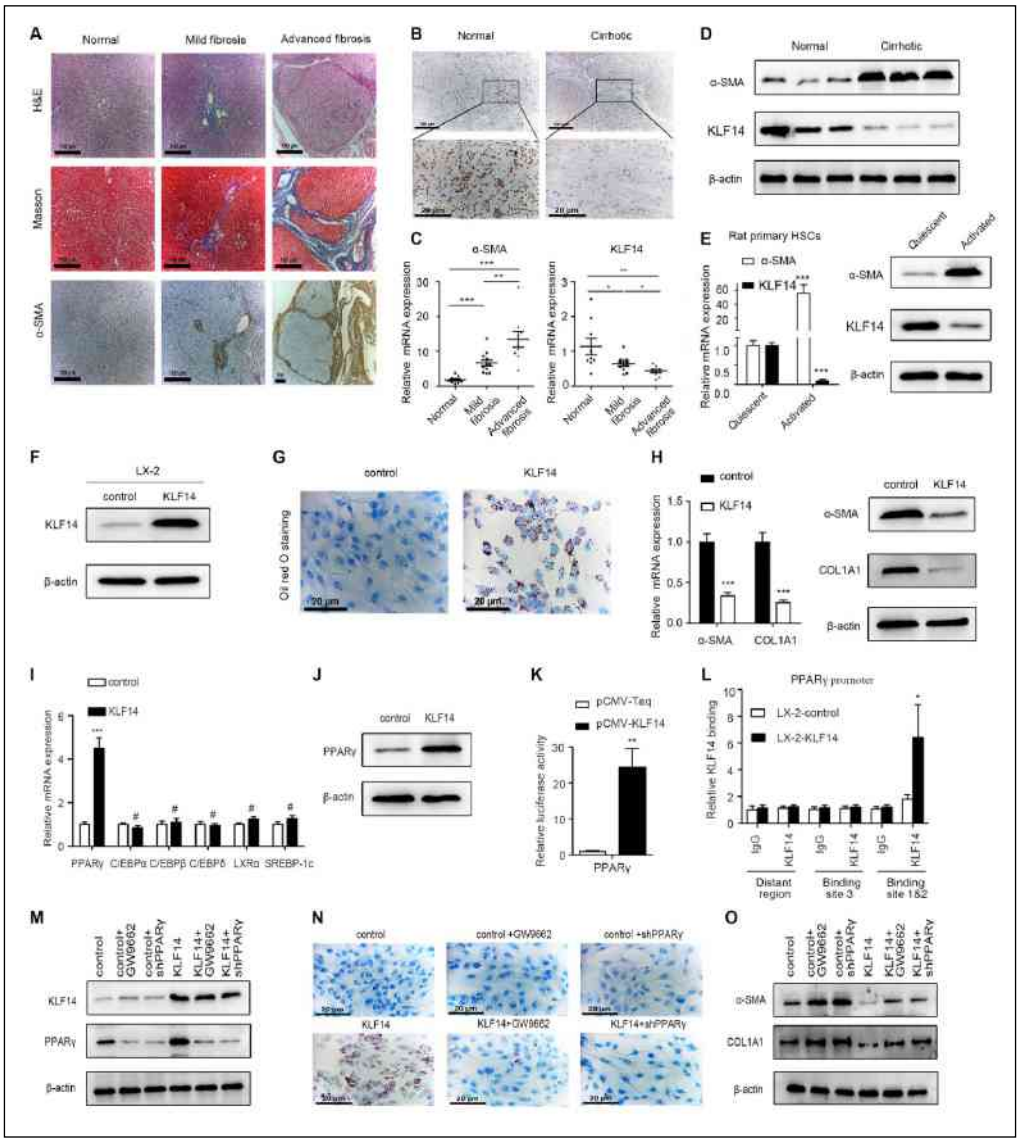

Figure 2. Adenovirus-mediated KLF14 overexpression mitigates TAA-established rat liver fibrosis through PPARγ.

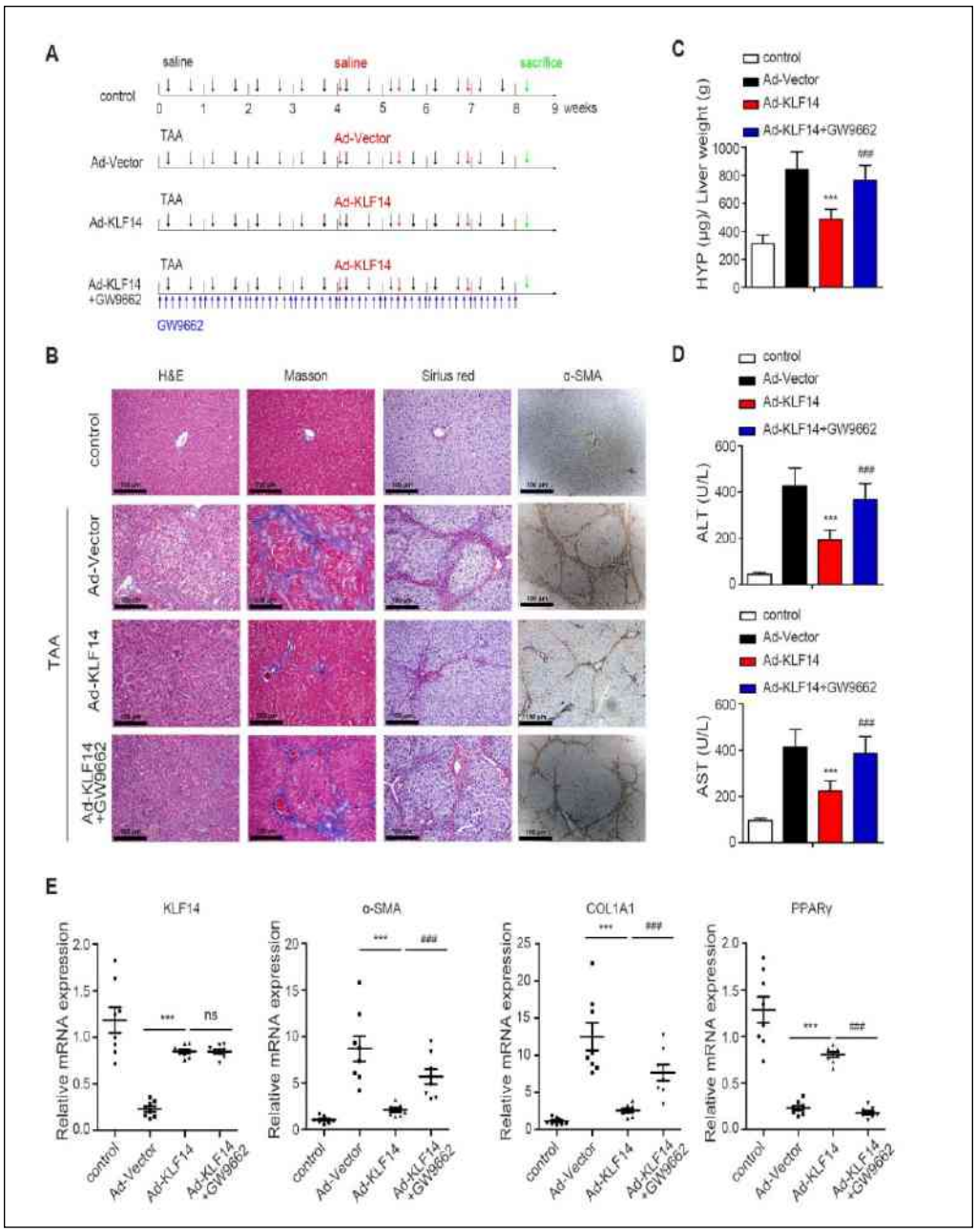

❖ AA-015

LSEC derived LOXL1 promotes hepatic sinusoid endothelial cell capillarization

Ning Zhang[1,2], Wei Chen[3,4], Aiting Yang[3,4], Xuzhen Yan[3,4], Wen Zhang[1,2], Hong YOU[1,2]
[1]Liver Research Center, Beijing Key Laboratory of Translational Medicine in Liver Cirrhosis, Beijing Friendship Hospital, Capital Medical University, Beijing, China , [2]National Clinical Research Center of Digestive Diseases, Beijing, China, [3]Beijing Clinical Research Institute, Beijing, China, [4]Experimental and Translational Research Center, Beijing Friendship Hospital, Capital Medical University, Beijing, China

Background: Our previous studies have found increased expression of lysyl oxidase-like 1 (LOXL1) stimulates hepatic stellate cell activation, promotes extracellular matrix (ECM) crosslinking, and accelerates liver fibrosis progression. Recent studies have confirmed that hepatic sinusoid endothelial cell (LSEC) capillarization is a characteristic lesion in liver fibrogenesis. Our preliminary experiments showed LOXL1 protein was highly expressed in LSECs from CCl4-treated mouse models. Considering the role of LOXL1 in ECM stability and the latter sequentially affects biological functions of LSEC, thus we tested the role of LOXL1 in LSEC capillarization in this study.

Method: In order to explore whether intracellular LOXL1 promotes LSEC capillarization, we transferred LOXL1 plasmid or empty vector into human LSEC (hLSEC) line, respectively. After 48 hours incubation, capillarization marker CD34 and vascular endothelial marker CD31 were detected. Alternatively, the role of extracellular LOXL1 secreted by hepatic stellate cells (LX-2) in LSEC capillarization was tested. Briefly, LOXL1 plasmid was overexpressed in LX-2 cells and culture medium was collected and used for LSEC culture. After 48 hours treatment, capillarization was assessed by detecting CD34 and laminin.

Result: In 12-week CCl4-treated mouse livers, LOXL1 was not limited at septal or portal areas but also located at LSECs, since it had the similar location pattern with CD31, the marker of LSEC. Increased intracellular LOXL1 expression significantly promoted LSEC capillarization as the marker CD34 mRNA and protein levels were elevated. However, extracellular LOXL1 secreted by LX-2 cells had no obvious effects on LSEC capillarization since CD34 and laminin protein showed no change after the treatment of culture medium from LX-2 cells in the setting of LOXL1 overexpression. Figure 1. Elevated expression of intracellular LOXL1 in LSEC can promote its capillarization. (A) Location and expression of CD31 and LOXL1 in CCl4-treated mice models (P0, Oil-treated mice; P12, CCl4 injection for 12 weeks). (B) Western blot analysis and (C) real-time PCR showed that CD34 expression was significantly increased after LOXL1 overexpression in LSECs. (D)

Secreted LOXL1 in the cultural medium. (E) CD34 and laminin (LN) protein expression in LSECs cultured in cultural medium of LX-2 cells in the context of LOXL1 overexpression.

Conclusion: Elevated expression of intracellular LOXL1 in LSEC can promote its capillarization, which deserves further study in the field of liver fibrosis.

Table and Figure:

Figure 1. Elevated expression of intracellular LOXL1 in LSEC can promote its capillarization.

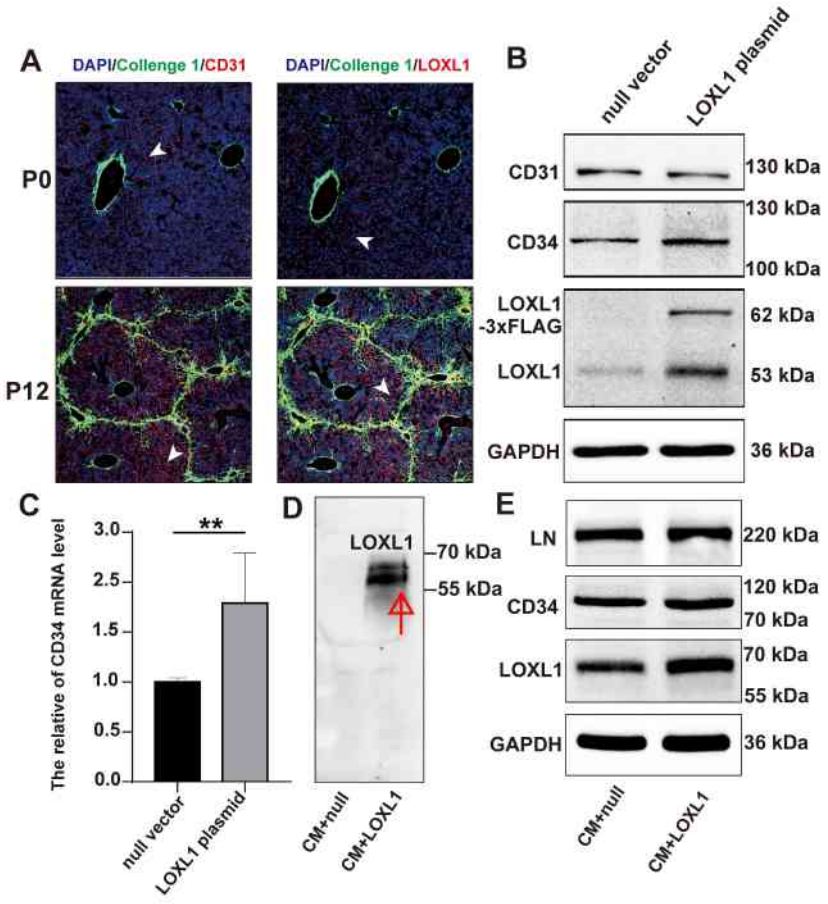

.

❖ AA-016

LAMC2 is induced by TGFβ1/Fosl2 pathway and regulates lipid metabolism in hepatocytes: novel insights into LAMC2 regulation and function

Aiting Yang[1,2], Xuzhen Yan[1,2], Hong You[1,2]
[1]Experimental and Translational Research Center, Beijing Friendship Hospital, Capital Medical University, 10050 Beijing, P.R. China., [2]Beijing Clinical Medicine Institute, 10050 Beijing, P.R. China.

Background: Laminin g2 (encoded by the LAMC2 gene) are multifunctional in health and disease, however its function in NASH is unknown.

Method: First, to mimic the in vivo microenvironment of NASH, especially fibrosis procedure, we examined Lamc2 expression and the lipid metabolism changes in hepatocyte in high TGFβ1 microenvironment. Second, to determine whether laminin-332 (Ln-332) stimulated lipids accumulation and lipogenic-enzyme induction, hepatocyte AML12 were seeded on plastic dish coated with Ln-332 or vehicle. Lastly, we evaluated the LAMC2 expression and explored the potential mechanisms of LAMC2 in the development of NAFLD/NASH.

Result: In vitro, we found that Lamc2 expression was required for TGFβ1 signaling and associates with altered lipid metabolism in AML12 hepatocyte treated with TGFβ1, importantly targeting Lamc2 reversed TGFb1 induced lipogenesis and fibrosis. Functionally, we observed that AML12 coated with Ln-332 have more lipid droplet accumulation compared with AML12 without Ln-332 coated. Along with their morphological presentation, AML12 coated with Ln-332 markedly increased the mRNA levels of key lipogenic genes such as fatty acid synthase (FAS), sterol regulatory element binding protein1c (SREBP-1c) and acetyl-CoA carboxylase 1 (ACC1) via cAMP/PI3K. In the mouse and human liver, LAMC2 were markedly up−regulated in steatotic livers. Mechanistically, we observed that Lamc2 was transcriptionally activated by TGFβ1/Fosl2 signaling, fosl2 inhibiton could alleviate diet induced NASH.

Conclusion: Therefore, we demonstrated that Laminin g2 play an important role in NASH, and Fosl2 was a key transcript factor of LAMC2 involved in modulation hepatic lipid metabolism and fibrosis.

❖ AA-017

CircRNA608-microRNA222-PINK1 axis regulates the mitophagy of hepatic stellate cells in NASH related fibrosis

Zixin Xu[1], Mingyi Xu[1], Huiyi Li[1]
[1]Department of Gastroenterology, Shanghai East Hospital, School of Medicine, Tongji University

Background: Increasing evidences have confirmed the relationship between mitophagy and nonalcoholic steatohepatitis (NASH). The exact mechanism of upstream circular RNAs (circRNAs) regulating PTEN-induced putative kinase 1 (PINK1) mediated mitophagy and its contribution to NASH-related liver fibrosis was explored in our study.

Method: Primary hepatic stellate cells (PHSCs) from C57BL/6 mice transfected into small interfering RNAs against PINK1 (si-PINK1) and negative control (si-NC) were prepared to perform circRNA sequence. Differentially expressed circRNAs, bioinformatic analysis and predicting software were performed to select axis of circ608/miR-222/PINK1. The expressions of circ608/miR-222/PINK1 were verified by RT-qPCR. The mitochondrial function was evaluated by immunofluorescence staining of COX4 and LC3B.

Result:PINK1-mediated mitophagy was inhibited in NASH-related liver fibrosis mice. CircRNA sequence revealed there were 37 DE-circRNAs between si-PINK1 PHSCs and si-NC PHSCs. Bioinformatic analysis showed these DE-circRNAs were related to enriched signaling pathways (such as Wnt, Rap1, mTOR, Hippo) regulating liver fibrosis and mitophagy. Circ608 was significantly down-regulated in lipotoxic HSCs and in livers of NASH-related liver fibrosis mice. MiR222 was identified to be the target miRNA of circ608 and was negatively regulated by circ608 in lipotoxic HSCs. MiR222 also had a binding site with PINK1 and could negatively regulate PINK1. So, the axis of circ608-miR222-PINK1 was proved. Circ608-miR222-PINK1 axis was identified participating in NASH-related liver fibrosis by regulating mitophagy. These results illustrated that circ608 might promote PINK1-mediated mitophagy though inhibiting miR222 in lipotoxic HSCs.

Conclusion: Circ608 could promote PINK1-mediated mitophagy of HSCs though inhibiting miR222 in NASH-related liver fibrosis.

Table and Figure:

Figure 1. Mitophagy was suppressed in NASH-related fibrosis mice model

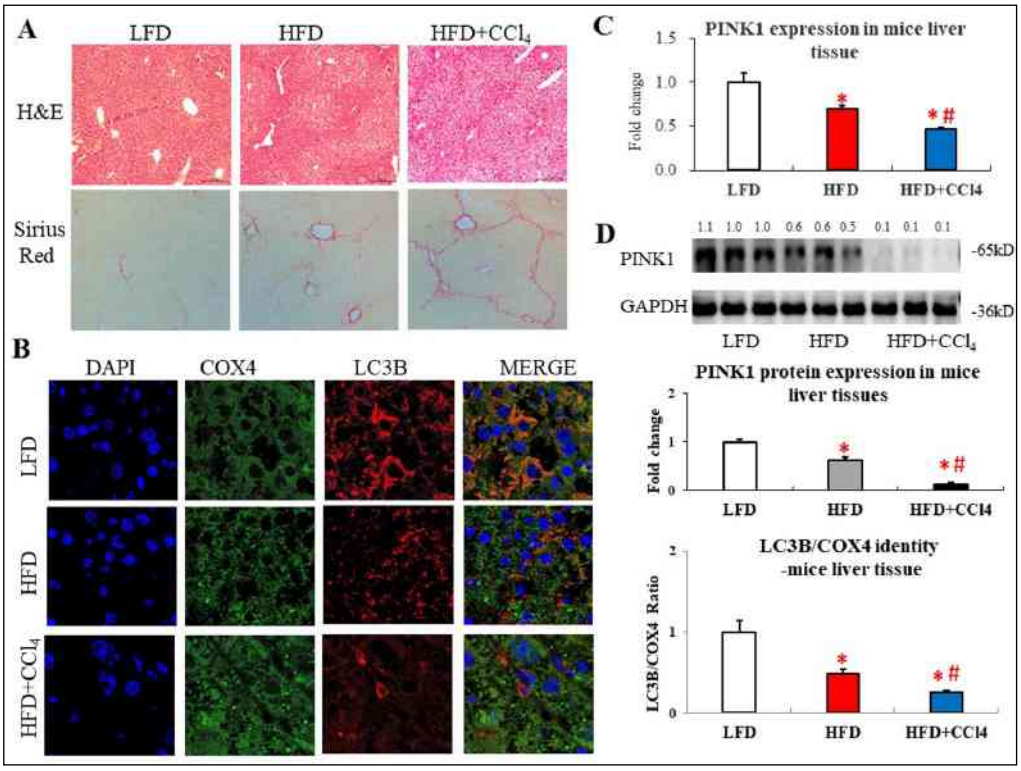

Figure 2. Circ608-miR222-PINK1 axis regulated PINK1 mediated mitophagy in lipotoxic LX2 cells

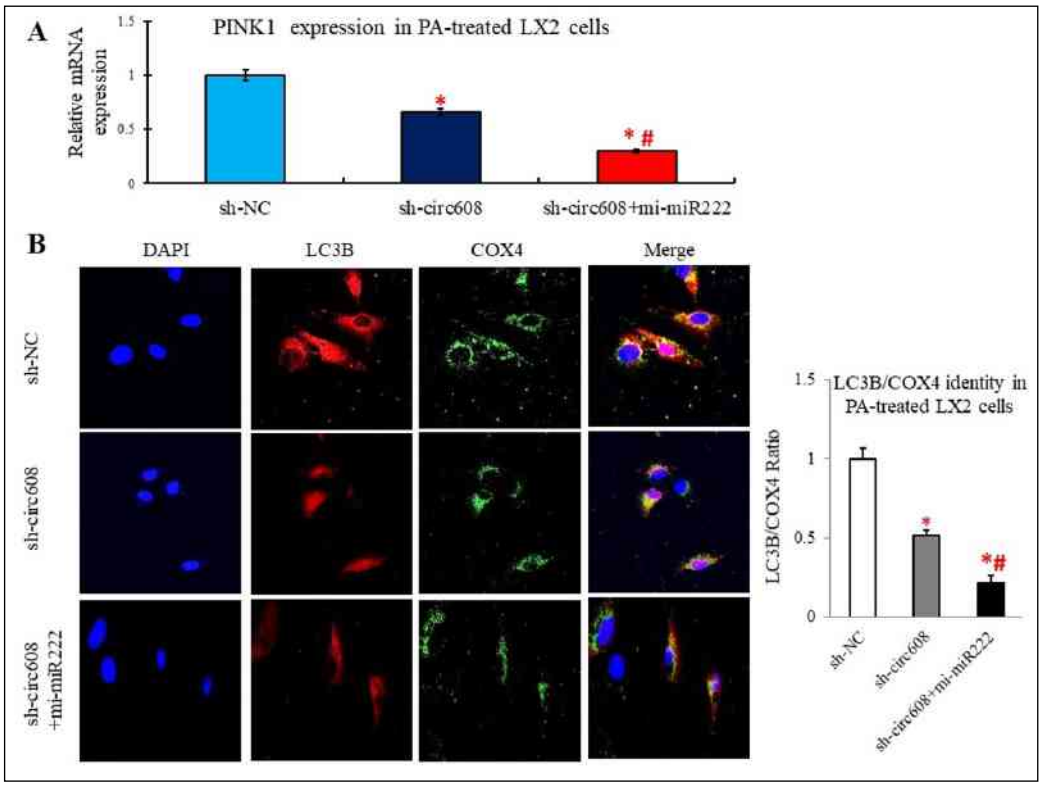

❖ AA-018

The effect and mechanism of KLF4 on hepatocyte apoptosis in chronic liver injury

Fan Xiu Ying[1], He Yi Huai[1], Luo Ya Wen[1]
[1]Affiliated Hospital of Zunyi Medical University

Background: In vivo and in vitro experiments were conducted to explore the expression characteristics of Krüppel-like factor 4 (KLF4) in chronic liver injury and its effect and mechanism on hepatocyte apoptosis.

Method:(1) The expression of KLF4 in the liver tissue of 35 patients with CHB was detected by immunohistochemistry, and the liver tissue of 10 patients with liver trauma was used as a control to analyze the expression characteristics of KLF4 in chronic liver injury.
(2) CCl4-induced mice were used for 4 and 8 weeks to establish a mouse model of chronic liver injury, and to explore the expression characteristics of KLF4 in the liver and its relationship with oxidative stress and apoptosis in chronic liver injury.
(3) The oxidative damage of LO2 cells was induced by H2O2, and the effect of oxidative stress on the expression of KLF4 in hepatocytes and apoptosis of hepatocytes were investigated.
(4) RelA expression was knocked down by RELA gene-specific short hairpin RNA (shRNA) to explore the mechanism of oxidative stress regulating KLF4 expression in hepatocytes.
(5) Pre-intervention of H2O2-induced LO2 cells by KLF4 gene-specific shRNA was used to explore the regulatory effect and mechanism of KLF4 on oxidative stress and apoptosis of hepatocytes.

Result:(1) Compared with the control group, the expression level of KLF4 in the liver tissue of CHB patients was significantly increased, and the positive staining of hepatic cell nucleus was the most significant ($P<0.01$).
(2) Compared with the control group, the CCl4-induced mice had obvious oxidative stress and hepatocyte apoptosis in the liver tissue, and the expression of KLF4 was increased at the same time ($P<0.01$). Similar to hepatitis patients, significantly increased in the nucleus of liver cells.
(3) In vitro experiments, compared with the control group, the expression of KLF4, UCP2 and apoptosis of LO2 cells induced by H2O2 increased ($P<0.05$).
(4) Compared with the model group, the expression of KLF4 and UCP2 decreased, and the oxidative stress and apoptosis increased after RelA knockdown ($P<0.05$).

(5) Compared with the model group, the expression of UCP2 decreased, and the oxidative stress and apoptosis increased after KLF4 knockdown ($P<0.05$).

Conclusion: In chronic liver injury, oxidative stress in hepatocytes up-regulates the expression of KLF4 in hepatocytes by activating NF-κB signaling; the up-regulated KLF4 negatively regulates oxidative stress by increasing the expression of UCP2, reducing hepatocyte apoptosis and liver injury.

❖ AA-019

Study of Transcription Factor 7-like 2 (TCF7L2) gene polymorphism in cirrhotic patients with diabetes

Mona Mahmoud Hassouna[1], Mohamed Sayed Mostafa[1], Mona Hamdy[2], Eman Abdelsameea[3], Mohamed Abbasy[4], Mary Naguib[5]

[1]Professor of clinical pathology, National Liver Institute , Menoufia University, [2] clinical pathology, National Liver Institute , Menoufia University, [3]Professor of Hepatology and gastroenterology,National Liver Institute , Menoufia University, [4]Assistant professor of hepatology and gastroenterology, National Liver Institute , Menoufia University, [5]Assistant professor of clinical pathology, National Liver Institute , Menoufia University

Background: Patients with chronic liver disease are at high risk of diabetes type 2 (T2D). Role of TCF7L2 gene in cirrhotic patients with diabetes is unclear. Aim: to study TCF7L2 gene polymorphisms (rs 290487) in cirrhotic patients with diabetes.

Method:25 cirrhotic patients with type 2 diabetes were compared to 25 cirrhotic HCV patients (non diabetic), 25 type 2 diabetic patients and 25 age and gender- matched healthy control group. After collection of relevant clinical and laboratory data, Single nucleotide polymorphism (SNP) in TCF7L2 gene (rs 290487) was performed by real time PCR technique.

Result: There was no significant difference among the four studied groups in terms of age and gender distribution. It was noticed that there were significant poorer liver function tests in cirrhotic patients with diabetes mellitus (DM) compared to cirrhotic non- diabetic patients and diabetic non- cirrhotic patients. In addition, cirrhotic patients with diabetes had significantly advanced stages of fibrosis as evidenced by elevated FIB- 4 score and APRI score compared to cirrhotic non- diabetic patients (p=0.001 and 0.013 respectively) and diabetic non cirrhosis group (p< 0.001).TCF7L2 rs290487 TT variant showed significantly increased diabetes risk in cirrhotic patients comparing with CC and CT genotypes. Cirrhotic diabetic patients had significantly higher incidence of TT with Odds ratio [OR] (95% CI) 14.667, p= 0.038 compared to control. The T allele showed OR (95%CI) 2.53, p= 0.025, this was associated with the dominant model (CC vs. CT+TT) p= 0.012 but not the recessive model (CC+CT vs. TT) p= 0.349. At the same time, calculation of odds ratio showed that TT genotype displayed significant statistical risk for DM more than CC "reference group" between cirrhotic diabetic patients and cirrhotic non-diabetic patients (p= 0.047) with OR (95% CI) 13.33 more risky than CC "reference group".

Conclusion:TCF7L2 rs290487polymorphism could be associated with increased risk of diabetes in cirrhotic patient. Further studies with larger sample size are needed to identify the possibility to use this polymorphism as potential genetic marker for T2DM in cirrhotic patients.

❖ AA-020

TM6SF2 variant as Risk Factors of Hepatocellular Carcinoma Development in Chronic Liver Disease

Gamal Raia[1], Eman Abdelsameea[2], Dalia Hamdy[3], Aml Abdelhamid Alsharnoby[2,4], Karema Diab[2,5]
[1]Professor of clinical pathology, National Liver Institute, Menoufia University,
[2]Professor of hepatology and gastroenterology National Liver Institute, Menoufia University,
[3]clinical pathology, National Liver Institute, Menoufia University,
[4]Assistant consultant of clinical pathology, National Liver Institute, Menoufia University,
[5]Lecturer of clinical pathology, National Liver Institute, Menoufia University

Background: Hepatocellular Carcinoma (HCC) is one of the most prevalent cancers worldwide. The transmembrane 6 superfamily member 2 (TM6SF2) gene is a non-synonymous single nucleotide polymorphism associated with nonalcoholic fatty liver disease. Single nucleotide polymorphisms (SNPs) of TM6SF2 gene play an important role in pathogenesis of HCC. We aimed to evaluate the role of rs58542926 polymorphism in development of HCC in chronic liver disease (CLD) patients.

Method:A total of 120 subjects, including 40 HCC patients, 40 patients with CLD and 40 healthy controls were selected. Real-time polymerase chain reaction (RT-PCR) was taken to determine TM6SF2 rs58542926 polymorphism.

Result: There was no significant difference among the three studied groups as regards age (p=0.06) and gender (p= 0.750) .Genotype distribution of CT, TT, CT+TT genotypes and T allele were significantly higher in HCC patients than CLD and control groups (p< 0.001, 0.005, and <0.001, respectively). CLD patients with CT genotype significantly increased risk of HCC development with 4.67 fold (OR= 4.67, 95% CI= 1.67–12.90), While patients who carrying TT genotype had significantly increased risk of HCC with 9.33 fold (OR =9.33, 95% CI =1.72- 50.61).Moreover, T allele was correlated with an increased risk of HCC (OR=5.44, 95% CI=2.09- 14.17) compared to C allele.

Conclusion:TM6SF2 rs58542926 genotype is associated with an increased risk of HCC in Egyptian population.

❖ AA-021

Hydrogen sulfide potential suppresses liver angiogenesis through inhibiting PI3K/Akt activation

Zhuqingzhu Gao[1], Hui Liu, Mingjie Tan, Huaxiang Yang, Keke Jin, Bihan Liu, Lei Li, Shanshan Wang, Huiguo Ding
[1]Department of Gastroenterology and Hepatology, Beijing You'an Hospital Affiliated to Capital Medical University

Background: Intrahepatic angiogenesis plays an important role in the development of cirrhotic portal hypertension and fibrosis. Hydrogen sulfide (H2S) plays a pivotal role in vascular pathophysiology. In this study, we investigated the effects of H2S on angiogenesis and molecular mechanism.

Method: Firstly, immunohistochemical staining was performed to examine cystathionine γ-lyase (CSE) and angiogenesis markers (CD34, VEGFR1) in 10 healthy and 10 cirrhotic liver tissues to observe the relationship between CSE and angiogenesis in liver cirrhosis. Secondly, the effect of NaHS, a donor of exogenous H2S, on tube formation ability, cell migration and proliferation of human umbilical vein endothelial cell (HUVEC). Besides, RT-qPCR was conducted to examine angiogenesis-related factor transcription level and transmission electron microscope was performed to observe the ultrastructural changes in HUVEC. Lastly, RNA sequencing and bioinformatics analysis were done in HUVEC exposed to exogenous H2S, then Western blotting and rescue assay confirmed the signaling pathway protein of PI3K/Akt.

Result: The decreased expression of CSE in the cirrhotic liver tissues was accompanied by increased angiogenesis (CD34 r=-0.49 $P<0.05$； VEGFR1 r=-0.80 $P<0.05$). In vitro, the tube formation ability, motility and viability of HUVEC were suppressed by NaHS ($P<0.05$). Decreased transcription levels of angiogenesis-related factors ($P<0.05$) and significant difference of cellular ultrastructure were observed. A total of 4656 mRNA transcripts were differentially expressed in the HUVEC stimulated by H2S, including 2332 upregulated and 2324 downregulated transcripts. Of them, 142 angiogenesis-related genes were collected. KEGG enrichment analysis showed significantly alteration of the PI3K/Akt signaling pathway in HUVEC exposed to NaHS. The p-PI3K and p-Akt were significantly inhibited by NaHS in HUVEC, which could be reversed by Y-P 740, a specific antagonist of PI3K ($P<0.05$). This antagonist also recovered NaHS-inhibited tube formation ability, motility and viability of HUVEC ($P<0.05$).

Conclusion: These results suggest that H2S potential inhibits angiogenesis through regulating PI3K/Akt signaling pathway, which serves as a potential therapeutic candidate to treatment cirrhotic portal hypertension.

Table and Figure:

Figure 1. CSE level decreased in cirrhotic patients, negatively correlated with angiogenesis markers

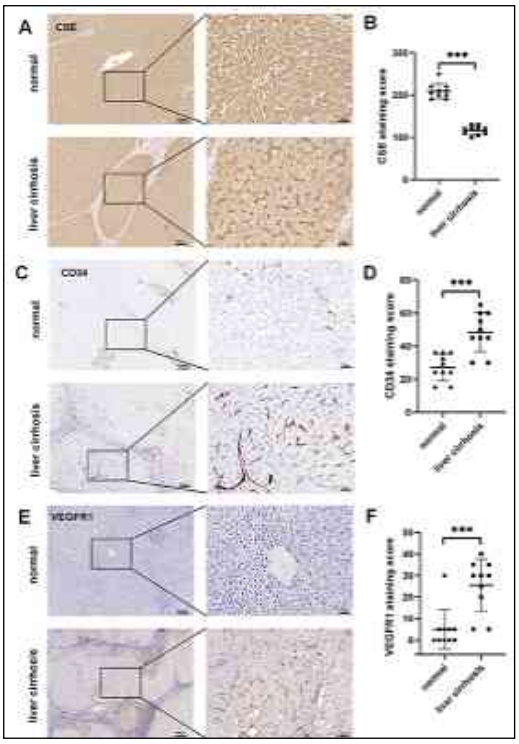

Figure 2. H2S directly suppressed angiogenesis via the PI3K/Akt signaling pathway

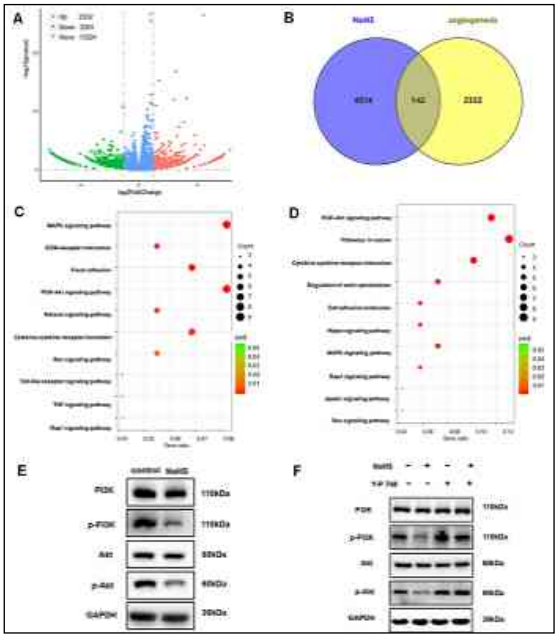

❖ AA-022

Association between diabetes and advanced fibrosis in chronic hepatitis B patients concurrent with nonalcoholic fatty liver disease

Jian Wang[1], Fajuan Rui[1], Rui Huang[1], Jiacheng Liu[1], Ruimin Lai[2], Yilin Liu[3], Chuanwu Zhu[4], Yuanwang Qiu[5], Zebao He[6], Shengxia Yin[1], Yuxin Chen[7], Xiaomin Yan[1], Weimao Ding[8], Qi Zheng[9], Chao Wu[1], Jie Li[1]

[1]Nanjing Drum Tower Hospital, The Affiliated Hospital of Nanjing University Medical School, [2]the First Affiliated Hospital, Fujian Medical University, [3]Nanjing Drum Tower Hospital Clinical College of Traditional Chinese and Western Medicine, Nanjing University of Chinese Medicine,, [4]The Affiliated Infectious Diseases Hospital of Soochow University, [5]The Fifth People's Hospital of Wuxi, [6]Taizhou Enze Medical Center (Group) Enze Hospital, [7]Institute of Viruses and Infectious Diseases, Nanjing University, [8]Huai'an No. 4 People's Hospital, Huai'an, [9]the First Affiliated Hospital, Fujian Medical University,

Background: Background Patients with chronic hepatitis B and concomitant nonalcoholic fatty liver disease were more likely to have advanced fibrosis. Clinical risk factors associated with the advanced fibrosis have not yet been well delineated. The aim of this study is to investigate the clinical characteristics and risk factors in advanced fibrosis patients with chronic hepatitis B patients concurrent with nonalcoholic fatty liver disease.

Method: Methods This study enrolled consecutive liver biopsy–proven chronic hepatitis B patients with nonalcoholic fatty liver disease from multiple medical centers of China between April 2004 and October 2020.

Result: Results There were 348 cases (69.0%) in non-advanced fibrosis (S0,S1,S2) and 156 cases (31.0%) in advanced fibrosis (S3,S4). 59.5% (25/42) of patients with diabetes had advanced fibrosis, and 28.4% (113/462) of non-diabetes patients had advanced fibrosis. Multivariate logistic analysis indicated that diabetes was an independent predictor of advanced fibrosis in all patients (odds ratio, 3.877; 95% CI: 1.428-10.528; p = 0.008) (Table 1), as well as in patients with normal alanine aminotransferase (odds ratio, 5.580; 95% CI: 1.085-28.706; p = 0.040), HBeAg positive (odds ratio, 4.979; 95% CI: 1.380-17.969; p = 0.014), alanine aminotransferase elevated (odds ratio, 3.613; 95% CI: 1.489-8.768; p = 0.005) and HBeAg negative (odds ratio, 3.548 CI: 1.132-11.117; p = 0.030).

Conclusion: Conclusions Diabetes is a critical factor associated with advanced fibrosis of with chronic hepatitis B patients concurrent with nonalcoholic fatty liver disease.

Table and Figure:

Figure 1.Table 1

Table 1 Predictors for fibrosis in all chronic hepatitis B patients concurrent with nonalcoholic fatty liver disease

	Univariate analysis		Multivariate analysis	
	OR (95% CI)	*P*	OR (95% CI)	*P*
Age (yr)	1.021 (1.002-1.040)	0.027		
Diabetes	3.716（1.943-7.107）	0.000	3.877 (1.428-10.528)	0.008
Inflammation grade (0-2)	Referent	0.000		0.000
Inflammation grade (3-4)	13.387（8.408-21.316）		12.813 (6.949-23.625)	
ALB (g/L)	0.901（0.860-0.944）	0.000		
male: ALT≤30; female: ALT≤19	Referent	0.000		
male: ALT>30; female: ALT>19	2.708（1.586-4.621）			
high density lipoprotein (mmol/L)	1.881（1.022-3.462）	0.042		
prothrombin time (S)	1.990（1.66-2.387）	0.000	1.428 (1.129-1.806)	0.003
HBeAg positive	1.751（1.185-2.588）	0.005		

❖ AA-023

mechanism of dact2 gene inhibiting the occurrence and development of liver fibrosis

Shenan Huang[1], *Zhili Wen*[1]
[1]*The Second Affiliated Hospital of Nanchang University*

Background: This paper mainly deals with the mechanism of dact2 gene inhibiting the development of liver fibrosis. Therefore, the method of control experiment is adopted. The results showed that dact2 gene can inhibit the activation of hepatic stellate cells by reducing the deposition of ECM. Meanwhile, TGF - β 1, Smad3, β - Catenin and CyclinD1 decreased by 50.02%, 46.73%, 47.58% and 37.50%, respectively. Gene transfer can be achieved by viral and non viral vectors. Its highly effective and stable expression characteristics make it widely used in clinical experimental research.

Method:in this experiment, we used lentivirus as a vector to construct lentivirus vector carrying dact2 gene, and packaged dact2 recombinant lentivirus and its control vector. HSC-T6 infected cells were observed. The effect of dact2 gene expression was activated by Wnt3a HSC-T6 cells. Immunoblot was used to detect α - SMA expression, TGF - β 1, Smad3, Smad7, β - Catenin and CyclinD1. The expression of MMP-2 and TIMP-1 was detected by real-time PCR. At the same time, dact2 recombinant lentivirus was injected into tail vein. Carbon tetrachloride was used to establish the liver fibrosis model. After 7 weeks of modeling, he staining was used to observe the pathological changes of liver tissue, hydroxyproline was used to analyze the changes of collagen content in liver tissue, the expression of protein was observed by immunohistochemistry, and the expression of fibrosis related genes was detected by real-time PCR.

Result:dact2 gene expression could inhibit the activation of HSC-T6 cells and reduce the expression of TGF - β 1. The percentage of Smad3, β - Catenin and cyclinD1 protein was 50.02%, 46.73%, 47.58% and 37.50% respectively ($P < 0.05$).

Conclusion: In theory, the structure and function of liver fibrosis can be restored by removing the pathogenic factors of liver fibrosis, alleviating the inflammatory reaction and carrying out effective anti fibrosis treatment. Pathogenesis of liver fibrosis: a variety of liver damage factors can cause liver damage and inflammation, and the body can repair the damaged liver to maintain a stable balance. Therefore, excessive ECM formation or reduction of ECM degradation for any reason may lead to ECM over deposition and

fibrosis. In the process of fibrosis, many cells in the liver interact with each other, forming a huge cross cell regulatory network, which affects the occurrence and development of the disease.

Table and Figure:

Figure 1. Determination of hydroxyproline in liver tissue

Figure 2. Real-time PCR detection of liver tissue

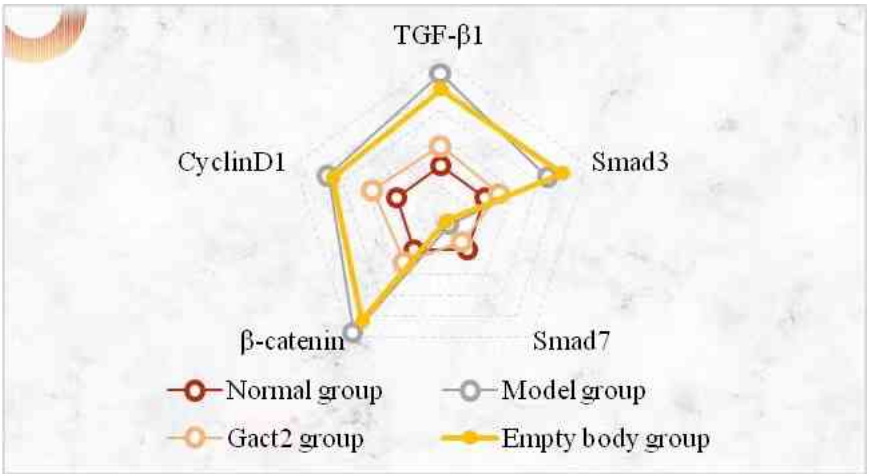

❖ AA-024

The improvement of Bortezomib on cirrhosis and its potential mechanism

Ling Wu[1], Xiaoquan Huang[1], Chunyan Xue[1], Chenyi Rao[1], Feng Li[1]
[1]Zhongshan Hospital, Fudan University

Background: China has the highest prevalence and death rate of cirrhosis in the world. The current treatment of liver cirrhosis mainly aims to prevent and treat complications, though the fact that some patients benefit from etiology treatment, effective treatment targeting cirrhotic liver itself still lacks. Activated hepatic stellate cell has been recognized as one of the crucial promoters in the progression of liver cirrhosis, being a prominent target in curing liver fibrosis and cirrhosis; On the other hand, bortezomib, a kind of proteasome inhibitor, has been found to be capable of improving fibrosis of skin, lung and kidney. We aimed to evaluate the efficacy of bortezomib in improving cirrhosis and its potential mechanism.

Method: Liver cirrhosis was induced by thioacetamide (TAA) in rats via intraperitoneal injection twice a week for 12 weeks. Cirrhotic rats were randomly divided into 2 groups: the treatment group (B) in which rats were injected with bortezomib at a dose of 0.1mg/kg through tail vein three times a week for 4 weeks, while the rats in the cirrhotic control group (CC) were injected with normal saline in the same way as the treating group. Rats with no intervention were set as the normal control group (NC). Liver and renal function indexes were detected to evaluate the toxicity of bortezomib; HE and Masson staining of liver tissues were compared to evaluate inflammation and fibrosis, hydroxyproline content was determined for a further evaluation of liver fibrosis. Expression of proteins which are related to fibrosis were detected through RT-qPCR and Western blot. Further, human hepatic stellate cell line LX-2 and liver cell line L02 were cultured under different concentrations of bortezomib for 24 hours, cell apoptosis were detected through flow cytometry.

Result: Alanine aminotransferase (ALT) and aspartate aminotransferase (AST) decreased in the treatment group, while renal function indexes as well as bilirubin presented no statistic difference between two groups, indicating a beneficial effect of bortezomib on liver function with no toxicity. Detections related to liver fibrosis including Masson staining, hydroxyproline content showed an improvement of cirrhosis in the treatment group,

consistent with fibrosis related protein mRNA and expression detected by RT-qPCR and Western blot, demonstrating the potential capacity of bortezomib in treating cirrhosis. In vitro experiments, hepatic stellate cells showed obvious apoptosis, while hepatocytes did not.

Conclusion: Bortezomib has the potential to improve liver cirrhosis with negligible toxicity. Inducing activated hepatic stellate cell apoptosis might be a potential mechanism underlying bortezomib improving cirrhosis.

Table and Figure:

Figure 1. Comparison of liver and renal function indexes and fibrotic detections in rats from different groups.

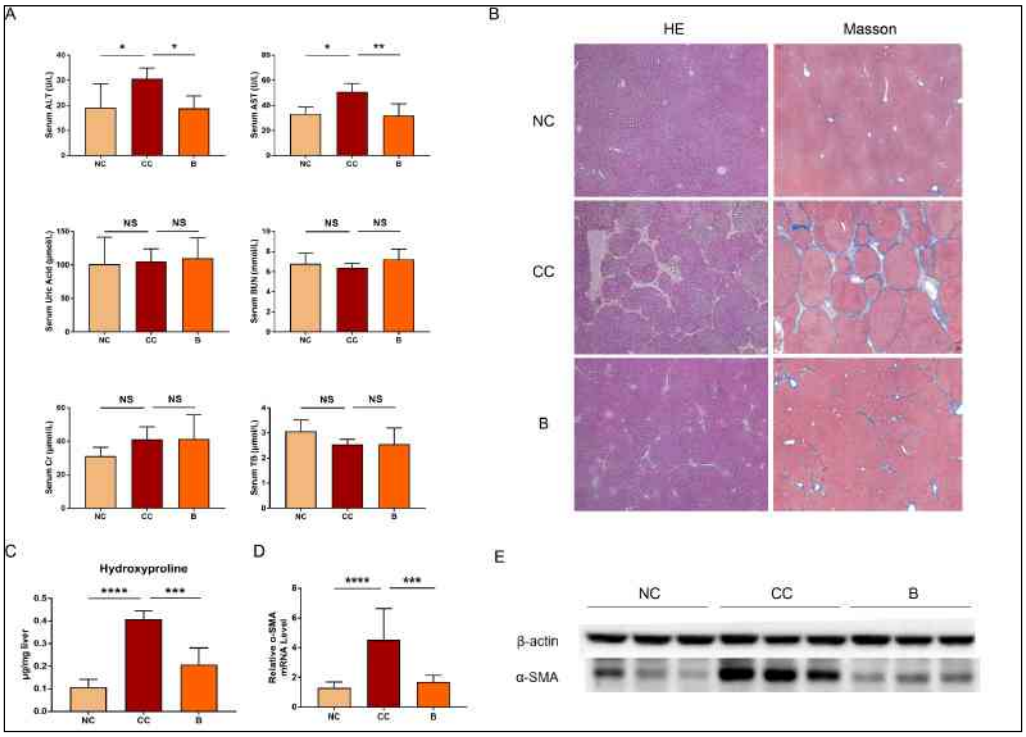

Figure 2. Apoptosis of activated hepatic stellate cells and hepatocytes after being stimulated by bortezomib in different concentrations.

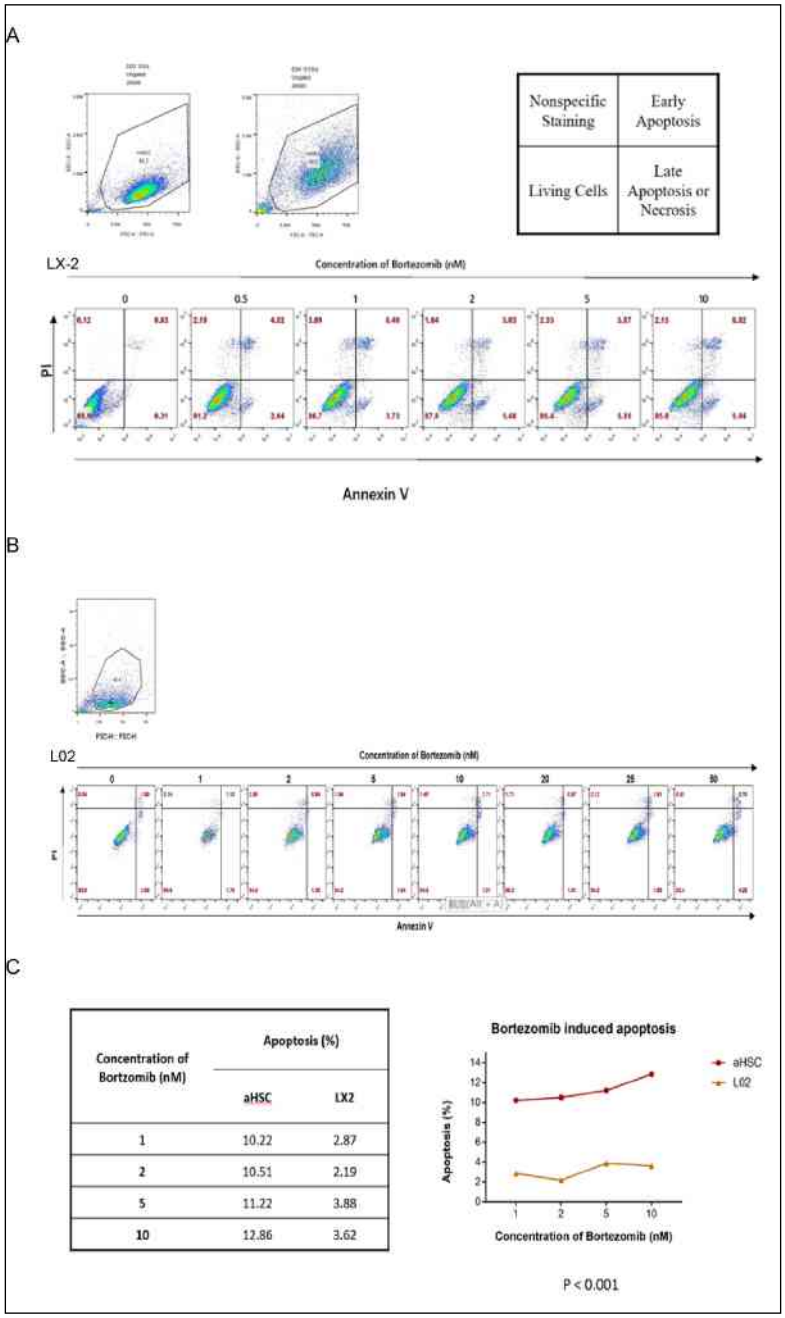

❖ AA-025

Ferroptosis pathway is involved in alcohol-induced hepatocyte death in vitro

Chen Feng[1], *Li Qianhui*[1], *Wang Fei*[1]
[1]*The Seventh Affiliated Hospital, Sun Yat-sen University*

Background: Translational medicine research targeting ferroptosis has become a promising new direction in disease prevention and treatment. Early studies have demonstrated that ferroptosis plays a critical role in the development process of various liver disease, such as non-alcoholic fatty liver disease, non-alcoholic steatohepatitis, autoimmune hepatitis, alcoholic liver disease and liver fibrosis. Based on the complexity of pathogenesis in the alcoholic liver disease and lack of effective clinical treatment, we adopt oxidative stress cell model in vitro to confirm the role and mechanism of ferroptosis in alcoholic-induced hepatocyte death.

Method: Ethanol and ferrostatin-1 was used to induce oxidative stress environment and to inhibit ferroptosis pathway in LX2 cells, respectively. The changes of cell activity, reactive oxygen species, levels of iron ions, oxidative stress-related indexes were detected by corresponding kits. The expression of ferroptosis-related genes in LX2 cells were detected by QRT-PCR and immunofluorescence assay.

Result: The IC50 value of LX2 cell damage caused by ethanol was 452.3mM, addition of 1μM ferrostatin-1 could significantly improve LX2 cell injury that induced by ethanol, as a concrete manifestation of increased cell activity, glutathione content and superoxide dismutase enzyme activity, along with decreased intracellular reactive oxygen species level and iron concentration. QRT-PCR results show that some genes related to ferroptosis pathway were changed in oxidative stress environment, the anomaly present as the expression level of SLC7A11, GPX4 decreased and ACSL4 increased, but the changes of these genes were significantly improved by adding ferroptosis inhibitors ferrostatin-1, the above results were also confirmed by cell immunofluorescence assay.

Conclusion: Our results suggest that ferrostatin-1 added to LX2 cell can enhance the antioxidant stress capacity in an environment induced by overdosed alcohol in vitro, ferroptosis pathway is involved in alcohol-induced hepatocyte death. These discoveries suggest that ferroptosis is a potential therapeutic target for alcoholic liver disease.

Table and Figure:

Figure 1. Research of ferroptosis in alcohol-induced hepatocyte death

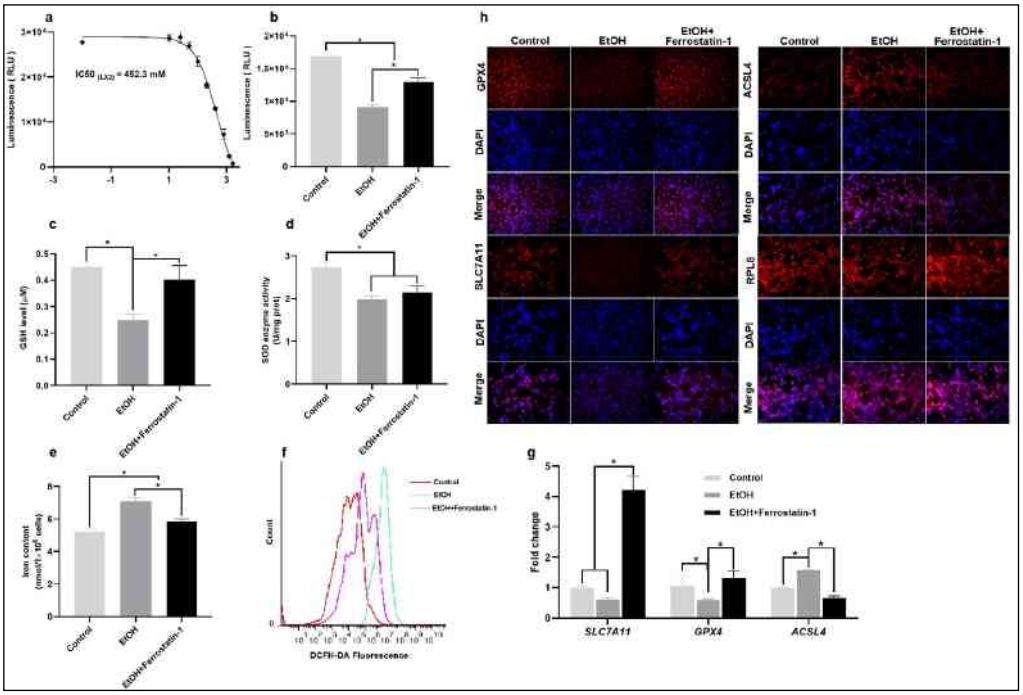

❖ AA-026

The mechanism of CLOCK molecular clock in the progression of liver fibrosis

Huijie Zhong [1], Jiawei Geng[1], Wenxue Wang[1]
[1]Department of Infectious Disease and Hepatic Disease, First People's Hospital of Yunnan Province, Affiliated Hospital of Kunming University of Science and Technology, Kunming, 650032, Yunnan, China.

Background: Hepatic fibrosis is an injury-repair response of the liver to react to a series of Chronic injury and inflammation, mainly characterized by excessive deposition of extracellular matrix. Hepatic fibrosis is a common pathological change in all chronic liver diseases. It is the key link of further deterioration to the development of cirrhosis, and also as the early reversible stage of cirrhosis. Liver metabolism has significant circadian rhythm, and molecular clock disorder would disrupt the cell cycle, inducing inflammation and many kinds of ways to participate in the occurrence and development of chronic liver disease. The continuous activation and proliferation of hepatic stellate cells play an important role in the formation of hepatic fibrosis. This study aims to explore the effect of regulating molecular clock gene CLOCK low expression on the activation and extracellular matrix secretion of hepatic stellate cells in vitro. Whether sustained activation and proliferation of activated hepatic stellate cells can be alleviated by targeting negative feedback protein of CLOCK molecule clock with small molecule drugs.

Method:(1) Cells are infected with lentivirus to construct hepatic stellate cell (LX2) . (2) TGF-β1 activates CLOCK low expression LX2 cell lines, after that measures cell proliferation and α-SMA protein expression. Which for testing the effect of molecule clock disturbance on LX2 cells activity. (3) Small molecule drugs KL001 / LH846 treated LX2 cells with low expression of Clock activated by TGF-β1, and the cell proliferation was measured by MTS method and the expression of α-SMA protein was detected by Western blot.

Result:(1) qRT-PCR and Western blot were used to verify that Clock stable cell lines with low expression of LX2 were successfully constructed. (2) Compared with blank and negative control group, LX2 cells with low Clock expression sustained activate and proliferate faster. (3) Small molecule drugs that are KL001 and LH846, targeting molecular clock negative feedback protein treated LX2 cells with low CLOCK expression activated by TGF-β1, it was found that the small molecule drug can inhibit the proliferation of LX2 cells, and inhibit the expression of extracellular matrix α-SMA.

Conclusion: Targeting drugs (KL001 and LH846) of molecular clock regulates molecular clock negative feedback proteins to slow the continuous activation and proliferation of LX2 cells induced by molecular clock disturbances.

Table and Figure:

Figure 1.

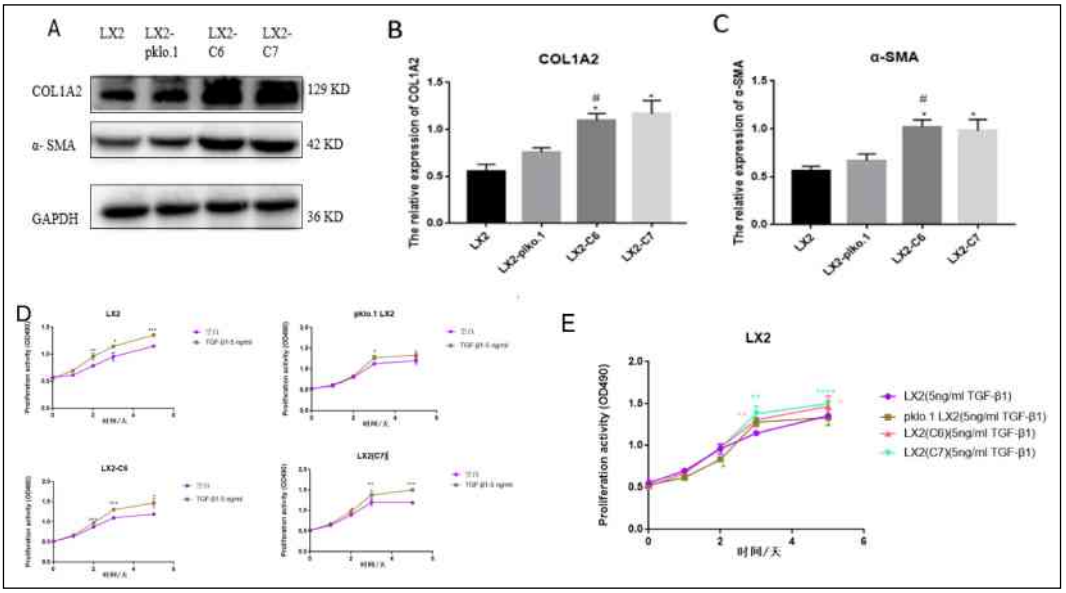

Figure 2.

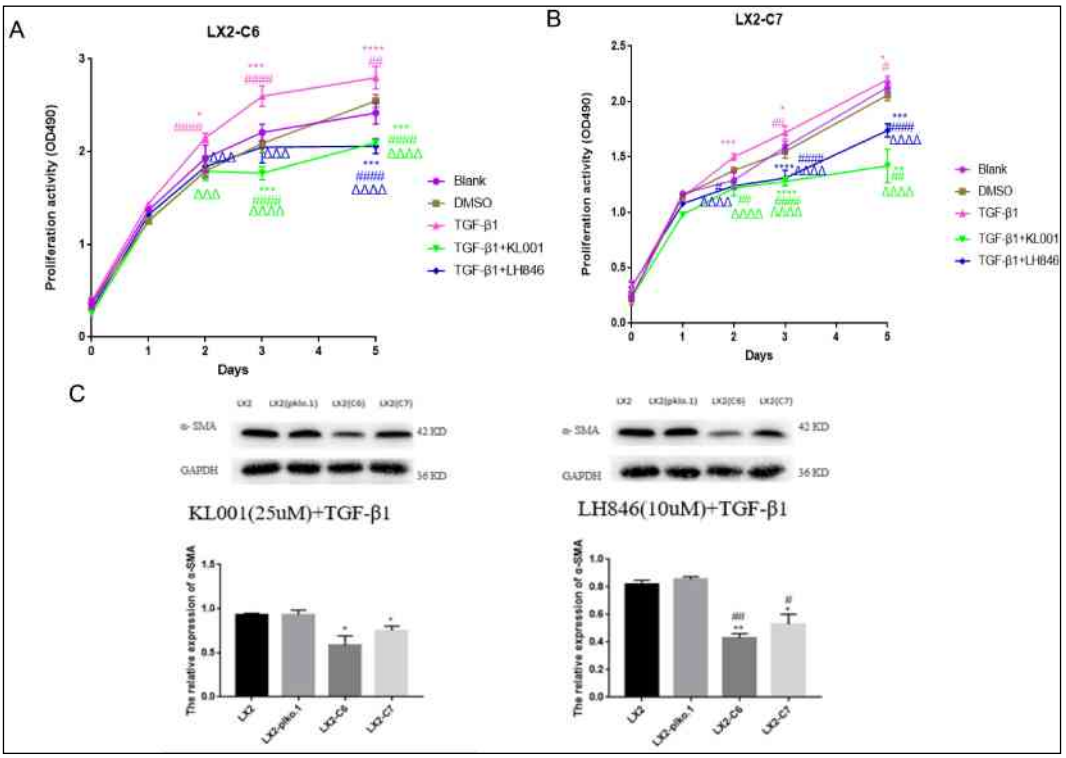

❖ AA-027

Mechanism of NK cell immune clearance senescent hepatic stellate cells induced by IL-10

Yizhen Chen[1], Yuehong Huang[1], Jiabing Chen[1], Yixuan Huang[1]
[1]Department of Gastroenterology and Fujian Institute of Digestive Disease, Fujian Medical University Union Hospital

Background: Natural killer cells (NK cells), one of the most important liver innate immune cells, secrete cytokines, and directly kill HSCs to antagonize the progression of liver fibrosis. Previous studies have shown that interleukin-10 (IL-10) induces senescence of activated hepatic stellate cells (HSCs) and inhibits the formation of hepatic fibrosis. However, it has not been reported whether IL-10-induced senescent HSCs can be selectively eliminated by NK cells. This study is to explored the specific mechanism of NK cells clearing IL-10-induced senescent HSCs, to elucidate the function of IL-10 reversing fibrosis.

Method:①Human HSCs line (LX2 cells) were treated with il-10 or Etoposide for 24h， and the LX2 senescence was assessed by β-galactosidase staining, flow cytometry and Western blot. ②Human NK cells line (NK92 cells) was co-cultured with LX2 cells. Cytotoxicity assay (LDH), crystal violet staining, flow cytometry and Western blot were performed to evaluate the cytotoxicity of NK92 cells to senescent LX2 and observe their expression of NK activated receptor (NKG2D) and its ligand (NKG2DL,including MICA/MICB, ULBP2 and PVR). ③LX2 cells and NK92 cells were treated with IL-10 respectively. The direct effect of IL-10 intervention on the two cells was observed by flow cytometry, Western blot and cellular immunofluorescence. ④Pretreated with exocytosis inhibitor (Concanamycin A) or granzyme B inhibitor (3,4-DCI) for 12h, NK92 cells were co-cultured with LX2 for 24h. LDH assay, Flow cytometry, and Western blot were used to assess the impact of inhibition of exocytosis and granzyme B of NK92 cells.

Result: Firstly, compared with the control, the LX2 cells in the IL-10 treatment group showed obvious senescence characteristics: the number of SA-β-Gal positive staining cells in the cytoplasm counted more, the quantitative detection activity of SA-β-Gal also increased significantly; besides, its cell cycle was blocked in G1 phase; additionally, the expression of proteins P21 and P53 increased. Subsequently, the co-culture of IL-10-treatmented LX2 cells with NK92 shown that LX2 could be significantly killed and

eliminated by NK92, the LDH value in the culture medium raised, and the number of surviving LX2 cells descend; further studies found that NK92 surface activated receptors such as NKG2D were significantly up-regulated, and the expression of cytotoxic substances was increased. At the same time, the expression of NKG2D ligands of LX2 also showed a trend of up-regulation. Afterward, the direct intervention of IL-10 had no obvious effect on NK92, but the expression of NKG2D-L of LX2 in IL-10 was significantly enhanced. Finally, the cytotoxicity of NK92 cells could be significantly inhibited, and the cytotoxicity to senescent LX2 was weakened more significantly than that of activated LX2.

Conclusion:NK cells kill and eliminate senescent HSCs induced by IL-10 through activating the NKG2D/NKG2DL pathway and exocytosis.

Table and Figure:

Figure 1.IL-10 induces senescence in HSCs

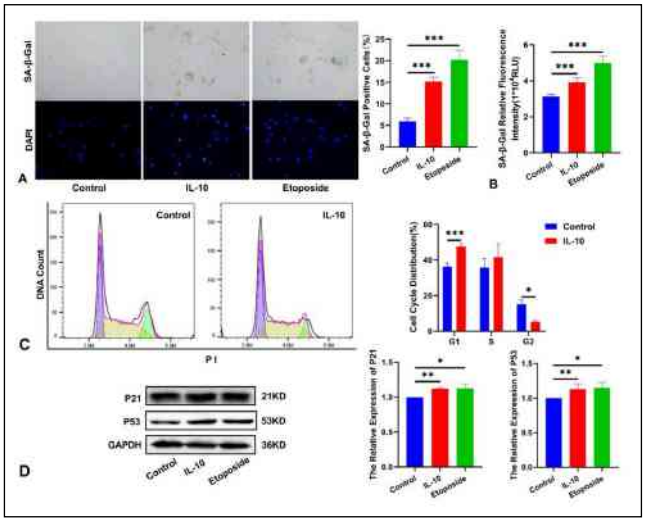

Figure 2.NK cells kill and clear senescent Hscs

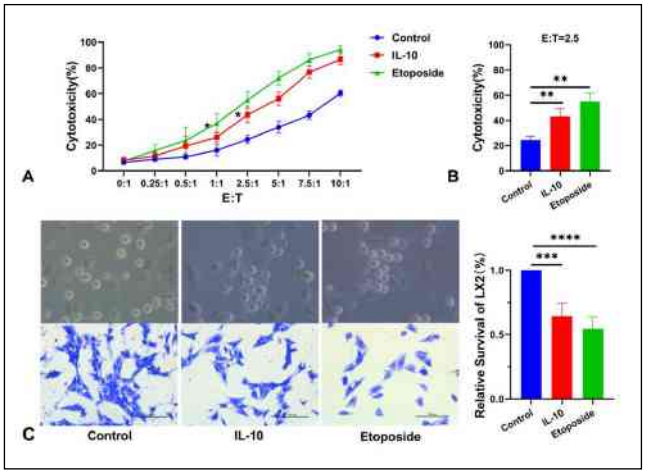

❖ AA-028

Clinical features and serum BMP9 levels in patients with portal pulmonary hypertension

Ruihua Zhang[1]
[1]*Department of Hepatology,The First Hospital of Jilin University*

Background: Portal pulmonary hypertension (POPH) is a serious complication of portal hy pertension with low morbidity and high mortality. Bone morphogenetic protein 9 (BMP9), a member of the bone morphogenetic protein family, can protect endothelial integrity and ma intain vascular homeostasis. It is known that the BMP9 signaling pathway is involved in the pathogenesis of pulmonary arterial hypertension, and POPH is a group 1 pulmonary arteri al hypertension (PAH). It is unclear whether BMP9 is involved in the pathogenesis of POP H.Our aim is to collect the clinical data of POPH patients, and to compare the expression l evels of BMP9 in POPH and other different forms of PAH.

Method: From April 2021 to the present, a total of 1650 patients with liver cirrhosis or portal hypertension underwent Doppler echocardiography. Finally, 14 patients were considered t o have POPH. The clinical data of these patients were collected, and 10 patients with POP H, 9 Serum samples from 9 patients with PAH caused by left heart disease, 9 patients with PAH caused by pulmonary disease, and 9 healthy individuals were detected by enzyme-linked immunosorbent assay (ELISA) to detect BMP9 levels.

Result:
1) The prevalence rate of POPH in patients with portal hypertension or liver cirrhosis was 0 84%. The basic information of 10 POPH patients selected in the experiment: the average a ge was 56.2±8.3 years old, 50% were female, and the most common cause was primary bi liary cirrhosis, 2 patients had a history of splenectomy, mean MELD: 11.8±11 points, mean hemoglobin: 98.1±34.5g/L, mean platelets 100.4±57.6*10^9/
L. 2) The expression levels of BMP9 in each group were detected, and the results were as follows: POPH group: 2.345±0pg/ml (compared with 17.6±8.1pg/
ml in healthy group, P<0.0001); PAH dcaused by left heart disease: 14.9±5.7pg/
ml ml (compared with 2.345±0pg/
ml in POPH group, P=0.0002); PAH caused by pulmonary disease: 12.6±7.0pg/
ml (compared with 2.345±0pg/ml in POPH group, P<0.0001); healthy group : 17.6±8.1pg/
ml.

Conclusion:

1) Compared with the healthy group, BMP9 in POPH patients was significantly decreased, and the decrease in BMP9 was considered to be related to the pathogenesis of POPH. 2) Compared with patients with PAH caused by left heart disease and PAH caused by pulmon ary disease, BMP9 in POPH group was significantly decreased. The application of BMP9 i s helpful to distinguish POPH from PAH caused by common clinical cardiopulmonary disea ses.

Table and Figure:

Figure 1. Serum BMP9 levels of patients in different groups

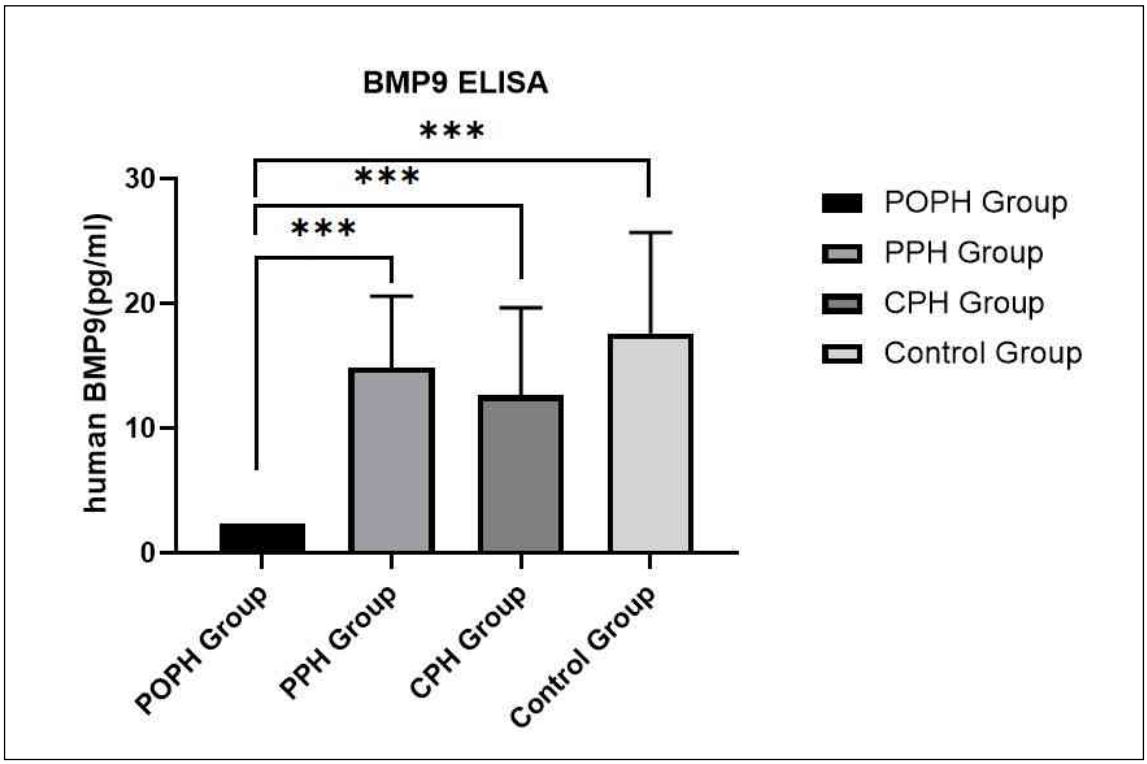

❖ AA-029

Hepatic CBS and CTH expression are significantly increased in Hepatic Fibrosis of Various Etiologies and Positively Correlated with Fibrotic Stage

Cichun Wu[1], Wei Zhang[1], Yao Liu[1], Lei Fu[1], Shifang Peng[1]
[1]Department of Infectious Diseases, Xiangya Hospital Central South University, Changsha 410008, China;

Background: Cystathionineβ-synthase (CBS) and cystathionineγ-lyase (CTH)have beenimplicated in the development of hepatic fibrosis in animal model.Theexpression pattern in human liver tissues of hepatic fibrosisis still unknown. We sought to investigate the expression and cellular localization of CBS\CTH in fibrotic liver tissues.

Method: Human liver pathology sections were collected from healthy individuals and patients with liver fibrosis of different etiologies. Pathological data were collected from the above patients. Immunohistochemistry and double immunofluorescence analysis as well as correlation analysis were used for the study.

Result: Immunohistochemistry and double immunofluorescence analysis showed that CBS\CTH were mainly located in hepatocytes. Compared with healthy controls, the expression of CBS\CTH was significantly increased in hepatic fibrosis of various etiologies. In hepatitis B-associatedhepatic fibrosis, the expression of CBS\CTH was positively correlated with the severity of hepatic fibrosis. In addition, CBS was positively correlated with the level of serum aspartate aminotransferase and total bilirubin, CTH was positively correlated with the level of serum aspartate aminotransferase, and both were negatively correlated with the level of platelets.

Conclusion: Our study suggests that CBS\CTH play an important role in the progression of hepatic fibrosis and are expected to become a potential target for intervention of hepatic fibrosis.

❖ AA-030

Incidence and factors influencing sleep disorders in patients with chronic hepatitis B infection

Cichun Wu[1], Jianping Xie[1], Fei Liu[1]
[1]Department of Infectious Diseases, Xiangya Hospital Central South University, Changsha, Hunan 410008, China

Background: Chronic hepatitis B (HBV) infection is a disease that imposes a considerable financial burden on patients and can lead to sleep disorders (SDs), resulting in a serious deterioration to patient quality of life. This study aimed to investigate the incidence and independent factors that influence SDs in patients with chronic HBV infection.

Method:A total of 747 patients with chronic HBV infection were recruited. All patients completed the Pittsburgh Sleep Quality Index (PSQI), Patient Health Questionnaire-9 (PHQ-9), Generalized Anxiety Disorder-7 scale, Social Support Rating Scale, Short Form 36 Health Survey (SF-36), and Visual Analogue Scale (VAS).

Result: The total PSQI score of patients with each type of chronic HBV infection was significantly higher compared to healthy Chinese adults($P<0.05$). The incidence of SDs in HBV carriers and patients with mild HBV, moderate HBV, severe HBV, liver failure, compensated cirrhosis, and decompensated liver cirrhosis was25%, 26%, 32%, 47%, 56%,31%, and 49%, respectively. The incidence of SDs in all patients with chronic HBV infection was 30%. Logistic regression analysis revealed that the course of disease, aspartate aminotransferase levels, PHQ-9scores, and VAS scores were independent risk factors for SDs, while the total SF-36 score was a protective factor for SDs (all $P<0.05$).

Conclusion:SDs occurred in 30% of patients with chronic HBV infection. The sleep quality of these patients is related to the course of disease, aspartate aminotransferase levels, the PHQ-9 score, the VAS score, and the total SF-36 score.

Table and Figure:

Figure 1. Comparison of SF-36 subscale scores between the two groups.

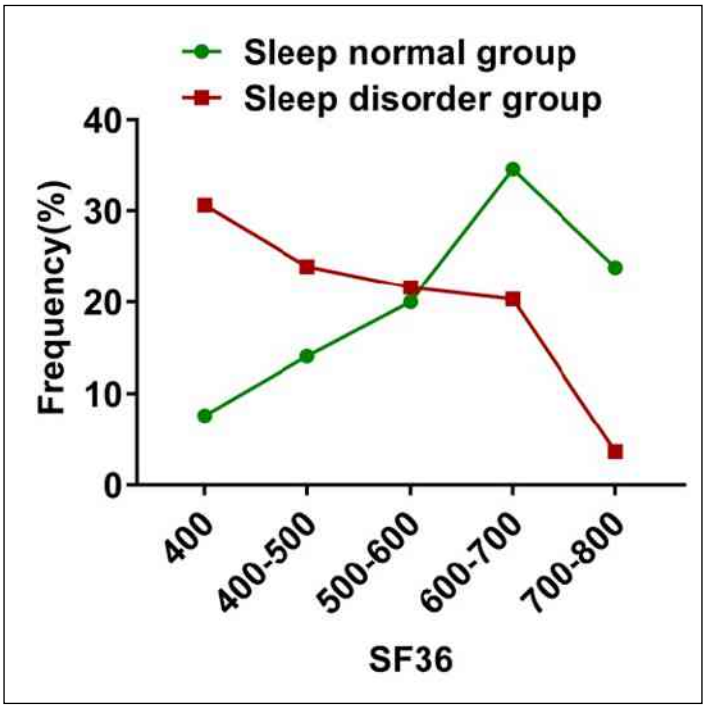

Figure 2. Comparison of the incidence of sleep disorders (SDs) in patients with different types of chronic hepatitis B virus (HBV) infection.

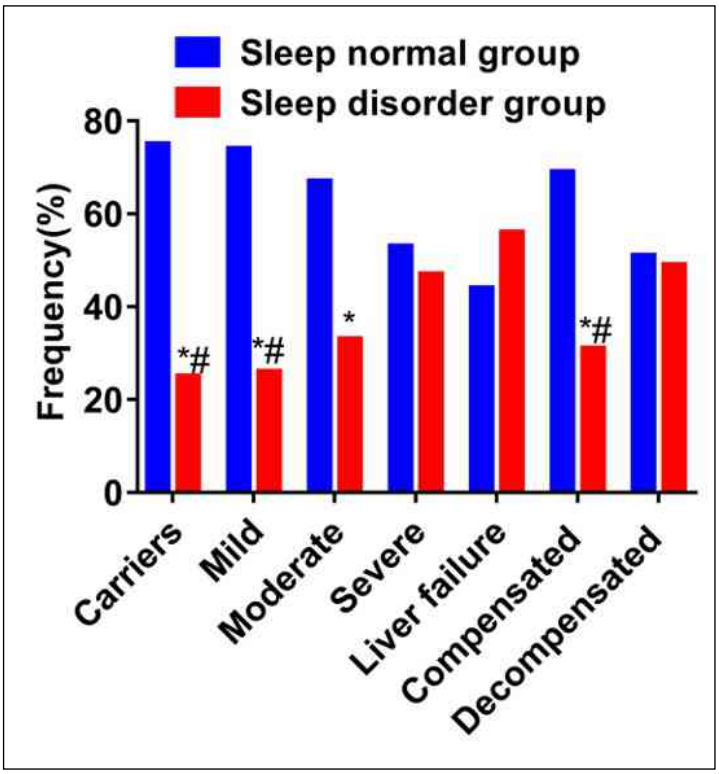

❖ AA-031

Prognosis of Spontaneous Bacterial Peritonitisin Patients with Hepatocellular Carcinoma

Mohamed Abdel-Samiee[1], Samah Awad[2], Amira Mohamed[3], Eman Abdelsameea[4], Hossam Abdel-Latif[5]
[1]Assistant consultant of hepatology and gastroenterology, National Liver Institute, Minoufia University,
[2]Assistant professor of Microbiolgy, National Liver Institute, Minoufia University,
[3]Student at hepatology and gastroenterolgy, National Liver Institute, Minoufia University,
[4]Professor of hepatology and gastroenterology, National Liver Institute, Minoufia University,
[5]Professor of hepatology and gastroenterology, National Liver Institute

Background: Background: Hepatocellular carcinoma (HCC) is the fourth most common cause of death from cancer. Spontaneous bacterial peritonitis (SBP) is associated with poor prognosis. Aim: We aimed at assessing the risk factors, differences in clinical characteristics and prognosis of SBP in patients with HCC in comparison to those without HCC.

Method: This study was conducted on cirrhotic patients who were admitted to the hospital with SBP, and divided into 2 groups; SBP group with HCC included 150 patients, and SBP group without HCC included 250 patients.

Result: Males represented 72% (n=108) in SBP group with HCC; their mean age was 55.8 ± 13.1 years old and SBP group included 171 males (68.4%), their mean age was 56.8 ± 10.5 years old. Regarding in-hospital mortality; it was 25.3% in SBP group with HCC and 18.8% in SBP group. Gastrointestinal bleeding was the most common cause of death in both groups. There was no significant difference between the two studied groups regarding patient outcome. The deceased patients had significantly higher levels of leucocytes and neutrophils in the ascitic fluid and a higher frequency of positive culture results than survived patients in the two studied groups. While there was no significant difference between survived and deceased patients regarding protein level in ascitic fluid or the causative organism.

Conclusion: Prognosis of SBP in patients with HCC seemed similar to patients without HCC.

Table and Figure:

Figure 1.

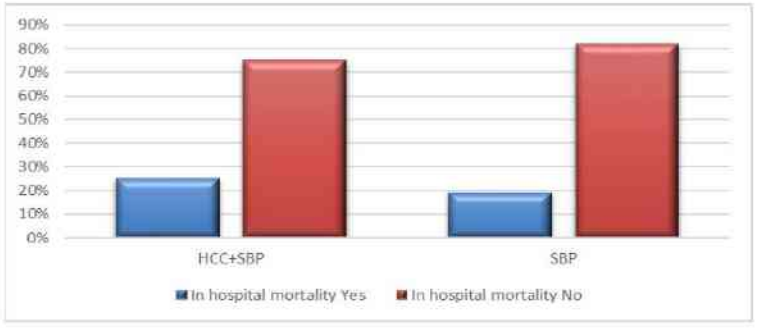

Figure 1: Comparison between the studied groups regarding in hospital mortality

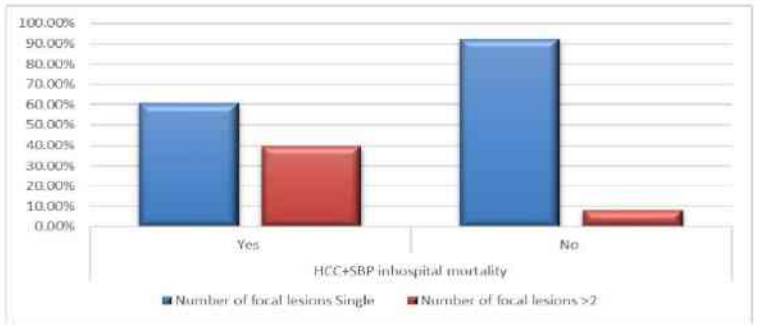

Figure 2: Number of focal lesions as regards in hospital mortality

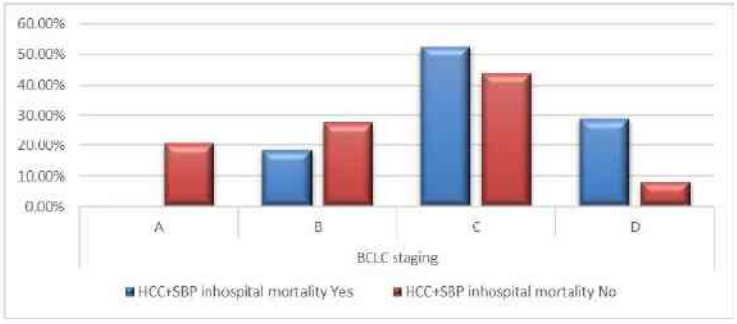

Figure 3: BCLC staging as regards in hospital mortality

❖ AA-032

Analysis on the influencing factors of hepatic fibrosis in patients with chronic hepatitis B virus infection complicated with metabolic associated fatty liver disease

Hongxia Wang[1], *Yan Wang*[2]
[1]山西医科大学, [2]山西白求恩医院

Background: Chronic HBV infection is a chronic infection with positive HBV surface antigen and/or HBV nucleic acid for more than 6 months. Metabolic-related fatty liver disease is a highly heterogeneous multi-system disease closely related to metabolic function. It used to be called non-alcoholic fatty liver disease. In early 2020, international experts changed its name to metabolic-related fatty liver disease . There is a greater relationship between chronic hepatitis B virus infection and metabolic-related fatty liver disease on the level of liver fibrosis. Liver fibrosis can be reversed before cirrhosis, but irreversible after cirrhosis. Chronic hepatitis B virus infection and metabolic-related fatty liver disease synergistically exacerbate liver damage. However, the mechanism that promotes liver fibrosis and affects liver cirrhosis has not been elucidated and needs further study.

Method:A total of 266 patients with chronic hepatitis B virus infection complicated with metabolic-related fatty liver disease were selected. According to the presence or absence of liver fibrosis, the patients were divided into control group: no liver fibrosis group (170 cases), observation group: liver fibrosis group (196 cases). The basic data of patients were collected; biochemical indexes; liver transient elasticity test; the influencing factors of liver fibrosis in patients with chronic hepatitis B virus infection and metabolic-related fatty liver disease were analyzed by nonparametric rank sum test, X2 test, and binary logistic regression.

Result:1. General information of patients The results showed that there were statistically significant differences in age and E value between the two groups (all $P<0.05$), but no significant differences in gender, CAP value and body mass index , see Table 1. 2. The blood biochemical results of the patients showed that compared with the patients in the control group, the levels of glutamate aminotransferase, aspartate aminotransferase, alkaline phosphatase, and glutamyl transfer in the observation group were The levels of enzymes and total bilirubin were significantly increased, and the levels of total cholesterol,

triglycerides, and high-density lipoprotein were significantly decreased, and the differences were statistically significant (P<0.05).see Table 2. 3. The results of multivariate analysis showed: glutamate aminotransferase, aspartate aminotransferase Elevated enzymes, glutamyl transferase, and lower triglycerides were the influencing factors of liver fibrosis in patients with chronic hepatitis B virus infection combined with metabolic-related fatty liver disease (all P<0.05), see Table 3.

Conclusion: Elevated levels of glutamate aminotransferase, aspartate aminotransferase, and glutamyltransferase are risk factors for liver fibrosis in patients with chronic hepatitis B virus infection combined with metabolic-related fatty liver disease, and triglyceride decreasing is a protective factor for them.

Table and Figure:

Figure 1. Table 1 and Table 2

Table 1 General information of 266 patients: M (P25, P75)

group	Number	Gender (male/female,example)	Age	BMI (kg/m²)	CAP (dB/m)	E (kpa)
control group	170	94/79	46 (39, 53)	24.69 (23.12, 27.09)	255 (228, 290)	4.85 (3.98, 6.50)
observation group	196	53/43	49 (44, 56)	25.97 (23.44, 27.68)	250 (221, 331)	10.60 (8.53, 19.03)
Statistics	-	X^2=0.070	Z=-2.929	Z=-1.548	Z=-0.493	Z=-13.543
P value	-	P=0.792	P=0.003	P=0.122	P=0.622	P<0.001

Table 2 Results of blood biochemical indexes of 266 patients: M(P25, P75)

group	control group (n=237)	observation group (n=266)	Z value	P value
FBG (mmol/L)	5.61 (5.14, 5.99)	5.77 (5.18, 6.24)	Z=-1.694	P=0.090
TC (mmol/L)	4.42 (3.55, 5.11)	3.76 (3.08, 4.74)	Z=-2.883	P=0.004
TG (mmol/L)	1.71 (1.16, 2.33)	1.17 (0.76, 1.90)	Z=-4.028	P<0.001
HDL (umol/L)	1.21 (1.01, 1.45)	1.11 (0.91, 1.30)	Z=-2.791	P=0.005
LDL (umol/L)	2.33 (1.79, 2.85)	2.07 (1.58, 2.80)	Z=-1.694	P=0.090
ALT (IU/L)	27.90 (19.00, 38.07)	32.00 (22.00, 69.50)	Z=-3.062	P=0.002
AST (IU/L)	23.00 (19.00, 29.08)	35.00 (25.50, 57.75)	Z=-7.026	P<0.001
ALP (IU/L)	76.00 (63.75, 89.48)	89.00 (74.00, 119.00)	Z=-4.474	P<0.001
GGT (IU/L)	22.00 (16.10, 30.78)	38.00 (26.00, 66.25)	Z=-6.343	P<0.001
TBIL (umol/L)	13.65 (10.00, 18.55)	16.20 (12.55, 28.28)	Z=-4.137	P<0.001

Figure 2. Table 3

Table 3 Multivariate analysis results of patients with chronic hepatitis B virus infection and metabolic-related fatty liver disease

Project	Regression coefficients	WaldX^2	P value	OR value	95%CI	
					lower limit	upper limit
年龄	0.008	0.326	0.568	1.008	0.981	1.035
ALT	-0.021	17.260	P<0.001	0.980	0.970	0.989
AST	0.089	19.172	P<0.001	1.093	1.050	1.137
TBIL	0.000	0.082	0.774	1.000	0.999	1.001
ALP	0.000	0.013	0.909	1.000	0.999	1.001
GGT	0.020	6.106	0.013	1.020	1.004	1.036
TC	0.003	0.097	0.755	1.003	0.985	1.021
TG	-0.603	8.932	0.003	0.547	0.368	0.812
HDL	0.061	3.132	0.077	1.063	0.993	1.137

❖ AA-033

Role of cytokines on the progression of liver fibrosis in mice infected with Echinococcus multilocularis

Fengming Tian[1], Tao Jiang[2], Xinwei Qi[2], Bin Li[1], Xuanlin Cai[2], Madinaimu Aibibula[1], Yumei Liu[2], Xiumin Ma[1]
[1]Tumor Hospital Affiliated to Xinjiang Medical University, [2]First Affiliated Hospital of Xinjiang Medical University

Background: Liver fibrosis is a significant pathological change of Echinococcus multilocularis (E. multilocularis) infection, as one of the histopathological phenomena in mice infected with E. multilocularis, it is associated with aberrant apoptosis of hepatocytes, collagen formation and liver immune cells inflammation. Although many CCL4-induced models have allowed us to gain a deeper understanding of the complexity of liver inflammation and repair, the composition of the ECM (extracellular matrix) in E. multilocularis infection is less well studied.

Method: The liver tissues were prepared for histological examinations, assessing liver pathological changes and fibrosis degrees （Figure 1A, B）. Liver histopathological features at 2, 8, 30, 90 and 180d were quantified by inflammatory severity score（Figure 1B, C）. The expression levels of inflammatory cytokines, fibrosis related cytokines and hepatic cell apoptosis were measured by qRT-PCR and immunohistochemistry (Figure 2).

Result: The mice infected with E. multilocularis resulted in distortions of the normal hepatic architecture with swollen hepatocytes around the central veins and interruption of hepatic tissue by numerous fibrous septa together with diffuse cellular infiltration around the fibrous bands and dilated portal areas. Furthermore, the vesicle structure could be observed in 90d and 180d infection (Figure 1A). At the early stage of infection, parasite stimulation triggers the rapid recruitment of immune cells. These infiltrated immune cells then produce a large number of cytokines, such as, iNOS (inducible Nitric Oxide Synthase), a pro-inflammatory cytokine; TGF-β (transforming growth factor) activated HSCs (hepatic stellate cells) to promote the proliferation of fibroblasts and secretion of ECM (extracellular matrix); MMP9 (matrix metalloproteinase 9) degraded basal ECM and facilitated its replacement by a highly dense interstitial matrix. At the middle and late stage of infection, the expression of IL-10 (interleukin-10), with general inhibitory effect was

increased (Figure 2). The imbalance of fiber formation and degradation aggravated liver fibrosis.

Conclusion: The disease is characterized by increased infiltration of immune cells around the lesion, creating an “immunosuppressive” microenvironment that is favor of persistent parasite infection. Along with expansion of parasitic infection, dynamic changes of cytokines expression were observed on the liver fibrosis progression, it is helpful to provide some new ideas for the prevention and treatment of liver fibrosis in mice infected with E. multilocularis. This work was supported by the National Natural Science Foundation (82060372, 81760372). Scientific Research Project of Science Department of Xinjiang Autonomous Region (2020E0277) and State Key Laboratory of Pathogenesis, Prevention and Treatment of High Incidence Diseases in Central Asia Fund (SKL-HIDCA-2020-YG3, SKL-HIDCA-2021-5).

Table and Figure:

Figure 1.

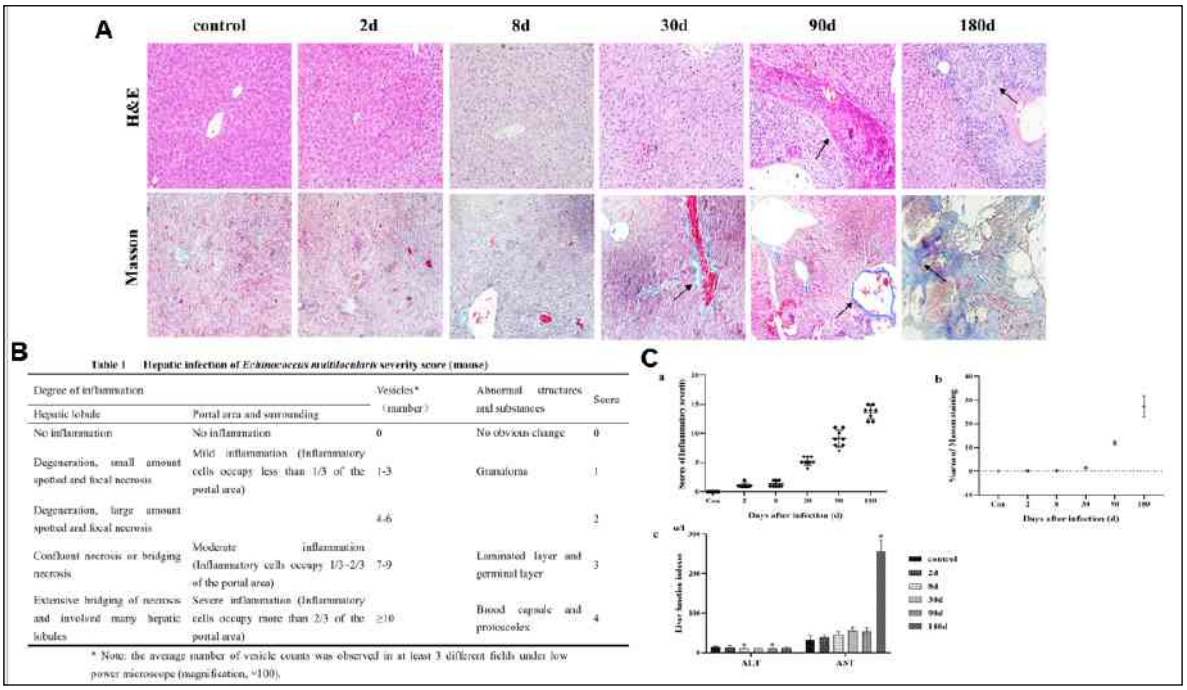

Table 1 Hepatic infection of *Echinococcus multilocularis* severity score (mouse)

Degree of inflammation		Vesicles* (number)	Abnormal structures and substances	Score
Hepatic lobule	Portal area and surrounding			
No inflammation	No inflammation	0	No obvious change	0
Degeneration, small amount spotted and focal necrosis	Mild inflammation (Inflammatory cells occupy less than 1/3 of the portal area)	1-3	Granuloma	1
Degeneration, large amount spotted and focal necrosis		4-6		2
Confluent necrosis or bridging necrosis	Moderate inflammation (Inflammatory cells occupy 1/3-2/3 of the portal area)	7-9	Laminated layer and germinal layer	3
Extensive bridging of necrosis and involved many hepatic lobules	Severe inflammation (Inflammatory cells occupy more than 2/3 of the portal area)	≥10	Blood capsule and protoscoles	4

* Note: the average number of vesicle counts was observed in at least 3 different fields under low power microscope (magnification, ×100).

Figure 2.

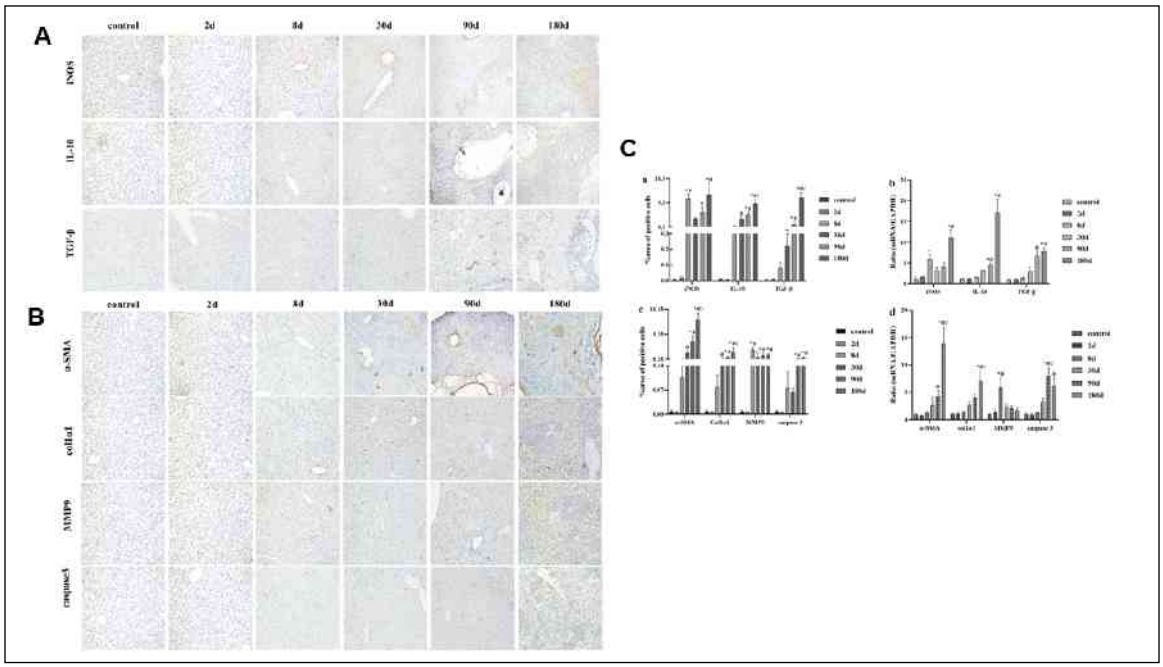
A
control
2d
8d
30d
90d
180d
iNOS
IL-10
TGF-β
B
α-SMA
collα1
MMP9
caspase3
C

❖ AA-034

Characterization of acute-on-chronic liver diseases: a multicenter prospective cohort study

Yuanyao Zhang[1], Zhongji Meng[2], Hai LI[3], Xianbo Wang[4], Xin Zheng[5], Yan Huang[6], Jinjun Chen[7], Yanhang Gao[8], Zhiping Qian[9], Feng Liu[10], Xiaobo Lu[11], Yu Shi[12], Yubao Zheng[13], Huadong Yan[14], Guohong Deng[15], Weituo Zhang[16]

[1]Postgraduate Training Basement of Jinzhou Medicical University. Taihe Hospital. Hubei University of Medicine,

[2]Taihe Hospital, Hubei University of Medicine,

[3]Department of Gastroenterology, Ren Ji Hospital, School of Medicine, Shanghai Jiao TongUniversity,

[4]Center of Integrative Medicine, Beijing Ditan Hospital, Capital Medical University,

[5]Department of Infectious Diseases, Tongji Medical College, Institute of Infection and Immunology, Union Hospital, Huazhong University of Science and Technology,

[6]Hunan Key Labor

atory of Viral Hepatitis, Department of Infectious Diseases, Xiangya Hospital, Central South University,

[7]Hepatology Unit, Department of Infectious Diseases, Nanfang Hospital, Southern Medical University,

[8]Department of Hepatology, The First Hospital of Jilin University,

[9]Department of Hepatology, The First Hospital of Jilin UniversityDepartment of Liver Intensive Care Unit, Shanghai Public Health Clinical Centre, Fudan University,

[10]Department of Infectious Diseases and Hepatology, The Second Hospital of Shandong University,

[11]Infectious Disease Center, The First Affiliated Hospital of Xinjiang Medical University,

[12]The State Key Laboratory for Diagnosis and Treatment of Infectious Diseases, The First Affiliated Hospital of School of Medicine, Zhejiang University,

[13]Department of Infectious Diseases, The Third Affiliated Hospital of Sun Yat-Sen University,

[14]Department of Infectious Diseases, Hwamei Hospital, Ningbo No. 2 Hospital, University of Chinese Academy of Sciences,

[15]Department of Infectious Diseases, Southwest Hospital, Third Military Medical University (Army Medical University),

[16]Clinical Research Center, Shanghai Jiao Tong University School of Medicine

Background: Patients with chronic liver diseases (CLD) will develop acute liver injury (ALI) under the attack of various precipitants, leading to significantly elevated alanine aminotransferase and/or total bilirubin levels, liver failure, or acute decompensation (AD) of liver cirrhosis, which is called acute on chronic liver diseases (AoCLD). This study intends to explore the clinical type, etiology, inducement, prognosis and prognostic factors of AoCLD, so as to provide theoretical guidance for the accurate diagnosis and prognosis of AoCLD.

Method: Patients with AoCLD from the Chinese Acute-on- Chronic Liver Failure (CATCH-LIFE) study cohort were included in this study, the demographic and clinical data, including age, gender, etiology, and predisposing factors, clinical examination and test data, complications, and outcomes (survival, liver transplantation, death) were analyzed. The 28-day and 90-day prognosis of each clinical type of AoCLD was analyzed using Kaplan-Meier, and the survival rate was compared using the log-rank test method.

Result:A total of 3599 patients with AoCLD were included in this study, including 1802 (50.1%) patients with acute decompensation of liver cirrhosis (LC-AD), 944 (26.3%) patients with acute-on-chronic liver failure (ACLF) (type-C ACLF in 596 patients, type-A ACLF in 121 cases, type-B ACLF in 227 cases), 327 (9.6%) cases with LC-A patients, and 578 (16.1%) cases with chronic hepatitis acute exacerbation (CHAE). The most common cause of CLD was HBV infection (71.2%), followed by alcoholic liver disease (18.8%). Among the inducements of AoCLD, HBV reactivation was the most common (61.3%), followed by bacterial infection (22.3%). At the end of 90 days of follow-up, the cumulative incidence of adverse events of each clinical subtype of AoCLD were: 52.0% (310/596) in type-C ACLF, 40.5% (49/121) in type-B ACLF, 26.9% (61/227) in type-A ACLF, 8.93% (161/1802) in LC-AD, 5.09% (14/275) in LC-A, and 1.38% (8/578) in CHAE, respectively.

Conclusion: In China, HBV infection is the main cause of AoCLD, and HBV reactivation is the main inducement of AoCLD. The most common clinical type of AoCLD is LC-AD, followed by ACLF, CHAE, and LC-A. Patients with LC-AD or ACLF have high short-term mortality, and early diagnosis and timely intervention should be applied to reduce the mortality of patients.

❖ AA-035

Prognosis of ABC clinical classification of acute-on-chronic liver failure and the prognostic evaluation of MELD 3.0 and COSSH-ACLF II

WANSHU LIU[1], LIJUN SHEN[1], FANGJIAO SONG[1], SHAOLI YOU[1], SHAOJIE XIN[1]
[1]Fifth Medical Center of Chinese PLA General Hospital

Background: Acute-on-chronic liver failure (ACLF) is a complex syndrome that results in a high short-term mortality rate of 50%–90%. Early diagnosis and prognosis for the effective treatment of ACLF is very important to decrease the high mortality rate. This study aims to investigate the prognosis of ABC subtype of acute-on-chronic liver failure (ACLF) and the value of evaluation prognosis by the latest end stage liver disease (MELD) 3.0 score and Chinese Group on the Study of Severe Hepatitis B (COSSH)-ACLF II score.

Method:ABC typing was performed of 1409 follow-up cohort. To evaluate the predictive abilities of 360-day mortality by different assessment methods, such as area under the receiver operating characteristic curve (AUROC) analysis, MELD, MELD 3.0, COSSH-II and COSSH-II 3 days after hospitalization (COSSH-II-3d). The differences in evaluation of prognosis were compared between different classifications and disease causes.

Result: The survival curve of 1409 patients with ACLF showed that the 360-day mortality of type A was significantly lower than that of type B and C (c2 = 80.133, p<0.01; Type A and C X2 = 76.198, p<0.01); There was no significant difference in survival rate between type B and C (X2=3.717, p>0.05). AUROC analysis, MELD, MELD 3.0, COSSH-II and COSSH-II-3d AUROC(95% CI) were 0.644, 0.655, 0.817 and 0.839 respectively (p<0.01). COSSH-II had better predictive ability for 360-day mortality in type A and HBV-ACLF, AUROC (95% CI) were 0.877 and 0.881, respectively (p<0.01). MELD 3.0 did not show better predictive power than MELD.

Conclusion:COSSH-II score greatly simplifies the calculation and evaluation, and has higher sensitivity and specificity for type A and HBV-ACLF. COSSH-II-3d has better evaluation value for prognosis, suggesting attention should be paid to ACLF treatment in the early stage of admission.

❖ AA-036

Analysis on the self-awareness rate and its influencing factors among the 15-69-year-old persons positive for HBsAg in China

Tongtong Meng[1], Ning Miao[2], Hui Zheneg[2], Fuzhen Wang[2], Zundong Yin[2], Liping Shen[3], Yu Wang[1], Jidong Jia[1], Yuanyuan Kong[4], Guomin Zhang[2]
[1]Liver Research Center, Beijing Friendship Hospital, Capital Medical University & National Clinical Research Center for Digestive Disease, [2]Department of National Immunization Program, Chinese Center for Disease Control and Prevention, [3]Chinese Center for Disease Control and Prevention, [4]Clinical Epidemiology and EBM Unit, Beijing Friendship Hospital, Capital Medical University & Beijing Clinical Research Institute

Background: The coverage of diagnosis and treatment of Hepatitis B virus (HBV) infection is low. Many people living with HBV are unaware of their hepatitis B status. Therefore, there is still a big gap between reaching the global target of 90% diagnosis rate of HBV infection by 2030 by the World Health Organization. We aimed to investigate the self-awareness rate of their HBV infection status and associated influencing factors in HBsAg-positive persons in China.

Method: In this cross-sectional study, we conducted a questionnaire survey on awareness of their HBV infection status in HBsAg-positive subjects aged 15-69 years found in the 2020 national viral hepatitis B seroepidemiological survey. The overall awareness rate in the whole HBsAg-positive subjects and the awareness rates of subgroups with different characteristics were calculated. The difference of awareness rate between groups was compared by the $\chi 2$ test. The multivariate logistic regression model was used to analyze the influencing factors associated with the awareness rate.

Result: The overall awareness rate of the respondents was 43.10% (1828/4241). The awareness rate for males was lower than for females (41.30% vs. 44.65%). The awareness rate was lower in the 60-69 age group than in other age groups (30.38% vs. 36.77%~57.58%). The awareness rate in rural areas was lower than in urban areas (39.43% vs. 47.32%). It was lower in areas with a per capita GDP below 54,000 yuan than in areas with a per capita GDP of 54,000 yuan and above (36.81% vs. 41.61%~50.30%). Respondents without co-liver diseases were lower than those with co-liver diseases (41.52% vs. 60.68%). Respondents without a family history of hepatitis B-related disease or unknown family history were lower than those with family history (43.58% vs. 68.26%, 24.71% vs. 68.26%). Multivariate logistic regression analysis found that males(OR=0.841, 95%CI: 0.734~0.964), high school education or below[primary school and below, middle

school, high school, OR (95%CI): 0.247(0.190~0.321), 0.451(0.352~0.577), 0.634(0.486~0.827)], rural areas(OR=0.822, 95%CI: 0.715~0.945), and regions with a per capita GDP of less than 80,000 yuan[54,000-80,000 yuan, OR (95%CI): 0.810(0.688~0.954); less than 54,000 yuan, 0.793(0.669~0.941)] were the negative influencing factors of awareness rate. While aged 30-39 years(OR=2.089, 95%CI: 1.626~2.683) and 40~49 years(OR=1.590, 95%CI: 1.250~2.023), co-liver diseases(OR=2.244, 95%CI: 1.754~2.871) and family history related to hepatitis B(OR=2.688, 95%CI: 2.242~3.223) were the positive factors of high awareness rate.

Conclusion: The overall awareness rate of HBsAg-positive people in China was 43.10%. To achieve the goal of 90% diagnosis rate of HBV infection by 2030, health publicity and advocacy for hepatitis B prevention and control should be further strengthened, and the scope of HBV screening should be expanded as well.

❖ AA-037

A combined radiomics-clinic model based on conventional MRI to predict liver fibrosis and necroinflammation

Zha Junhao[1], *Ju Shenghong*[1]
[1]*Jiangsu Key Laboratory of Molecular and Functional Imaging, Department of Radiology, Zhongda Hospital, Medical School of Southeast University, Nanjing, China*

Background: Patients with liver fibrosis, especially≥F2, are at significantly increased risk for liver-related morbidity and mortality. Necroinflammatory activity is also a histological hallmark of advanced liver disease. Although liver biopsy is the current gold standard, it still has limitations, including risks of procedure-related complications, sampling error, and interobserver variability. Clinical fibrotic scores, such as FIB-4, APRI or the ultrasound elastography are able to provide useful inputs. However, these tools have limiting gray zones for proper scoring. Radiomics analysis has recently gained attention as a promising method to characterize chronic liver diseases and guide clinical decision making. Multiple pieces of information, in terms of MR tissue texture, clinical biomarkers, should be taken into consideration, and this mimics the diagnosis in real clinical senarios. Hence, We hypothesized that CRC models may allow comprehensively classifing ≥F2 or ≥G2.

Method: In this retrospective study, 394 consecutive patients at center 1 with biopsy-proven liver fibrosis and necroinflammatory activity from May 2015 to December 2018 were randomly placed in a training(n=276) or test(n=118) cohort at a ratio of 7:3. 2880 radiomics features extracted from 3D whole liver on T2FS and T1WI delay-phase MR images (VOIT2FS,VOIT1delay) were analyzed separately to form the radiomics scores(R-score). The optimal R-scores and clinical biomarkers were integrated into the radiomics-clinic model(CRC) for predicting fibrosis staging(≥F2) or necroinflammatory activity grading(≥G2), respectively. The performance of the models was assessed and compared with FIB-4 and APRI. The decision curve analysis were established from the CRC models. We also conducted validation 1 using an independent 96 subjects from January 2019 to August 2020 at center 1, and external validation 2 using an independent cohort of 47 subjects at center 2.

Result: Whole liver radiomics features extracted from conventional MRI are accessible and reliable for assessing liver fibrosis. A human-in-the-loop strategy is developed to achieve better automated segmentation performance of ResUnet network. We identified five risk

factors(T1delay R-score, T2FS R-score, and 3 clinical biomarkers: ALB, GGT, PLT) for ≥F2 and six risk factors(T1delay R-score, T2FS R-score, and 4 clinical biomarkers: ALB, ALP, AST, TBA) for ≥G2, respectively. The combined radiomics-clinic model demonstrates good performance for predicting ≥F2(AUC 0.82, 0.78, 0.82, and 0.83 in the training, test, validation 1, and external validation 2 cohort, respectively) and ≥G2(AUC 0.88, 0.86, 0.78 and 0.89 in the training, test, validation 1 and external validation 2 cohort, respectively). In comparison, the AUCs of CRC model outperformed Radiomics model alone, FIB-4, and APRI. DCA indicated the CRC models have potential in clinical application.

Conclusion: The CRC models provide a promising approach for detecting liver fibrosis(≥F2) and necroinflammatory activity(≥G2)

Table and Figure:

Figure 1. Diagnostic Performance of CRC Model for ≥F2 and ≥G2 in the Training, Test and Validation Cohort

Parameter	Diagnostic Performance			
	Training	Test	Validation 1	Validation2(External)
Clinically significant fibrosis , stage ≥F2				
AUC	0.82	0.78	0.82	0.83
Sensitivity(%)	83.2(74.1-90.1)	73.1(61.8-82.5)	82.4(69.1-91.6)	91.4(76.9-98.2)
Specificity(%)	71.8(64.7-78.2)	62.5(45.8-77.3)	71.1(55.7-83.6)	75.0(42.8-94.5)
Necroinflammatory grade, ≥G2				
AUC	0.88	0.86	0.78	0.89
Sensitivity(%)	75.4(67.1-82.5)	71.4(57.8-82.7)	61.5(44.6-76.6)	80.0(63.1-91.6)
Specificity(%)	83.6(76.5-89.2)	90.3(80.1-96.4)	82.5(70.1-91.3)	66.7(34.9-90.1)

Figure 2. Area under receiver operating characteristic (ROC) comparison of CRC model, Radiomics model, FIB-4,and APRI in training, test, and validation set; DCA results

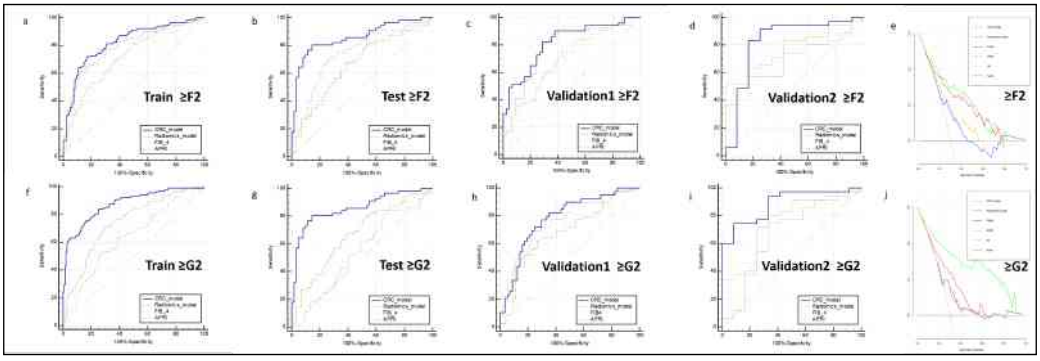

❖ AA-038

Prediction of the risk of rebleeding after the first esophageal variceal ligation based on Nomography

Li Sai[1], Li Yong[2], Shi Liangrong[1]
[1]Interventional Radiology Center, Department of Radiology, Xiangya Hospital Central South University, Changsha 410005, Hunan, China, [2]Department of Gastroenterology, Xiangya Hospital, Central South University, Changsha 410005, Hunan, China

Background: Esophageal variceal ligation (EVL) is one of the main treatments for esophageal varices. Sequential therapy may reduce the occurrence of rebleeding events after EVL. However, there are some patients with poor compliance who fail to regularly complete sequential treatment, which seriously affects the efficacy of therapy. This study aimed to investigate the risk factors affecting rebleeding in the short- and long-term for patients who underwent EVL for the first time and to predict the risk of rebleeding, to reduce the financial burden on patients.

Method: This study retrospectively selected patients who underwent EVL for cirrhotic esophageal varices in the Xiangya Hospital Central South University between January 2017 and December 2021. A total of 629 patients who did not regularly complete sequential treatment after the first operation were included. Before the first operation of EVL, the patients' clinical data, serological data, imaging data, endoscopic data were collected through the electronic medical record system. Patients were divided into bleeding and nonbleeding groups according to whether they had a bleeding event at 8 weeks and 6 months postoperatively. Cox regression was used to analyze factors influencing short- and long-term rebleeding after first EVL, and Nomography was used to visualize the results and predict the risk of rebleeding.

Result:1. A total of 1213 patients with cirrhotic esophageal varices who underwent EVL were included in this study, including 629 patients who did not routinely complete sequential therapy after the first EVL, representing 51.9%. 2. Eight weeks after the first EVL, there were 219 patients who experienced a bleeding event and 410 patients who did not, with a rebleeding rate of 34.8% within 8 weeks. Multivariate Cox regression analysis showed that male, severe varices, prothrombin activity, platelet count, and history of blood transfusion were independent risk factors for rebleeding in the short term. The established Cox regression model had an area under the receiver operating curve (AUC) of 0.77 (95% CI: 0.63-0.87), with a sensitivity of 0.633 and a specificity of 0.874. 3. Six months after the

first EVL, there were 504 patients who experienced a bleeding event, 125 patients who did not, and the rebleeding rate within 6 months was 80.1%. By multivariate Cox regression analysis, severe varices, platelet count, and the width of the main portal vein were independent risk factors for long-term rebleeding. The established Cox regression model had an AUC of 0.81 (95% CI: 0.68-0.91), sensitivity of 0.591, and specificity of 0.882.

Conclusion: The severe varices and platelet count are independent risk factors for short- and long-term rebleeding after first-time EVL, and the Cox regression model constructed in this study showed good performance in predicting bleeding events and was more visually displayed by Nomogram.

Table and Figure:

Figure 1. Nomography visualized the results. (A) Risk prediction of rebleeding within 8 weeks of first EVL (B) Prediction of risk of rebleeding within 6 months of first EVL procedure. BT: blooding transfusion history; Variability: degree of esophageal varices; PTR: prothrombin time rate; PLT: platelet, WPV: width of the portal veins.

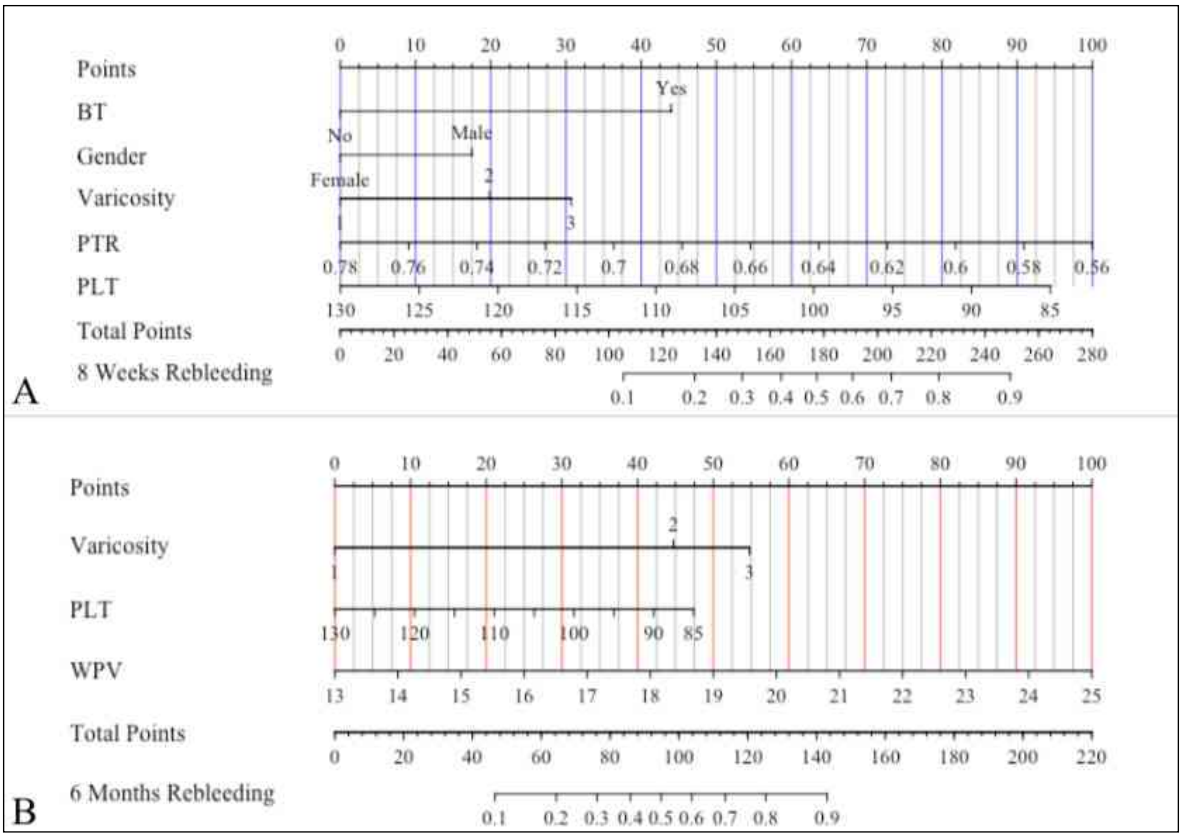

❖ AA-039

Liver cirrhosis could be identified non-invasively with a new threshold by liver stiffness measurement in hepatitis B patients during antiviral therapy

Xiaoning Wu[1], Yameng Sun[1], Jialing Zhou[1], Mingyi Xu[2], Yongpeng Chen[3], Chenghai Liu[4], Huichun Xing[5], Lei Li[6], Wei Jiang[7], Hongxin Piao[8], Hong Zhao[5], Bingqiong Wang[1], Shuyan Chen[1], Tongtong Meng[1], Qiushuang Guan[1], Xiaojuan Ou[1], Hong You[1], Jidong Jia[1]

[1]Beijing Friendship Hospital, Capital Medical University, [2]Shanghai First People's Hospital, [3]Nanfang Hospital of Southern Medical University, [4]Shuguang Hospital, Shanghai University of Traditional Chinese Medicine, [5]Beijing Ditan Hospital, Capital Medical University, [6]Beijing Youan Hospital, Capital Medical University, [7]Shanghai Zhongshan Hospital, Fudan University, [8]The Affiliated Hospital of Yanbian University

Background:HBV-related cirrhotic patients are still at high risk of developing decompensated complications and hepatocellular carcinoma even after they initiated antiviral therapy. Identifying of cirrhosis is the basis of properly monitoring in chronic hepatitis B (CHB) patients. However, the performance of liver stiffness measurement (LSM) to identify liver cirrhosis in CHB patients who have been on antiviral treatment is uncertain.

Method: Adults with CHB who had LSM and liver biopsy simultaneously at least 6 months after initiation of antiviral therapy were enrolled from three clinical studies (NCT01938781, NCT01938820, NCT01943617). Liver cirrhosis was defined as F4 according to the METAVIR scoring system. LSM was performed using FibroScan (Echosens, Paris, France) or Fibrotouch (Wuxi Hisky Medical Technology Co., Ltd., Wuxi, China). The performance of LSM to identify liver cirrhosis in CHB patients during antiviral therapy was analyzed by using area under receiver operating characteristic curve (AUROC).

Result: Four hundred and twenty patients were enrolled and eligible for statistical analysis. All patients were treated with Entecavir. Patients were all HBVDNA undetectable with a median ALT of 24.0 (17.0, 33.0) at the liver biopsy. The median time from initiation of antiviral therapy to liver biopsy was 1.5 (1.2, 1.9) years. One hundred and sixteen (27.6%) patients were staging at F4 according to the METAVIR scoring system. LSM in non-cirrhosis and cirrhosis patients were 7.7 ±4.3 kPa and 12.0 ±5.7 kPa (P<0.001) respectively. The value of AUROC for diagnosis of cirrhosis by LSM was 0.796 (95% confidence interval 0.755-0.834), The cut-off value was 7.9 kPa with a sensitivity of 81%, a specificity of 66%, a positive predictive value is 47%, and a negative predictive value is 90%. Adjusted AUROC using the Obuchowski method confirmed the good performance. The new threshold is lower than the previous one of 10.7 kPa for diagnosis of cirrhosis

which was derived from untreated patients. With this new threshold during antiviral treatment, about 29.3% (34/116) of patients could be identified non-invasively.

Conclusion:HBV-related cirrhosis during antiviral therapy could be identified non-invasively with a new threshold of 7.9 kPa by liver stiffness measurement.

❖ AA-040

Optimal liver stiffness measurement values for diagnosis of significant fibrosis in hepatitis B patients during antiviral treatment

Jialing Zhou[1], Xiaoning Wu[1], Yameng Sun[1], Mingyi Xu[2], Yongpeng Chen[3], Chenghai Liu[4], Huichun Xing[5], Lei Li[6], Wei Jiang[7], Hongxin Piao[8], Hong Zhao[5], Yuemin Nan[9], Shuyan Chen[1], Tongtong Meng[1], Qiushuang Guan[1], Xiaojuan Ou[1], Hong You[1], Jidong Jia[1]

[1]Beijing Friendship Hospital, Capital Medical University, [2]Shanghai First People's Hospital, [3]Nanfang Hospital of Southern Medical University, [4]Shuguang Hospital, Shanghai University of Traditional Chinese Medicine, [5]beijing ditan hospital, [6]Beijing Youan Hospital, [7]Shanghai Zhongshan Hospital, Fudan University, [8]The Affiliated Hospital of Yanbian University, [9]the Third Hospital of Hebei Medical University

Background: Not all chronic hepatitis B (CHB) patients with liver fibrosis who have initiated potent antiviral treatment could achieve liver fibrosis reversion. Identifying on-treatment significant fibrosis is helpful to refine the stratification of disease progression and define the potential anti-fibrotic population. However, the optimal liver stiffness measurement (LSM) to for the diagnosis of significant fibrosis in antiviral treatment hepatitis B patients remains unclear.

Method: Patients with CHB from three clinical studies (NCT01938781, NCT01938820, NCT01943617) who had LSM and liver biopsy simultaneously during antiviral therapy were enrolled. Significant liver fibrosis was defined as ≥F2 according to the METAVIR scoring system. LSM were performed using FibroScan (Echosens, Paris, France) or Fibrotouch (Wuxi Hisky Medical Technology Co., Ltd., Wuxi, China). The correlation between LSM and fibrosis stage was analyzed by the Spearman's rank correlation coefficient (r). Area under receiver operating characteristic curve (AUROC) was used to assess LSM diagnostic performance.

Result: Four hundred and twenty patients were included. 315 (75%) of patients were male, the median age was 46.0 (43.0, 48.0), the median time from initiation of antiviral treatment to liver biopsy was 2.1± 1.6 years. All patients were treated with Entecavir and achieved HBVDNA undetectable as well as ALT normalization at liver biopsy. About 87 % of patients were staged as significant liver fibrosis. LSM in F0 to F4 was 5.3 ±0.8, 6.8 ± 4.4, 7.3 ± 4.3, 9.5 ± 4.2, and 12.0 ±5.7 kPa, respectively. A significant correlation was found between LSM fibrosis stage (r=0.602, P < 0.001). Diagnostic performance of LSM to identify patients with histological fibrosis stage ≥F2 was AUROC 0.741 (95% confidence interval 0.697-0.783). The optimal cut-off of LSM values for significant fibrosis were 6.6 with sensitivity of 68%, specificity of 73%, the positive predictive value is 40%, negative

predictive value is 94%. AUROC using the Obuchowski method confirmed this good performance. For diagnosis of significant fibrosis in hepatitis B patients during antiviral treatment, the new threshold is similar to the cut-off of 7.3 kPa which is derived from untreated patients.

Conclusion: The optimal liver stiffness measurement values for the diagnosis of significant fibrosis during antiviral treatment in hepatitis B patients is 6.6 kPa.

❖ AA-041

Digital Droplet PCR (ddPCR) for Detection and Quantitation of Hepatitis Delta Virus

Yuan Tian[1], Ling Xu[1], Xiangying Zhang[1], Yaling Cao[1], Zihao Fan[1], Huaibin Zou[1], Zhongping Duan[1], Feng Ren[1]
[1]BeijingYouanHospital, Capital Medical University

Background: The prevalence of hepatitis delt virus (HDV) far exceeds our expected level, there remains a lack of reliable quantitative assays for HDV RNA detection. We sought to develop a new method based on digital droplet PCR (ddPCR) for HDV quantitative detection.

Method: With plasmid (pMD19T) containing HDV full-genome, we determined the method for ddPCR-based HDV RNA quantification. To compare various assays for HDV detection, 30 cases diagnosed hepatitis D and 14 controls were examined by ELISA, RT-PCR and ddPCR. 728 HBV-related patients including 182 chronic hepatitis B (CHB), 182 liver cirrhosis (LC), 182 hepatocellular carcinoma (HCC) and 182 liver failure (LF) were screened for HDV infection.

Result: The limit of detection of ddPCR for HDV is significantly low, which lower limit of detection (LLoD) and lower limit of quantitation (LLoQ) to be 0.18 copies/reaction (95% CI: 0.0012151- 0.76436) and 5.51 copies/reaction (95% CI: 1.15-6.4*105), respectively. Among the 44 samples, ELISA detected 30 cases positive, ddPCR reported 24 samples and RT-PCR reported 10 samples positive for HDV RNA. Moreover, the positive rates of anti-HDV were 1.1%, 3.3%, 2.7% and 7.1% in patients with CHB, LC, HCC, and LF; the detection rates of RT-PCR in HDV RNA were 0%, 16.67%, 15.4% and 20%, however, the detection rates of ddPCR were 0%, 33.33%, 30.77% and 60%.

Conclusion: We establish a high sensitivity and specificity quantitative HDV RNA detection method based on ddPCR. HBV-related end-stage liver disease, especially liver failure, are associated with a remarkably high rate of HDV infection.

❖ AA-042

HVPG-guided regression of portal hypertension with cirrhotic patients: A meta-analysis

Wang Min, Zhang Guan-hua, Wang Yu
Liver Research Center, Beijing Friendship Hospital, Capital Medical University,
95 Yong-an Road, Xi-Cheng District, Beijing 100050, China.

Background and aims: Hepatic venous pressure gradient (HVPG) is a golden standard for assessing portal hypertension（PH）in cirrhosis. Reduced HVPG is associated with decreased risk of decompensated events (mainly variceal bleedings) and mortality in cirrhotic patients. Here, we performed a meta-analysis to confirm this effect in cirrhotic patients.

Methods： We collected data of available studies from the PubMed, Embase and Cochrane Library. Responder is defined as a reduction of HVPG by ≥10% from baseline in compensated cirrhosis and a reduction of HVPG to ≤12 mmHg or by ≥20 % from baseline following pharmacological treatment in decompensated cirrhosis.

Results: Fourteen studies were identified including 1031 patients. In cirrhosis mixed with decompensated and compensated stage, pooled odds ratios (OR) of bleedings and death/ liver transplant for responders were, respectively 0.14, (95%CI: 0.09-0.21;P＜0.001) and 0.42,(95%CI: 0.25-0.70;P=0.001). In 7 studies with definitely decompensated cirrhosis, responder had significantly lower odds of variceal bleedings than non-responders. (OR, 0.17; 95%CI,0.10-0.29). Only 2 studies were compensated cirrhosis, responders had significantly lower odds of decompensation than non-responders. (OR, 0.11; 95%CI,0.06-0.25;P＜0.001).

HVPG reductions in those responders were divided into three subgroups：19-25%, 26-29% and ≥30%，the ORs of bleedings for three subgroups is 0.27(95%CI,0.12-0.57), 0.13(95%CI,0.05-0.27), and 0.69(95%CI,0.26-1.82), respectively.

Conclusions： In a meta-analysis of clinical trials, we found that HVPG reduction by≥10 % of baseline might be essential for PH regression in compensated cirrhosis, and to <12 mmHg or by≥20% in decompensated cirrhosis.

Table and Figure:pic1

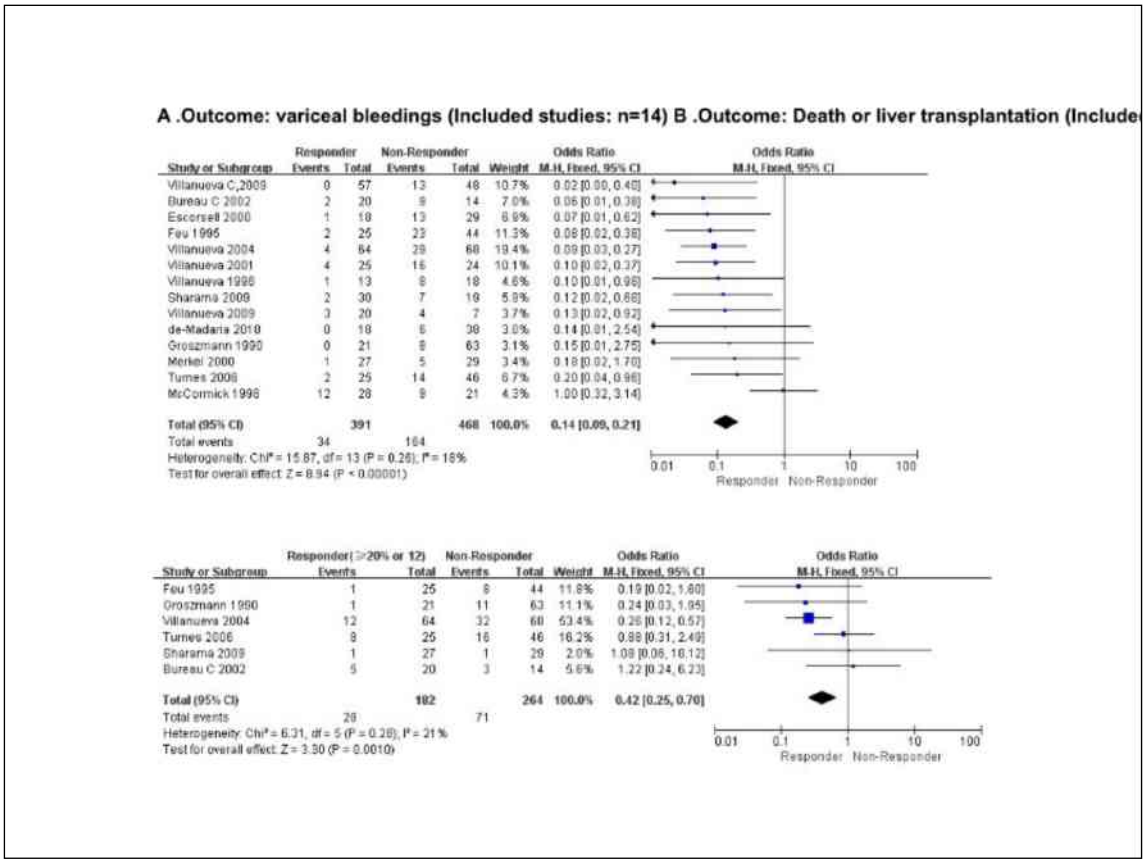

pic2

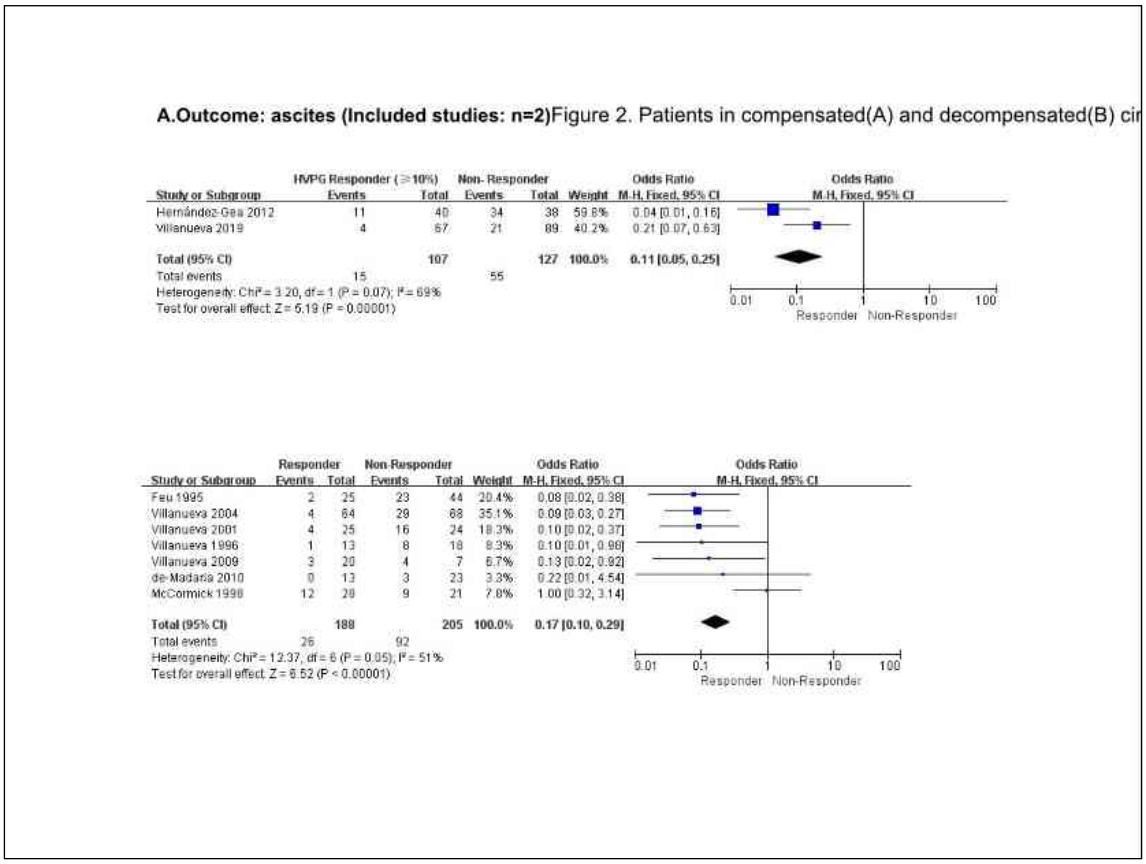

Pic3

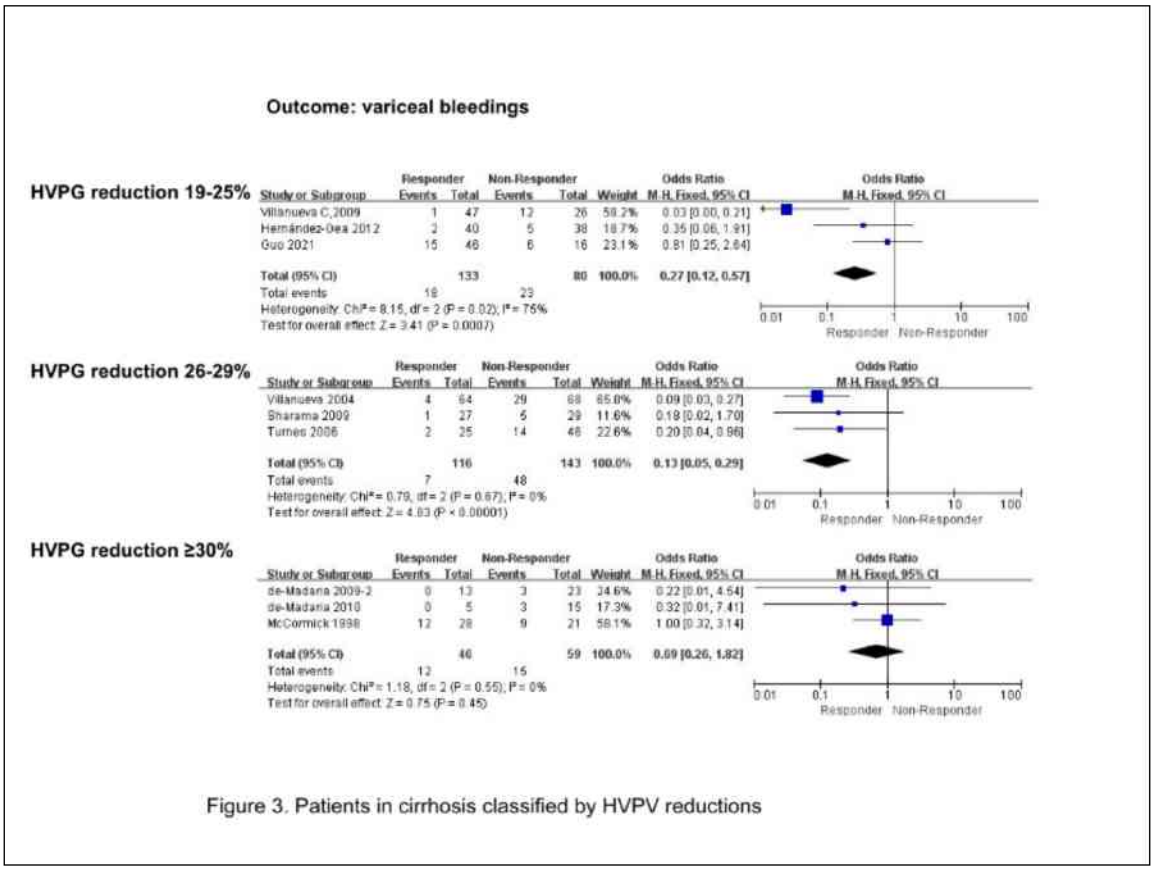

Figure 3. Patients in cirrhosis classified by HVPV reductions

❖ AA-043

The analysis of clinical, pathological and follow-up characteristics in patients with classical PBC-AIH overlap syndrome and PBC with AIH features

Liping Guo[1], Simin Zhou[1], Weirong Wang[1], Jiangpeng Liu[1], Bangmao Wang[1], Lu Zhou[1]
[1]Tianjin Medical University Gerenal Hospital

Background: To analyze the clinical, pathological and follow-up characteristics of PBC with AIH features diagnosed by AIH scoring system and classical PBC-AIH overlap syndrome diagnosed by Paris criteria.

Method: To retrospectively analyze and reassess 88 PBC patients who underwent liver biopsy. 61 cases of PBC patients with AIH features were selected according to AIH scoring criteria, 21 cases of classical PBC-AIH patients were selected according to Paris criteria, and 25 cases of pure PBC patients were selected respectively. The clinical, pathological and follow-up characteristics were compared among each group.

Result: Compared to pure PBC patients, the AIH score, IgG level and incidence of interfacial hepatitis in PBC patients with AIH features were higher, the level of ALP and TBil, the incidence of liver cell cholestasis were lower(all $P<0.05$); compared to classic PBC-AIH patients, the levels of ALT, AST, ALP, GGT and TBil in PBC patients with AIH features were lower(all $P<0.05$); 19 patients were diagnosed consistently in PBC with AIH features group and classic PBC-AIH group. Compared to inconsistent patients, the AIH score, incidence of jaundice or skin pruritus, levels of ALT, AST, GGT and TBil were higher in these consistent patients(all $P<0.05$); compared to classic PBC-AIH patients, the incidence of cirrhosis complications at first visit were higher, the treatment response were poorer and cirrhosis with/without complications at follow-up endpoint were more prominent in PBC patients with AIH features. As Paris criteria was the gold standard, a receiver operating characteristic(ROC) curve was drawn with the AIH scores of 88 PBC patients. The AUC value was 0.714, the 95% confidence interval was 0.599 ~ 0.829, and the diagnostic sensitivity and specificity of the AIH scoring system to distinguish PBC-AIH overlap syndrome were 90.5% and 37.3% respectively.

Conclusion: The AIH scoring system had a high sensitivity and poor specificity for the diagnosis of PBC-AIH. Compared to classic PBC-AIH patients, the liver enzyme levels of PBC patients with AIH features were lower. The diagnosis of PBC-AIH should not be blindly relied on Paris criteria in clinical, but more attention should be paid to those PBC

patients with AIH features whose liver enzymes were not up to the standard of Paris criteria. In the future, a new scoring system for overlap syndrome should be constructed on the basis of the original AIH scoring system, so as to identify the PBC-AIH overlapp syndrome in the early stage.

Table and Figure:

Figure 1.ROC curve drawn by AIH integral

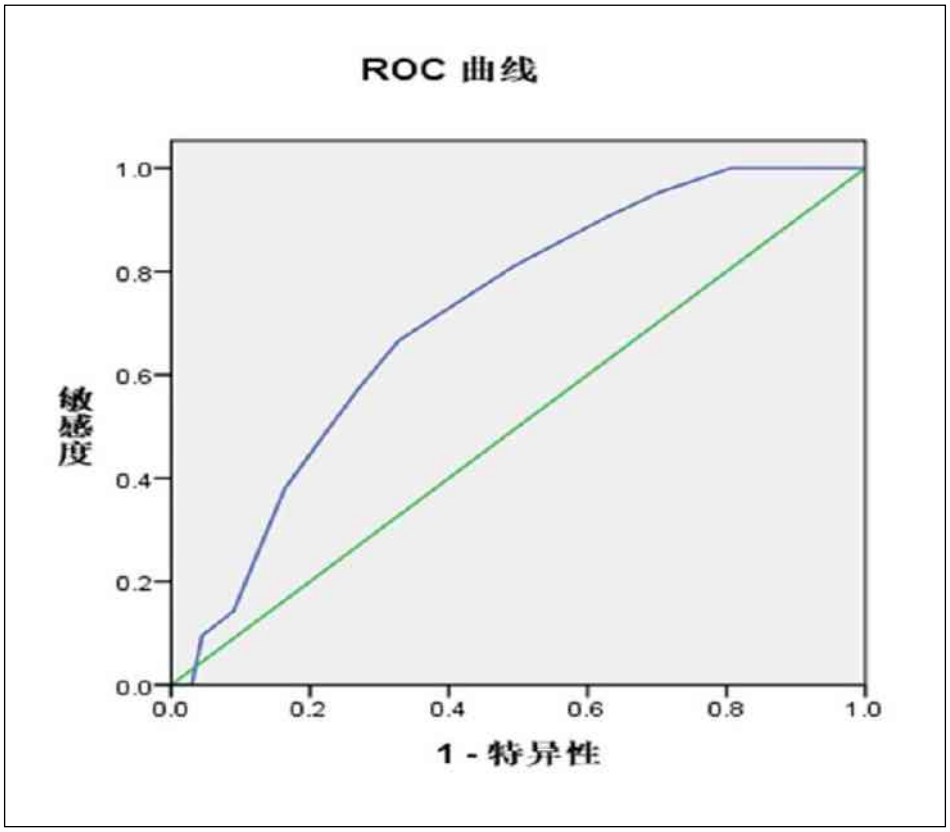

❖ AA-044

CRISPR/Cas13-assisted Hepatitis B Virus Covalently Closed Circular DNA Detection

Ling Xu[1], Xiangying Zhang[1], Yuan Tian[1], Zihao Fan[1], Yaling Cao[1], Yingmin Ma[1], Hao Li[1], Zhongping Duan[1], Feng Ren[1]
[1]Beijing YouAn Hospital, Capital Medical University

Background: The formation of an intranuclear pool of covalently closed circular DNA (cccDNA) in the liver is the main cause of persistent hepatitis B virus (HBV) infection. Here, we established highly sensitive and specific methods to detect cccDNA based on CRISPR-Cas13a technology.The formation of an intranuclear pool of covalently closed circular DNA (cccDNA) in the liver is the main cause of persistent hepatitis B virus (HBV) infection. Here, we established highly sensitive and specific methods to detect cccDNA based on CRISPR-Cas13a technology.

Method: We used plasmid-safe ATP-dependent DNase (PSAD) enzymes and HindIII to digest loose circle rcDNA and double-stranded linear DNA, amplify specific HBV cccDNA fragments by rolling circle amplification (RCA) and PCR, and detect the target gene by using CRISPR-Cas13a technology. The CRISPR-Cas13a-based assay for the detection of cccDNA was further clinically validated using HBV-related liver tissues, plasma, whole blood and peripheral blood mononuclear cells (PBMCs).

Result: Based on the sample pretreatment step, the amplification step and the detection step, we established a new CRISPR-Cas13a-based assay for the detection of cccDNA. After the amplification of RCA and PCR, 1 copy/μl HBV cccDNA could be detected by CRISPR/Cas13-assisted fluorescence readout. We used ddPCR, qPCR, RCA-qPCR, PCR-CRISPR and RCA-PCR-CRISPR methods to detect 20, 4, 18, 14 and 29 positive samples in liver tissue samples from 40 HBV-related patients, respectively. HBV cccDNA was almost completely undetected in the 20 blood samples of HBV patients (including plasma, whole blood and PBMCs) by the above five methods.

Conclusion: We developed a novel CRISPR-based assay for the highly sensitive and specific detection of HBV cccDNA, presenting a promising alternative for accurate detection of HBV infection, antiviral therapy evaluation and treatment guidance.

❖ AA-045

Histological regression and clinical benefits in patients with liver cirrhosis after long-term anti-HBV treatment

Shuyan Chen[1], Yameng Sun[1], Jialing Zhou[1], Xiaoning Wu[1], Tongtong Meng[1], Bingqiong Wang[1], Hui Liu[2], Tailing Wang[3], Chen Shao[2], Xinyu Zhao[1], Xiaoqian Xu[1], Yuanyuan Kong[1], Xiaojuan Ou[1], Jidong Jia[1], Hong You[1]

[1]Liver Research Center, Beijing Friendship Hospital, Capital Medical University, Beijing Key Laboratory of Translational Medicine on Liver Cirrhosis, National Clinical Research Center of Digestive Diseases, Beijing, China, [2]Department of Pathology, Beijing Youan Hospital, Capital Medical University, Beijing, China, [3]Department of Pathology, China-Japan Friendship Hospital, Beijing, China

Background: To determine histological regression and clinical improvement after long-term antiviral therapy in hepatitis B virus-related cirrhosis patients.

Method: Treatment-naïve chronic hepatitis B patients with histologically or clinically diagnosed liver cirrhosis were enrolled. Liver biopsies were performed after 5 years entecavir-based antiviral treatment. Patients were followed up every 6 months. Cirrhosis regression was evaluated based on Metavir system and P-I-R score. Clinical improvement was evaluated before and after the long-term treatment.

Result: Totals of 73 patients with HBV-related liver cirrhosis were enrolled. Among them, 30 (41.1%) patients were biopsy proved liver cirrhosis and the remaining 43 (58.9%) cirrhotic patients were diagnosed by clinical features. Based on Metavir system and P-I-R score, 72.6% (53/73) patients attained histological regression. Furthermore, 30.1% (22/73) were defined as significant regression (Metavir decrease ≥ 2 stage), 42.5% (31/73) were mild regression (Metavir decrease 1 stage or predominantly regressive by P-I-R system if still cirrhosis after treatment) and 27.4% (20/73) were the non-regression. Compared to levels of clinical characteristics at baseline, HBV DNA, ALT, AST and liver stiffness significantly decreased after 5 years of anti-HBV treatment, while serum levels of platelets and albumin improved remarkably ($P < 0.05$). In multivariate analysis, only the pre-treatment liver stiffness level was associated with significant regression (OR = 0.887, 95%CI: 0.802-0.981, P = 0.020).

Conclusion: After long-term antiviral therapy, patients with HBV-related cirrhosis are easily to attain improvements in clinical parameters, while a certain percentage of these patients still cannot achieve histological reversal.

❖ AA-046

Rapid and Portable HBV DNA Detection Based on CRISPR/Cas13a Technology for Low-Level Viremia Patients

Zihao Fan[1], Yuan Tian[1], Ling Xu[1], Yaling Cao[1], Sisi Chen[1], Zhenzhen Pan[1], Yao Gao[1], Xiangying Zhang[1], Zhongping Duan[2], Feng Ren[1]
[1]Beijing Institute of Hepatology, Beijing Youan Hospital, Capital Medical University, Beijing, China, [2]Beijing YouAn Hospital, Capital Medical University, Beijing, China

Background: The World Health Organization (WHO) has developed a strategy to eliminate hepatitis B virus (HBV) infections as a public health threat by 2030. However, an increasing number of patients are presenting with low-level viremia (LLV) with the widespread use of antiviral medications. The diagnostic efficiency and coverage area of HBV infection are low. Hence, this study intended to develop a rapid and portable HBV DNA detection test strip to achieve high-sensitivity and high-specificity point-of-care testing (POCT) detection.

Method: We established, optimized, and evaluated a colloidal gold test strip for the rapid and convenient detection of HBV DNA based on CRISPR/Cas13a combined with recombinase-aided amplification (RAA) technology. Furthermore, 180 HBV-infected patients (including patients with different viral loads, LLV patients and dynamic plasma samples of patients on antiviral therapy) were enrolled for clinical validation.

Result:POCT detection of HBV DNA was established based on CRISPR-Cas13a technology with a sensitivity of 101 copies/μl (<10 IU/ml for clinical samples) and a specificity of 100%. HBV DNA gradient concentration plasmids and clinical samples were effectively identified by this approach. The positive coincidence rate for LLV patients was 87%, while the negative coincidence rate was 100%. The positive coincidence rate reached 100% in LLV patients (>100 IU/ml). The sensitivity, specificity, positive predictive agreement (PPA) and negative predictive agreement (NPA) values of dynamic plasma detection in patients on antiviral therapy were 100%, 92.15%, 93.75%, and 100%, respectively.

Conclusion: We developed a rapid and portable HBV DNA detection test strip based on RAA-CRISPR/Cas13a that can achieve high-sensitivity and high-specificity POCT detection in LLV patients.

❖ AA-047

Comparison of the GLIM criteria with specific screening tool for diagnosing malnutrition in hospitalized patients with cirrhosis: a cross-sectional study

Wanting Yang[1,2], Chao Sun[1,2,3]
[1]Department of Gastroenterology and Hepatology, Tianjin Medical University General Hospital, Anshan Road 154, Heping District, Tianjin 300052, China, [2]Tianjin Institute of Digestive Disease, Tianjin Medical University General Hospital, Anshan Road 154,Heping District, Tianjin 300052, China, [3]Department of Gastroenterology, Tianjin Medical University General Hospital Airport Hospital, East Street 6, Tianjin Airport Economic Area, Tianjin 300308, China

Background: The Global Leadership Initiative on Malnutrition (GLIM) has recently been built to diagnose malnutrition, however its validity among cirrhotics remains enigmatic. We aimed to investigate the prevalence of malnutrition according to GLIM criteria and compare the differences in relation to specific screening tool.

Method: We conducted a cross-sectional study by analyzing hospitalized cirrhotics. The Royal Free Hospital-Nutritional Prioritizing Tool (RFH-NPT) was performed as the screening tool. The estimated prevalence was showed with and without the initial screening process. Diversely combined phenotypic and etiologic criteria and distinct BMI cut-offs was applied to detect frequency of malnourished patients hospitalized for decompensated cirrhosis.

Result: Totally, 363 patients were recruited with median age of 64 years and 51.2% female. The prevalence of malnutrition according to GLIM criteria with and without prior RFH-NPT screening was 33.3% and 36.4%, respectively. Low BMI and inflammation was the most prevalent combination resulting in the malnutrition diagnosis (42.4%), followed by low BMI and reduced food intake (39.4%). In contrast, the least prevalence was present by combining reduced muscle mass with inflammation to diagnose malnutrition. Furthermore, the frequency of malnourished and well-nourished participants was not statistically different by using divergent BMI reference values across study population.

Conclusion:GLIM criteria may serve a specific proxy to diagnose malnutrition along with prior RFH-NPT screening. Relevant investigation is supposed to report the applied combination of phenotypic/etiologic criteria, taking consideration of significant impact of different models. More attempts are warranted to delineate the prognostic role of GLIM criteria in the context of cirrhosis.

Table and Figure:

Figure 1. Cut-off values for the phenotypic and etiologic GLIM criteria. GLIM, Global Leadership Initiative on Malnutrition; BMI, body mass index; SMI, skeletal muscle index; NLR, neutrophil-to-lymphocyte ratio.

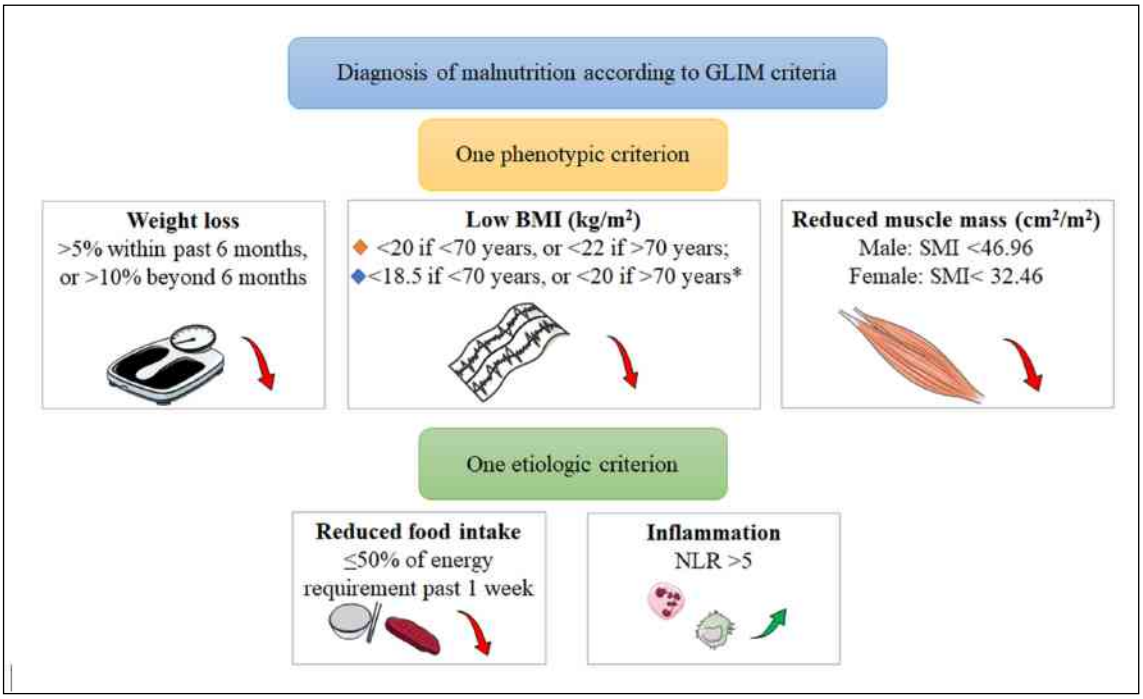

Figure 2. Comparison of diagnosis of malnutrition according to GLIM criteria with and without screening by RFH-NPT scheme. The circles represent the proportion of patients being identified at each of the two processes screening with RFH-NPT and malnutrition diagnosis. RFH-NPT, Royal Free Hospital-Nutrition Prioritizing Tool; GLIM, Global Leadership Initiative on Malnutrition.

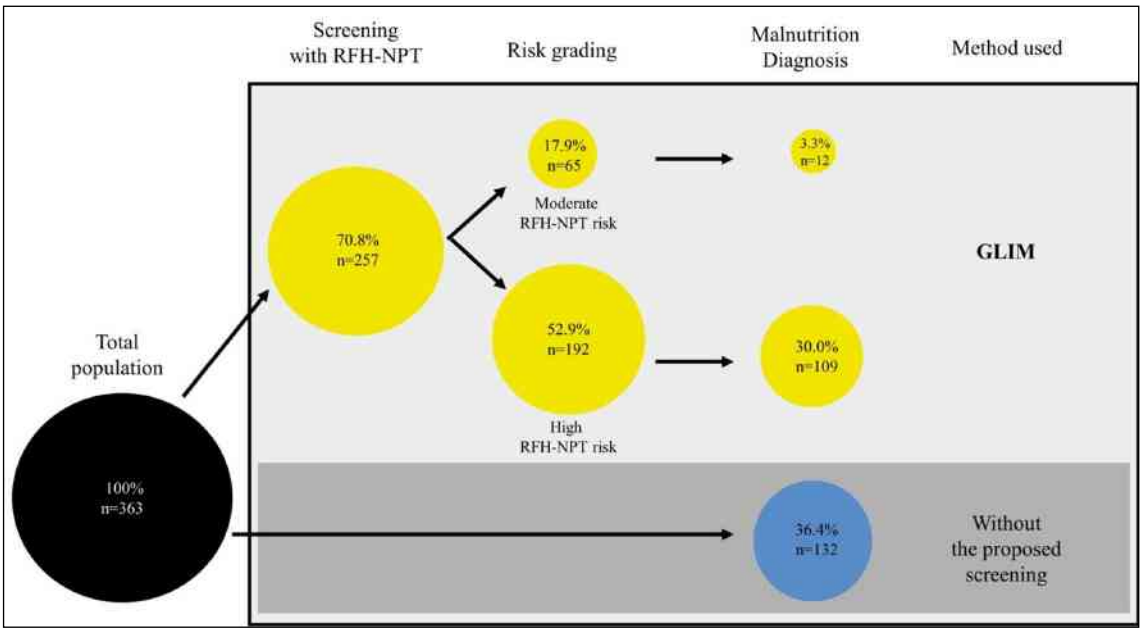

❖ AA-048

The Angiogenesis-related Biomarkers of Idiopathic Non-cirrhotic Portal Hypertension: An Immunohistochemical Study

Zijin Liu[1], Hui Liu[1], Huiguo Ding[1], Zhuqing Gao[1], Mingjie Tan[1]
[1]Beijing Youan Hospital

Background: Angiogenesis may play a key role in portal hypertension progression. Few researches focus on the immunohistochemical (IHC) expression of angiogenesis-related biomarkers in idiopathic non-cirrhotic portal hypertension (INCPH) patients.

Method: This study aims to: (1) investigate the expression pattern of some angiogenesis-related biomarkers in INCPH and liver cirrhosis (LC) patients (2) determine the correlation between clinical, imaging information and these biomarkers expression in INCPH patients; (3) investigate the correlation between the prognosis of INCPH and these biomarkers expression.

Result:IHC showed LC tissue had significantly higher proportion of CD34 and vascular endothelial growth factor receptor 1(VEGFR1) compared with INCPH patients(P<0.01). Leukocyte cell-derived chemotaxin-2 (LECT2) and glutamine synthetase (GS) were mainly distributed around central vein in INCPH, while in LC patients, LECT2 and GS were distributed around fibrous septa area. CD34 positive area proportion were positively correlated with splenic length(P=0.04), spleen thickness(P=0.03), ascites(P=0.01), and gastric varices(P<0.01). VEGFR1 were positively correlated with spleen thickness(P<0.01). and negatively correlated with right posterior hepatic notch sign(P=0.03). During the follow-up period, the angiogenesis-related biomarkers expression had no correlation with INCPH’s prognosis.

Conclusion:LC tissue had significantly higher proportion of CD34 and VEGFR1 compared with INCPH patients. The LECT2 and GS distribution area was different between LC and INCPH patients. CD34 positive area proportion was positively correlated with splenic length, spleen thickness, ascites, gastric varices. VEGFR1 were positively correlated with spleen thickness and negatively correlated with right posterior hepatic notch sign.

Table and Figure:

Figure 1. Different expression of CD 34 between INCPH and LC patients.

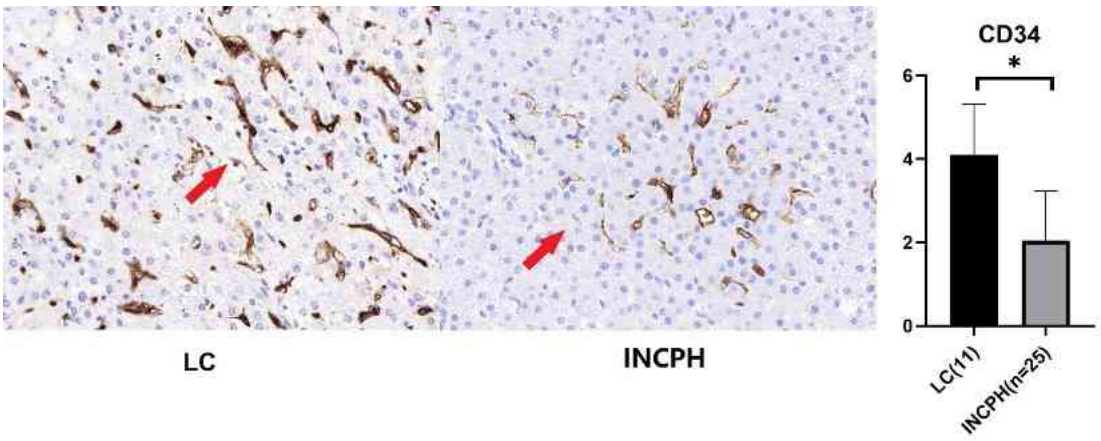

Figure 2. Different expression of VEGFR1 between INCPH and LC patients.

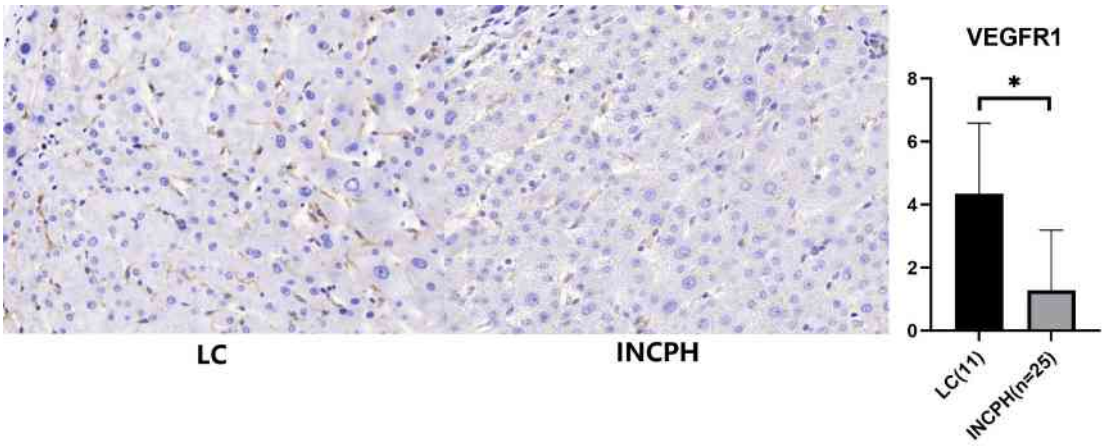

❖ AA-049

Screening of overlapping differential expression genes in liver fibrosis and the diagnostic value in predicting HBV-related severe liver fibrosis

Shuya Zhang1, Ying Liu1, Jun Huang1, Guifu Dai1, Yuqi Guo1
[1]School of Life Science, Zhengzhou University

Background: Corresponding author: Jun Huang, huangjun@zzu.edu.cn; Guifu Dai, daiguifu@zzu.edu.cn；Yuqi Guo, guoyuqi@zzu.edu.cn Funding: National Natural Science Foundation of China (Project Reach Youth, Grant No.8190120757); Key Research and Development Projects in Henan Province (Science and Technology Research,Grant No. 222102310622) Liver fibrosis, the result of uninterrupted chronic liver damage, is closely associated with the incidence of server liver diseases referring to cirrhosis and hepatocellular carcinoma. Chronic liver injury caused by different etiologies, such as toxicants, viral hepatitis (HBV/HCV), nonalcoholic steatohepatitis, alcohol abuse, etc. can be accompanied by the development of liver fibrosis. Accurate diagnosis of liver fibrosis and timely etiological removal or advance drug treatment can effectively prevent or even reverse liver fibrosis and largely avoid the occurrence of end-stage liver diseases. Therefore, it is crucial to identify the clinical biomarkers of liver fibrosis and apply them for clinical diagnosis and subsequent combined drug therapy.

Method: In combination with transcriptome and bioinformatics, high-throughput sequencing data of liver fibrosis caused by multiple etiologies in humans or mice were collected from GEO database, and the overlapping up-regulated differential genes of liver fibrosis induced by various etiological factors were preliminarily obtained. A classical mouse model of liver fibrosis was established to compare the expression of overlapping differential expression genes（DEGs） in liver tissue samples with fibrosis and normal liver tissue samples. Finally, the expression levels of overlapping DEGs in different pathological stages of HBV-related liver fibrosis were compared and the possibility of overlapping DEG as a risk factor for predicting the severity of HBV-related liver fibrosis was evaluated.

Result:12 genes were screened and found to be overall up-regulated in liver fibrosis caused by HBV, CCL4 and alcoholic fatty liver injury. In the subsequent mouse model and patients with HBV related liver fibrosis, it was verified that the expression of a ferroptosis-related gene was up-regulated and closely related to the occurrence and development of

fibrosis, which could be used as a biomarker for predicting the severity of HBV-related liver fibrosis, and its function and clinical application value were worthy of further study.

Conclusion: Through searching the overlapping up-regulated genes of liver fibrosis caused by multiple etiologies and verifying them in vivo animal experiments, we found that the ferroptosis-related gene was abnormally expressed in the process of liver fibrosis, which could be used as a biomarker for clinical diagnosis of severe HBV-related liver fibrosis.

❖ AA-050

A model based on two-dimensional shear wave elastography for acute-on-chronic liver failure development in patients with acutely decompensated hepatitis B cirrhosis

Songsong Yuan[1], Xingzhi Huang [2], Xiaoping WU[1], Pan Xu[2], Aiyun Zhou[2]
[1]Department of Infection Disease, The First Affiliated Hospital of Nanchang University,
[2]Department of Ultrasonography, the First Affiliated Hospital of Nanchang University

Background: To evaluate the accuracy of two-dimensional (2D) shear wave elastography (SWE), develop and validate a novel prognostic model in predicting acute-on-chronic liver failure (ACLF) development in patients with acutely decompensated hepatitis B cirrhosis.

Method: This prospective cohort study enrolled 221 patients in the First Affiliated Hospital of Nanchang University from September 2019 to January 2021, and randomly assigned them to the derivation and validation cohorts (7:3 ratio). Ultrasound, 2D SWE, clinical and laboratory data were collected, and outcome (ACLF developed) was recorded during a 90-day follow-up period. We evaluated the ability of 2D SWE to predict the outcome, developed a model for predicting ACLF development in the derivation cohort, and assessed the model in the validation cohort.

Result:2D SWE values were significantly higher in patients with ACLF development ($P<0.05$). The accuracy of 2D SWE in predicting the outcome was better than that of serum parameters of liver fibrosis (all $P<0.05$). The SWE model for ACLF development had good calibration and discrimination [concordance index (C-index): 0.855 and 0.840 respectively] in derivation and validation cohorts, outperforming serum prognostic scores (all $P<0.05$).

Conclusion: The 2D SWE model, superior to serum prognostic scores in predicting ACLF development, could be a noninvasive tool to guide the individual management of patients with acutely decompensated hepatitis B cirrhosis.

Table and Figure:

Figure 1. Image shows liver stiffness measured with 2D SWE in patients with acutely decompensated hepatitis B cirrhosis. The rectangular elasticity box (4 cm × 3 cm) was placed 1–2 cm under the liver capsule in the parenchyma area free of large vessels. Regions of interest ranged from 10 to 20 mm in diameter and were positioned in the elasticity box. 2D, two-dimensional; SWE, shear wave elastography.

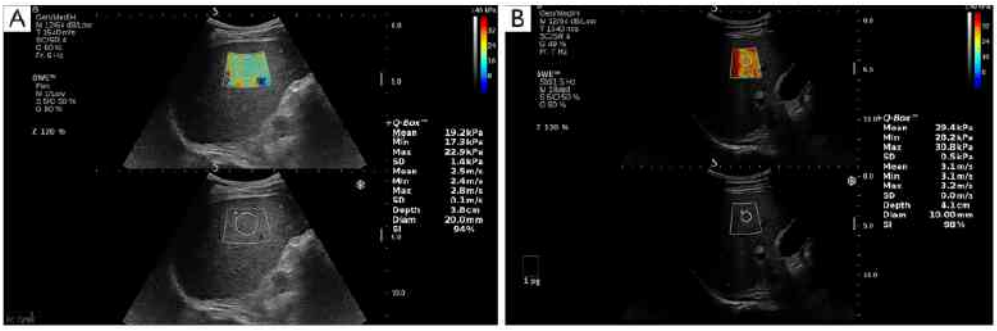

Figure 2. Generation and evaluation of the nomogram. (A) Nomogram to predict 90-day ACLF development; (B,C) the calibration curve estimates 90-day ACLF development predicted by nomogram in the derivation and validation cohorts. ACLF , acute-on-chronic liver failure; ALP , alkaline phosphatase; PTA, prothrombin activity, PVv, peak velocity of portal vein; SWE, shear wave elastography.

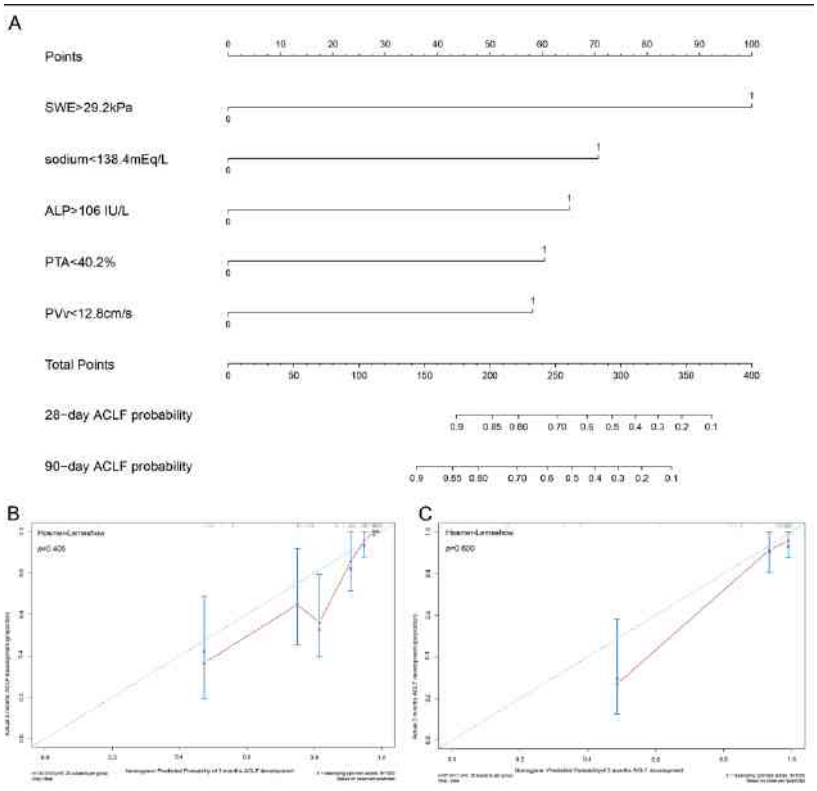

❖ AA-051

Liver Cancer Classification based on Computerized Tomography Scan Image using Probabilistic Neural Network Model Algorithm

Rifaldy Fajar[1], *Baddeha Lelayati*[1], *Evy Elfiany*[1]
[1]*Computational Biology and Medicine Laboratory, Yogyakarta State University*

Background: The most common type of liver cancer is Hepatocellular carcinoma (HCC), which begins in the main type of liver cell (hepatocyte). Hepatocellular carcinoma occurs most often in people with chronic liver diseases, such as cirrhosis caused by hepatitis B or hepatitis C infection. Examinations carried out to determine the presence of HCC are by measuring the level of Alpha-Fetoprotein in the blood, radiographic diagnoses such as ultrasound examination, CT-Scan, and MRI, as well as performing a liver biopsy. HCC is often not identified because the symptoms of HCC are masked by the underlying disease. So we need a method to make it easier to identify HCC disease through CT-Scan images. In this study, an alternative machine learning algorithm is used, namely the Probabilistic Neural Network that works to classify HCC.

Method: The method used in this study is Probabilistic Neural Network to identify HCC disease. The steps taken to identify HCC disease are starting with pre-processing using Gaussian filtering to improve image quality by reducing noise in the image, then segmentation using thresholding, morphology operators and find contour which aims to get image segmentation in the heart, as well as to feature extraction using a gray level co-occurrence matrix to analyze the texture of the image as input for the identification process. The image data used in this study were obtained from The Cancer Imaging Archive (TCIA) and Radiopedia.org.

Result: The test results obtained indicate that the proposed method is able to identify HCC disease with an accuracy obtained of 94%. The use of the gray level co-occurrence matrix method for the feature extraction process works well for recognizing objects so that they can identify HCC and normal categories.

Conclusion: The Probabilistic Neural Network method can identify HCC disease quite well based on the accuracy obtained exceeding 90%.

❖ AA-052

Evaluation of liver transient elastography combined with aMAP in patients with chronic hepatitis B virus infection in uncertain period

Limin Wang[1], Yuan Huang[2], Wenping Zhao[2], Jingyue Wang[2], Si Xie[2]
[1]Beijing Tsinghua Changgung hospital,Children liver disease department, [2]Beijing Tsinghua changgung hospital, Department of hepatobiliary and pancreatic medicine

Background: To evaluate the effect of liver transient elastography combined with aMAP liver cancer risk assessment on patients with chronic hepatitis B virus (HBV) infection in uncertain period.

Method: Collect the information of patients with chronic HBV infection in uncertain clinical in Beijing Tsinghua Changgeng hospital from January 2018 to December 2021, and calculate aMAP and liver transient elastography.

Result:1.The study included 155 patients with chronic HBV infection in uncertain period, 102 males (65.8%), 53 female（34.2%）, median age of 37 (P2531,P75 47) years. 56 cases (36.1%) had ALT higher than the normal high value , 44 cases had (28.4%) HBeAg positive , and HBV DNA was positive in 88 cases (56.8%). 2. The median of liver transient elasticity in this group was 7.3 (P256.1, P75 8.6). The highest aMAP was 65.2. The percentage of people with low, middle and high risk of liver cancer accounted for 78.1%, 14.2% and 7.7% respectively. 3. The median of liver transient elasticity in HBeAg positive patients was 7.1 (P25 5.5, P75 8.9), which was lower than that in HBeAg negative patients 7.8 (P25 6.5, P25 9.6), P 0.03. The proportion of high, middle and low risk of liver cancer with aMAP score in HBeAg positive patients and negative patients was 4.5% vs9.5% respectively 0%、11.4%VS15. 3% and 84.1% vs75 7%, P 0.24. 4. There were 42 cases (27.1%) with liver transient elastography higher than 8.0, and the rate of the patients with high, middle and low risk of liver cancer with aMAP score compared with liver transient elastography less than 8.0 was 21.4% VS2, respectively 7%、23.8%VS10. 6% and 54.8% vs86 7%, P = 0.00.

Conclusion: Chronic HBV infection in uncertain period patients with liver transient elastography 8.0 is significantly higher proportion of high risk of liver cancer with aMAP than that less than 8.0 , and antiviral treatment should be taken.

❖ AA-053

Analysis of clinical characteristics of early primary biliary cholangitis

Yujin Zhu[1], Chunyan Wang[2], Jing Li[1]
[1]Tianjin Medical University, [2]Tianjin Second People's Hospital

Background: To investigate the clinical features of early primary biliary cholargitis,for the early clinical identification of primary biliary cholargitis,timely treatment and monitoring.

Method: From January 2016 to November 2021,clinical date of 69 patients diagnosed with pathologically confirmed primary biliary cholargitis,the Tianjin's Second People's Hospital.According to the pathological stages,they were divided into stage Ⅰ，Ⅱ，Ⅲ，Ⅳ period.The general date,serum biochemistry,immunoglobulins and autoimmunity antibodies of the patients were analyzed retrospectively.

Result: Early stage(Istage+IIstage) of primary biliary cholargitis patients with ALT、AST slight elevation(All <2 times normal value upper limit),comparison among the three groups had statistical significance(P<0.05). In the early stage of primary biliary cholargitis cases, 31.57% ALP was normal ,mild increase in the rest patients,and GGT elevation was more pronounced(>5 times normal value upper limit),cpmparison among the three groups about ALP had statistical significance(P<0.05).The lcterus index was not significantly increased,the ALB and A/G decreased with the disease progression.The difference among the three groups was statistical significance(P<0.05).IgM,IgG was slightly elevation,CHO was slightly elevation,TG was normal,but the difference among the three groups was no statistical significance(P>0.05).The early detection rate of AMA,Gp120 was 57.90%, 15.79%,higher than that of phase III and phase IV respectively,and AMA was the hightest. The early detection rate of ANA was hightest in cytoplasmic granulosa type 39.47%.When AMA and AMA-M2 were negative,the positive rate of ANA centromere type was the highest.

Conclusion: In early primary biliary cholargitis patients,liver function was normal or slightly abnormal,and GGT was the main index of cholestasis,with or without specific autoantibodies,it has certain significance for diagnosis.

Table and Figure:

Figure 1. Comoarision of biochemical and immunoglobulin levels of liver function in different stages

	Early stage (n = 38)	III stage (n = 19)	IV stage (n = 12)	H	P
ALT	53.50 (30.50~133.28)	53.00(24.00~140.00)	80.00(42.78~127.38)	0.938	0.626
AST	54.70 (33.75~106.00) *	69.00(39.00~114.50)	112.20(81.18~136.25)	6.629	0.036
TBA	7.50 (3.00~36.80) *	18.00(7.00~43.50)	28.20(18~111.50)	7.395	0.025
TBIL	15.85 (11.48~35.33) *	15.50(13.60~23.30) *	61.15(28.13~114.25)	11.075	0.004
DBIL	5.30 (3.53~18.03) *	8.00(1.90~11.60) *	42.25(15.80~67.25)	11.323	0.003
ALB	42.30 (38.40~45.00) *	39.90(38.10~43.50)	35.75(30.45~41.00)	11.024	0.004
A/G	1.20 (1.10~1.40) *	1.20(0.90~1.40)	0.90(0.70~1.08)	13.354	0.001
ALP	197.50 (114.50~414.00) *	238.00(153.00~411.40)	463.50(329.60~770.53)	9.855	0.007
GGT	267.25(146.50~686.93)	514.00(297.80~758.00)	336.45(264.90~648.00)	3.098	0.212
CHO	5.66 (4.60~7.02)	6.17(5.14~7.36)	6.77(4.91~6.99)	1.362	0.506
TG	1.26 (0.94~1.68)	1.60(1.26~2.10) *	1.05(0.75~1.46)	8.168	0.017
IgG	16.45 (13.19~19.37)	17.40(14.70~22.72)	20.00(13.98~24.43)	2.532	0.282
IgA	2.73 (2.08~3.46)	3.46(2.58~4.51)	3.40(2.40~4.44)	4.983	0.083
IgM	2.97 (1.74~4.47)	3.57(2.16~4.900)	3.67(1.92~6.77)	0.835	0.659
C3	0.30 (0.26~1.94)	0.33(1.03~2.09)	0.34(0.98~1.92)	1.303	0.245
C4	0.08(0.03~0.39)	0.09(0.12~0.47)	0.09(0.08~0.37)	0.836	0.384

Figure 2. Comparison of autoantibody levels in different stages

		Early stage (%)	III stage (%)	IV stage (%)	P
AMA		22 (57.90)	11 (57.90)	6 (50.00)	0.882
AMA-M2		16 (42.11)	12 (66.67)	3 (25.00)	0.100
Sp100		5 (13.16)	3 (15.79)	5 (41.67)	0.100
Gp210		6 (15.79)	2 (10.53)	1 (8.33)	0.897
ACA		2 (5.26)	0 (0)	2 (16.67)	0.142
SSA/Ro52		6 (15.79)	3 (15.79)	3 (25.00)	0.828
ANA	Cytoplasmic granulosa	15 (39.47)	10 (52.63)	4 (33.33)	0.509
	Centrometric pattern	7 (18.42)	4 (21.05)	3 (25.00)	0.919
	Nuclear membrane type	7 (18.42)	5 (26.32)	3 (25.00)	0.725

❖ AA-054

Comprehensive analysis of competing endogenous RNA network focusing on long non-coding RNA involved in cirrhotic hepatocellular carcinoma

Yuli Zhang[1], Dinggui Chen[2], Miaomiao Yang[2], Xianfeng Qian[2], Chunmei Long[2], Zhongwei Zheng[2]
[1]Department of Pharmacy, The Third People's Hospital of Changzhou, Changzhou City, Jiangsu Province 213001, China,
[2]Department of Gastroenterology, The Third People's Hospital of Changzhou, 300 Lanling North Road, Changzhou City, Jiangsu 213001, China

Background: The role of long noncoding RNAs- (lncRNAs-) associated competing endogenous RNA (ceRNA) in the field of hepatocellular carcinoma (HCC) biology is well established, but the involvement of lncRNAs competing interactions in the progression of liver cirrhosis to HCC is still unclear. We aimed to explore the differential expression profiles of lncRNAs, microRNAs (miRNA), and messenger RNAs (mRNAs) to construct a functional ceRNA network in cirrhotic HCC.

Method: The lncRNA, miRNA, and mRNA expression datasets were obtained from Gene Expression Omnibus and The Cancer Genome Atlas. Based on miRanda and TargetScan, the HCC-specific ceRNA network was constructed to illustrate the coexpression regulatory relationship of lncRNAs, miRNAs, and mRNAs. The potential prognostic indicators in the network were confirmed by survival analysis and validated by qRT-PCR.

Result:A total of 74 lncRNAs, 36 intersection miRNAs, and 949 mRNAs were differentially expressed in cirrhotic HCC samples compared with cirrhosis samples. We constructed a ceRNA network, including 47 lncRNAs, 35 miRNAs, and 168 mRNAs. Survival analysis demonstrated that 2 lncRNAs (EGOT and SERHL), 4 miRNAs, and 40 mRNAs were significantly associated with the overall survival of HCC patients. Two novel regulatory pathways, EGOT-miR-32-5p-XYLT2 axis and SERHL-miR-1269a/miR-193b-3p-BCL2L1/SYK/ARNT/CHST3/LPCAT1 axis, were built up and contribute to the underlying mechanism of HCC pathogenesis. The higher-expressed SERHL was associated with a higher risk of all-cause death. The expressions of SERHL-miR-1269a-BCL2L1 were significantly different using qRT-PCR in vitro studies.

Conclusion: LncRNAs EGOT and SERHL might serve as effective prognostic biomarkers and potential therapeutic targets in cirrhotic HCC treatment.

Table and Figure:

Figure 1. Prognosis prediction for differentially expressed lncRNAs

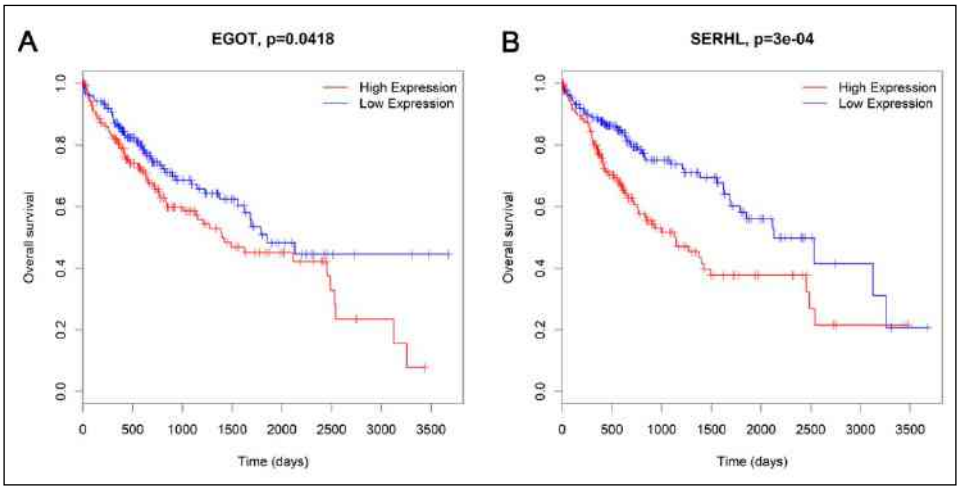

Figure 2. Nomogram to predict the probability of 5-year survival in HCC patients based on AFP, serum albumin, pathologic stage, and lncRNA.

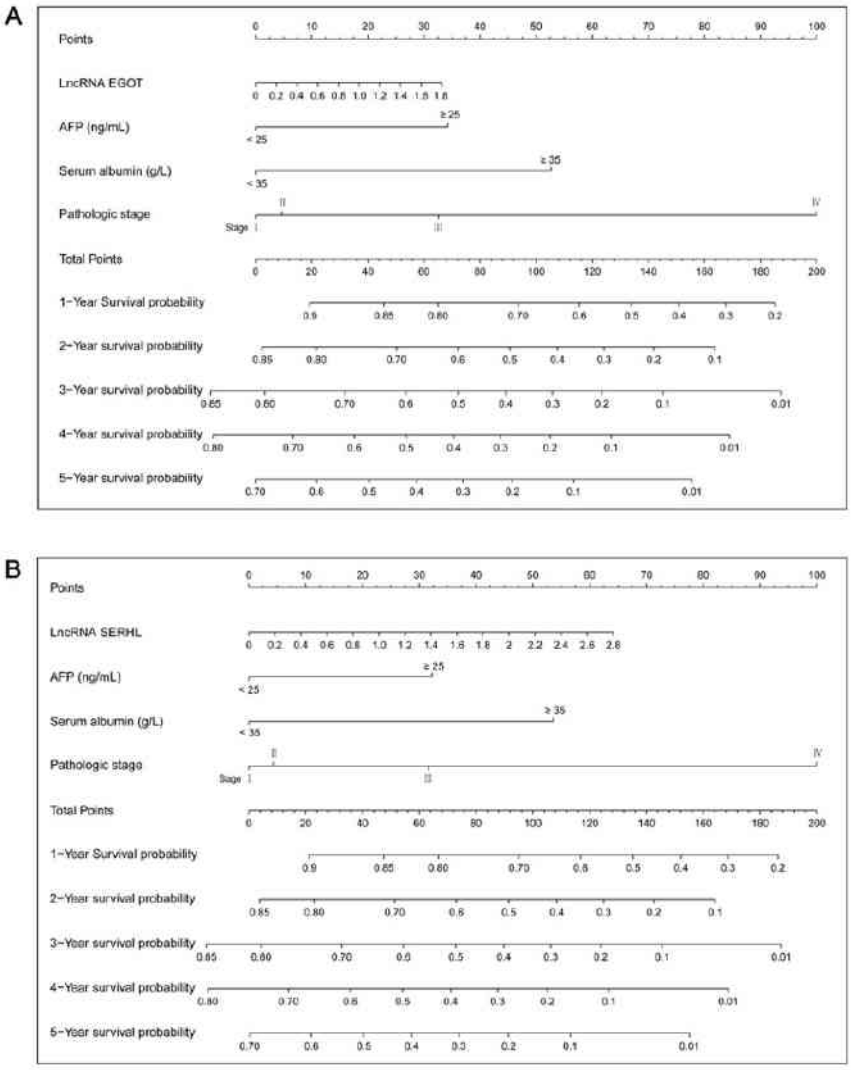

❖ AA-055

CHI3L1 detects over 12% of AFP/AFP-L3/DCP triple negative HCC cases and the four-biomarker panel offers much improved performance for HCC diagnosis

Biaoyang Lin[1], Yanji Jiang[2], Yunxiang Zhou[3], Yingchun Liu[2], Qian Guo[4], Shicheng Zhan[3], Cunli Nong[5], Yingying Ma[1], Hongping Yu[2,3]
[1]Zhejiang Uinv, [2]Guangxi Medical University Cancer Hospital, [3]Guangxi Medical University, [4]Liuzhou Worker's Hospital,, [5]Liuzhou Worker's Hospital

Background: Hepatocellular carcinoma (HCC) remains a major global health burden, with an estimated incidence over 1 million cases by 2025. Early detection of HCC is the most effective way to an effective therapy and to prolong survival time for the patients. Currently, AFP, AFP-L3 and DCP triple marker combination are the best combination biomarker panel, and a recent meta-analysis showed an overall sensitivity and specificity of 88% and 79% respectively. There is still room for improvement. Chitinase 3 like protein 1(CHI3L1) is liver enriched protein involved in the activation of astrocytes and macrophages in the liver. Here we aim to study whether CHI3L1 have added value to improve HCC diagnosis alone or in combination with AFP, AFP-L3 and DCP.

Method: We analyzed the serum levels of CHI3L1, AFP, AFP-L3 and DCP for 847 clinically diagnosed HCC cases (The HCC group) and 400 healthy individuals (the healthy group). ROC analysis was conducted for the individual marker and their combinations.

Result: The serum level of each of the four biomarker CHI3L1, AFP, AFP-L3 and DCP was statistically significantly higher in the HCC group compared with the heathy group (P <0.001). ROC analysis showed that the AUC and the Kappa values for diagnosing HCC using CHI3L1 were 0.906 and 0.665 respectively with the optimal cutoff values of 72.68 ng/ml for the dataset, which surpassed the performance of any of the three single biomarkers (Table 1). The combination of CHI3L1 with AFP, AFP-L3 and DCP further improved the performance with an AUC and the Kappa values of 0.977 and 0.845 respectively (Table 1). In addition, CHI3L1 alone help to identify 107 cases (12.63%) of AFP, AFP-L3, DCP triple negative HCC cases in 847 cases using the cutoff values of 72.68 ng/ml.

Conclusion:CHI3L1 detects over 12% of AFP/AFP-L3/DCP triple negative HCC cases and the four biomarker panel using CHI3L1, AFP, AFP-L3 and DCP offers much improved performance for HCC diagnosis. #LB and YJ are co-first authors

Table and Figure:

Figure 1. The AUC for HCC diagnosis using CHI3L1，AFP，AFP-L3，DCP or their combinations

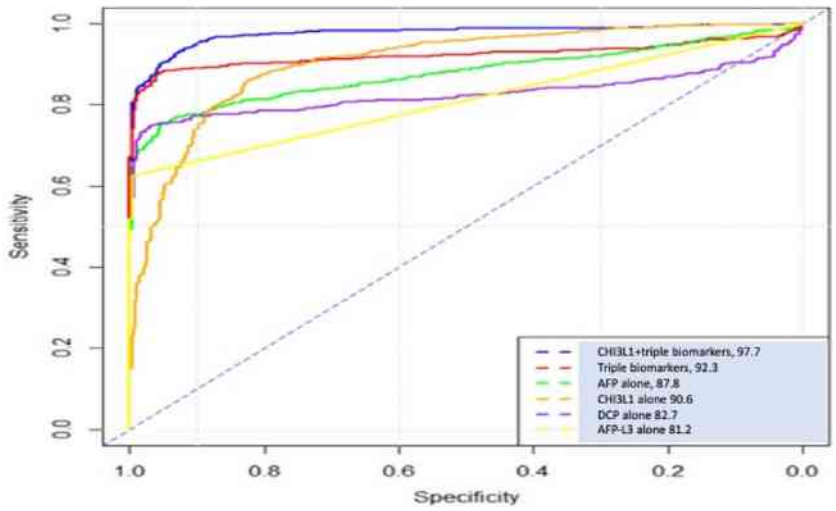

Figure 2. Table 1: Performance of CHI3L1, AFP, AFL-L3, DCP and their combinations

Table 1: Performance of CHI3L1, AFP, AFL-L3, DCP and their combinations

biomarker	Sensitivity	Specificity	AUC	AUC (95CI%)	Cutoff	Kappa
CHI3L1	0.861	0.825	90.6	88.9-92.4	72.68	0.665
AFP	0.75	0.955	87.8	85.9-89.2	6.011	0.498
DCP	0.74	0.978	82.7	80.4-85.0	33.96	0.611
AFP-L3	0.625	0.998	81.2	78.9-83.4	0.83	0.514
AFP/AFP-L3/DCP	0.878	0.958	92.3	90.7-93.9	1.647	0.791
CHI3L1+AFP/AFP-L3/DCP	0.933	0.927	97.7	96.9-98.4	3.971	0.845

❖ AA-056

Identification transcriptional landscape and potential biomarker genes of HBV-related fibrosis by weighted gene co-expression network analysis

Yuwei Liu[1]
[1]*Department of Hepatology, The First Hospital of Jilin University*

Background: Liver fibrosis is a progressive disease with multiple etiology. HBV infection is the major etiology of liver fibrosis and cirrhosis. We aimed to construct a co-expression network to explore the transcriptional landscape and potential biomarker genes of HBV related fibrosis.

Method: The transcriptional profiles were obtained from the GSE84044 dataset. Weighted gene co-expression network analysis (WGCNA) was used to determine the co-expression modules and genes. Functional enrichment analysis was conducted to analyze the top Gene Ontology (GO) term and the Kyoto Encyclopedia of Genes and Genomes (KEGG) pathway. Protein-protein interaction was conducted to identify the hub genes. Receiver Operating Characteristic (ROC) curve analysis was performed to evaluate the predictive power for liver fibrosis of the hub genes.

Result: 226 genes in modules were significantly associated with fibrosis. GO and KEGG enrichment analysis suggested they were mainly related to oxidation-reduction process, complement and coagulation cascades, and carbon metabolism. Six hub genes (SPARC, THBS2, LUM, DCN, IGFBP7, and ITGAV) related to fibrosis were determined. Compared with COL1A1, SPARC had a better predictive power in patients with advanced fibrosis (S≥3), while SPARC, THBS2, LUM, IGFBP7, and ITGAV had a better predictive power in patients with early cirrhosis (S=4).

Conclusion: The results identified the transcriptional landscape and hub genes of HBV related fibrosis, which provided a framework and information to explore the mechanism and potential therapeutic targets of liver fibrosis.

Table and Figure:

Figure 1. Identify trait-related modules and genes

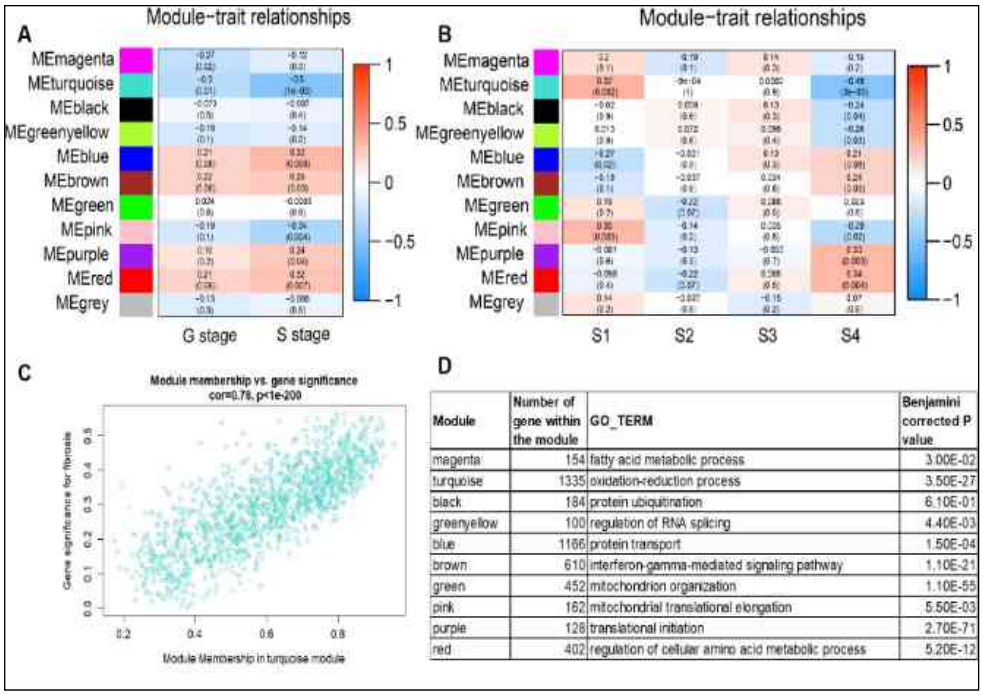

Module	Number of gene within the module	GO_TERM	Benjamini corrected P value
magenta	154	fatty acid metabolic process	3.00E-02
turquoise	1335	oxidation-reduction process	3.50E-27
black	184	protein ubiquitination	6.10E-01
greenyellow	100	regulation of RNA splicing	4.40E-03
blue	1166	protein transport	1.50E-04
brown	610	interferon-gamma-mediated signaling pathway	1.10E-21
green	452	mitochondrion organization	1.10E-55
pink	162	mitochondrial translational elongation	5.50E-03
purple	128	translational initiation	2.70E-71
red	402	regulation of cellular amino acid metabolic process	5.20E-12

Figure 2. Identify the predictive value of the hub genes by ROC analysis

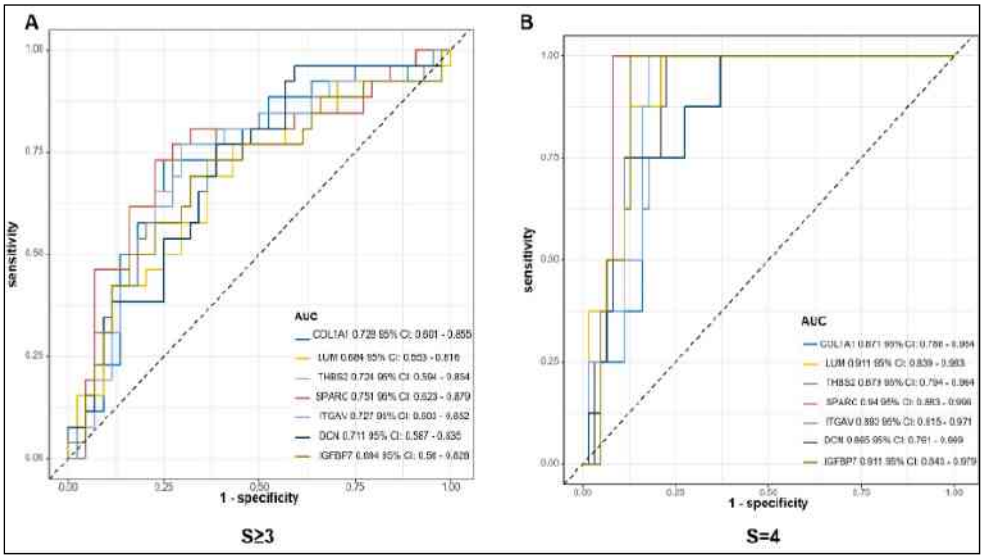

❖ AA-057

A non-invasive model based on the virtual portal pressure gradient to predict the first variceal hemorrhage in cirrhotic patients

Shuo Zhang[1], Weiping Song[1], Bo Yang[1], Haoyu Jia[1], Shuai Chen[1], Jing Li[1], Changqing Yang[1]
[1]Department of Gastroenterology and Hepatology, Tongji Hospital, School of Medicine, Tongji University, Shanghai 200092, China

Background: This study aimed to establish a non-invasive model based on the virtual portal pressure gradient to predict the first variceal hemorrhage in patients with cirrhosis.

Method: This single-center study prospectively enrolled cirrhotic patients as the training and validation cohorts during different time periods. The portal pressure gradient-detection software 1.0 was used to perform virtual portal pressure gradient calculation, which involves 2 steps including three-dimensional reconstruction of portal vein tree and subsequent application of computational fluid dynamics. All patients were given standard primary prophylaxis against variceal hemorrhage and followed-up for 2 years. Data from the training cohort were assessed using univariate and multivariate Cox regression and Kaplan-Meier analyses, by which a nomogram with its dynamic form was developed to estimate the probability of variceal hemorrhage.

Result: In the training cohort (n=128), 37 (28.9%) experienced variceal hemorrhage during 2-year follow-up. Four variables including virtual portal pressure gradient≥10.5 mmHg (P<0.001), platelet<56 ×109/L (P=0.048), albumin<32 g/L (P<0.001) and INR≥1.2 (P=0.022) were identified as independent risk factors of variceal hemorrhage, among which virtual portal pressure gradient showed the best diagnostic performance (AUC=0.875). Subsequently, these predictors were incorporated into the nomogram, of which C-indexes were 0.891 and 0.926 for the training and validation cohorts, respectively. Calibration curves demonstrated a great calibration ability of the model. At the threshold probabilities of 0.1-0.6 (1-year) and 0.1-1.0 (2-year), this nomogram could offer more net benefits in decision curve analysis.

Conclusion: The virtual portal pressure gradient-based nomogram could be used for risk stratification of the first variceal hemorrhage in patients with cirrhosis.

Table and Figure:

Figure 1. Nomogram for prediction of the first variceal hemorrhage in cirrhotic patients with high-risk varices

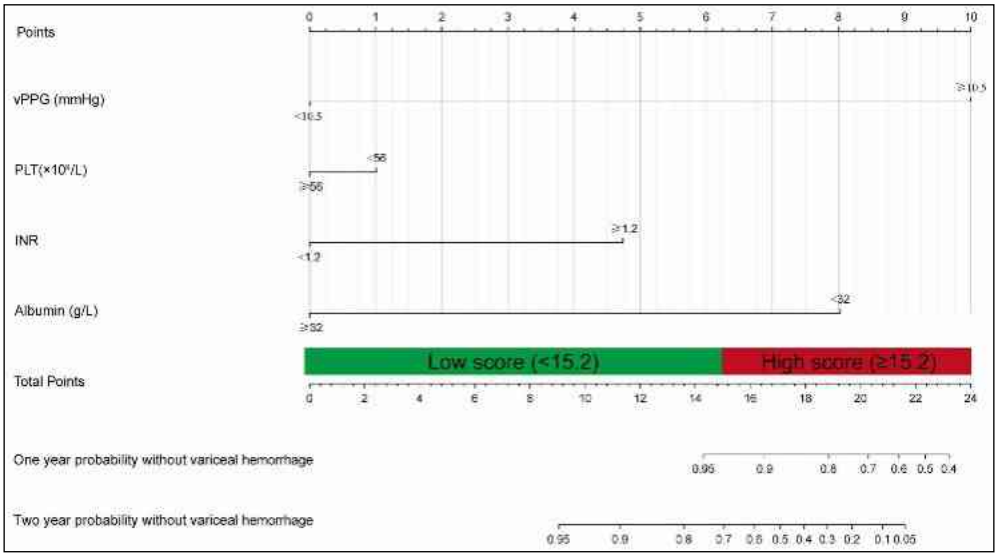

Figure 2. Validation and evaluation of the nomogram

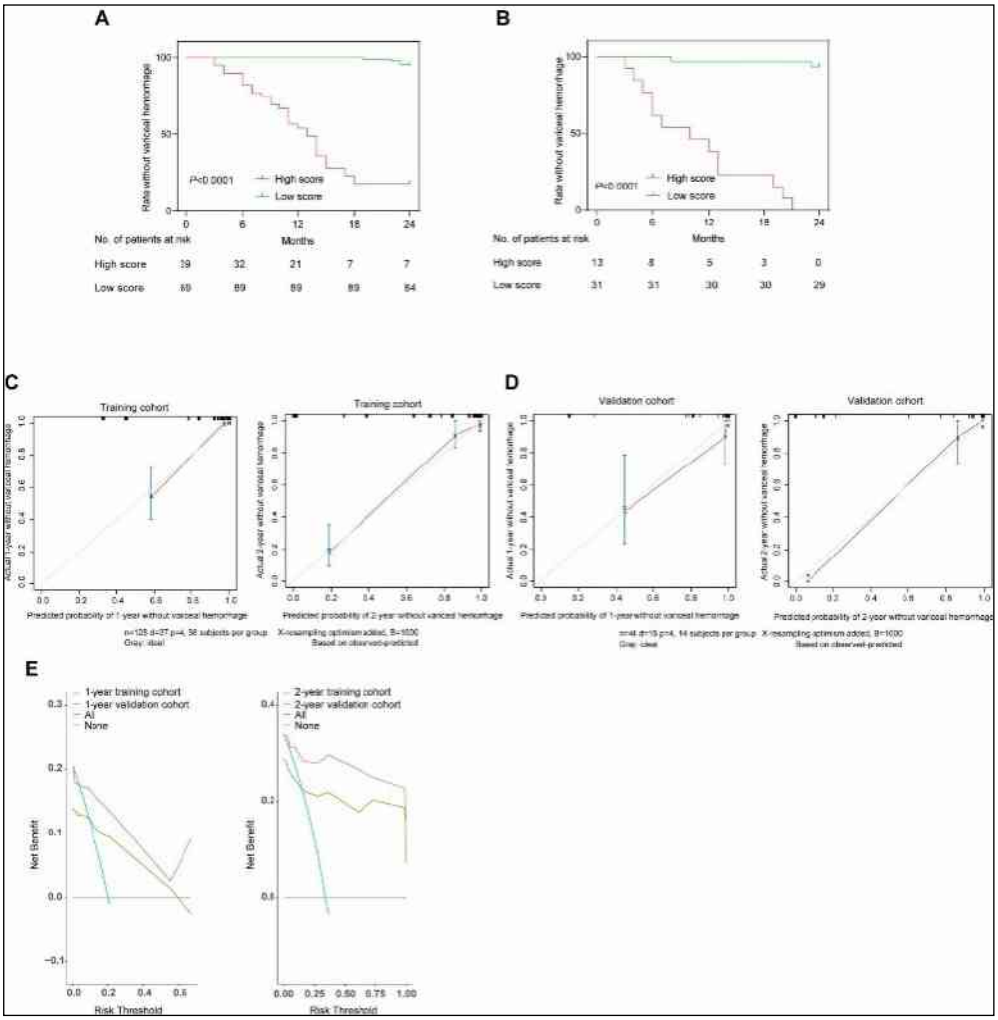

❖ AA-058

An N-terminal Propeptide of Type 3 Collagen-Based Sequential Algorithm can identify high-risk steatohepatitis and severe fibrosis in MAFLD

Liangjie Tang[1], Gang Li[1], Mohammed Eslam[2], Peiwu Zhu[3], Suidan Chen[3], Howard Howai Leung[4], Ouyang Huang[3], Grace Laihung Wong[4], Yujie Zhou[5], Morten Karsdal[6], Diana Julie Leeming[6], Pei Pei[7], Cong Wang[7], Haiyang Yuan[3], Christopher D Byrne[8], Giovanni Targher[9], Jacob George[2], Vincent Waisun Wong[4], Minghua Zheng[1]

[1]The First Affiliated Hospital of Wenzhou Medical University, [2]University of Sydney, [3] The First Affiliated Hospital of Wenzhou Medical University, [4]The Chinese University of Hong Kong, [5]Shanghai Jiao Tong University, [6]Nordic Bioscience Biomarkers and Research A/S, [7]Fosun Diagnostics (Shanghai) Co., Ltd, [8]Southampton General Hospital, [9]University and Azienda Ospedaliera Universitaria Integrata of Verona

Background: With metabolic dysfunction-associated fatty liver disease (MAFLD) incidence and prevalence increasing, there is an urgent need for non-invasive diagnostic tests to accurately screen high-risk patients for liver inflammation and fibrosis. We aimed to develop a novel sequential algorithm based on N-terminal propeptide of type 3 collagen (PRO-C3) for disease risk stratification in patients with MAFLD.

Method:A derivation and independent validation cohort (327 and 142 biopsy-confirmed patients with MAFLD) were studied. We compared the diagnostic performance of various non-invasive scores in different disease states, and a novel sequential algorithm was constructed by combining the best performing non-invasive scores.

Result: For patients with high-risk progressive steatohepatitis (i.e., steatohepatitis + NAFLD activity score ≥ 4 + F ≥ 2), the AUROC of FAST score was 0.801 (95% confidence interval (CI): 0.739-0.863), and the negative predictive value (NPV) was 0.951. For advanced fibrosis (≥ F3) and cirrhosis (F4), the AUROC of ADAPT and Agile 4 were 0.879 (95% CI: 0.825-0.933) and 0.943 (95% CI: 0.892-0.994), and the NPV was 0.972 and 0.992. Sequential algorithm of ADAPT + Agile 4 combination was better than other combinations for better risk stratification of patients with severe fibrosis (AUROC=0.88), with similar results in the validation cohort. Meanwhile, in all subgroup analyses (stratifying by sex, age, diabetes, NAS, BMI and ALT), ADAPT + Agile 4 had good diagnostic performance.

Conclusion: The new sequential algorithm reliably identifies liver inflammation and fibrosis in MAFLD, making it easier to exclude low-risk patients and recommending high-risk patients for clinical trials.

Table and Figure:

Figure 1.(A) The area under the receiver operating characteristic curves (AUROC) for predicting F≥ 3 fibrosis. (B) Decision curve analysis (DCA) for the combined diagnosis of non-invasive fibrosis scores. The Sankey diagrams showed the distribution of patients in the true positive (TP), true negative (TN), false positive (FP), false negative (FN), and indeterminate groups.

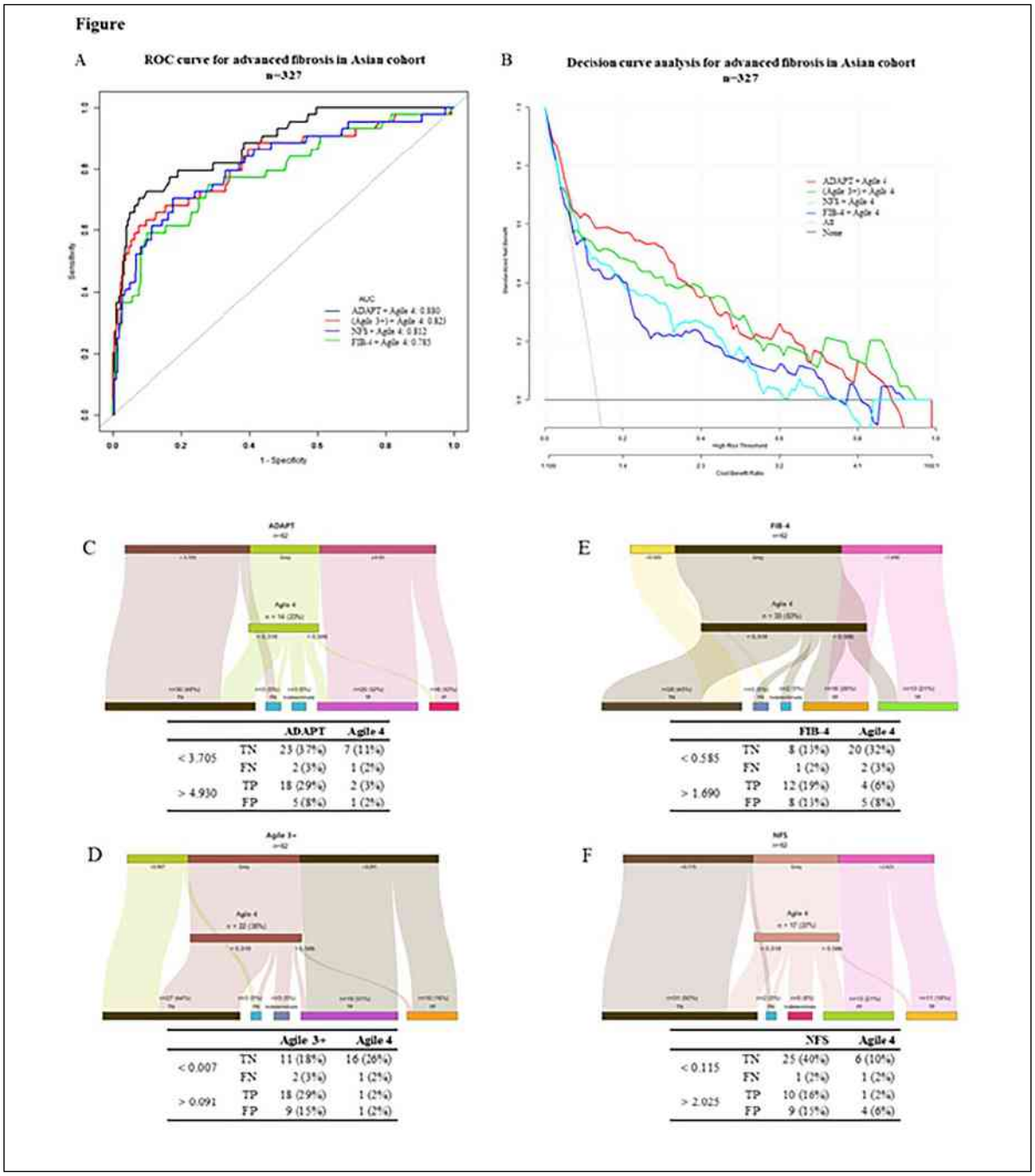

		ADAPT	Agile 4
< 3.705	TN	23 (37%)	7 (11%)
	FN	2 (3%)	1 (2%)
> 4.930	TP	18 (29%)	2 (3%)
	FP	5 (8%)	1 (2%)

		Agile 3+	Agile 4
< 0.007	TN	11 (18%)	16 (26%)
	FN	2 (3%)	1 (2%)
> 0.091	TP	18 (29%)	1 (2%)
	FP	9 (15%)	1 (2%)

		FIB-4	Agile 4
< 0.585	TN	8 (13%)	20 (32%)
	FN	1 (2%)	2 (3%)
> 1.690	TP	12 (19%)	4 (6%)
	FP	8 (13%)	5 (8%)

		NFS	Agile 4
< 0.115	TN	25 (40%)	6 (10%)
	FN	1 (2%)	1 (2%)
> 2.025	TP	10 (16%)	1 (2%)
	FP	9 (15%)	4 (6%)

Figure 2. Flow chart for the 3-step serial combination of tests in the sequential algorithm.

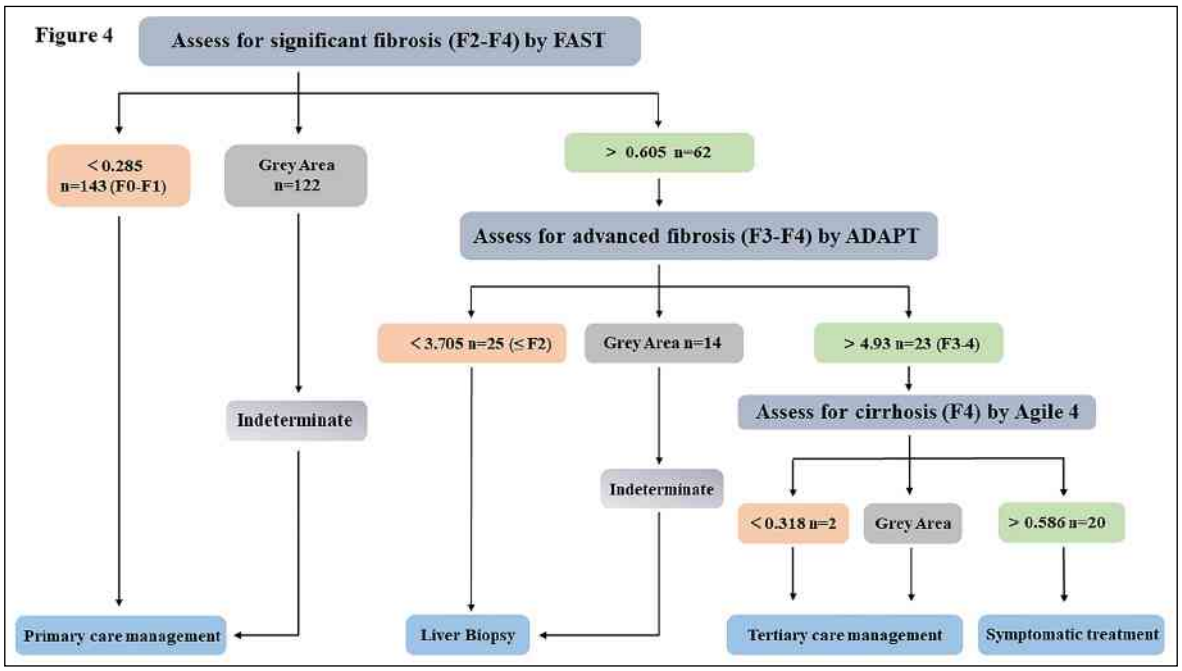

❖ AA-059

Mitofusin 2 Gene Polymorphisms and Metabolic dysfunction Associated Fatty Liver Disease: a case-control study in a Chinese population

Xiwei Yuan[1], Mengmeng Hou[2], Yiqi Wang[2], Siyu Zhang[2], Lu Li[2], Yingjun Mi[2], Huijuan Du[2], Songhao Yu[2], Yuemin Nan[2]

[1]Department of Traditional and Western Medical Hepatology, Third Hospital of Hebei Medical University, shijiazhuang, China, [2]Third Hospital of Hebei Medical University

Background: Mitofusion-2 (Mfn2) may have a role in the development of mitochondrial oxidative stress, insulin resistance and endoplasmic reticulum stress. Such conditions promote the development of metabolic dysfunction associated fatty liver disease (MAFLD). The current study explored the association between common single nucleotide polymorphisms (SNPs) of Mfn2 and MAFLD in a northern Han Chinese population.

Method: Six SNPs of the Mfn2 gene (rs2336384, rs873458, rs873457, rs4846085, rs2878677 and rs2236057) were genotyped using the ligase detection reaction (LDR) in 466 MAFLD patients and 423 healthy controls. Genotype and allele frequencies were calculated, along with haplotype analysis and pairwise linkage disequilibrium.

Result: The genotype distribution of rs2336384, rs2878677 and rs2236057 among the MAFLD patients showed a different pattern from that of healthy controls ($P<0.05$), indicated by Chi-square analyses. The C allele prevalence of rs2878677 was higher in the MAFLD patients ($P<0.05$). Binary logistic regression analysis showed that an increased risk of MAFLD was significantly correlated with the patients carrying the GG genotype of rs2336384; CC genotype of rs873457; TT genotype of rs4846085; TT genotype of rs2878677 and the AA genotype of rs2236057 (OR=1.585, P=0.006; OR=1.485, P=0.0017; OR=1.388, P=0.048; OR=1.722, P=0.002; OR=1.560, P=0.012, respectively). The Rs2336384 SNP was significantly associated with MAFLD in males and the rs2878677 SNP in females when stratified by gender. Haplotype analysis revealed that the GGCTTA haplotype was negatively associated with MAFLD.

Conclusion: The current findings suggest a strong link between Mfn2 gene polymorphisms and metabolic dysfunction associated fatty liver disease.

Table and Figure:

Figure 1. Linkage disequilibrium (LD) block defined by the Haploview program based on the solid spine of LD method. a. represents LD result of D'; b. represents LD result of r2.

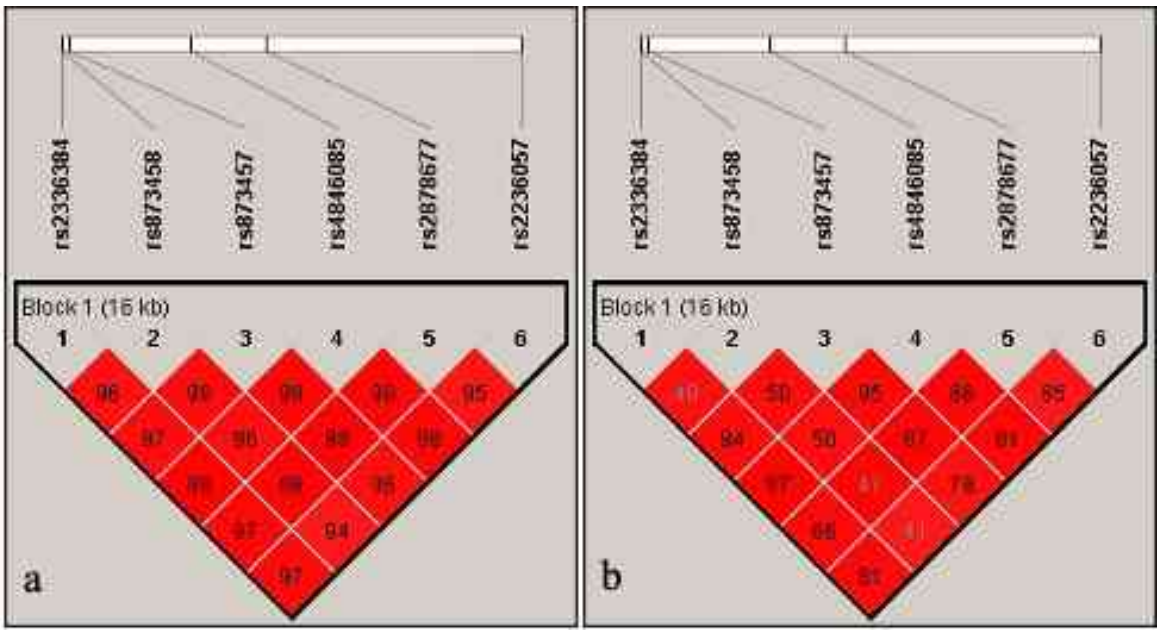

Figure 2. Haplotype Analyses of the Mfn2 Polymorphisms in MAFLD and Control Subjects

Table 4. Haplotype Analyses of the Mfn2 Polymorphisms in MAFLD and Control Subjects

Haplotype						Frequency		X^2	*P*	Male		X^2	*P*	Female		X^2	*P*
M1	M2	M3	M4	M5	M6	Control	MAFLD			Control	MAFLD			Control	MAFLD		
G	G	C	T	T	A	0.452	0.397	4.796	**0.029**	0.451	0.399	3.350	0.067	0.453	0.410	1.966	0.161
T	A	G	C	C	G	0.353	0.359	0.170	0.680	0.361	0.384	1.108	0.293	0.348	0.334	0.204	0.651
T	G	G	C	C	G	0.145	0.158	0.628	0.428	0.142	0.130	0.228	0.633	0.146	0.174	2.054	0.152
G	G	C	T	T	G	0.023	0.020	0.048	0.826	0.022	0.029	0.855	0.355	0.023	0.019	0.334	0.564
G	G	C	T	C	G	0.019	0.024	0.591	0.442	0.019	0.022	0.002	0.961	0.019	0.016	0.007	0.935

M1: rs2336384, M2: rs873458, M3: rs873457, M4: 4846085, M5: 2878677, M6: 2236057.

❖ AA-060

CHI3L1 as a non-invasive marker for effective selecting of chronic HBV patient with normal ALT levels but with advanced liver fibrosis for treatments

Biaoyang Lin[1], Yunhua Liu[2], Shengjun Wu[3], Hongfei Zhang[4]
[1]Zhejiang Univ , [2]The Second Hospital of Yunnan Province, [3]Sir Run Run Shaw Hospital, School of Medicine, Zhejiang University, [4]Changfeng Hospital of Jumei Medical group

Background:WHO has mandated a goal for reaching 80% treatment rate for eligible HBV patients by 2030. However, the current treatment rate for eligible HBV patients is only about 8% worldwide due to lack of effective and noninvasive means to identify those eligible patients. Therefore, we aim to test the utility of using CHI3L1 for the identification of occult ongoing liver fibrosis for those chronic HBV patients with normal ALT levels.

Method: Serum CHI3L1 levels were measured by the ELISA kit with CFDA approval and CE mark status from Hangzhou Proprium Biotech Co. Ltd (Hangzhou, China).

Result: We found that 20 of 61 (46.5%) chronic HBV patients with biopsy-confirmed fibrosis stage > 2 or inflammation >2 and normal ALT have CHI3L1 level greater than 79 ng/ml, which was previously established to identify fibrosis stage > 2 for HBV patients. Furthermore, we identified 10 naïve chronic patients (no prior antiviral treatments) with CHI3L1 > 79 ng/ml but normal ALT (<40), and subjected them to entecavir treatments. Nine of the 10 patients showed reduced CHI3L1 levels at week 12.
Finally, we recruited 405 patients who underwent antiviral treatment and measured the CHI3L1 in 2-3 month intervals. 73.09% showed improved fibrosis (CHI3L1 reduced > 5 ng/ml), 7.16% showed stable fibrosis and 19.75% still showed progressive fibrosis, which await longer antiviral treatments.

Conclusion:CHI3L1 is a non-invasive surrogate serum marker for effectively identifying chronic HBV patient with normal ALT levels but with occult ongoing liver fibrosis passing stage 2 for starting antiviral treatments.

Table and Figure:

Figure 1. Proposed schema for using CHI3L1 for initiating treatment for chronic HBV patients with normal ALT levels.

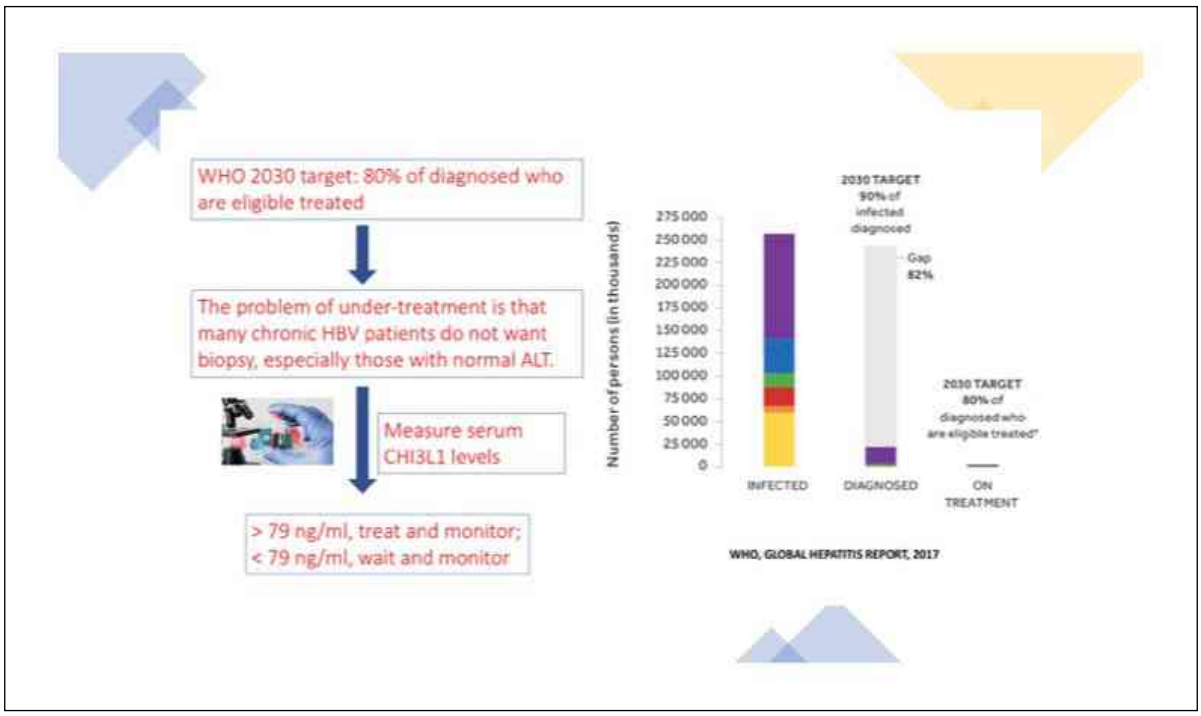

❖ AA-061

AFL score, a novel risk score based on Liver stiffness measurement, presents a good prediction accuracy in predicting the development of hepatocellular carcinoma in patients with chronic hepatitis

Zhang Xiao Xiao[1], Nan Yue Min[2]
[1]Department of Traditional and Western Medical Hepatology, Third Hospital of Hebei Medical University,
[2]Department of Traditional and Western Medical Hepatology, Third Hospital of Hebei Medical University,

Background: To investigate the impact of liver stiffness measurement (LSM) on the incidences of hepatocellular carcinoma (HCC) and establish a novel risk model based on the LSM to predict the probability of HCC in chronic hepatitis B (CHB) patients.

Method: We retrospectively collected 288 CHB patients with valid LSM and complete follow-up data between January 2016 and March 2020. Patients were divided into two groups by presence or absence of HCC during follow-up, and the baseline characteristics were compared. Univariate and multivariable Cox regression analyses were applied to identify the independent risk predictors and establish a risk prediction model for HCC development. Furthermore, a comparison of the new model and other previous HBV-related HCC scores was conducted to evaluate the prediction performance.

Result:5.9% (17/288) of patients developed HCC during a mean duration of 37.0 months. Patients who developed HCC were older and more likely to have a higher PT, LSM value and lower PLT. A significantly higher proportion of HCC patients had baseline cirrhosis, alcoholism history, family history and diabetes mellitus compared with non-HCC patients. A predictive model and nomogram abbreviated as AFL score including age, family history and LSM was constructed to predict the risk of HCC development, which exhibited a good predictive accuracy evidenced by considerable high discrimination, with a concordance index (C-index) of 0.87 and time-dependent area under the curve (TDAUC) of 0.83, 0.84, 0.90 at 3-,4- and 5-years, respectively. Compared with other existing HBV-related HCC risk prediction models, the AFL score can more accurately predict subsequent HCC development confirmed by the highest C-index and a stable trend within 5 years.

Conclusion: The AFL score based on the LSM value provides a reliable and accurate prediction and assessment of HCC development in patients with CHB, which is beneficial to risk stratification and early intervention.

❖ AA-062

Evaluation of the association of single nucleotide polymorphism with fibrosis progression in patients with chronic hepatitis C infection after eradication

Qian Kang[1], Tan Ning[1], Hongyu Chen[2], Xiaoyuan XU[2]
[1]Peking university first hospital, [2]Peking University First Hospital

Background: The relationship of single nucleotide polymorphisms (SNPs) in patatin-like phospholipase domain containing 3 (PNPLA3) rs738409, transmembrane 6 superfamily member 2 (TM6SF2) rs58542926, and membrane bound Oacyltransferase domain containing 7 (MBOAT7) rs641738 with outcomes in patients with hepatitis C infection (HCV) is unclear. This study aimed to evaluate the association of PNPLA3, TM6SF2, and MBOAT7 with the baseline fibrosis stage and progression of liver fibrosis after HCV eradication with direct antiviral agents (DAAs).

Method:A total of 171 patients who received the DAAs at the Peking University First Hospital between June 2015 and June 2020 were included in the retrospective cohort. Transient elastography was used to determine liver stiffness measurements (LSMs) at the baseline, the end of treatment (EOT), 24 weeks after treatment (W24), and the last follow-up (LFU) visit. We used the QIAamp Blood Mini Kit (Qiagen) for whole blood genomic DNA extraction and polymerase chain reaction for PNPLA3, TM6SF2, and MBOAT7 amplification of the target gene.

Result: After 46 (23-59) months of follow-up in 171 CHC patients, multivariate Cox regression analysis showed that patients with patatin-like phospholipase domain containing 3 (PNPLA3) rs738409 CG genotype were approximately 1.5 times risk to develop advanced liver fibrosis and cirrhosis than patients with CC genotype (HR = 1.566; 95% CI = 1.02-2.575, P = 0.017). Patients with the GG genotype were approximately twice risk to develop advanced fibrosis and cirrhosis as those with the CC genotype (HR = 2.109; 95% CI = 1.36-3.271, P = 0.001). Transmembrane 6 superfamily member 2 (TM6SF2) rs58542926 CT/TT genotype was associated with the development of advanced fibrosis and cirrhosis (HR = 1.322, 95% CI = 1.003-1.857, P = 0.045; HR = 1.855, 95% CI = 1.35-2.765, P = 0.015).

Conclusion: There are significant associations between PNPLA3 rs738409 and TM6SF2 rs58542926 polymorphisms and baseline fibrosis stage and fibrosis progression in CHC

patients after HCV eradication with DAAs therapy. Therefore, such patients should be monitored and followed up to reduce the risk of fibrosis progression.

Table and Figure:

Figure 1. Univariate Cox regression analysis of PNPLA3 rs738409 and TM6SF2 rs58542926 genotypes on the cumulative probability of progression to advanced (³F3) fibrosis in 172 patients with a known duration of HCV infection. Similar results were observed in multivariate Cox regression analysis.

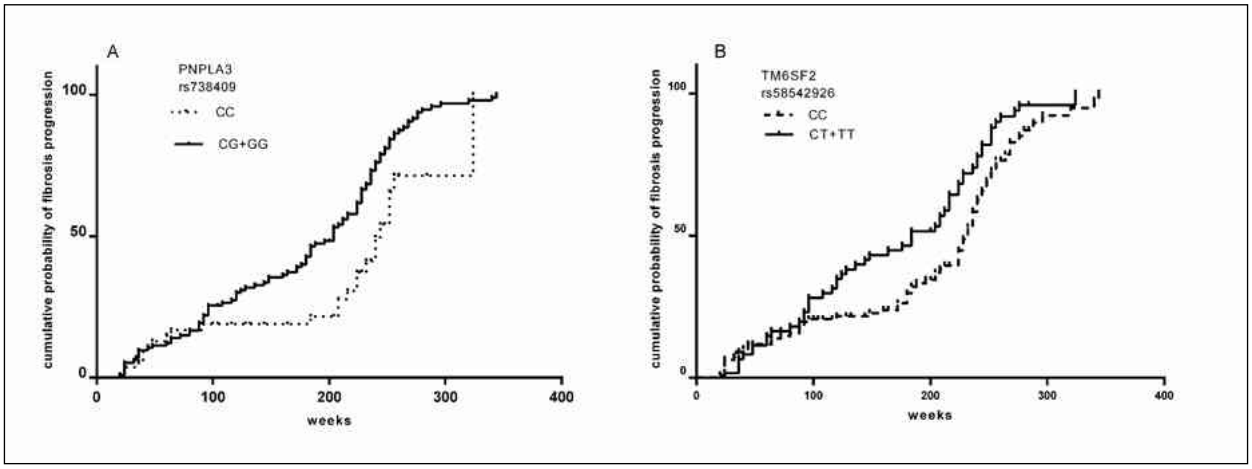

❖ AA-063

Correlation between serum liver fibrosis markers and early esophageal and gastric varices among patients with compensated liver cirrhosis: a cross-sectional analysis

Ling Mei[1], Qingling Chen[1], Jia Li[2]
[1]Department of Gastroenterology and Hepatology, Second People's Clinical College of Tianjin Medical University, Tianjin Second People's Hospital, [2]Department of Gastroenterology and Hepatology, Tianjin Second People's Hospital

Background:portal hypertension is a common complication of chronic liver diseases that is responsible for most clinical consequences of liver cirrhosis. In patients with portal hypertension, esophagogastric variceal bleeding is a leading cause of death. The majority of research focuses on high-risk esophageal and gastric varices and bleeding, with only a few on early varices. However, it is found that early intervention of esophageal and gastric varices can better improve the prognosis and reduce mortality, there is still no relevant research. Endoscopy can only observe varices on the surface of esophagus and gastric mucosa. Ultrasonic endoscopy is a combination of endoscopy and ultrasonic imaging. It can detect varices around esophagus and gastric based on gastroscope, and detect esophageal collateral veins and perforating veins earlier, which is helpful for the early diagnosis of varices. Therefore, the aim of this study was to explore the correlation between serum fibrosis markers and early esophageal and gastric varices in patients with compensatory cirrhosis.

Method: This study included 477 patients with compensated liver cirrhosis. The selected patients were categorized into two groups. Early esophageal and gastric varices group was esophageal and gastric varices were found by endoscopic ultrasonography, but not by gastroscopy, whereas the no esophageal and gastric varices group was endoscopic ultrasonography and gastroscope without varices. All patients underwent a complete biochemical workup, endoscopic ultrasonography and gastroscope. Multiple logisitic regression analysis was used to explore the association of serum fibrosis markers with early esophageal and gastric varices.

Result: Among the 477 patients with compensated liver cirrhosis 198 patients without esophageal and gastric varices and 279 patients with early esophageal and gastric varices. There was a positive correlation between serum fibrosis markers and early portal hypertension. In univariate logistic regression analysis, patients with early portal

hypertension had lower platelet count (P = 0.034), higher aspartate aminotransferase (P = 0.046), total bilirubin (P = 0.041), hyaluronic acid (P < 0.001), laminin (P < 0.001), type III procollagen (P = 0.005), type IV collagen (P = 0.002) and liver stiffness measurement (P = 0.001). Multivariate analysis showed that laminin（OR 1.011;95% CI 1.004,1.017,P=0.001） was an independent risk factor for predicting early esophageal and gastric varices in patients with compensatory cirrhosis.

Conclusion:hyaluronic acid, laminin, type III pro-collagen, and collagen IV levels were significantly associated with early portal hypertension. Higher laminin was independently associated with early esophageal and gastric varices among patients with compensated liver cirrhosis.

Table and Figure:

Figure 1. Correlations between serum fibrosis markers and clinical characteristics of patients

Variables statistics	Hyaluronic acid （ng/ml）		Laminin（ng/ml）		Type III pro-collagen（ng/ml）		Collagen type IV （ng/ml）	
	r	P	r	P	r	P	r	P
Age（years）	0.168	<0.001	0.006	0.895	-0.131	0.004	-0.116	0.011
Child class (A/B)	0.273	<0.001	0.216	<0.001	0.301	<0.001	0.291	<0.001
ALT(U/L)	0.210	<0.001	0.254	<0.001	0.439	<0.001	0.420	<0.001
AST（U/L）	0.331	<0.001	0.352	<0.001	0.518	<0.001	0.529	<0.001
TBIL (μmol/L)	0.266	<0.001	0.290	<0.001	0.289	<0.001	0.256	<0.001
ALB（g/L）	-0.401	<0.001	-0.302	<0.001	-0.431	<0.001	-0.494	<0.001
PLT($X10^9$/L)	-0.314	<0.001	-0.249	<0.001	-0.150	<0.001	-0.267	<0.001
PT（s）	0.212	<0.001	0.217	<0.001	0.300	<0.001	0.339	<0.001
LS(kPa)	0.484	<0.001	0.430	<0.001	0.469	<0.001	0.568	<0.001
Splenic diameter （mm）	0.149	0.001	0.088	0.059	0.159	0.001	0.204	<0.001
EGD(-)EUS(-/+)	0.142	0.002	0.253	<0.001	0.130	0.004	0.127	0.006

ALT alanine aminotransferase, AST aspartate aminotransferase, TBIL total bilirubin, ALB albumin, PLT platelet, PT prothrombin time, LS liver stiffness
EGD （-）esophagogastroduodenoscopy negative, EUS（-/+） endoscopic ultrasound negative or positive

Figure 2. Univariate and multivariate analysis of factors associated with early esophageal and gastric varices

Variables	Univariate analysis		Multivariate analysis	
	OR（95%CI）	P	OR（95%CI）	p
Age（years）	1.004（0.989，1.020）	0.612		
Male，n（%）	0.865（0.600，1.247）	0.436		
Aetiology of cirrhosis (HBV/HCV/other)	0.839（0.643，1.095）	0.197		
Child category (A/B)	2.158（0.988，4.713）	0.054		
ALT(U/L)	1.001（1.000，1.001）	0.246		
AST（U/L）	1.001（1.000，1.002）	0.046	0.999(0.998,1.001)	0.529
TBIL（umol/L）	1.008（1.000，1.016）	0.041	1.004(0.995,1.012)	0.387
ALB（g/L）	0.981（0.949，1.015）	0.247		
PLT($X10^9$/L)	0.996（0.993，1.000）	0.034	0.999(0.996,1.003)	0.676
PT（s）	1.056（0.971，1.149）	0.205		
Hyaluronic acid（ng/ml）	1.001（1.001，1.002）	<0.001	1.000(0.999,1.001)	0.562
Laminin（ng/ml）	1.015（1.009，1.020）	<0.001	1.011（1.004，1.018）	0.001
type III pro-collagen（ng/ml）	1.040（1.012，1.069）	0.005	0.999(0.995,1.002)	0.494
Collagen type IV（ng/ml）	1.004（1.001，1.006）	0.002	1.003(0.968,1.040)	0.862
LS（Kpa）	1.032（1.113，1.051）	0.001	1.013(0.988,1.038)	0.308
Splenic diameter(mm)	1.003（0.993，1.013）	0.569		

ALT alanine aminotransferase, AST aspartate aminotransferase, TBIL total bilirubin, ALB albumin, PLT platelet, PT prothrombin time, LS liver stiffness

❖ AA-064

The value of blood IGFBP7 in evaluating the degree of liver fibrosis in patients with chronic hepatitis B virus infection

Huanqin Han[1], Lixian Wu[1]
[1]Affiliated Hospital of Guangdong Medical University

Background: The activation of hepatic stellate cells (HSCs) is one of the key links in the occurrence and development of liver fibrosis. The expression of IGFBP7, mainly derived from hepatic stellate cells (HSCs), may be increased upon HSC activation. However, whether the concentration of IGFBP7 in the blood circulation increases during liver fibrosis has not been reported. We initially explored the value of blood IGFBP7 as a biomarker of liver fibrosis in patients with chronic hepatitis B (CHB).

Method: Sixty-four patients with chronic HBV infection (HBV group, including HBV carriers, CHB patients, and patients with hepatitis B cirrhosis) and 10 age- and sex-matched healthy subjects (normal control group) were enrolled. Their clinical data were collected and patients with conditions affecting the accuracy of the LSM were excluded. Their liver stiffness value (LSM) was detected by FibroTouch, and 1 ml of their fasting serum was collected and stored in a -80°C refrigerator for testing. According to the clinical data and LSM, HBV group were divided into F0-1 group (no liver fibrosis), F2-3 group (liver fibrosis), F3-4 group (significant liver fibrosis or cirrhosis), and F4 group (liver cirrhosis). The blood IGFBP7 values of each subgroup were compared, and the correlation between LSM and blood IGFBP7 in the HBV group was analyzed; the sensitivity and specificity of blood IGFBP7 in diagnosing liver fibrosis grades2-3 were calculated.

Result: There were 64 cases in the HBV group, including 24 cases in the F0-1 group, 17 cases in the F2-3 group, 8 cases in the F3-4 group, and 15 cases in the F4 group. The serum IGFBP7 in the HBV group was (83.82±51.11) ng/ml, which was higher than that in the normal control group (44.55±17.43) ng/ml (P<0.001). The LSM value and blood IGFBP7 of each subgroup in the HBV group were all in the F4 group>F3-4 group>F2-3 group>F0-1 group (all P<0.05). And, LSM value was significantly correlated with blood IGBP7 (r=0.742, P<0.001). Based on LSM as the surrogate gold standard, the area under the curve (AUC) of the receiver operating curve (ROC) of serum IGFBP7 for the diagnosis of liver fibrosis grades 2-3 in chronic HBV-infected patients was 0.852 (95%CI 0.739-0.965, SE 0.085) (P<0.001). When the blood IGFBP7 was 56.64 ng/ml as the cut-off

value (maximum Youden index), the sensitivity of diagnosing grades 2-3 of fibrosis was 66.7% and the specificity was 95.2%.

Conclusion: Serum IGFBP7 was significantly positively correlated with the degree of liver fibrosis in patients with chronic HBV infection, and had high sensitivity and specificity in the diagnosis of grade 2-3 liver fibrosis in patients with CHB. Blood IGFBP7 is expected to be used to screen early liver fibrosis and cirrhosis in patients with chronic HBV infection.

Table and Figure:

Figure 1. Trend chart of liver stiffness value and blood IGFBP7 in HBV-infected patients. According to liver stiffness value (LSM), patients with chronic HBV infection were divided into F0-1, F2-3, F3-4, and F4 with gradually increasing degree of liver fibrosis. In the four groups, the mean value of blood IGFBP7 measured in the four groups was consistent with the mean value of LSM. (*P<0.05)

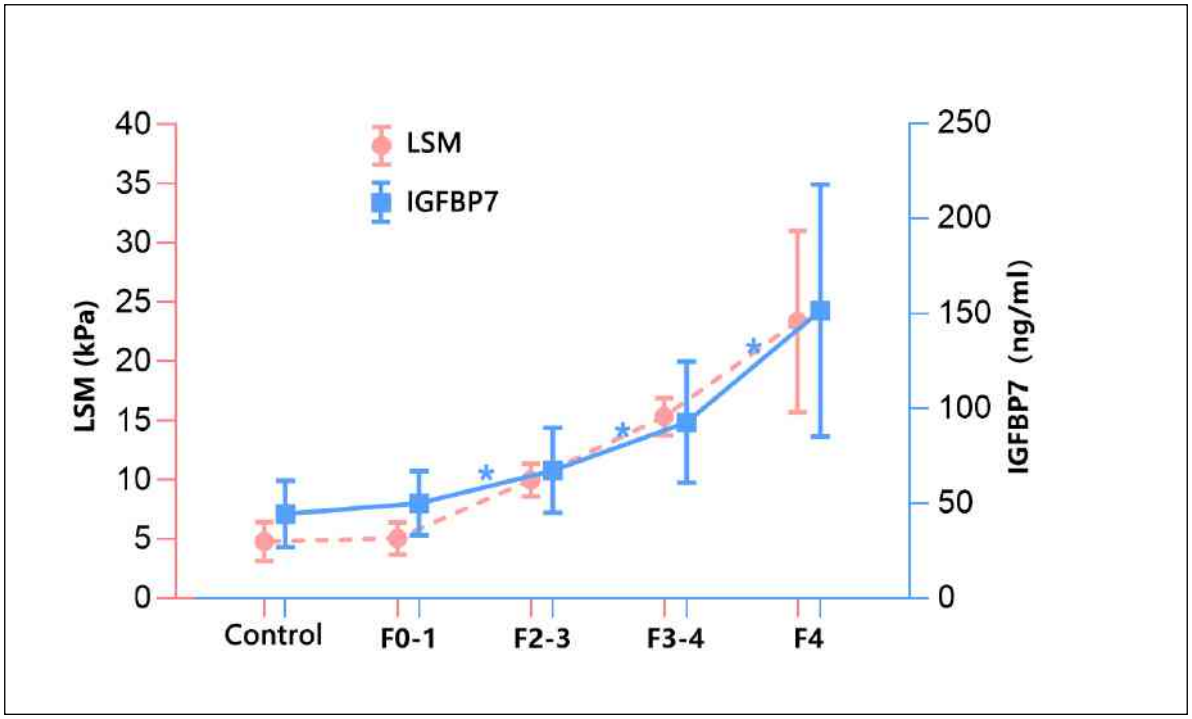

Figure 2.LSM and serum IGFBP7 in patients with chronic HBV infection with different degrees of fibrosis

	Control (n=10)	F0-1 (n=24)	F2-3 (n=17)	F3-4 (n=8)	F4 (n=15)
Age（years）	46.10±17.19	34.79±9.65	47.35±10.55	49.13±12.77	55.53±9.79
BMI（kg/m²）	21.20±2.47	22.50±2.82	23.14±2.98	20.61±2.41	22.33±2.41
SCr (μmol/L)	77.29±14.61	80.65±17.64	78.93±14.98	74.00±15.19	76.64±19.43
eGFR (ml/min)	91.57±11.84	99.14±18.10	95.07±14.98	99.00±15.68	93.38±15.69
ALT (M, IQR) (U/L）	22.60 (15.75~28.65)	34.00 (17.40~47.90)	29.50 (20.90~31.93)	67.70 (29.85~122.90)	38.70 (29.35~87.35)
TBil (M, IQR) (μmol/L)	10.65 (7.95~18.88)	9.25 (6.85~13.15)	10.40 (6.98~14.85)	9.75 (8.18~14.35)	15.95 (11.58~25.20)
PLT (×10⁹/L)	248.00±59.31	267.04±58.62	178.27±67.91	161.75±62.60	107.64±45.20
LSM (kPa)	4.77±1.63	5.03±1.35	9.96±1.39	15.31±1.57	23.35±7.64
serum IGFBP7 (ng/ml)	44.55±17.43	50.11±16.77	67.48±22.41	92.77±31.84	151.53±66.36

❖ AA-065

Identification and validation of novel biomarkers for hepatocellular carcinoma, liver fibrosis/cirrhosis and chronic hepatitis B via transcriptome sequencing technology

Dan Dan Zhao[1], Pei Lin Guo[1], Chen Dong[1], Yu Hui Tang[1], Yuemin NAN[1]
[1]Third Hospital of Hebei Medical University

Background: At present, there are no accurate diagnostic biomarkers for distinguishing among hepatitis B virus (HBV)-related liver diseases. This research aimed to identify and validate a novel biomarker panel in patients with HBV-related hepatocellular carcinoma (HCC), liver fibrosis/liver cirrhosis (LF/LC) and chronic hepatitis B (CHB).

Method: Transcriptomics sequencing was conducted on the liver tissues of 5 patients with HCC, 5 patients with LF/LC, 5 patients with CHB, and 4 healthy controls. The expression levels of selected mRNAs and proteins were verified in validation set (n=200) and testing set (n=400) via enzyme-linked immunosorbent assay (ELISA).

Result: We identified 3 potential mRNAs by using short time-series expression miner and weighted gene co-expression network analysis. ELISA tests on the validation cohort indicated that the plasma levels of SHC adaptor protein 1 (SHC1), SLAM family member 8 (SLAMF8), and interleukin-32 (IL-32) gradually increasing trends in the four groups. Furthermore, a diagnostic model APFSSI (age, PLT, ferritin, SHC1, SLAMF8 and IL-32) was established to distinguish among CHB, LF/LC and HCC. The performance of the APFSSI model for discriminating CHB from healthy subjects (AUC=0.966) was much greater compared to SHC1 (AUC=0.900), SLAMF8 (AUC=0.744) and IL-32 (AUC=0.821). When distinguishing LF/LC from CHB, APFSSI was the most outstanding diagnostic parameter (AUC=0.924), which was superior to SHC1, SLAMF8 and IL-32 (AUC=0.812, 0.684 and 0.741, respectively). Likewise, APFSSI model with greatest AUC values displayed an excellent performance for differentiating between HCC and LF/LC than other variables (SHC1, SLAMF8 and IL-32) via ROC analyses. Finally, the results in the test set were consistent with those in the validation set.

Conclusion:SHC1, SLAMF8 and IL-32 can differentiate among patients with HCC, LF/LC, CHB and healthy controls. More importantly, the APFSSI model greater improves the diagnostic accuracy of HBV-associated liver diseases.

Table and Figure:

Figure 1. Development and validation of the APFSSI model

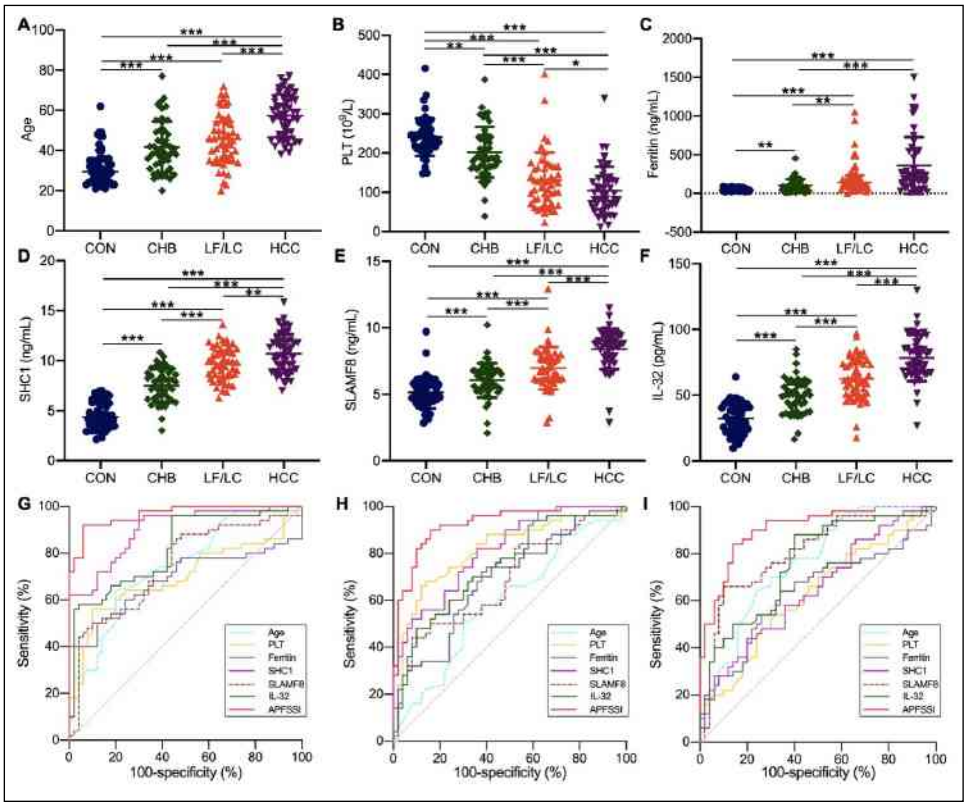

Figure 2. Further evaluation of the APFSSI model in the test set

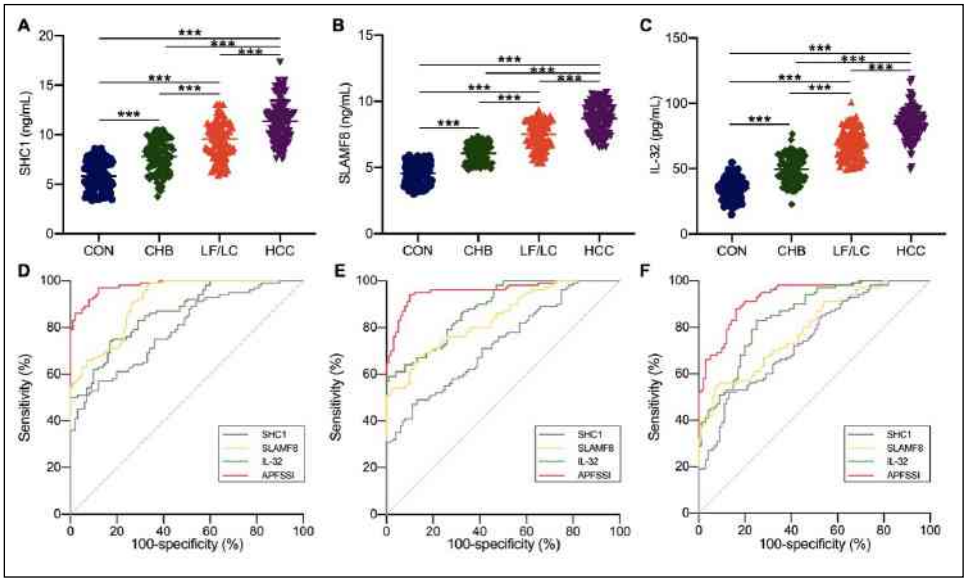

❖ AA-066

Prediction of upper gastrointestinal bleeding by serum chitinase-3-like protein 1 in patients with liver cirrhosis

Hang Yang[1,2], Chunxia Guo[1,2], Jia Li[2]
[1]Department of Hepatology, Second People's Clinical College of Tianjin Medical University, Tianjin, China, [2]Department of Hepatology, Tianjin Second People's Hospital, No. 7, Sudi South Road, Nankai District, Tianjin, 300192, China

Background: Upper gastrointestinal bleeding is one of the most frequent causes of morbidity and mortality in the course of liver cirrhosis. Chitinase-3-like protein 1 is an liver cirrhosis biomarker.The aim of this study was to assess the prediction sensitbility and specificity of the serum chitinase-3-like protein 1 to predict the risk of upper gastrointestinal bleeding in the in patients with liver cirrhosis.

Method: Two hundred and ninety-nine liver cirrhosis patients were enrolled in this etrospective study. All participants underwent serum chitinase-3-like protein 1 level detection and one year follow-up.Further information on the general characteristics of the patients is shown in Attachment1.Further information on the general characteristics of the patients by upper gastrointestinal bleeding is shown in Attachment2.Through binary logistic regression analyses of the clinical data, the factors affecting upper gastrointestinal bleeding were identified.Receiver operating characteristic curves were used to evaluate the predictive value of serum chitinase-3-like protein 1.

Result: Among the 299 liver cirrhosis patients, 40 (13.4%) had upper gastrointestinal bleeding, and 259 (86.6%) hadn't.Binary logistic regression analysis was used to explore the risk factors associated with upper gastrointestinal bleeding in liver cirrhosis patients.Patients had upper gastrointestinal bleeding were older ($P = 0.002$) ; had higher serum chitinase-3-like protein 1 ($P < 0.001$) ; had longer INR ($P < 0.001$) ; and had lower serum albumin ($P < 0.001$) and serum prealbumin ($P < 0.001$).The receiver operating characteristic curve showed that the best serum chitinase-3-like protein 1 cut-off value was 206.5 g/L, with 76.90% sensitivity and 73.70% specificity for the prediction of upper gastrointestinal bleeding (Area u nder the curve= 0.806, 95% CI 0.740−0.872).

Conclusion: Serum chitinase-3-like protein 1 can be used as a noninvasive method to predict upper gastrointestinal bleeding for patients with liver cirrhosis.

Table and Figure:

Figure 1. General characteristics of the patients with liver cirrhosis

Variables	n=299	Data available for analysis	Missing values
Age (years)	55.2 ± 11.4	299	0
Gender (male %)	173 (57.9)	299	0
Pathogenyn, n (%)		299	0
Chronic hepatitis B	156 (52.2)		
Hepatitis C	29 (9.7)		
Others	114 (38.1)		
compensated cirrhosis, n (%)	202 (67.6)	299	0
ALT (U/L)	21.0 (15.0, 28.0)	299	0
AST (U/L)	26.0 (20.0, 35.0)	299	0
Albumin (g/L)	40.0 (33.6, 45.0)	299	0
Prealbumin (mg/L)	136.4 (88.2, 190.3)	264	35 (11.7)
TBil (μmol/L)	18.3 (13.3, 28.9)	299	00
CHI3L1 (ng/mL)	136.0 (77.0, 243.0)	299	0
INR	1.1 (1.0, 1.2)	297	2 (0.7)
PLT(×10⁹/L)	94.0 (60.0, 158.0)	299	0

Data are expressed as mean (± standard deviation), median (quartile 25, quartile 75) or number (proportion)

ALT alanine aminotransferase, AST aspartate aminotransferase, TBIL total bilirubin, CHI3L1 Chitinase-3-like protein 1, INR international normalized ratio, PLT platelet

Figure 2. General characteristics of the patients with liver cirrhosis by upper gastrointestinal bleeding

Variables	No bleeding (n=259)	Bleeding (n=40)	*P*
Age (years)	54.3 ± 11.1	61 (52.5, 66.8)	0.003
Gender (male %)	141 (54.4)	32 (80.0)	0.002
Pathogenyn, n (%)			
Chronic hepatitis B	135 (52.1)	21 (52.5)	0.965
Hepatitis C	21 (8.1)	8 (20.0)	0.038
Others	103 (39.8)	11 (27.5)	0.137
compensated cirrhosis, n (%)	194 (74.9)	8 (20.0)	< 0.001
ALT (U/L)	21.5 (16.0, 28.0)	17.0 (12.8, 25.2)	0.027
AST (U/L)	26.0 (20.0, 34.0)	27.0 (20.5, 38.8)	0.264
Albumin (g/L)	41.2 (35.1, 45.3)	31.8 (26.4, 35.9)	< 0.001
Prealbumin (g/L)	154.1 (104.3, 195.9)	76.5 (50.8, 99.1)	< 0.001
TBil (μmol/L)	17.7 (13.3, 27.6)	21.8 (13.0, 41.3)	0.173
CHI3L1 (ng/mL)	113.0 (71.0, 214.0)	272.0 (193.5, 555.8)	< 0.001
INR	1 (1, 1.2)	1.2 (1.1, 1.3)	< 0.001
PLT(×10⁹/L)	98 (61.0, 161.0)	80.5 (54.3, 147.0)	0.257

Data are expressed as mean (± standard deviation), median (quartile 25, quartile 75) or number (proportion)

ALT alanine aminotransferase, AST aspartate aminotransferase, TBIL total bilirubin, CHI3L1 Chitinase-3-like protein 1, INR international normalized ratio, PLT platelet

❖ AA-067

Performance of non-invasive surrogates to predict the prognosis of portal hypertension: a systematic review and meta-analysis

Xiaoqian Xu[1], Hao Wang[1], Min Li[1], Xinyu Zhao[1], Bingqiong Wang[1], Jidong Jia[1], Yuanyuan Kong[1], Hong You[1]
[1]Beijing Friendship Hospital, Capital Medical University

Background: Measurement of hepatic venous pressure gradient (HVPG) and endoscopy are limited applied in the clinical monitoring of portal hypertension (PH) due to their invasiveness. Simple, non-invasive tests or indexes to predict the prognosis of PH were thus needed.

Method: PubMed, EMBASE and the Cochrane Library were systematically searched. Prospective studies, with endpoints defined by PH changes (PH regression/ progression measured by HVPG or endoscopy) or PH-related disease progression and with the data necessary to calculate the true and false positive, true and false negative predicting results were included.

Result: In six studies finally included, only one study reported predictive performance of non-invasive tests for PH regression, with a small sample size of 23. Using change in liver stiffness measurement (LSM) ratio between baseline and second measurement, the sensitivity, specificity and areas under the receiver operating characteristic (AUROC) of predicting PH regression were 1.00 (95%CI: 0.61, 1.00), 0.77 (95%CI: 0.53, 0.90), and 0.79 (95%CI: 0.58, 0.93) respectively. While, using LSM at second measurement, the sensitivity, specificity and AUROC were 0.83 (95%CI: 0.44, 0.99), 0.65 (95%CI: 0.41, 0.83), and 0.63 (95%CI: 0.40, 0.82), respectively. All six studies reported the predictive performance of non-invasive tests for PH-related disease progression. For serum markers (platelet count, platelet count to spleen diameter ratio, GB score, and MELD score), the pooled sensitivity, specificity, and areas under the summary receiver operating characteristic (AUSROC) curves for predicting PH-related disease progression were 0.64 (95%CI: 0.27, 0.89), 0.80 (95%CI: 0.72, 0.86) and 0.81(95%CI: 0.78, 0.85), respectively. For imaging-based markers to predict the progression of PH, including LSM and platelet count to spleen diameter ratio, the pooled sensitivity, specificity and AUSROC of predicting PH-related disease progression were 0.85 (95%CI: 0.68, 0.98), 0.75 (95%CI: 0.66, 0.82) and 0.76 (95%CI: 0.72, 0.80), respectively.

Conclusion: Evidence on non-invasive surrogates of PH prognosis was insufficient, especially for PH regression. Based on a few available studies, the specificities and AUSROCs were similar between serum and imaging-based tests. Moreover, imaging-based markers, mainly LSM, seem to show a relatively better performance than serum markers.

❖ AA-068

Dynamic MELD score at 1 week after artificial liver support treatment predicts 90-day prognosis of HBV-ACLF

Yuanyao Zhang[1], Zhongji Meng[2], Deqiang Ma[2], Yinhua Zhang[2], Sen Luo[2]
[1]Taihe Hospital, Hubei University of MedicinePostgraduate Training Basement of Jinzhou Medical University, Taihe Hospital, Hubei University of Medicine, [2]Department of Infectious Diseases, Hubei Clinical Research Center for Precise Diagnosis and Therapy of Liver Cancer, Taihe Hospital, Hubei University of Medicine

Background: To investigate the efficacy of ALSS in the treatment of hepatitis B virus-related acute-on-chronic liver failure (HBV-ACLF) with different clinical types, and to explore factors predicting the short-term prognosis of HBV-ACLF patients who received artificial liver support system (ALSS) therapy.

Method: The data of HBV-ACLF patients who received ALSS treatment from January 2016 to December 2020 in the Department of Infectious Diseases of Taihe Hospital in Shiyan City were retrospectively analyzed. Multivariate COX regression was used to analyze the factors associated with 90-day prognosis of HBV-ACLF patients.

Result:A total of 313 HBV-ACLF patients were finally included in the analysis, including 121 cases of type A, 59 cases of type B, and 133 cases of type C. The clinical effective rates of ALSS treatment were significantly higher in type A HBV-ACLF (68.8%), than in type B (55.9%) and type C (22.6%) HBV-ACLF, (P<0.001). ΔMELD at one week of ALSS treatment was an independent factor of 90-day prognosis in HBV-ACLF patients. The cut-off values of ΔMELD for predicting 90-day prognosis in A, B, and C HBV-ACLF were -5.7, -4.5, and -1.5, respectively. The cumulative survival rate of patients with ΔMELD lower than the cut-off value was significantly higher than those with ΔMELD higher than the cut-off value (in all the three clinical types of HBV-ACLF, P<0.001).

Conclusion:ALSS treatment can improve the outcomes of HBV-ACLF, especially in type A and type B HBV-ACLF, and ΔMELD is effective in evaluating the dynamic status of the disease and predicting the short-term prognosis of HBV-ACLF patients who received ALSS treatment.

❖ AA-069

Application of non-invasive serological model and transient elastography in assessment of liver fibrosis in primary biliary cholangitis

Qian Wang[1], *Yingmei Tang*[1]
[1]*The Second Affiliated Hospital of Kunming Medical University*

Background: Primary biliary cholangitis is a chronic liver disease characterized by progressive cholestasis，the degree of fibrosis is closely related to the prognosis. Therefore, it is particularly important to accurately determine the degree of liver fibrosis. Liver biopsy is a recognized reference standard for evaluating liver fibrosis, but because it is invasive and not acceptable to patients, non-invasive tests are proposed.

Method: This article retrospectively analyzed the literature to explore the application of Instantaneous elastography and non-invasive serological models in the assessment of liver fibrosis in PBC.

Result: Obstructive enzymes such as ALP and GGT in PBC patients tend to be elevated, and bilirubin, albumin, platelet counts, etc. may also be changed in the late stage. Therefore, some scholars have proposed a variety of non-invasive serological assessment models of PBC liver fibrosis based on the above characteristics. Literature data indicate that the INPR, AAR, APRI, FIB-4, TPR，RPR alone or in combination with related autoantibodies can better predict liver fibrosis. However, some scholars hold different views. In conclusion, due to the limited data, there is currently no guideline that explicitly addresses a noninvasive serological model as a recommendation for fibrosis in PBC. Transient elastography is an emerging technique in recent years. It evaluates the degree of fibrosis according to the propagation speed of shear waves in the liver, and its diagnostic performance is superior to other simple non-invasive indicators. The 2021 European Society of Hepatology guidelines state that it is the best surrogate marker for diagnosing advanced fibrosis/cACLD in PBC patients and recommend 10 kPa as the cut-off value for liver stiffness. The two most commonly used tests are Fibro Scan and Fibro Touch. FibroTest and FibroMeter are unverified on PBC.

Conclusion: The current research on non-invasive liver fibrosis diagnosis is mainly based on other chronic liver diseases, and its practicability and accuracy in cholestatic liver disease, especially in PBC patients, remains to be studied. Therefore, larger-scale, multi-center prospective studies are still needed for verification in the future.

❖ AA-070

Indocyanine Green 15-minute Retention Test as a non-invasive marker of Esophageal Varices in compensated liver cirrhosis

Xiaojing Cheng[1], Xu Han[2]
[1]Tianjin Second People's Hospital, [2]Tianjin Second People's Hospital

Background: Non-invasive markers are useful for the assessment of esophageal varices(EV) in patients with compensated liver cirrhosis. The aim of our study was to evaluate the performance of ICG-R15 as a non-invasive marker of EV, measured with the gold standards (upper endoscopy).

Method: The clinical data of patients with compensated liver cirrhosis were retrospectively analyzed. All patients underwent laboratory tests, abdominal ultrasound, upper endoscopy and ICG 15-minute retention test. We evaluated the sensibility and specificity of ICG retention test and other non-invasive tools for the diagnosis of EV. They were divided in to no or mild esophageal varices group, and moderate or severe esophageal varices group referred to the "Trial Scheme for Endoscopic Diagnosis and Treatment of Gastrointestinal Varicose Veins and Bleeding (2009)" . Measurement data that conformed to the normal distribution were expressed as mean ± standard deviation (`x ± s) , and the comparison between the two groups was performed with T test or analysis of variance. Median and interquartile intervals were used for measurement data that didn't meet the normal distribution[M(P25,P75)] ,and the comparison between the two groups was performed with rank sum test. The comparison of count data between groups was performed with χ2 test, and those who did not meet the χ2 test conditions used Fisher's exact test. The risk factors were analyzed by binary Logistic regression model, and OR values of risk factors and 95% of OR values were calculated.

Result:144 consecutive patients (88M/56F, 51.7 ± 11.06 years) were enrolled. The ICG-R15, PVD (portal vein diameter), TBIL, PT, INR, ARR (AST/ALT ratio), APRI (AST/platelet ratio index), Splenic area, Lok index, Park index and Liver stiffness in the no or mild EV group were lower than those in the moderate or severe EV group, while the ICG-K(Indocyanine green elimination rate), EHBF (Effective hepatic blood flow) , ALB, PLT, and PSDR (platelet count/spleen diameter ratio) were higher than those in the moderate or severe EV group, and the differences were statistically significant (P< 0.05). ICG-R15, splenic area, APRI and PLT were independent risk factors for moderate OR severe esophageal and gastric varices (OR = 1.115, 1.025, 0.281, 0.987, P<0.05). The predictive

value of ICG-R15 for moderate and severe varices was 17.7%, the sensitivity was 0.662, and the specificity was 0.849. The diagnostic performance of ICG-R15 as a noninvasive marker of mild EV group and moderate or severe EV group can be interpreted by examining the area under the receiver operating characteristic (ROC) curve (AUROC) to be 0.815.

Conclusion:ICG R15 is an effective tool for the assessment of EV in patients with compensated liver cirrhosis. Although we are still far from the replacement of endoscopy, ICG-R15 seems to be able to identify patients with advanced liver disease in which endoscopy is mandatory, and to rule out the presence of EV in patients with compensated liver cirrhosis.

❖ AA-071

A novel non-invasive index for the prediction of liver fibrosis in chronic hepatitis B patients with concurrent nonalcoholic fatty liver disease

Jian Wang[1], Jiacheng Liu[2], Yilin Liu[2], Yiguang Li[3], Li Zhu[4], Ruifei Xue[5], Suling Jiang[5], Minxin Mao[2], Yu Geng[2], Weimao Ding[6], Chuanwu Zhu[4], Rui Huang[1], Jie Li[1], Chao Wu[1]
[1]Nanjing Drum Tower Hospital, The Affiliated Hospital of Nanjing University Medical School,
[2]Nanjing Drum Tower Hospital Clinical College of Nanjing University of Chinese Medicine,
[3]The Fifth People's Hospital of Wuxi, [4]The Affiliated Infectious Diseases Hospital of Soochow University,
[5]Nanjing Drum Tower Hospital Clinical College of Nanjing Medical University, [6]Huai'an No. 4 People's Hospital

Background: Few accurate non-invasive indexes are available to evaluate liver fibrosis in chronic hepatitis B (CHB) patients with nonalcoholic fatty liver disease (NAFLD). We aimed to establish a predictive index for advanced fibrosis in CHB patients with NAFLD.

Method:A total of 267 treatment-naïve CHB patients with NAFLD underwent liver biopsy were enrolled from four hospitals and randomly divided into a derivation set (n=134) and a validation set (n=133). Receiver operating characteristic (ROC) curve was used to compare predicting accuracy of different indexes.

Result: In the derivation set, alanine aminotransferase, aspartate aminotransferase (AST), prothrombin time, presence of hypertension, and type 2 diabetes were significantly associated with advanced fibrosis (≥S3). Based on these parameters, a novel index namely AAPHD for predicting advanced fibrosis was developed. The areas under the ROC curves (AUROCs) of AAPHD index in predicting advanced fibrosis was 0.88 (95%CI: 0.82-0.94). The optimal cut-off value of AAPHD was -2.870, with a sensitivity of 72.73% and a specificity of 90.10%. The predicting accuracy of AAPHD for advanced fibrosis was significantly superior to AST-to-platelet ratio index (APRI)(AUROC=0.70), fibrosis-4 score (FIB-4)(AUROC=0.69), and NAFLD fibrosis score (NFS)(AUROC=0.68). In the validation set, the AUROCs of AAPHD (AUROC=0.88) remains significantly higher than that of FIB-4 and NFS, while it was comparable with APRI for predicting advanced fibrosis.

Conclusion:AAPHD is a promising non-invasive index for predicting advanced fibrosis with high accuracy in CHB patients with NAFLD. The application of AAPHD may reduce the necessary for liver biopsy in CHB patients with NAFLD.

Table and Figure:

Figure 1. Receiver operating characteristic (ROC) curves of non-invasive tests for predicting advanced liver fibrosis in derivation set (A) and validation set (B).

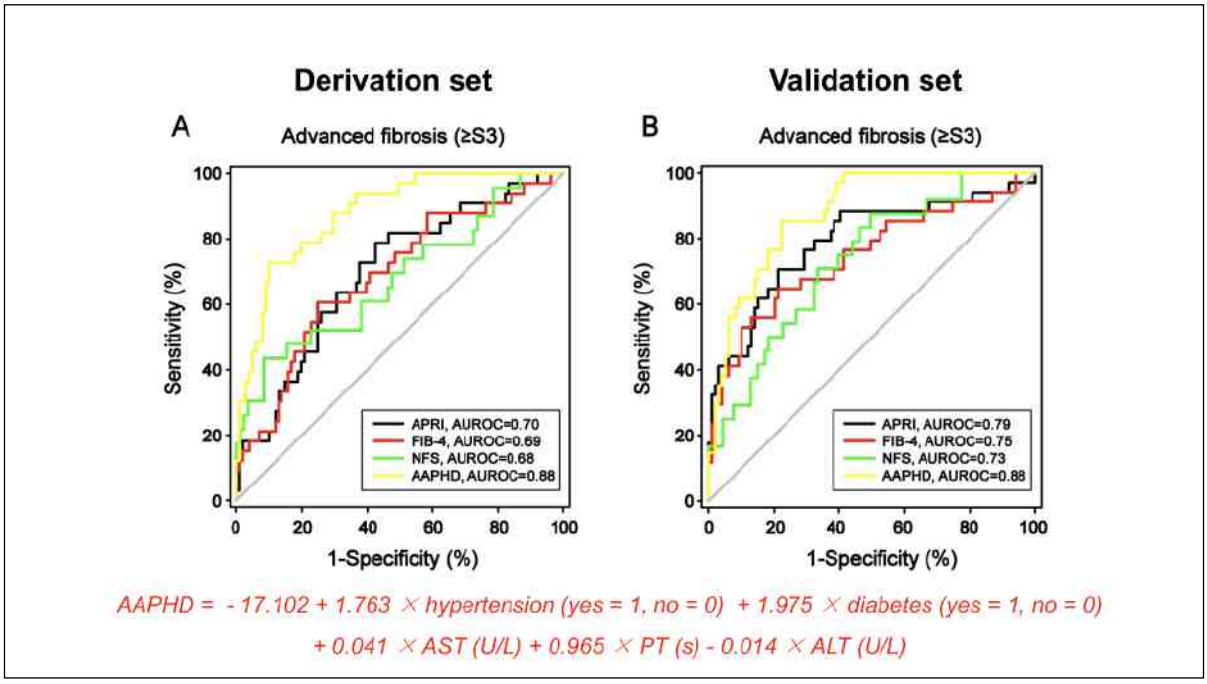

❖ AA-072

Combined model with acoustic radiation force impulse to rule out high-risk varices in HBV-related cirrhosis with viral suppression

Haiyu Wang[1]
[1]Hepatology Unit, Department of Infectious Diseases, Nanfang Hospital, Southern Medical University, Guangzhou, China

Background: To prospectively evaluate the performance of spleen stiffness measurement(SSM) and liver stiffness measurement(LSM) via acoustic radiation force impulse (ARFI) imaging alone or combined with platelet counts(PLT) in ruling out high-risk varices(HRV) in HBV-related cirrhotic patients with maintained viral suppression.

Method: Patients with cirrhosis enrolled between June 2020 and November 2021 were divided into derivation cohort and validation cohort(ClinicalTrials.gov:NCT04123509). LSM and SSM ARFI-based, and esophagogastroduodenoscopy(EGD) were performed at enrollment. Antiviral regimen(s) and virological responses, evaluated every 3-6 months, were recorded.

Result: In the derivation cohort, overall 236 HBV-related cirrhotic patients with maintained viral suppression were enrolled, and the prevalence of HRV was 19.5% (46/236). AUROC curves for LSM and SSM for the detection of HRV were 0.744 and 0.851, respectively. With the aim of identifying HRV, by the AUROC curves, the most accurate LSM and SSM cut-off of 1.46m/s and 2.28m/s were chosen, respectively. The new criteria is LSM<1.46m/s and PLT>150×109/L criteria which can spared 9.3% (22/236) of EGD and no HRV was missed (0/46). The SSM cut-off (≤2.28m/s) was well validated in safely ruling out HRV in these patients (the percentage of missed HRV was 4.3%). The combined model (LSM<1.46m/s and PLT>150×109/L combined with SSM ≤ 2.28m/s) can spare 38.6% (91/236) of EGDs and 4.3% (2/46) of HRV cases were misclassified. In the validation cohort, we analysed 239 HBV-related cirrhotic patients with maintained viral suppression, and the prevalence of HRV was 18.4% (464/239). We validated the new criteria (LSM<1.46m/s and PLT>150×109/L), SSM ≤2.28m/s and the combined model (LSM<1.46m/s and PLT>150×109/L combined with SSM ≤ 2.28m/s) which can spared 13% (31/239), 25.5% (61/239) and 33.9% (81/239) of EGD respectively, and the HRV missed rate were < 5% (0 vs 4.5% vs 4.5%).

Conclusion:A non-invasive prediction model combining LSM<1.46m/s and PLT>150×109/L criteria with SSM ≤ 2.28m/s exhibited excellent performance in ruling out HRV and make

it possible to avoid a significantly large number (38.6% vs 33.9%) of unnecessary EGDs in HBV-related cirrhotic patients with maintained viral suppression. This simple combined model could serve as a convenient and efficient non-invasive method for HRV screening that can guide the future surveillance strategy.

Table and Figure:

Figure 1. Baseline characteristics of HBV-related cirrhotic patients with maintained viral suppression in derivation cohort and validation cohort

Variable	Derivation cohort (n=236)	Validation cohort (n=239)
Age (years)	48(41-55)	48(40-54)
Male gender- no. (%)	199(84.3)	205(85.8)
Body mass index (kg/m^2)	23(21-26)	24(21-26)
Child Pugh Score- no. (%)		
A	226(95.8)	216(90.4)
B	10(4.2)	23(9.6)
MELD score	7(6-8)	7(6-9)
Anti-HBV drugs- no. (%)		
Entecavir	170(72.0)	177(74.1)
Other nucleos(t)ides	66(28.0)	62(25.9)
Maintained viral responses duration(months)	36.5(20.4-71.0)	32.4(14.1-65.9)
Laboratory results		
Platelet counts (×10^9/L)	142(97-182)	138(91-183)
INR	1(0.95-1.06)	1(0.9-1.1)
AST (U/L)	25(21-32)	25(20-31)
ALT (U/L)	27(19-35)	25(19-32)
Total bilirubin (umol/L)	14.8(11.1-19.7)	15.8(12.0-20.3)
Albumin (g/L)	45.2(42.7-47.7)	45.4(41.6-47.5)
Creatinine (μmol/L)	77(68-87)	79(68-89)
Non-invasive tests		
LSM(m/s)	1.74(1.56-2.09)[#]	1.82(1.56-2.17)
SSM(m/s)	2.46(2.15-2.73)[&]	2.52(2.27-2.93)[$]
Spleen length(mm)	109(95-126)	111(95-128)
Spleen thickness(mm)	34(29-43)	35(30-44)
Esophageal varices- no. (%)		
No varices	76(32.2)	73(30.5)
Grade 1*	115(48.7)	123(51.5)
Grade 2	22(9.3)	17(7.1)
Grade 3	23(9.7)	26(10.9)
Low-risk varices	190(80.5)	195(81.6)
High-risk varices*	46(19.5)	44(18.4)

Figure 2. Operating characteristics for different non-invasive tests in ruling out high-risk varices in HBV-related cirrhotic patients with maintained viral suppression in derivation cohort and validation cohort

Patients	Derivation cohort (n=236)			Validation cohort (n=239)		
	LSM<1.46 m/s and PLT>150×10^9/L	SSM(2.28m/s)	Combined model	LSM<1.46 m/s and PLT>150×10^9/L	SSM(2.28m/s)	Combined model
True positive (n)	46	44	44	44	42	42
False positive (n)	168	111	101	164	136	116
True negative (n)	22	79	89	31	59	79
False negative (n)	0	2	2	0	2	2
Sensitivity (%)	100	95.65	95.65	100	95.45	95.45
Specificity (%)	11.58	41.58	46.84	15.90	30.26	40.51
PPV (%)	21.50	28.39	30.34	21.15	23.60	26.58
NPV (%)	100	97.53	97.80	100	96.72	97.53
LR-positive	1.13	1.64	1.80	1.19	3.15	1.60
LR-negative	0	0.10	0.09	0	0.15	0.11
EGDs spared (%)	9.3	34.3	38.6	13.0	25.5	33.9
HRV missed/HRV total (%)	0	4.3	4.3	0	4.5	4.5

❖ AA-073

VEGFR2-targeted Ultrasound Molecular Imaging of Angiogenesis to Evaluate Liver Allograft Fibrosis

Chen Qiu[1]
[1]中山大学附属第三医院

Background: Liver allograft fibrosis (LAF) is a common challenge threatening patient survival after liver transplantation, making a potent imaging technique vital for clinical management. Till now, ultrasound (US) elastography has been regarded the most promising non-invasive evaluation method which, however, is susceptible to inflammation and also insensitive to early-stage pathological changes. This study intended to achieve accurate diagnosis of LAF basing on VEGFR2-targeted US molecular imaging (USMI) in rat LAF models.

Method:(1) Preparation and detection of MBVEGFR2: MBVEGFR2 was fabricated using biotin-avidin method. The binding of the antibody to the surface of microbubbles was verified by fluorescence microscopy imaging. (2) Animal experiments: ① Establishment of LAF in rats: LAF models of different stages were builded after liver ischemia-reperfusion injury surgery. ② In vivo USMI: basing on the microbubble burst-reperfusion method, after intravenous injection of MBVEGFR2 or MBCON, US imaging was performed on the liver region of the rats. The quantitative molecular signal intensity values of each group were further analyzed and US elastography was measured at the same time. The USMI quantitative values and elastic measurement values were compared with the pathological gold standard respectively.

Result: (1) Preparation and detection of MBVEGFR2: the antibodies successfully linked to the surface of microbubbles under fluorescence microscope observation. (2) Animal experiments: ①The LAF models of different stages were successfully builded which were verified by pathological and serological tests. The results confirmed that the fibrosis severity peaked 7 days after the surgery whereas the inflammatory peaked 1 day after the surgery. ②Based on a thorough comparison with US elastography at multiple diseasestages, VEGFR2 targeted US molecular imaging (USMI) was validated to be highly potent for LAF early diagnosis and staging: the linear correlation (R2) between either the quantitative value of USMI or elastography measurement value and the pathological fibrosis score (Metavir score) was 0.77 vs. 0.35 ($P < 0.05$), respectively.

Conclusion: In this study, basing on USMI of MBVEGFR2, LAF were accurately staged especially for early stage LAF which confirming the more excellent sensitivity of this technology than that of US elastography. The study provided new methods and new ideas for non-invasive dynamic monitoring of LAF.

❖ AA-074

Contrast-free ultrasensitive ultrasound imaging for in-vivo quantitative evaluation of hepatic microcirculation in cirrhotic rats

Wei Zhang[1], Chengwu Huang[2], Tinghui Yin[1], Xiaoyan Miao[1], Huan Deng[1], Rongqin Zheng[1], Jie Ren[1], Shigao Chen[2]
[1]Department of Ultrasound, Laboratory of Novel Optoacoustic (Ultrasonic) Imaging, The Third Affiliated Hospital of Sun Yat-sen University, [2]Department of Radiology, Mayo Clinic College of Medicine and Science

Background: Liver microcirculation dysfunction plays a vital role in the occurrence and development of liver diseases, and thus there is a clinical need for in vivo and noninvasive evaluation of liver microcirculation. The purpose of this study is to evaluate the feasibility of ultrasensitive ultrasound microvessel imaging (UMI) in visualization and quantification of hepatic microvessels in rats.

Method: In vivo studies were carried out to image hepatic microvasculature in Sprague Dawley rats (four control and five cirrhotic rats). Contrast-free ultrasensitive UMI was achieved by removing tissue clutters and extracting blood flow signals using a spatial-temporal singular value decomposition-based clutter filter. In vivo conventional power Doppler (PD) and in vitro micro-CT were performed as benchmarks. UMI-based quantifications for describing perfusion status, tortuosity, and integrity of microvessels were compared between control and cirrhotic groups by using a students' t-test. Correlations between quantification parameters and pathological fibrosis, perfusion function, and hepatic hypoxia were evaluated.

Result:UMI showed superior sensitivity in detecting minute vessels below the liver capsule, as compared with the conventional PD and qualitatively validated by micro-CT. Decreased perfusion (indicated by vessel density (P=0.001), fractional moving blood volume (FMBV) (P=0.001) and perfusion index (P=0.046), and increased tortuosity (indicated by sum of angles metric (SOAM) (P=0.005) were demonstrated in the cirrhotic group compared to the control group using UMI. UMI-based quantification parameters including vessel density (R2=0.768, P=0.002), FMBV (R2=0.810, P<0.001) and SOAM (R2=0.619, P=0.012) showed good linear correlations with pathologically-derived microvessel density labeled with Dextran. And vessel density (R2=0.827, P<0.001), FMBV (R2=0.742, P=0.003) and SOAM (R2=0.755, P=0.002) also showed good linear correlations with hepatic tissue hypoxia.

Conclusion: Contrast-free UMI was able to provide in vivo imaging and quantification of hepatic microvessels, which showed a great potential in the noninvasive evaluation of hepatic microcirculation dysfunction in liver diseases.

Table and Figure:

Figure 1. Representative UMI images acquired in the control and cirrhotic groups

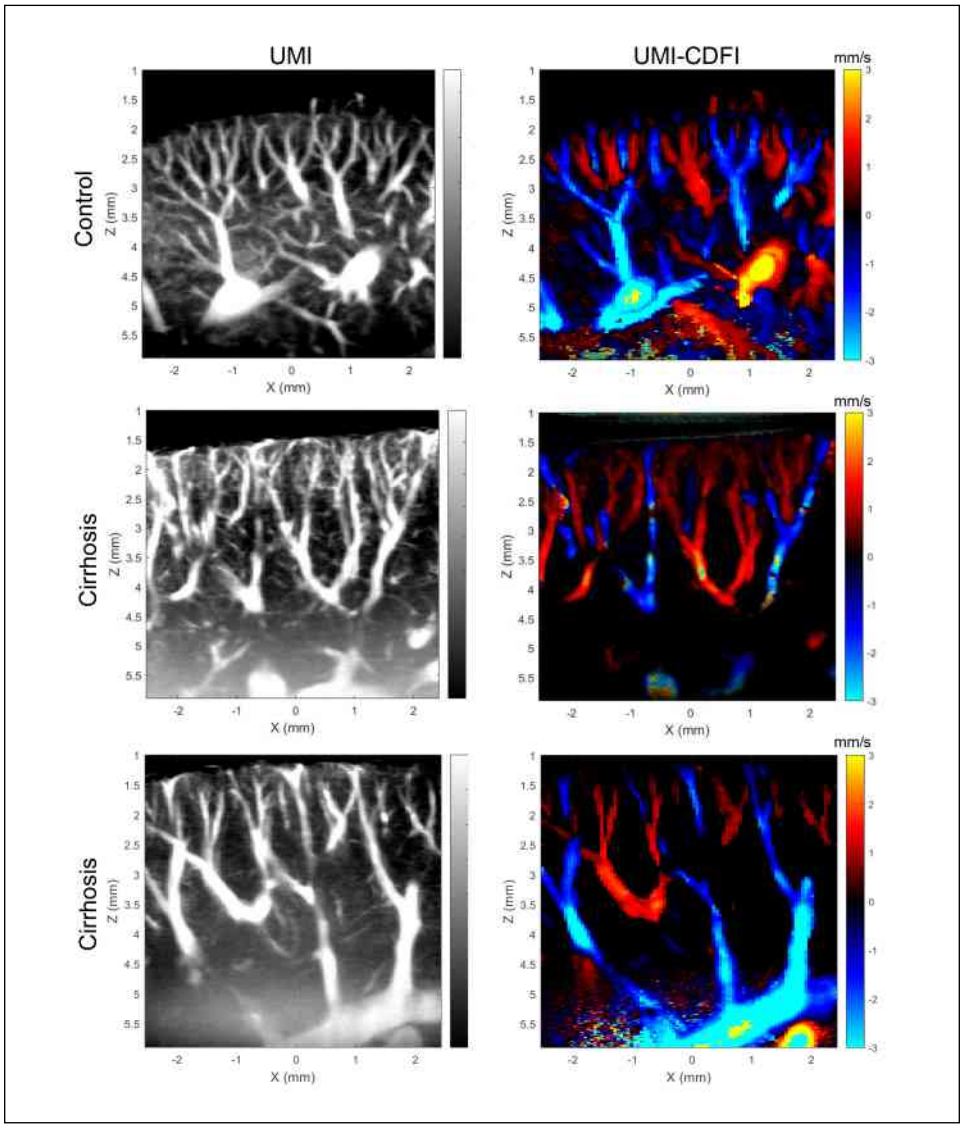

Figure 2. Linear regression between value of expression of Hypoxyprobe, microvessel density of Dextran and UMI based quantification parameters

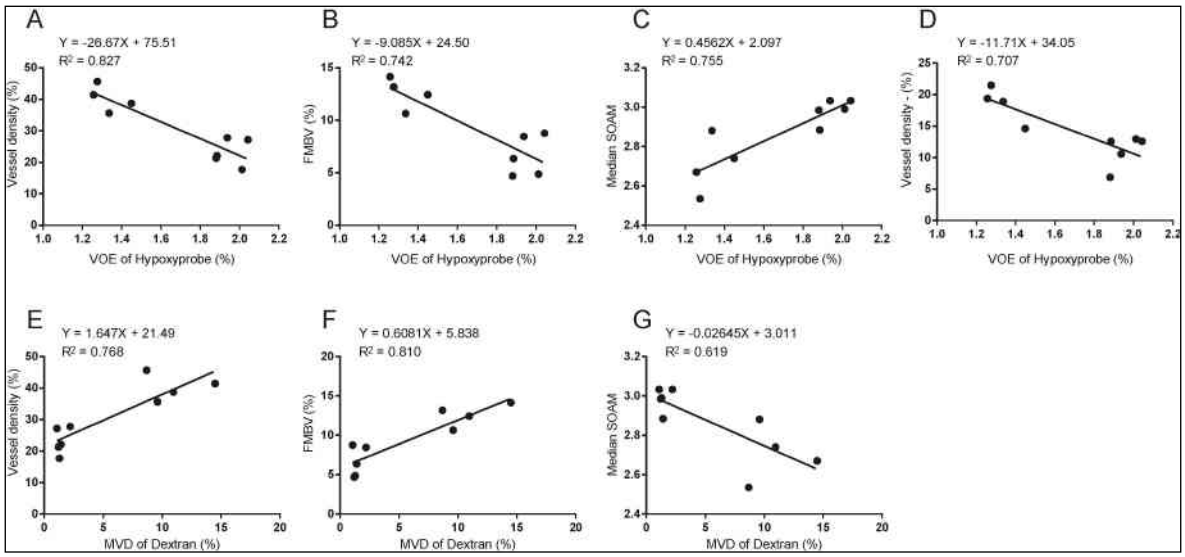

❖ AA-076

Splenic vein embolization as a safe and efficient treatment for patients with hepatic encephalopathy related to large spontaneous splenorenal shunts

Qiao Ke[1]
[1]Mengchao Hepatobiliary Hospital of Fujian Medical University

Background: Although splenic vein embolization (SVE) has been performed for the management of patients with hepatic encephalopathy (HE) related to large spontaneous splenorenal shunts (SSRS) in recent years, its role remains poorly defined. In this study, we aimed to explore the safety and efficacy of SVE for HE patients with large SSRS.

Method: Data for cirrhotic patients who were confirmed to have recurrent or persistent HE related to large SSRS and underwent SVE from January 2017 to April 2021 were retrospectively collected and analyzed at our center. The primary endpoints were the change of HE severity at 1 week after embolization and the recurrence of HE during the follow-up period. The secondary endpoints were procedure-related complications and changes in laboratory indicators and hepatic function (Child-Pugh score/grade and model for end-stage liver disease score).

Result: Of the eight cirrhotic patients included in the study, six were diagnosed with persistent HE, and the others were diagnosed with recurrent HE. Embolization success was achieved for all patients (100%), and no immediate procedure-related complications, de novo occurrence, or aggravation of symptoms related to portal hypertension were observed during the long-term follow-up. HE status was assessed at 1 week after embolization. The results demonstrated that the symptoms were mitigated in three patients and resolved completely in five patients. During the follow-up period, all patients were free of HE within 1 month after embolization, but one patient experienced the recurrence of HE within 6 months and another one experienced the recurrence of HE within 1 year. Compared with the preoperative parameters, the Child-Pugh score and grade were significantly improved at 1 week and 1 month after embolization (all $P<0.05$), and the serum ammonia level was significantly lower at 1 month after embolization ($P<0.05$).

Conclusion:SVE could be considered as a safe and efficient treatment for patients with HE related to large SSRS, but further validation is required.

Table and Figure:

Figure 1. Contrast-enhanced computed tomography (CT) showing large spontaneous splenorenal shunt (white arrow; A. transverse plane; B. coronal plane).

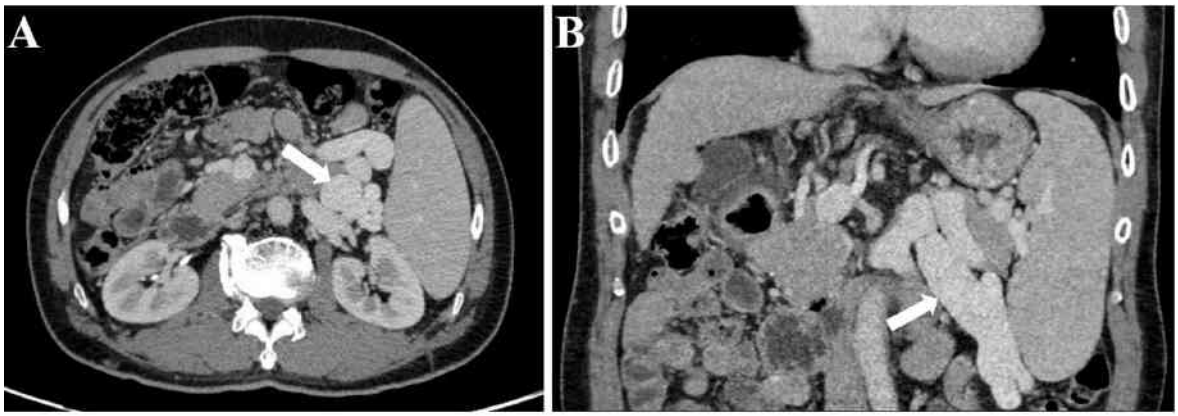

Figure 2. Fluoroscopy and digital subtraction images (A, before embolization, splenic venography shows the hepatofugal flow in the splenic vein and a large splenorenal shunt, black arrow shows the large shunt; B, before embolization, shunt venography shows the blood flow in shunt enters systemic circulation, black arrow shows the large shunt; C, before embolization, superior mesenteric venography shows hepatofugal flow in the splenorenal shunt, black arrow shows the large shunt; D, after embolization, superior mesenteric venography shows increased hepatopetal flow in the portal vein and no flow in splenic vein, black arrow shows the embolic site).

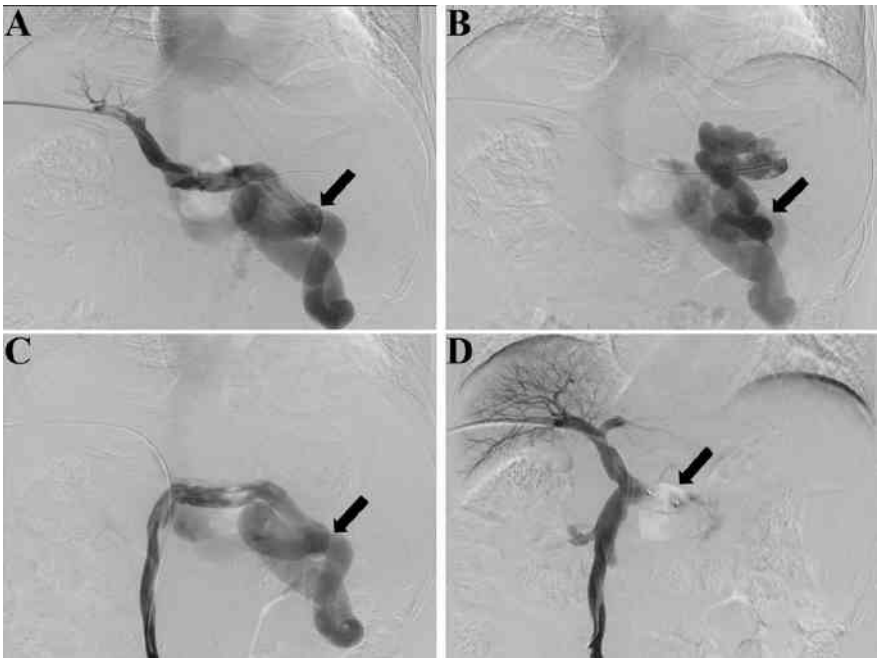

❖ AA-077

Assessing Hepatic Stiffness in Hepatic fibrosis using Monoexponential Diffusion Weighted Imaging and Intravoxel Incoherent Motion Diffusion Weighted Imaging

Jie Yuan[1]
[1]Shuguang Hospital Affiliated to Shanghai University of Traditional Chinese Medicine

Background: To compare monoexponential diffusion-weighted imaging (DWI) and intravoxel incoherent motion (IVIM) for assessing hepatic stiffness in hepatic fibrosis patients and to determine the optimal high and low b values of DWI.

Method:A total of 92 patients were enrolled in the study. All MRI examinations were performed on a 3.0T scanner. All patients underwent DWI with multiple b values. The monoexponential model was applied to calculate the apparent diffusion coefficient (ADC). The biexponential IVIM parameters, slow diffusion coefficient (D), fast diffusion coefficient (D*) and perfusion-related diffusion fraction (f) were calculated. A two-dimensional gradient echo sequence was used for magnetic resonance elastography (MRE) measurements. Correlation analysis was conducted between IVIM and DWI parameters and MRE data.

Result: The patient cohort consisted of 43 males and 49 females with an average age of 52.4 ± 13.7 years. There was an excellent negative correlation between MRE shear stiffness and D value obtained in IVIM (r=-0.826, P<0.001). There was a good correlation between MRE and the ADCtotal value using DWI at all b values (r=-0.789, P<0.001). Good correlation was also found between the ADC value (b=200 and 1200 s/mm2) and MRE (r=-0.716, P<0.001). Moderate correlation was obtained between MRE shear stiffness and ADC values (b=200 and 1500 s/mm2, b=200 and 500 s/mm2, b=200 and 800 s/mm2, b=100 and 500 s/mm2, b=0 and 500 s/mm2) (r=-584, -0.570, -0.516, -0.469, -0.415, respectively, with all P<0.001). On comparing the different b value combinations, b200 and 1200 s/mm2 was found to yield the best correlation between DWI diffusion parameters and MRE calculations.

Conclusion:DWI and IVIM imaging offer an alternative to MRE for diagnostic assessment of hepatic fibrosis by measurement of fluid diffusion parameters. A combination of b values of 200 and 1200 s/mm2 is recommended for examination of patients to minimize scan times.

Table and Figure:

Figure 1. Maps of a 32-year-old female of chronic hepatitis B. A: Biexponential model parameter D map, D=1.21×10–3 mm2/s. B: Biexponential model parameter D* map, D*=6.18×10–3 mm2/s. C: Biexponential model parameter f map, f=7.10%. D: Monoexponential model parameter ADC map, ADC=0.98×10–3 mm2/s. E: Shear-wave maps. F: Elastogram of MRE shows liver stiffness of 2.47kPa.

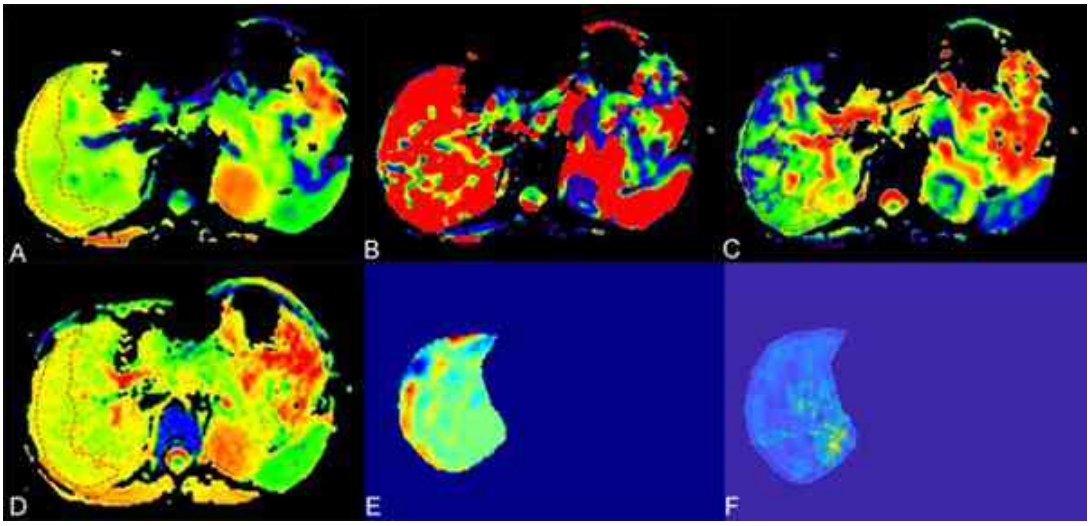

Figure 2. Linear regression of MRE and D of IVIM and ADCtotal and ADCb200 and 1200 calculated from DWI. ADC all had significant correlation with MRE (r = -0.826, -0.789, -0.716, respectively, all P<0.001)

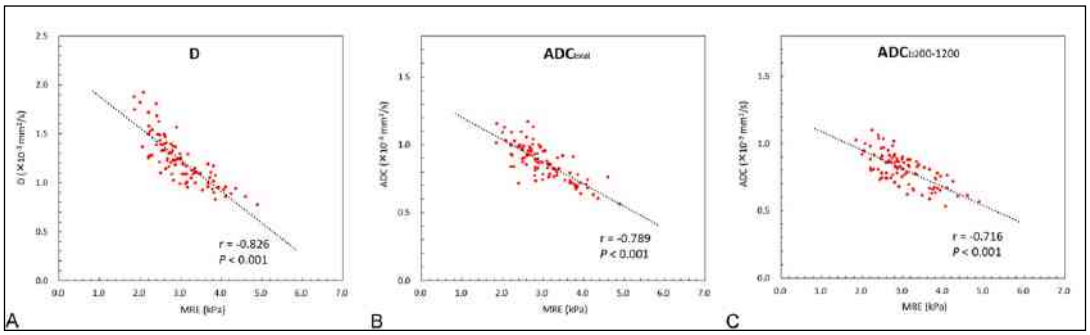

❖ AA-078

Association of myosteatosis with various body composition abnormalities in patients with decompensated cirrhosis: a pilot study

Xiaoyu Wang[1], Guo Gaoyue[1], Chao Sun[1]
[1]Tianjin Medical University General Hospital

Background: Myosteatosis is linked to dismal outcomes in the context of cirrhosis. However, association of myosteatosis with various body composition abnormalities remains enigmatic. We aimed to clarify the determinants of myosteatosis and its reciprocal relationship with other body composition profiles and length of hospitalization (LOH).

Method: We retrospectively analyzed the data of 473 consecutive cirrhotic patients hospitalized for decompensation. Computed tomography-based segmentation of the cross-sectional area at the third lumbar vertebra level was used to evaluate body composition abnormalities. The categories of myosteatosis were built according to our previously outcome-based cutoffs for each gender.

Result: Totally, 83 patients (17.55%) were stratified as myosteatotic, of whom 85.54% have concomitant high visceral adiposity indicative of increased visceral adipose tissue index (VATI). The prevalence of sarcopenia showed no significant difference between the groups with and without myosteatosis. Multivariate analysis showed advanced age (OR = 1.097, P <0.001), higher visceral to subcutaneous ratio of adipose tissue area ([VSR]; OR = 1.574, P = 0.032) and higher VATI (OR = 1.026, P <0.001) are independently associated with myosteatosis. Correlation analyses revealed a strong relationship between IMAC and VATI (ρ = 0.48, P <0.001) SATI (ρ = 0.36, P <0.001) and age (ρ = 0.36, P <0.001). None of the skeletal muscle or adipose tissue indicators was significantly related to longer LOH.

Conclusion: Higher VSR, higher VATI and advanced age are associated with myosteatosis among patients with cirrhosis at decompensation phase. It is tempting to target divergent adipose tissue depots aimed at proper intervention/prevention for myosteatosis.

Table and Figure:

Figure 1. Table 1 Characteristics of 473 cirrhotic patients with or without myosteatosis.

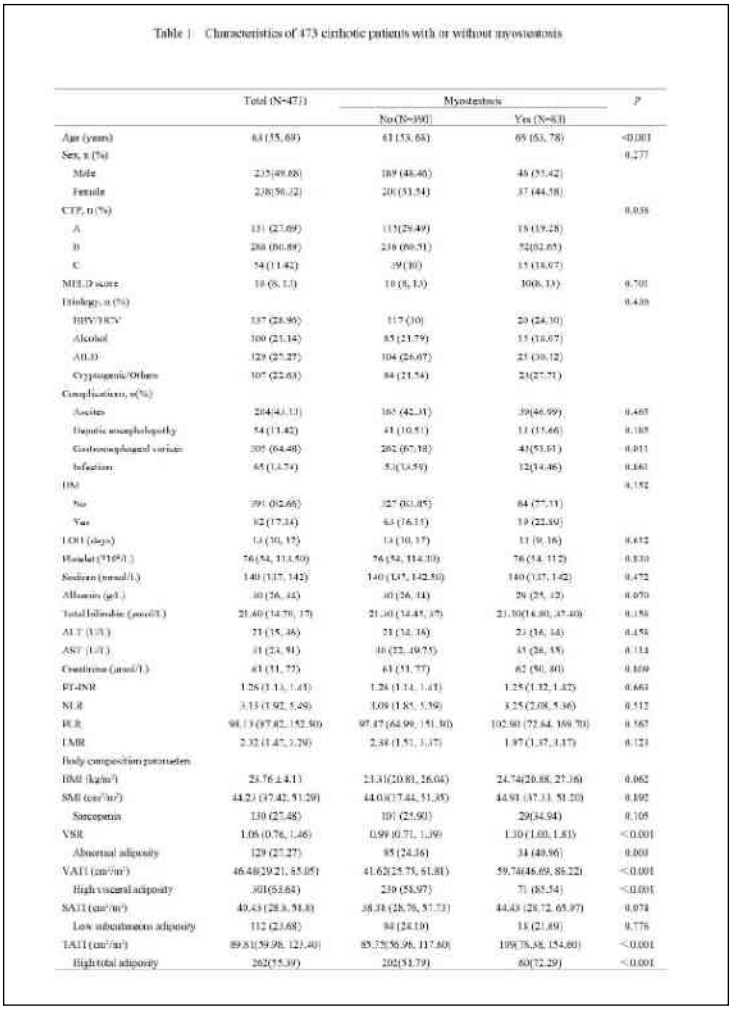

Table 1 Characteristics of 473 cirrhotic patients with or without myosteatosis

	Total (N=471)	Myosteatosis		P
		No (N=390)	Yes (N=83)	
Age (years)	63 (55, 69)	63 (53, 68)	69 (63, 78)	<0.001
Sex, n (%)				0.277
Male	235(49.88)	189 (48.46)	46 (55.42)	
Female	236(50.12)	201 (51.54)	37 (44.58)	
CTP, n (%)				0.038
A	131 (27.69)	115(29.49)	16 (19.28)	
B	288 (60.89)	236 (60.51)	52(62.65)	
C	54 (11.42)	39 (10)	15 (18.07)	
MELD score	10 (8, 13)	10 (8, 13)	10(8, 13)	0.701
Etiology, n (%)				0.430
HBV/HCV	137 (28.96)	117 (30)	20 (24.10)	
Alcohol	100 (21.14)	85 (21.79)	15 (18.07)	
AILD	129 (27.27)	104 (26.67)	25 (30.12)	
Cryptogenic/Others	107 (22.63)	84 (21.54)	23(27.71)	
Complications, n(%)				
Ascites	204(43.13)	165 (42.31)	39(46.99)	0.465
Hepatic encephalopathy	54 (11.42)	43 (10.51)	11 (13.66)	0.385
Gastroesophageal varices	305 (64.48)	252 (67.38)	43(53.01)	0.011
Infection	65 (13.74)	53(13.59)	12(14.46)	0.843
DM				0.152
No	391 (82.66)	327 (83.85)	64 (77.11)	
Yes	82 (17.34)	63 (16.15)	19 (22.89)	
LOH (days)	13 (10, 17)	13 (10, 17)	11 (9, 16)	0.032
Platelet (*10^9/L)	76 (54, 114.50)	76 (54, 114.10)	76 (54, 112)	0.830
Sodium (mmol/L)	140 (137, 142)	140 (137, 142.50)	140 (137, 142)	0.472
Albumin (g/L)	30 (26, 34)	30 (26, 34)	29 (25, 32)	0.070
Total bilirubin (μmol/L)	21.40 (14.70, 37)	21.30 (14.45, 37)	21.30(14.80, 37.40)	0.158
ALT (U/L)	23 (15, 36)	23 (14, 36)	23 (16, 34)	0.458
AST (U/L)	33 (24, 51)	30 (22, 49.75)	43 (28, 58)	0.114
Creatinine (μmol/L)	63 (51, 77)	63 (51, 77)	62 (50, 80)	0.809
PT-INR	1.26 (1.13, 1.43)	1.26 (1.14, 1.43)	1.25 (1.12, 1.42)	0.661
NLR	3.13 (1.92, 5.48)	3.08 (1.85, 5.39)	3.25 (2.08, 5.36)	0.512
PLR	98.13 (67.82, 152.90)	97.47 (64.99, 151.90)	102.90 (72.64, 169.70)	0.167
LMR	2.32 (1.47, 3.29)	2.44 (1.51, 3.37)	1.97 (1.37, 3.17)	0.121
Body composition parameters				
BMI (kg/m²)	23.76 (20.41)	23.31(20.01, 26.04)	24.74(20.88, 27.16)	0.062
SMI (cm²/m²)	44.2 (37.42, 51.29)	44.0 (37.44, 51.35)	44.93 (37.13, 51.20)	0.892
Sarcopenia	130 (27.48)	101 (25.90)	29(34.94)	0.105
VSR	1.06 (0.76, 1.46)	0.99 (0.71, 1.39)	1.30 (1.00, 1.81)	<0.001
Abnormal adiposity	129 (27.27)	95 (24.36)	34 (40.96)	0.003
VATI (cm²/m²)	46.48(29.21, 85.05)	41.62(25.75, 61.81)	59.74(46.69, 86.22)	<0.001
High visceral adiposity	301(63.64)	239 (61.97)	71 (85.54)	<0.001
SATI (cm²/m²)	40.43 (28.8, 51.8)	38.38 (28.76, 51.73)	44.43 (28.72, 65.97)	0.074
Low subcutaneous adiposity	112 (23.68)	94 (24.19)	18 (21.69)	0.776
TATI (cm²/m²)	89.81(59.98, 123.40)	85.75(56.98, 117.60)	109(76.88, 154.80)	<0.001
High total adiposity	262(55.39)	202(51.79)	60(72.29)	<0.001

Figure 2. The correlation coefficience of IMAC, VSR, VATI with age, BMI, SMI,SATI, and LOH.

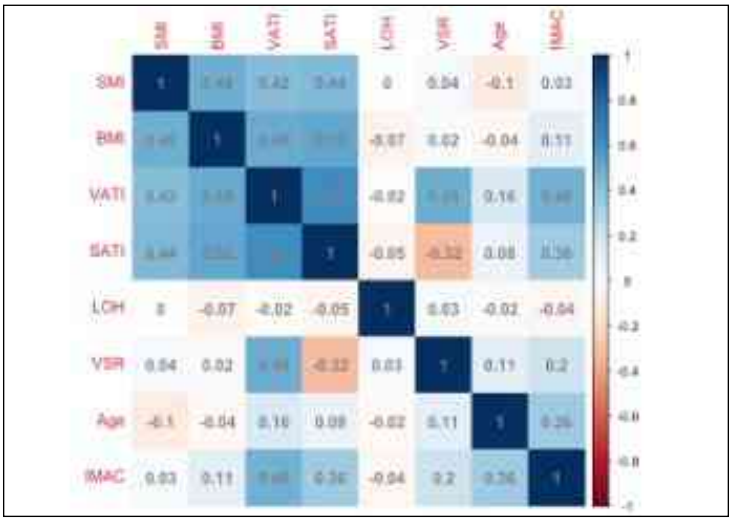

❖ AA-081

Qushi Huayu decoction attenuated hepatic lipid accumulation via JAK2/STAT3/ CPT-1A-related fatty acid β-oxidation in mice with non-alcoholic steatohepatitis

Qinmei Sun[1], Xin Wang[1], Yiyang Hu[1,2,3], Qin Feng[1,2,3]
[1]Institute of Liver Diseases, Shuguang Hospital affiliated to Shanghai University of Traditional Chinese Medicine, [2]Shanghai Key Laboratory of Traditional Chinese Clinical Medicine, Shanghai 201203, China., [3]Key Laboratory of Liver and Kidney Diseases, Shanghai University of Traditional Chinese Medicine, Ministry of Education, Shanghai 201203, China.

Background: Non-alcoholic fatty liver disease (NAFLD) has become the most common chronic liver disease worldwide. Qushi Huayu Decoction (QHD), a traditional Chinese recipe, has been clinically used in treating NAFLD for long time. It has been previously demonstrated that QHD could alleviate hepatic steatosis and inflammation in non-alcoholic steatohepatitis (NASH) animal. CPT-1A-related mitochondrial fatty acid β-oxidation is the primary mechanism responsible for fat consumption. The Janus Kinase 2 (JAK2) / signal transducer and activator of transcription 3 (STAT3) pathway has been proved to regulate CPT-1's transcription in liver. Whether fatty acid β-oxidation is involved in lipid consumption when QHD treating NASH remains unclear. In this study, we investigated the effect of QHD in hepatic fatty acid β-oxidation and the underlying mechanism relating to JAK2/STAT3 pathway.

Method: Male C57BL/6J mice was fed with normal or high-fat and high-carbohydrate diet for 18 weeks. In the beginning of 13th week, mice on HFHC diet were randomly divided into HFHC, QHD-L, QHD-H and obeticholic acid groups. And then, different dose of QHD (2.875 mg/kg/d and 11.5 mg/kg/d) or obeticholic acid (10 mg/kg) were administrated by intragastric gavage for 6 weeks. The effects of QHD on general condition, glucose and lipid metabolism, liver histopathology and liver enzymes were evaluated. Moreover, hepatic lipid accumulation was measured using lipid droplets staining, hepatic triglyceride and free fatty acid. Further, the mRNA and protein levels of hepatic CPT-1A, a rate-limiting enzyme of fatty acid β-oxidation, were qualified to evaluate the level of lipid consumption. And then, the content of ATP in liver was qualified to indicate the level of cellular energy metabolism. Lastly, the potential signaling pathway responsible for fatty acid β-oxidation was identified by estimating the relative expression protein level of Janus kinase 2, phosphorylated JAK2, signal transducer and activator of transcription 3 and phosphorylated-STAT3 in the liver.

Result: The results showed that QHD significantly improved NASH in mice, as reflected by reducing body weight, improving serum glucolipid metabolism, decreasing hepatic enzymes activities, reducing hepatic triglyceride and free fatty acids, and ameliorating hepatic steatosis, inflammation in pathology. From a mechanistic point of view, hepatic ATP content increased significantly after QHD treatment. The expression of CPT-1A mRNA and protein both increased drastically, too. Furthermore, both the total protein and nuclear p-STAT3 in liver were significantly down-regulated after QHD treatment. And the hepatic p-JAK2 protein was significantly inhibited by QHD, too.

Conclusion:QHD reduced hepatic lipid accumulation in NASH mice by increasing fatty acid β-oxidation, and this effect may be related to the JAK2/STAT3/CPT-1A signaling pathway. The study provided a scientific basis for the clinical use of QHD in treating NASH.

❖ AA-082

Salvianolic acid B ameliorates liver fibrosis by inhibiting hepatocytes ferroptosis via activation of ECM1/xCT/GPX4 pathway

Yadong Fu[1,2,3], Xiaoxi Zhou[1], Weiguo Fan[2], Siqi Gao[1,3], Zhiyang Ling[2], Bing Sun[2], Ping Liu[1,3], Jiamei Chen[1]

[1]Institute of Liver Diseases, Key Laboratory of Liver and Kidney Diseases (Ministry of Education), Shuguang Hospital Affiliated to Shanghai University of Traditional Chinese Medicine, Shanghai 201203, China, [2]State Key Laboratory of Cell Biology, Shanghai Institute of Biochemistry and Cell Biology, Center for Excellence in Molecular Cell Science, Chinese Academy of Sciences; University of Chinese Academy of Sciences, Shanghai 200031, China, [3]Institute of Interdisciplinary Medicine, Shanghai University of Traditional Chinese Medicine, Shanghai 201203, China

Background: Extracellular matrix protein 1 (ECM1), mainly secreted by hepatocytes in liver, plays an important role in maintaining liver homeostasis and physiological functions. Hepatocyte ferroptosis promotes the occurrence and progression of liver fibrosis. Salvianolic acid B (Sal B), one of the main active ingredients of Salvia miltiorrhiza, has potent antioxidative and anti-fibrotic effects, but its pharmacological mechanism is still unclear. We investigated the role of ECM1 in hepatocyte ferroptosis, and the pharmacological mechanism of Sal B against liver fibrosis.

Method: We performed studies with hepatocyte-specific ECM1 knockout mice (ECM1Δhep), and wild type mice (WT, controls). Liver fibrosis was induced by intraperitoneal injection of CCl4 three times weekly for 6 weeks, and intervened with Sal B, sorafenib or cilengitide in the beginning of 4th week. Liver tissues were collected from mice and analyzed using histopathologic and molecular analysis. A hepatocyte injury model induced by CCl4 and a hepatocyte ferroptosis model induced by Erastin were incubated with Sal B, recombinant human ECM1 protein and ferrostatin-1 (Fer-1) in vitro.

Result:CCl4-induced hepatic lipid peroxidative damage, hepatocyte ferroptosis and liver fibrosis were accelerated in ECM1Δhep mice compared with control mice. Hepatocyte ferroptosis induced by CCl4 or Erastin was significantly reduced after ECM1 treatment by interacting with xCT. Hepatocytes produced the highest levels of ECM1 in livers of mice. Ectopic expression of ECM1 or soluble TGFBR2 in liver prevented fibrogenesis in ECM1-KO mice and prolonged their survival.Ectopic expression of ECM1 in liver also reduced the severity of CCl4-induced fibrosis in mice. Sal B treatment significantly attenuated inflammatory, hepatocyte injury, hepatic iron metabolism, hepatic lipid peroxidative damage and hepatic fibrosis. Mechanistically, we found that Sal B protected against

hepatocyte ferroptosis by activating the ECM1/xCT/GPX4 pathway, which was supported by the result that ECM1 knockout by using ECM1Δhep mice blocked the Sal B-mediated anti-fibrotic effect.

Conclusion:ECM1 inhibits lipid peroxidation to prevent hepatocyte ferroptosis and represents a novel therapeutic target for the treatment of liver fibrosis. Sal B exerts significant protective effects against hepatocyte ferroptosis through activation of ECM1/ xCT/GPX4 pathway, consequently attenuating hepatic fibrosis.

Table and Figure:

Figure 1.A schematic illustration shows that the mechanism of protection against hepatocyte ferroptosis of Sal B.

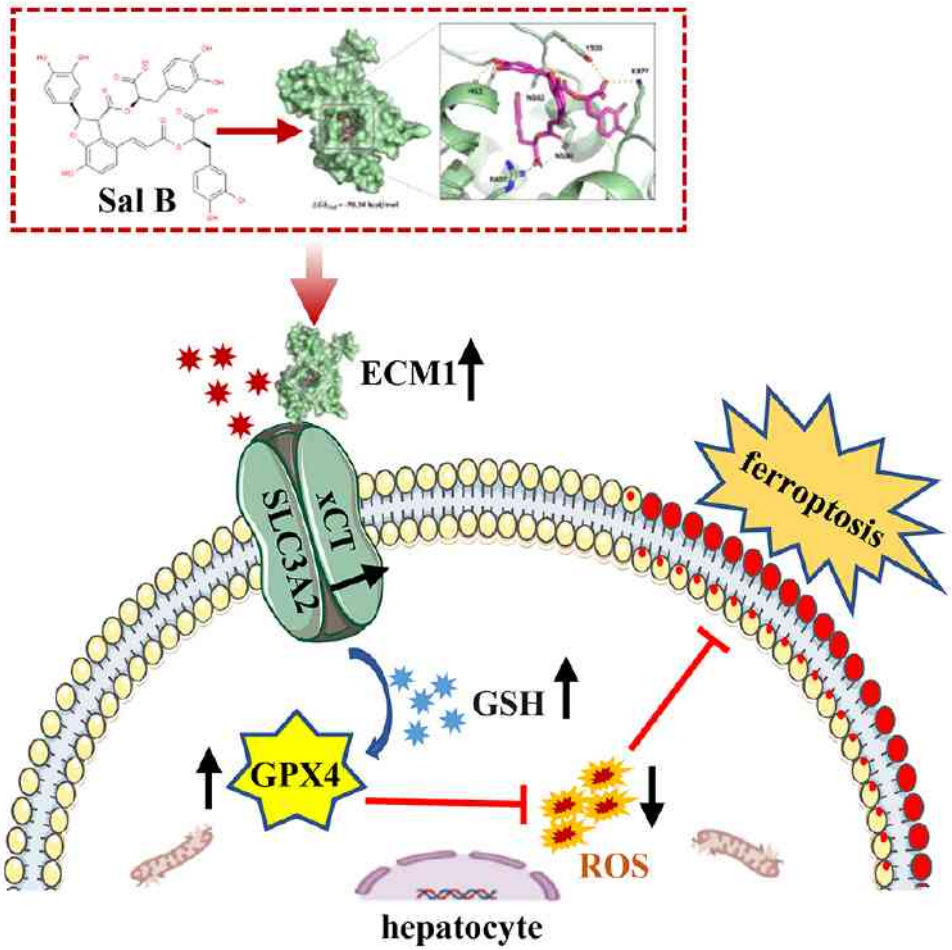

❖ AA-083

The Impact of National Centralized Drug Procurement Policy on Antiviral Utilization and Expenditure for Chronic Hepatitis B in China

Xinyu Zhao[1], Min Li[1], Hao Wang[1], Xiaoqian Xu[1], Xiaoning Wu[2], Yameng Sun[2], Bingqiong Wang[2], Shuyan Chen[2], Hong You[3], Jidong JIA[3], Yuanyuan Kong[1]
[1]Clinical Epidemiology & EBM Unit, Beijing Friendship Hospital, Capital Medical University; National Clinical Research Center for Digestive Diseases, Beijing, China., [2]Liver Research Center, Beijing Friendship Hospital, Capital Medical University, Beijing Key Laboratory of Translational Medicine on Liver Cirrhosis, National Clinical Research Center of Digestive Diseases, Beijing, China., [3]Liver Research Center, Beijing Friendship Hospital, Capital Medical University; National Clinical Research Center for Digestive Diseases, Beijing, China.

Background: The National Centralized Drug Procurement (NCDP policy) was launched in mainland China in April 2019, with entecavir (ETV) and tenofovir disoproxil fumarate (TDF) being included in the procurement list. However, the impacts of NCDP policy on the utilization and expenditure of antiviral therapy for CHB in mainland China is still unclear, so we conducted the current study based on the administrative database of the National Healthcare Security Administration (NHSA).

Method: The procurement records, including monthly purchase volume, expenditure, and price of nucleos(t)ide analogs (NAs), were derived from the NHSA from April 2018 to March 2021. The changes in volumes and expenditures of the first-line NAs and bid-winning products were calculated. The effects of price, volume, and structure related to drug expenditure were calculated by A.M. Index System Analysis. The changes in the proportion of CHB patients receiving antiviral treatment were also reported.

Result: The purchase volume of NAs significantly increased from 134.3 to 318.3 million DDDs, whereas the expenditure sharply decreased from 1623.41 to 490.43 million RMB (Figure 1). The proportions of first-line NAs rose from 72.51% (ETV 69.00%, TDF 3.51%) to 94.97% (ETV 77.42%, TDF 17.55%) (Figure 1). A.M. analysis showed that the NCDP policy decreased the expenditure of all NAs (S=0.91) but increased that of the first-line NAs in the bid-winning list (S=1.13). Assuming the population size of CHB patients remains stable and a compliance rate of ≥75%, the proportion of CHB patients receiving first-line antiviral therapy would increase from 6.36-8.48% to 11.56-15.41% (table 1).
Conclusion: The implementation of the NCDP policy significantly increased the utilization of first-line NAs for CHB patients at a lower expenditure. The findings could provide

evidence for optimizing antiviral therapy strategy and allocating medical resources in China.

Table and Figure:

Figure 1. Figure 1. The quarterly change of volume (A), expenditures (B), and proportions of purchase volume (C) of HBV-related NAs from Apr 2018 to Feb 2021.

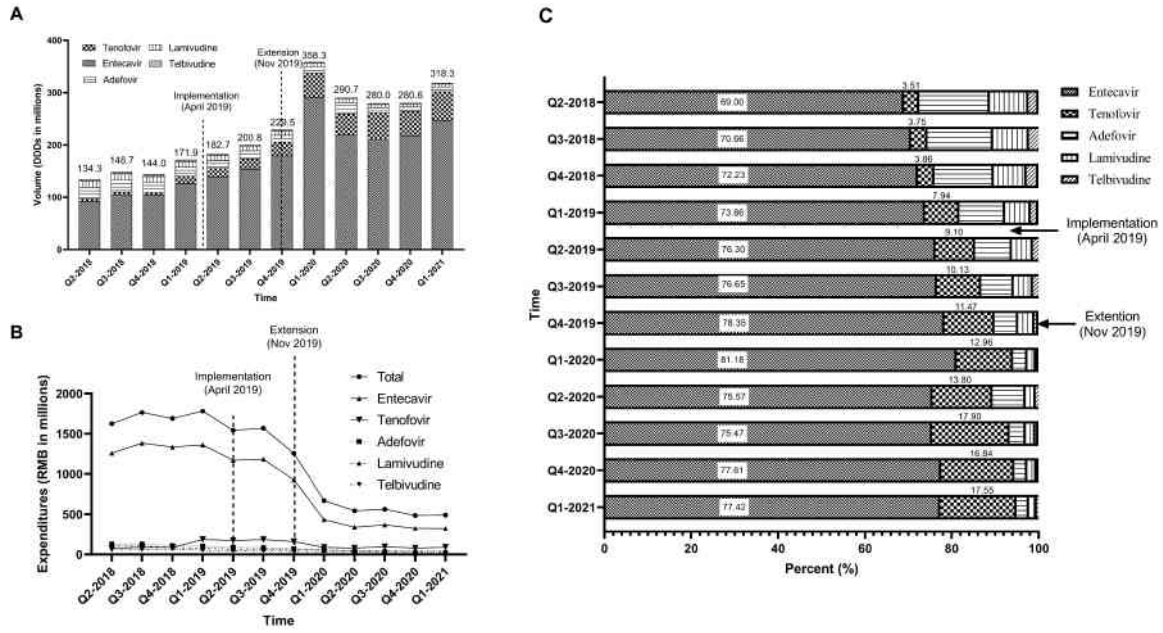

Figure 2. Table 1. Changes in the proportion of CHB patients receiving antiviral treatment before and after the implementation of “4+7” policy

Table 1. Changes in the proportion of CHB patients receiving antiviral treatment before and after the implementation of "4+7" policy

	Apr 2018–Mar 2019		Apr 2019–Mar 2020		Apr 2020–Mar 2021	
Groups	Number* (n)	Percentage (%)	Number* (n)	Percentage (%)	Number* (n)	Percentage (%)
Total NAs						
Compliance rate						
100%	1640626	6.36	2661061	10.31	3204251	12.42
75%	2187502	8.48	3548082	13.75	4272335	16.56
50%	3281252	12.72	5322123	20.63	6408502	24.84
25%	6562505	25.44	10644246	41.26	12817004	49.68
First-line NAs#						
Compliance rate						
100%	1255169	4.86	2393733	9.28	2982164	11.56
75%	1673558	6.49	3191643	12.37	3976219	15.41
50%	2510337	9.73	4787465	18.56	5964329	23.12
25%	5020674	19.46	9574930	37.11	11928657	46.24
First-line NAs in the bid-winning list						
Compliance rate						
100%	55273	0.21	843135	3.27	1671132	6.48
75%	73697	0.29	1124180	4.36	2228176	8.64
50%	110546	0.43	1686270	6.54	3342264	12.95
25%	221092	0.86	3372539	13.07	6684527	25.91

Abbreviations: Apr: April; Mar: March.

*: Number of CHB patients receiving antiviral treatment.

#: First-line NAs included entecavir and tenofovir.

❖ AA-084

Aloin Attenuates Hepatic Stellate Cell Activation and CCl4-induced Liver Fibrosis by Inhibiting the TGF-β/Smad Signaling Pathway

Junjie Bai1, Baolin Qian1,2, Tianying Cai1, Yifan Chen1, Tongxi Li1, Yonglang Cheng1, Ziming Wu1, Chen Liu1, Yichao Du3 and Wenguang Fu1,3
1Department of General Surgery (Hepatopancreatobiliary Surgery), The Affiliated Hospital of Southwest Medical University, Luzhou, Sichuan, China.
2Key Laboratory of Hepatosplenic Surgery, Ministry of Education, The First Affiliated Hospital of Harbin Medical University, Harbin, Heilongjiang, China.
3Academician (Expert) Workstation of Sichuan Province, The Affiliated Hospital of Southwest Medical University, Luzhou, Sichuan, China.

Background: Liver fibrosis is an excessive accumulation of extracellular matrix (ECM) components in liver tissue, which is considered to be a wound-healing response to liver damage, for which there is no effective treatment. Aloin (Alo), an anthraquinone compound isolated from the aloe plant, has been found to have anti-inflammatory and antioxidant abilities in a variety of disease models, but whether it has a protective effect in liver fibrosis is still unclear. In this study, we investigated the potential mechanisms underlying the antifibrotic effect of Aloin.

Method: We established a mouse liver fibrosis model by intraperitoneal injection of carbon tetrachloride (CCl4) and a cellular model by stimulating hepatic stellate cells (HSCs) with transforming growth factor β1 (TGF-β1).

Result: Aloin attenuated CCl4-induced liver injury and reduced serum alanine aminotransferase (ALT), aspartate aminotransferase (AST) and hydroxyproline (HYP). Meanwhile, Aloin attenuated CCl4-induced inflammation by down-regulating inflammatory factors (IL-1β, IL-6 and TNF-α) and up-regulating the expression of anti-inflammatory factor IL-10. Additionally, Aloin inhibited the activation of hepatic stellate cells, reduced the expression of α-SMA (α-smooth muscle actin) and Collagen Type I (COL1A2), and improves liver fibrosis by inhibiting the TGF-β/Smad signaling pathway.

Conclusion: In vivo and in vitro studies confirmed that Aloin attenuated liver fibrosis through inhibition of the TGF-β/Smad2/3 signaling pathway, while mitigating CCl4 and TGF-β1-induced inflammation. It provided a basis for the prevention and treatment of liver fibrosis.

Table and Figure:

Figure 1. Chemical structure of aloin presented in (A) two-dimensional and (B) three-dimensional models.

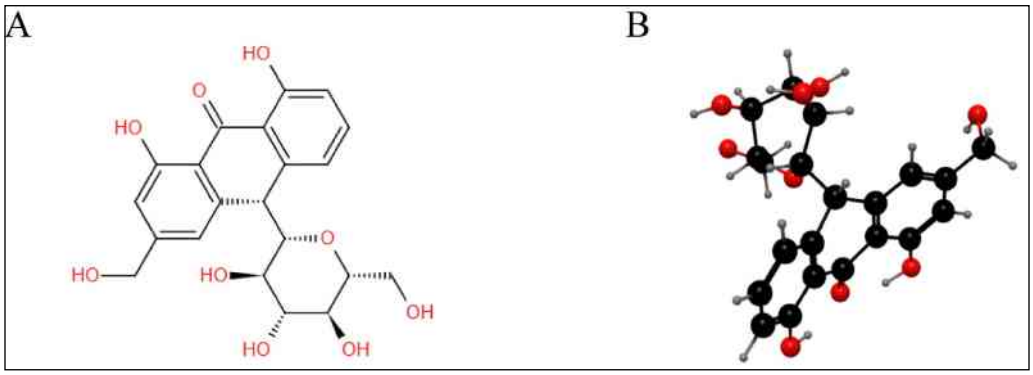

Figure 2. Aloin treatment attenuated CCl4-induced liver injury in mice. (A) Experimental design. (B) Body weight. (C) Liver index. (D) Hydroxyproline content in serum. (E) Alanine aminotransferase content in serum. (F) Aspartate aminotransferase content in serum. Data are expressed as mean ± standard deviation. *** P < 0.001 versus the Control group; # P < 0.05, ## P < 0.01 and ### P < 0.001 versus the CCl4 group; ns: no significance.

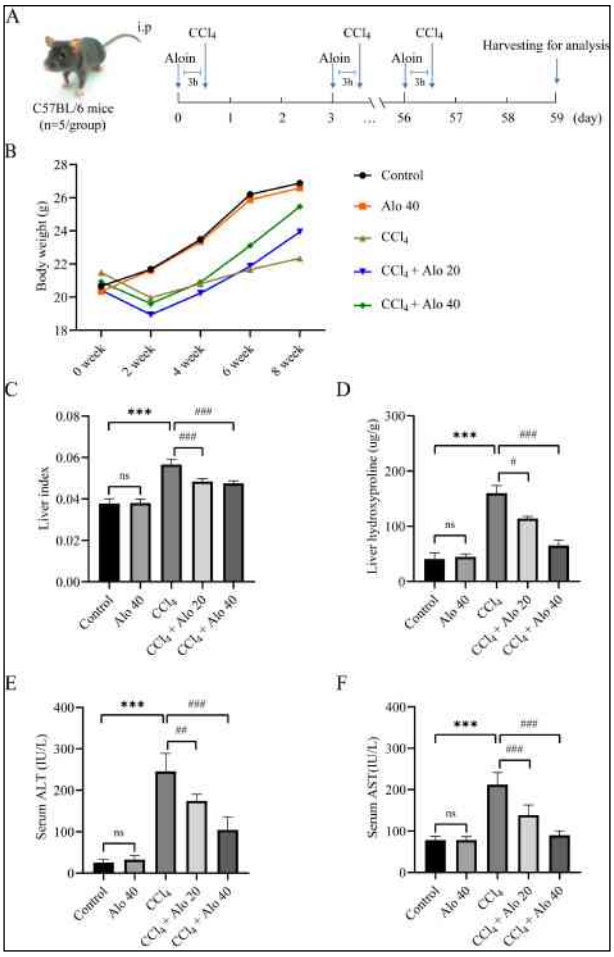

❖ AA-085

Anti-fibrosis effect of traditional Chinese medicine compound Biejiaruangan in patients with chronic hepatitis B

YaChao Tao[1], Enqiang Chen[2]
[1]Center of Infectious Diseases, West China Hospital of Sichuan University, No.37 Guo Xue Xiang, Wuhou District, Chengdu 610041, China, [2]West China Hospital of Sichuan University

Background: Liver fibrosis is the intermediate stage and a common pathway leading to cirrhosis and cancer. It is reversible and can be improved. Compound Biejiaruangan (CBJRG) tablet acts as the first traditional Chinese medicine to treat liver fibrosis and has been widely used in clinical setting. This study aimed to explore the efficacy of CBJRG tablet in alleviating liver fibrosis in patients with chronic hepatitis B (CHB).

Method: All enrolled patients achieved virological response at baseline and received 24-week CBJRG in the context of antiviral therapy. The evaluation of anti-fibrosis effect of CBJRG was performed through comparing the differences of live stiffness measurements (LSM) values, aspartate aminotransferase-to-platelet ratio index (APRI) scores and fibrosis index based on four factors (FIB-4) scores between pre- and post-treatment.

Result:A total of 120 eligible patients were enrolled. LSM values ($p<0.01$), APRI scores ($p<0.01$) and FIB-4 scores ($p<0.01$) were significantly lower after 24-week treatment in all patients. Positive correlations were observed between APRI, FIB-4 scores and LSM values both at baseline and after treatment. At the end of our follow up, 55 patients improved and 17 patients worsened in fibrosis stages. Further investigation revealed that the significant reduction of LSM values, APRI and FIB-4 scores and the improvement of fibrosis stages were only observed in patients receiving after 24-week CBJRG in the context of ETV therapy, not in patients receiving CBJRG plus other antiviral drugs.

Conclusion:CBJRG tablet can help to alleviate the degree of liver fibrosis in patients receiving ETV antiviral therapy.

❖ AA-086

Advances in aspirin to slow down liver fibrogenesis

Chenrui Zhang1, Yingmei Tang1
1 The Second Affiliated Hospital of Kunming Medical University

Background: The progression of liver fibrosis involves extensive necrosis of hepatocytes, diffuse proliferation of fibrous tissue, formation of pseudobullets and regenerative nodules, and eventually cirrhosis. During this process, platelets can accelerate the liver fibrosis process by promoting intrahepatic microthrombosis and direct activation of hepatic stellate cells. Aspirin is a classical inhibitor of platelet aggregation, and some researches have now found that aspirin may have an inhibitory effect on liver fibrosis.

Method: New research advances in aspirin to slow down the process of liver fibrosis are reviewed.

Result: Aspirin may act to prevent and inhibit the process of liver fibrosis by indirectly inhibiting the stimulatory effect of platelets and intrahepatic prostaglandin synthase-2 on hepatic stellate cell activation.

Conclusion: The mechanism by which aspirin inhibits the progression of liver fibrosis is still unclear, and aspirin may have the effect of preventing the development of liver fibrosis and delaying the progression of liver fibrosis in patients with liver disease. Further investigation of the therapeutic effects of aspirin in patients with liver fibrosis may provide new therapeutic avenues for the reversal of cirrhosis.

❖ AA-087

Very Low Level Viremia and Occasional Low Level Viremia Suggests Hindered Fibrosis Regression

Zhengzhao Lu[1], Yameng Sun[1], Shuyan Chen[1], Tongtong Meng[1], Bingqiong Wang[1], Jialing Zhou[1], Xiaoning Wu[1], Xinyan Zhao[1], Xiaojuan Ou[1], Jidong Jia[1], Hong YOU[1]
[1]Liver Research Center, Beijing Friendship Hospital, Capital Medical University, Beijing Key Laboratory of Translational Medicine on Liver Cirrhosis, National Clinical Research Center of Digestive Diseases, Beijing, China

Background: Maintained virological response (MVR) could reverse liver fibrosis and low level viremia (LLV) promotes fibrosis progression of chronic hepatitis B patients under antiviral treatment. We aimed to assess whether very low level viremia (VLLV) and occasionally detectable HBV DNA were associated with decreased regression of liver fibrosis.

Method: Chronic hepatitis B patients with paired liver biopsies at baseline and after 260 weeks of antiviral therapy were enrolled. Levels of HBV DNA were measured by sensitive real-time quantitative PCR (lower limit of detectable was 20 IU/mL) every 26 weeks. VLLV was defined as HBV DNA detectable (>20 IU/mL) at least once but persistently less than 100 IU/mL. Occasional low level viremia (OLLV) was defined as HBV DNA detectable only once but less than 2,000 IU/mL during at least 3 times of HBV DNA tests. Fibrosis regression was defined as Ishak stage decrease ≥ 1 or as predominantly regressive classified by P-I-R system (Beijing Classification).

Result:A total of 111 CHB patients with HBV DNA persistently <2,000 IU/mL and good compliance after 52 weeks of antiviral therapy were included in this analysis. Fibrosis regression was observed in 67 (60.4%) patients, indeterminate in 14 (12.6%) patients, and progression in 30 (27.0%) patients. Among them, 68 (61.3%) patients were in MVR group, 37 (33.3%) in VLLV group and 24 (21.6%) in OLLV group. Fibrosis regression rate was lower in VLLV than in MVR but higher than in the remaining patients (MVR vs. VLLV vs. remaining: 67.6% [46/68] vs. 51.4% [19/37] vs. 33.3% [2/6], p=0.030). Also fibrosis regression rate was lower in OLLV than in MVR but higher than in the remaining patients (MVR vs. OLLV vs. LLV were 67.6% [46/68], 56.5% [13/23] and 40.0% [8/20], p=0.009).

Conclusion: Very low level viremia and occasional low level viremia may associate with a decreased fibrosis regression.

Table and Figure:

Figure 1. Distribution of fibrosis regression, indeterminate, and progression in patients with maintained virological response, very low level viremia and the remaining patients.

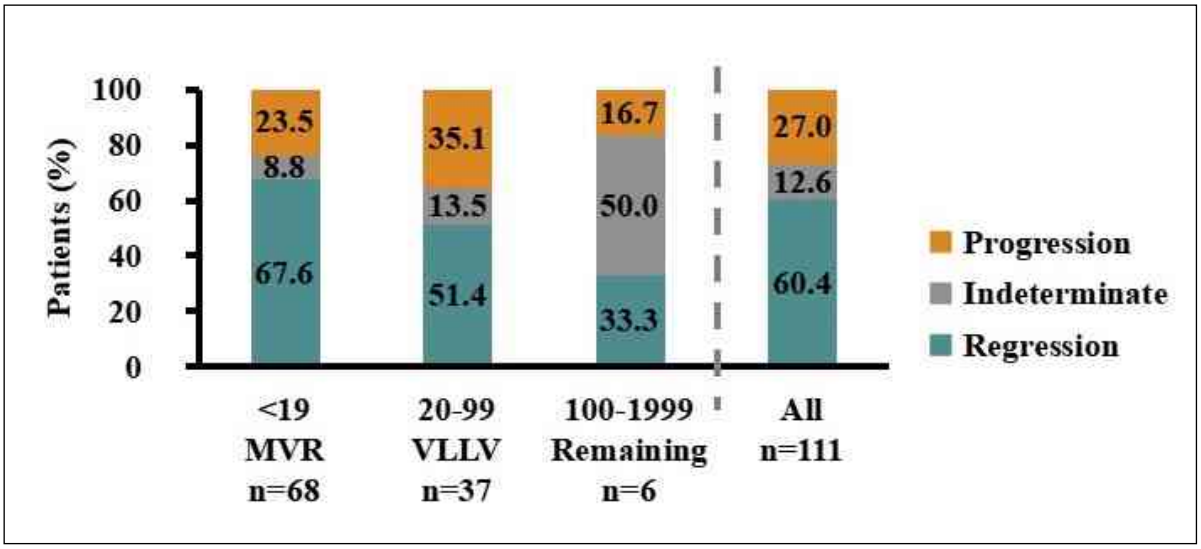

Figure 2. Distribution of fibrosis regression, indeterminate, and progression in patients with maintained virological response, occasional low level viremia and the remaining patients.

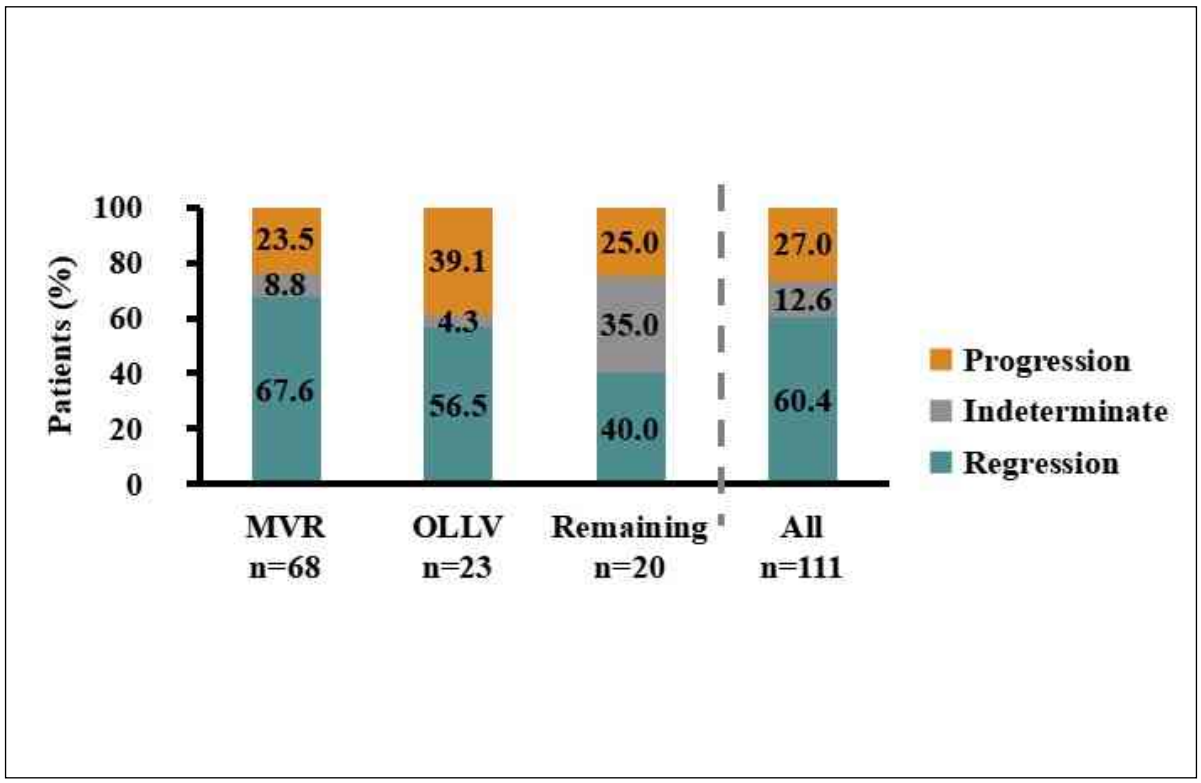

❖ AA-088

Glycemic control improves the prognosis of patients with hepatitis B virus related acute-on-chronic liver failure

Weizhen Weng[1], Xiaohua Peng[2], Jing Zhang[1], Bingliang Lin[1]
[1] the third Affiliated Hospital of Sun Yat-sen University, [2]the seventh Affiliated Hospital of Sun Yat-sen University

Background: Hepatitis B virus-related acute-on-chronic liver failure (HBV-ACLF) is a severe and life-threatening complication. However, there is limited information on the impact of diabetes mellitus (DM) and blood glucose control on HBV-ACLF in a large population. We aimed to evaluate the impact of diabetes mellitus on the prognosis of HBV-ACLF, and to access whether glycemic control improves the prognosis.

Method: In this retrospective observational study, we identified 2166 cases of HBV-ACLF hospitalized from January 2010 to March 2018, of whom 251 had diabetes mellitus. Patients were divided into different groups according to the diagnosis of diabetes mellitus and level of fasting blood glucose (FBG). Diabetic patients who had been hospitalized for more than one week (n=205) were divided into three subgroups according to FBG: the normal FBG group (Group A, n=66, FBG <6.1 mmol/L), the impaired FBG group (Group B, n=40, FBG between 6.1-7.0 mmol/L) and the high FBG group (Group C, n=99, FBG ≥7.0 mmol/L). Survival was estimated by the Kaplan-Meier method, and evaluated with a stratified log-rank test. A Cox regression was performed to estimate the hazard ratios (HR) and 95% confidence intervals (CI) for ACLF-related mortality. A ROC curve analysis was performed to evaluate the predictive value of FBG for a 90-day prognosis.

Result: In patients with diabetes, 90-day transplant-free mortality was significantly higher than in patients without diabetes (39.8% vs 54.3%). These patients were elderly, with higher pneumonia accidence and acute kidney injury. Cox multivariate regression analysis showed that DM was an independent risk factor. The cumulative 90-day survival rates were 56.1%, 62.5%, and 37.4% in the normal FBG group (Group A), the impaired FBG group (Group B) and the high FBG group (Group C), respectively. A lower mortality was observed in patients with a mean fasting blood glucose below 6.77 mmol/L within one week of hospitalization.

Conclusion: Patients with diabetes increase the risk of 90-day mortality. Controlling FBG at an appropriate level in diabetic patients may improve the prognosis of HBV-ACLF.

Table and Figure:

Figure 1. Patients' survival rate with different levels of FBG and cut-off for FBG

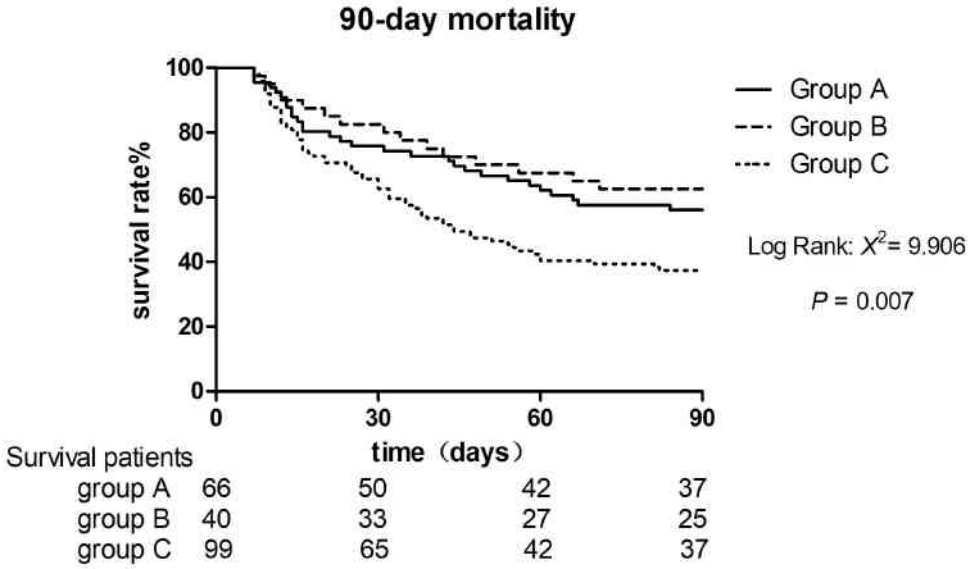

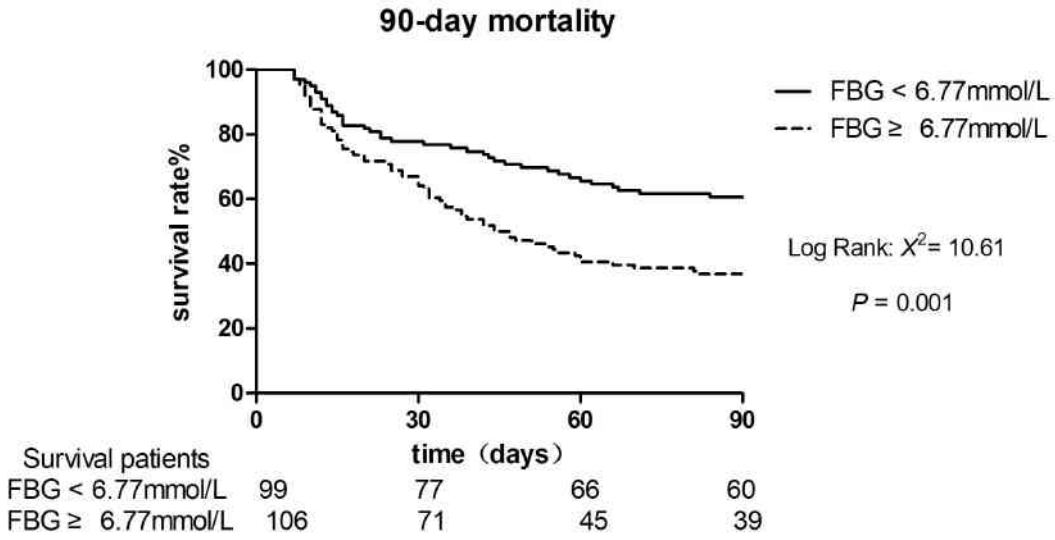

❖ AA-089

Exosomes Derived from Human Umbilical Cord Mesenchymal Stem Cells Ameliorate Experimental Non-alcoholic Steatohepatitis by Regulating Nrf2/NQO-1 Pathway

Yaxing Kang[1], Yiran Song[1], Yuxin Luo[1], Jinbo Guo[1], Xiaonan Liang[1], Jia Song[1], Jun Yu[1], Xiaolan Zhang[1]
[1]The Second Hospital Of Hebei Medical University

Background: Non-alcoholic steatohepatitis (NASH) may progressively lead to hepatic cirrhosis and liver carcinoma, and excessive oxidative stress provides an essential role in the progression of NASH. However, no approved effective therapy for NASH is currently available. Exosomes derived from mesenchymal stem cells (MSCs) perform the functions such as inhibiting inflammation, anti-oxidative stress, regulating immunity, but it is not clear whether MSCs exosomes protect against NASH through antioxidant effects. Therefore, this study was conducted to investigate the effects of exosomes on NASH and explore the role of exosomes on oxidative stress in NASH both in vivo and in vitro.

Method: In vivo, C57BL/6J male mice were fed with high fat and high cholesterol diet (HFHC) and methionine choline deficiency diet (MCD). Mice were treated with or without MSCs exosomes by tail intravenous injection. The key indicators were measured, including liver damage, lipid metabolism and oxidative stress. In vitro, Human hepatocellular carcinoma cells HepG2 exposed to palmitic acid (PA) and mouse immortalized hepatocytes AML12 exposed to methionine choline-deficient (MCD) medium were cultured. The therapeutic effect of exosomes in steatotic cells was also evaluated. To elucidate the signaling pathways, ML385 was applied to intervene in vitro.

Result: In vivo the studies showed that MSCs exosomes histologically improved hepatic steatosis and inflammatory cell infiltration; reduced serum ALT, liver TG levels and improved liver-related inflammatory parameters, including the increment of M2 macrophages and CD206 mRNA, reduction of M1 macrophages and hepatic TNF-α, IL-6, CD11c mRNA; modified the aberrant expression of lipid-related genes, including SREBP-1c, PPAR-α, Fabp5, CPT1α, ACOX and FAS. In addition, MSCs exosomes increased the protein ratio of p-Nrf2/Nrf2, as well as the activity of SOD and GSH and the protein expression of NQO-1; decreased the protein and mRNA expression of CYP2E1 and the levels of hepatic MDA. In vitro MSCs exosomes depressed the fluorescence intensity of Nile Red, cellular TG and ROS; promoted the protein expression of p-Nrf2 and

NQO-1. Furthermore, the Nrf2-specific inhibitor ML385 reversed the partial therapeutic effects of MSCs exosomes.

Conclusion: These results obviously showed that MSCs exosomes improved NASH probably through modulating Nrf2/NQO-1 anti-oxidative signaling, suggesting that MSCs exosomes hold promise as a novel therapeutic agent for NASH.

❖ AA-090

Lower alanine aminotransferase threshold for initiating anti-HBV therapy for chronic hepatitis B benefits to identify more patients need to treat

Mengyang Zhang[1], Yameng Sun[1], Shuyan Chen[1], Xiaoning Wu[1], Jialing Zhou[1], Bingqiong Wang[1], Tongtong Meng[1], Hong You[1]
[1]Liver Research Center, Beijing Friendship Hospital, Capital Medical University, Beijing Key Laboratory of Translational, Medicine on Liver Cirrhosis, National Clinical Research Center of Digestive Diseases, Beijing, China.

Background:A non-negligible proportion of chronic hepatitis B (CHB) patients with normal alanine aminotransferase (ALT) show significant histological lesions and are at a high risk of liver-related events. Therefore, the aim of our study is to determine whether a lower ALT threshold for treatment benefits to identify more patients who need antiviral therapy.

Method: Treatment-naive patients with chronic HBV infection and liver biopsies were selected from an existing cohort. ALT threshold was set as 40, 35, 30, 25, 20, 15 and 10IU/L manually to determine the benefit of a lower ALT threshold and to detect the best threshold for both males and females. Diagnostic accuracy and cut-off value were explored by the area under the receiver operating characteristic curve (AUC).

Result:A total of 86% of patients had significant inflammation, 68% of patients had significant fibrosis and 91% of patients had significant inflammation or fibrosis. ALT was positively associated with necroinflammation score ($R = 0.269$, $P < 0.001$), while was not correlated with fibrosis. The highest proportion of significant inflammation or fibrosis was in the new-covered patients, who met the criteria of initiating treatment when 30IU/L of threshold was taken for males, and 25IU/L for females. The AUCs of ALT in males and females were 0.653 and 0.751 for significant inflammation or significant fibrosis ($P = 0.016$ and 0.041), and the cut-off value was 28.5IU/L and 25.5IU/L respectively. An ALT threshold of 30/25 IU/L (males/females) provided a sensitivity of 0.94, a specificity of 0.25, and an accuracy of 0.85.

Conclusion: Lower ALT threshold for treatment of CHB brings benefits to identify more patients who need therapy. A threshold of 30/25IU/L (male/female) could be recommended for Chinese CHB patients.

Table and Figure:

Figure 1. Distributions of significant histological lesions with different ALT thresholds in new-covered CHB patients.

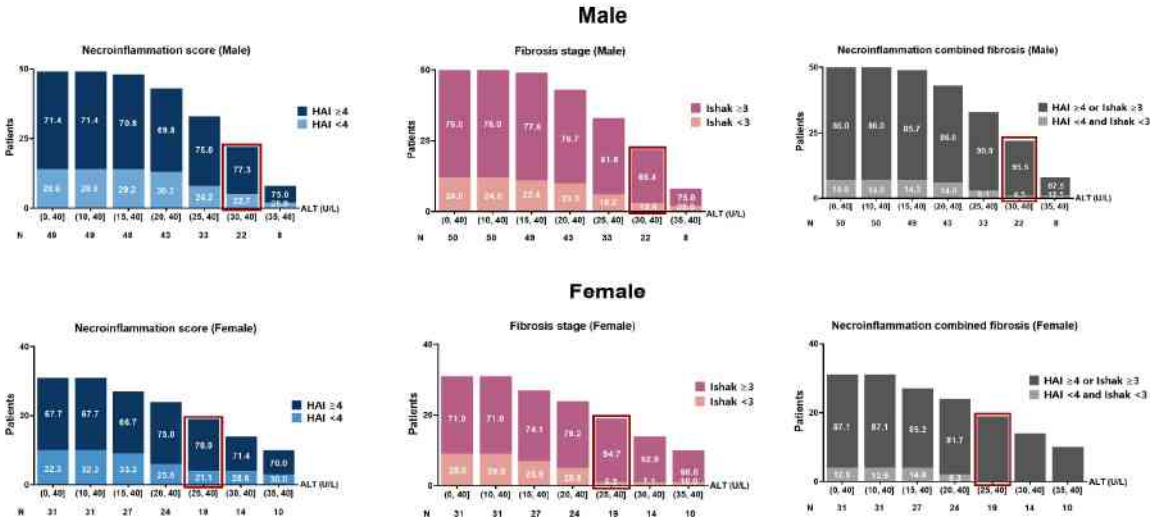

Figure 2. Diagnostic accuracy of a threshold of 30/25IU/mL (male/female) for identifying

	HAI ≥4	Ishak ≥3	HAI ≥4 or Ishak ≥3
Male-30U/L			
Sen	0.91	0.89	0.90
Spe	0.26	0.12	0.26
Youden index	0.18	0.01	0.16
Accuracy	0.82	0.65	0.84
PPV	0.88	0.70	0.92
NPV	0.26	0.12	0.26
+LR	1.24	1.01	1.22
-LR	0.33	0.92	0.38
Female-25U/L			
Sen	0.92	0.93	0.90
Spe	0.43	0.25	0.67
Youden index	0.35	0.18	0.57
Accuracy	0.84	0.69	0.89
PPV	0.89	0.69	0.97
NPV	0.43	0.25	0.67
+LR	1.61	1.24	2.71
-LR	0.19	0.28	0.14

CHB patients with significant histological lesions.

❖ AA-091

Prevalence and predictors of cirrhosis among US adults with surface antigen negative hepatitis B: a nationwide population-based study

Shuaiwen Huang[1]
[1]Department and Institute of Infectious Disease, Tongji Hospital, Tongji Medical College, Huazhong University of Science and Technology, Wuhan, Hubei, China

Background: Evaluation of cirrhosis appears to be easily overlooked in the clinic for the population with HBsAg-negative (hepatitis B surface antigen-negative) hepatitis B [also defined as resolved hepatitis B (RHB)]. Herein, we determine the prevalence of cirrhosis among US adults with RHB.

Method: Data come from the National Health and Nutrition Examination Survey 2001-2018. 3115 US adults with RHB were enrolled in this study. We assessed cirrhosis by using the Fibrosis-4 (FIB-4) and aspartate aminotransferase to platelet ratio index (APRI) score.

Result: Out of 50201 NHANES adults, 45087 were tested for anti-HBc/HBsAg, of whom 3115 met the inclusion criteria (anti-HBc-positive/HBsAg-negative with available data for FIB-4/APRI). The proportion of US adults with RHB was 4.46% (95% CI, 4.17%-4.75%), affecting 9.87 million US adults. According to the results of the FIB-4, the weighted prevalence of cirrhosis among US adults with RHB was 3.76% (95%CI: 2.80–4.72%), which project to 371,112 (95% CI: 276,360-465,864) American adults with RHB who coexisted cirrhosis. Cirrhosis among anti-HBs-negative RHB adults (6.28%, 95%CI: 4.10-8.45%) was significantly higher than in anti-HBs-positive (3.08%, 95%CI:2.07-4.08%). Results were similar when APRI was used.

Conclusion: According to the FIB-4, 3.76% of US adults with RHB had cirrhosis, more than 10 times higher than in the general population of the US. There is a disparity in cirrhosis prevalence between anti-HBs-negative and anti-HBs-positive populations. Our data highlight the importance of cirrhosis screening in RHB infection to prevent advanced liver disease, especially among those who are anti-HBs-negative.

Table and Figure:

Figure 1. Flow diagram of subject selection.

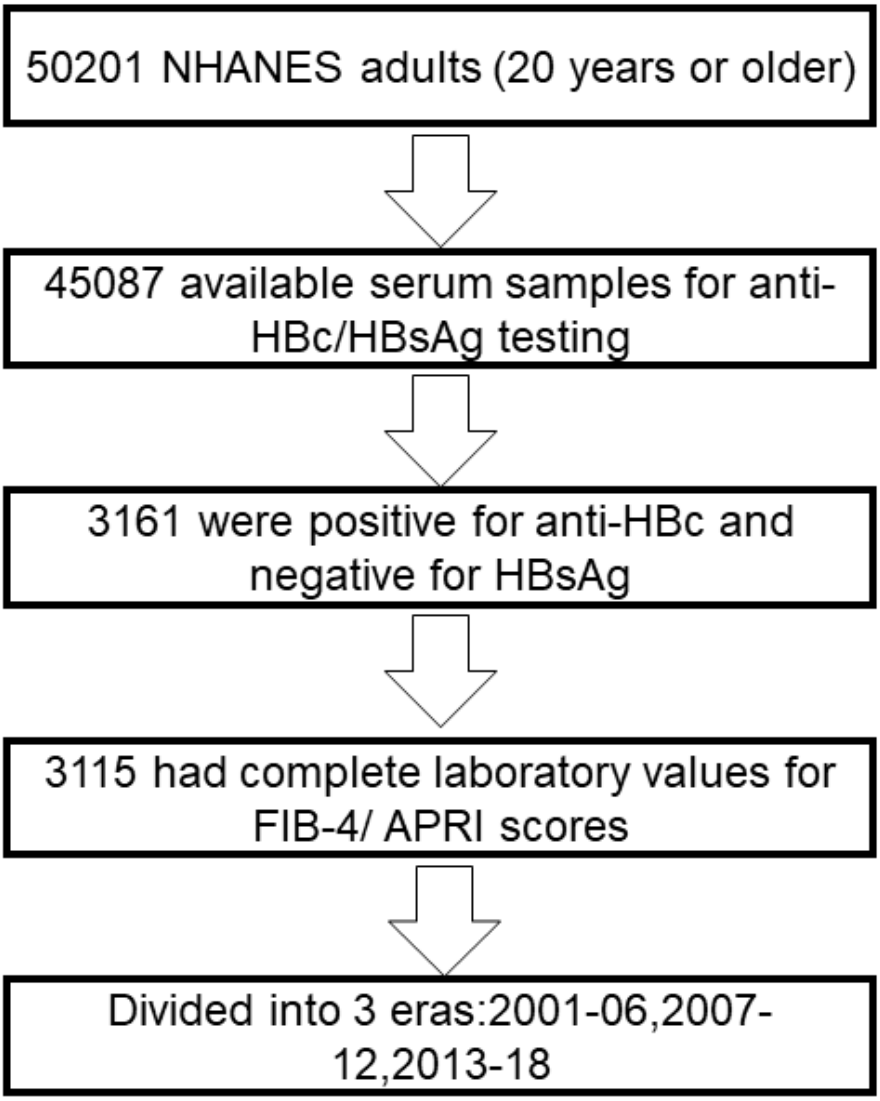

❖ AA-092

Effectiveness and safety of avatrombopag in liver cancer patients with severe thrombocytopenia: stratified analysis by presence or absence of chronic liver disease

Jiafeng Chen[1,2], Ao Huang[1,2], Jianzhang Wu[3], Xiutao Fu[1,2], Yinghong Shi[1,2], Jia Fan[1,2], Jian Zhou[1,2], Zhenbin Ding[1,2]
[1]Department of Liver Surgery & Transplantation, Liver Cancer Institute, Zhongshan Hospital, Fudan University, [2]Key Laboratory of Carcinogenesis and Cancer Invasion, Chinese Ministry of Education, [3]Department of General Surgery, Zhongshan Hospital, Fudan University

Background: Thrombocytopenia is common in patients with chronic liver disease (CLD) and worsens with the degree of liver cirrhosis and this situation is much more complicated in liver cancer patients. Thus, it is necessary to investigate novel agents in order to prevent hemorrhagic events during anti-cancer treatment. Avatrombopag, a small-molecule thrombopoietin receptor agonist, has been approved for the treatment of patients with thrombocytopenia and CLD who would undergo invasive procedure. To date, the accumulated evidence of avatrombopag in liver cancer patients is few. In the current study, we evaluated the retrospective data of avatrombopag in liver cancer patients with thrombocytopenia and CLD, aiming to evaluate their clinical outcomes including platelet count increase result and thrombotic or bleeding events, as well as the anti-cancer treatment response indirectly contributed by the thrombopoietic effect of avatrombopag.

Method: Liver cancer patients who received avatrombopag were retrospectively enrolled. The major inclusion criteria were: patients with liver cancer who were 18 years old or more and the platelet count was below 50×109/L at baseline. Avatrombopag dosage, peak platelet count, absolute platelet count increase, combination treatment with other thrombopoietic agents, and the anti-cancer treatment response were analyzed. Platelet transfusion, hemorrhage events requiring rescue procedures, and vein thrombosis events during or after avatrombopag treatment period were also recorded.

Result: A total of 93 liver cancer patients were included, with 72 and 21 in the CLD and non-CLD group. Patients in the CLD group were caused by hepatitis B or C and had lager spleen volume and higher Fibroscan value. Baseline platelet counts were similar between the two groups (37.0 vs. 39.0; P = 0.594) while patients without CLD had higher peak platelet (134.0 vs. 74.0; P = 0.015) and absolute increment (101.0 vs. 41.0; P = 0.020) after avatrombopag treatment. All patients in the non-CLD group had reached the target

platelet count ≥ 50×109/L while 9 patients failed in the CLD group. Regression analysis revealed that splenectasis impeded the increase of platelet while combination use of avatrombopag with other thrombopoietic agents significantly increased platelet count than avatrombopag alone. Patients who responded well to avatrombopag displayed a tendency towards higher disease control rate (80.0 vs. 55.6%, P = 0.227) . No adverse effects of thrombosis and hemorrhagic complications were observed.

Conclusion: In conclusion, our study suggests avatrombopag is effective for liver cancer patients with severe thrombocytopenia and CLD. The off-label use of avatrombopag in liver cancer patients without CLD also displays impressive thrombopoietic effect. Avatrombopag is a safe and effective alternative to platelet transfusion, simplifying the management of thrombocytopenia in liver cancer patients with or without CLD, minimizing hemorrhage risk, and safeguarding anti-cancer treatment.

Table and Figure:

Figure 1. Thrombopoietic effect of avatrombopag in liver cancer patients with and without CLD

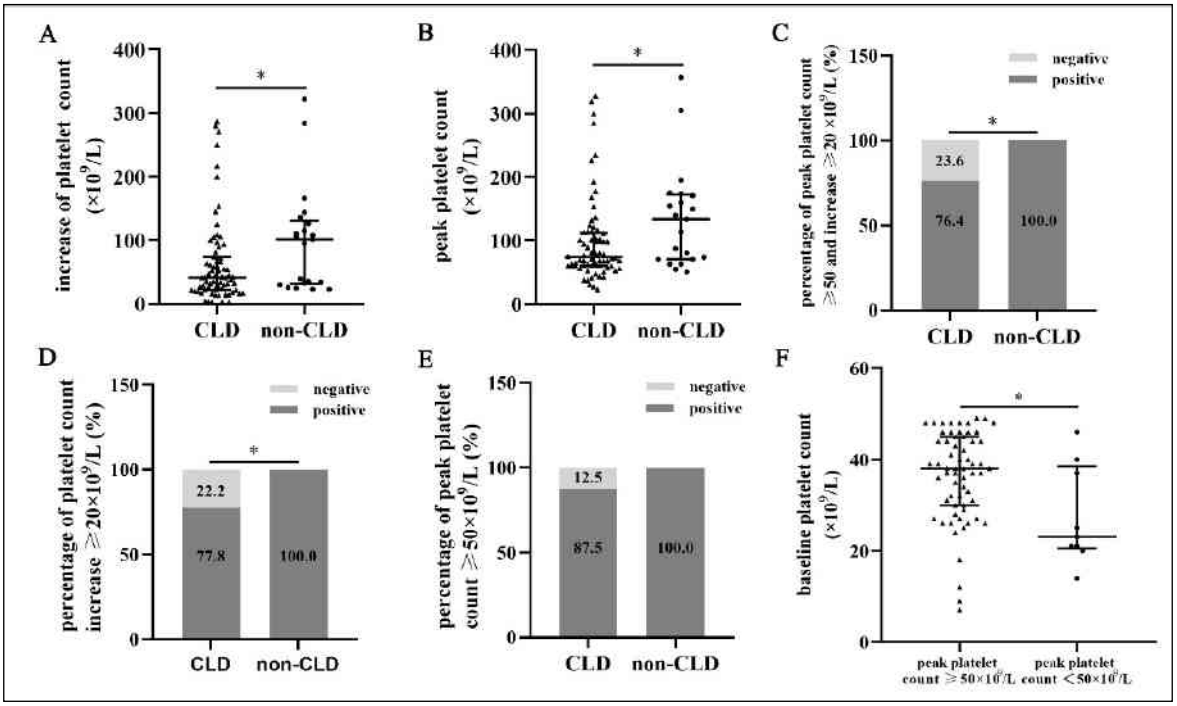

Figure 2. Thrombopoietic effect of combination treatment of avatrombopag with other thrombopoietic drugs and repeated use in liver cancer patients.

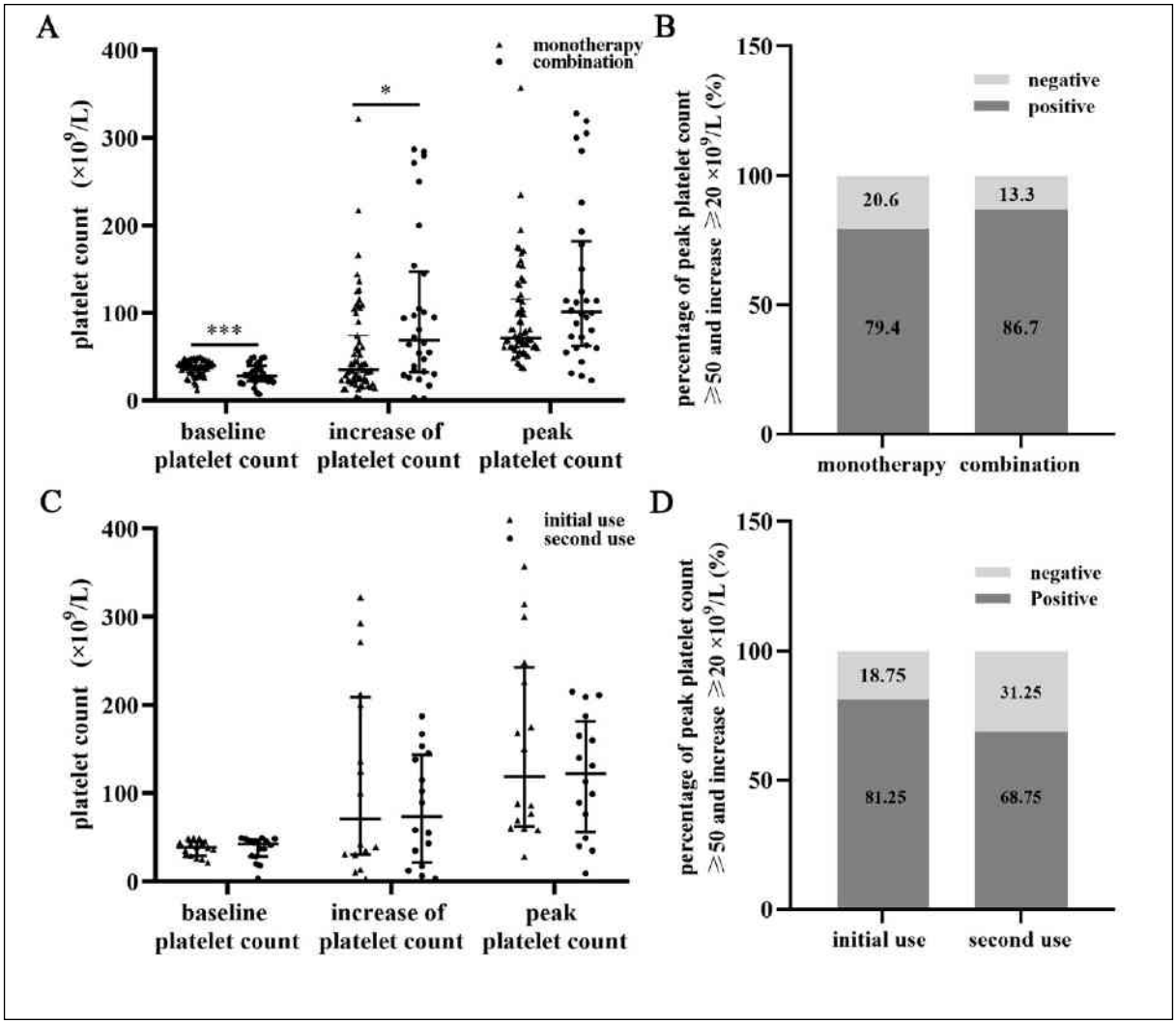

❖ AA-093

Multistate outcome analysis improves predictability of clinical course of HBV-related cirrhosis on antiviral therapy

Yuanyuan Kong[1], Hong You[1], Sam S Lee[2], Jidong Jia[1], Regression of HBV-induced Compensated Liver Cirrhosis Group
[1]Beijing Friendship Hospital, Capital Medical University, Beijing, China,
[2]Cumming School of Medicine, University of Calgary, Calgary, Canada

Background: Multistate or ordinal outcome models better evaluate the development of decompensation events in alcohol-associated or untreated hepatitis C cirrhosis. Here we formulated a multistate outcome model to evaluate the progression to decompensation events and hepatocellular carcinoma (HCC) in nucleos(t)ide analogue (NA)-treated CHB patients with compensated cirrhosis.

Method:A prospective cohort of 1163 NA-treated CHB patients with compensated cirrhosis were followed every 6 months for up to 7 years. The cumulative incidences of decompensation events and HCC were analyzed by cumulative incidence function method. A multistate model was formulated to calculate the state transition probability (STP) and state occupation probability (SOP).

Result: After a median follow-up of 5.5 years, 94% of the patients achieved HBV DNA suppression. The overall disease progression rate was 19.7%, with HCC diagnosed in 10.2%, nonbleeding decompensation in 7.5%, and variceal bleeding in 2.2%. Variceal bleeding had a higher STP to second decompensation, whereas nonbleeding events had a higher STP to HCC. Among patients in whom variceal bleeding occurred first, the 1, 3, and 5-year incidences of HCC were stable at 11.2%, whereas when nonbleeding events occurred first, HCC steadily increased from 11.1% to 19.4% and 25.0%. Baseline alcohol intake and serum albumin ≤35 g/L predicted variceal bleeding and INR >1.2 predicted nonbleeding events, whereas age >45 years, male sex, and platelets ≤150×109/L predicted HCC.

Conclusion: This multistate outcome model could depict the temporal pattern of different decompensation events and HCC development in NA-treated CHB patients with compensated cirrhosis.

❖ AA-094

Exploring the Immune Infiltration and Gene Features in Viral Hepatitis-associated Liver Fibrosis with Transcriptome data

Jiali Pan[1], Yu Tian[2], Fengling Hu[3], Jinghang Xu[1], Ning Tan[1], Yifan Han[1], Qian Kang[1], Hongyu Chen[1], Yuqing Yang[1], Xiaoyuan Xu[2]*

[1]Department of Infectious Diseases, Peking university first hospital,

[2]Department of Gastroenterology, Peking university first hospital,

[3]Department of thoracic surgery, Peking University Third Hospital

Background:A persistent inflammatory stimulus to the liver induced by the virus may lead to liver fibrosis. In this process, the innate and adaptive immunity of the organism plays an important role. However, the relevant immune mechanisms are still unclear. In this study, we propose to use the GEO database to systematically explore the immune cell infiltration and identify potential hub genes, and provide new insights for the treatment of viral hepatitis-associated liver fibrosis.

Method: Three transcriptomic data matrices for testing and one for validation were downloaded from the GEO database. Immune cell infiltration was assessed using the CIBERSORT algorithm. The characteristic subgroups were obtained by intersecting the results obtained from Lasso regression and Wilcox Text. The hub gene was explored next. Both hub genes and characteristic immune cell subpopulations were verified in the validation group. Finally, the association of hub genes with immune infiltrating cells was explored in the validation group using Spearman correlation analysis. R (version 4.1.3) was utilized for data analysis and visualization.

Result: We found 10 differential immune infiltrating cells in viral hepatitis-associated liver fibrosis and non-fibrosis, including M0-2 macrophages, naive B cells, plasma cells, resting CD4+ memory T cells, T follicular helper cells, T regulatory cells, resting mast cells and activated mast cells. Six significant hub genes were identified including STAT1, CXCL10, PTPRC, IFIT3, OAS2, and MX1. They also differed significantly in the subgroups of non-fibrosis, mild to moderate fibrosis and severe fibrosis, and these differences were also demonstrated in the validation group. All six hub genes were significantly associated with M1 and M2 macrophages, and were positively associated with M1macrophages and negatively associated with M2 macrophages.

Conclusion: We systematically identified 10 immune infiltrating cells that differ significantly between non-fibrosis and fibrosis and identified 6 signature genes. The six hub genes may be involved in viral hepatitis-associated liver fibrosis by promoting the polarization of M0 macrophages to M1 and inhibiting the conversion to M2. These genes may be potential therapeutic targets in inhibiting liver fibrosis in viral hepatitis.

❖ AA-095

Resistant-associated substitutions do not affect HCV RNA and HCV core antigen clearance during direct-acting antiviral agent treatment in a real-world setting

Hongyu Chen[1], Jianxiang Liu[2], Qian Kang[1], Hao Luo[1], Tan Ning[1], Jiali Pan[1], Yuqing Yang[1], Ran Cheng[1], Yifan Han[1], Min Yu[1], Dan Liu[1], Hongli Xi[1], Yanyan Yu[1], Xiaoyuan Xu[1]
[1]Departments of Infectious Diseases, Peking University First Hospital, NO.8, Xishiku Street, Xicheng District, Beijing 100034, China, [2]Departments of Gastroenterology, Peking University First Hospital, NO.8, Xishiku Street, Xicheng District, Beijing 100034, China

Background: Since oral direct-acting antiviral agents (DAAs) became available, the global hepatitis C treatment situation has undergone tremendous changes. However there are still many issues worthy of attention in treatment.

Method: We selected 53 HCV-infected patients who were treated and followed up in the Peking University First Hospital from December 2017 to January 2021 to detect the RASs in HCV. Pearson correlation analysis was used to analyze HCV RNA and HCV cAg, the Fisher exact test and chi-square test was used to compare the effects of RASs on the rate of decline of HCV RNA and HCV core antigen (cAg) during DAA treatment.

Result: The RASs and its prevalence on the NS3 are mainly Y56F 2.56% (1/39), Q80K 23.08% (9/39), S122G 71.79% (28/39), and V170I 38.46% (15/39). On the NS5A were R30Q 10.53% (4/38), P32A 5.26% (2/38), P58S 2.63 % (1/39), and Y93H 21.05% (8/38). On NS5B were C316N 71.05% (27/38), C451H 2.63% (1/38), and I585C 2.63% (1/38). There was no significant correlation between the RASs (Y93H, V179I, Q80K, S122G, C316N) and HCV genotype ($p > 0.05$). The baseline serum HCV RNA and HCV cAg had a significant medium-degree correlation ($r = 0.601$, $p = 0.002$). After 1 week of DAA treatment was weak correlation ($r = 0.413$, $p = 0.032$). Q80K, S122G, V170I, Y93H, and C316N had no effect on the clearance of HCV RNA and HCV cAg within the first week of DAA treatment ($p>0.05$).

Conclusion: The HCV genotype may have a limited impact on the presence of the five RASs (Y93H, V179I, Q80K, S122G, and C316N) as shown in this study. HCV RNA and HCV cAg have a correlation, especially at baseline is the highest; the appearance of some RASs has no effect on DAA treatment in most chronic hepatitis C patients.

Table and Figure:

Figure 1. Prevalence of RASs in enrolled patients

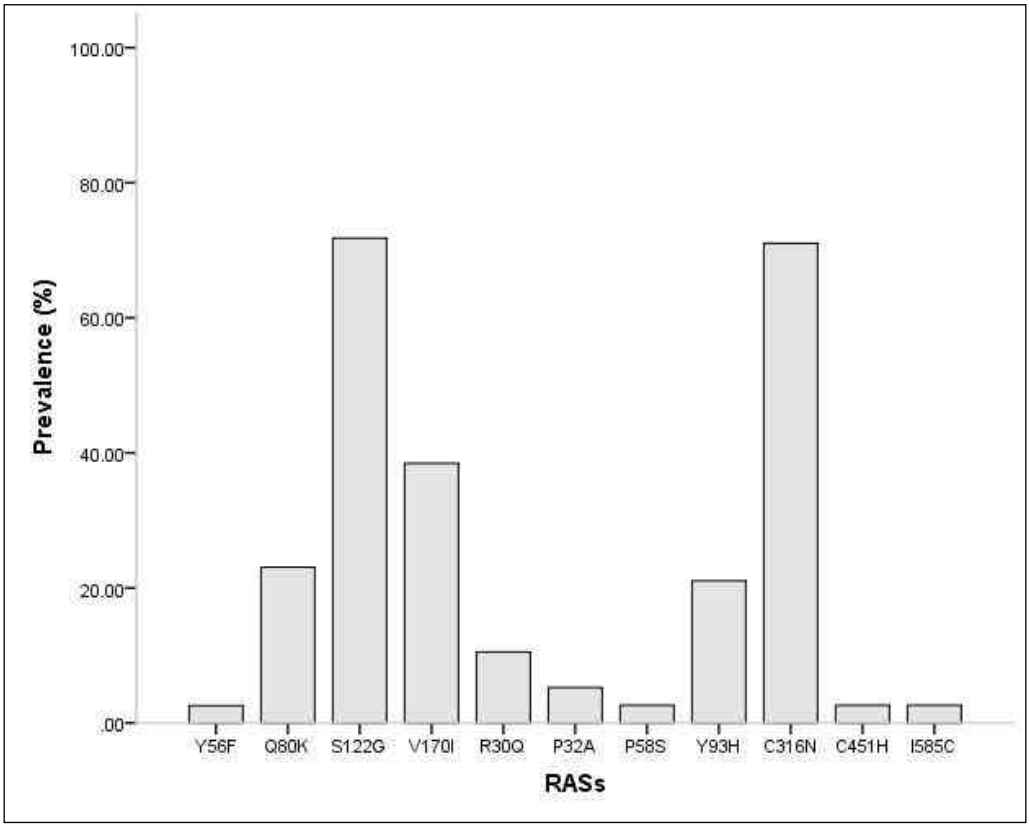

Figure 2.HCV RNA and HCV cAg correlation analysis

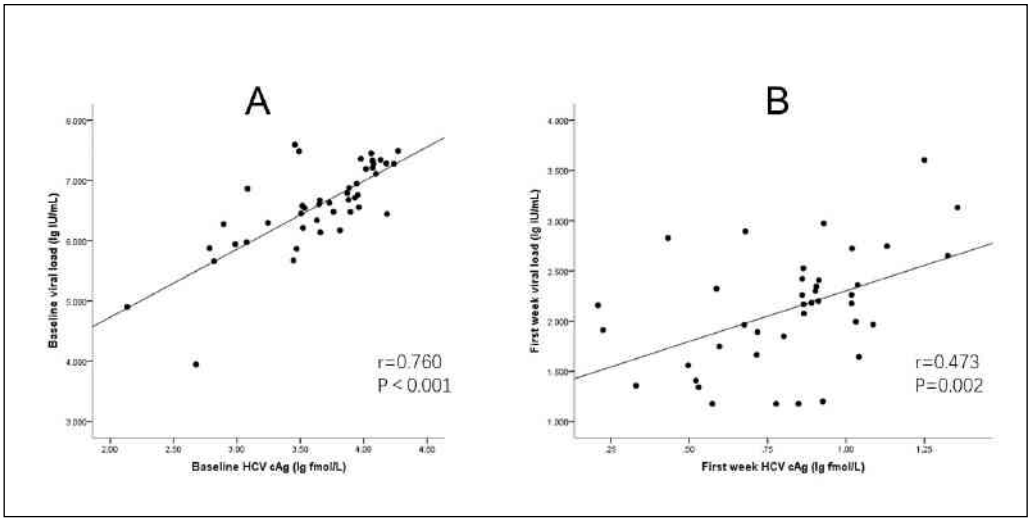

❖ AA-096

Applicationof aMAP hepatocellular carcinoma risk assessment in outpatients with chronic hepatitis B virus infection

Limin Wang[1], Yuan Huang[2], Si Xie[2], Jingyue Wang[2]
[1]Beijing Tsinghua Changgung hospital ,Children liver disease department, [2]Beijing Tsinghua changgung hospital, Department of hepatobiliary and pancreatic medicine

Background: To evaluate the aMAP risk of hepatocellular carcinoma in outpatients with chronic hepatitis B virus infection.

Method: The information of chronic HBV infected patients in the outpatient department of Beijing Tsinghua Changgung hospital were collected, from January 2018 to December 2021. Then calculate the aMAP score, and the risk of HCC was stratified.

Result: This study included 709 patients with chronic HBV infection, 22.4% of all had complicated with alcoholic liver disease and 11.8% with diabetes mellitus. 18.6% of the patients were complicated with fatty liver, 19.0% with liver cirrhosis, 9.7% with liver cancer. 71.2% of the patients have taken oral antiviral drugs, and 28.8% had not antiviral drugs. 2. The highest aAMP was 75.2, and the rate of low, medium and high risk of HCC were 70.0%, 23.1% and 6.9% respectively; 3. The proportion of HCC high-risk patients with alcohol liver disease, diabetes mellitus and liver cirrhosis were higher than that of patients without alcohol liver disease, diabetes and cirrhosis (9.4%VS6.2%, 11.9%VS6.2%, 19.3%VS4.0%). The mean annual change of aMAP was 0.93 ± 2.05 in patients without antiviral treatment higher than -1.15 ± 1.72 in patients with antiviral treatment P=0.00 (F = 39.36). 4. The proportion of patients with HCC high risk during the pre-HCC three years was 38.4%, 26.7% and 33.3% respectively. The median of aMAP was more than 50 in three years before diagnosis liver cancer, which was earlier than the increase of AFP.

Conclusion:aMAP is a simple convenient tool of HCC screening for outpatient with chronic HBV infection. The proportion of HCC high risk with aMAP was higher in patients associated with alcohol liver disease, diabetes and cirrhosis in chronic HBV infection patients than that without complications. Oral antiviral therapy could reduce aMAP in patients with chronic HBV infection.

Table and Figure:

Figure 1. Table1. Distribution and proportion of high, medium and low risk with aMAP score in each subgroup

N(%)		High-risk N=49	Medium-risk N=164	Low-risk N=496	Z	P
Gender	Male	21（5.0）	105（25.0）	294（75.0）	-0.42	0.67
	Female	28（9.7）	59（20.4）	202（69.9）		
Combined Alcoholic liver disease	Yes	15（9.4）	55(34.6)	89（56.0）	-4.25	0.00
	No	34（6.2）	109（19.8）	407（74.0）		
Combined Diabetes	Yes	10（11.9）	25（29.8）	49（58.3）	-2.59	0.01
	No	39（6.2）	139（22.2）	447（71.5）		
Combined fatty liver disease	Yes	6（4.5）	33（25.0）	93（70.4）	-0.32	0.74
	No	43（7.5）	131（22.7）	403（69.8）		
Combined liver cirrhosis	Yes	26（19.3）	56（41.5）	53（39.2）	-8.99	0.00
	No	23（4.0）	108（18.8）	443（77.2）		
Combined liver cancer	Yes	6（8.7）	33（47.8）	30（43.5）	-4.75	0.00
	No	43（6.7）	131（20.5）	466（72.8）		
Antiviral treatment	Yes	27（5.4）	124（24.8）	350（69.9）	-0.33	0.74
	No	22（10.6）	40（19.2）	146（70.2）		
ALT	≥40IU/l	6（3.0）	22（10.7）	177（86.3）	-6.02	0.00
	<40 IU/l	43（8.5）	142（28.2）	319（63.2）		
HBeAg	Positive	5（3.0）	18（11.0）	141（86.0）	-5.06	0.00
	Negative	44（8.1）	146（26.8）	355（65.1）		
HBVDNA	≥30 IU/ml	13（4.2）	52（16.6）	248（79.2）	-4.83	0.00
	<30IU/ml	36（9.1）	112（28.3）	248（62.6）		
HBsAg	>250IU/ml	21（3.9）	92（17.3）	420（78.8）	-9.11	0.00
	≤250 IU/ml	28（15.9）	72（40.9）	76（43.2）		

Figure 2. Table 2. Reviewed aMAP of HCC patients before diagnosis 1-3 years

Table 2. Reviewed aMAP of HCC patients before diagnosis 1-3 years

N（%）	High-risk	Medium-risk	Low-risk
Pre-diagnosis HCC 3 years N=13	5（38.4）	3（23.0）	5（38.5）
Pre-diagnosis HCC 2 years N=15	4（26.7）	4（26.7）	7（46.7）
Pre-diagnosis HCC 1 years N=15	5（33.3）	6（40.0）	4（26.7）
diagnosis HCC N=69	6（8.7）	33（47.8）	30（43.5）

❖ AA-097

Systematic review and meta-analysis: Impact of antiviral therapy on portal hypertensive complications in HBV patients with advanced chronic liver disease

Yuanyuan Kong[1], Tingting Lv[2], Min Li[2], Shiv K Sarin[3], Mattias Mandorfer[4], Jidong Jia[2], on behalf of the BAVENO Cooperation: an EASL consortium
[1]Beijing Friendship Hospital, Capital Medical University, Beijing, China,
[2] Beijing Friendship Hospital, Capital Medical University, Beijing, China,
[3]Institute of Liver and Biliary Sciences, Vasant Kunj, New Delhi,
[4]Medical University of Vienna, Vienna, Austria

Background: The efficacy of treatment with nucleos(t)ide analogues (NAs) in non-cirrhotic chronic hepatitis B (CHB) patients is well-established. However, its impact on complications of portal hypertension in advanced chronic liver disease (ACLD) is less well-characterized.

Method:MEDLINE/PubMed, EMBASE, Web of Science, Cochrane Central Register of Controlled Trials, and abstracts of major international hepatology meetings were searched for publications from Jan 1, 1995 to Nov 30, 2021. Randomized control trials and observational studies reporting the efficacy of NAs in ACLD patients were eligible. Pooled risk ratios (RRs) for outcomes of interest were calculated with a random-effect or fixed-effect model, as propriate.

Result: Thirty-nine studies including 14 212 ACLD patients were included. NA treatment was associated with reduced risks of overall hepatic decompensation events (RR, 0.51; 95% confidence interval [CI]: 0.37-0.71) such as variceal bleeding (RR, 0.44; 95% CI: 0.26-0.74) and also ascites (RR, 0.10; 95% CI: 0.01-1.59) on a trend-wise level. Moreover, the risks of hepatocellular carcinoma (HCC) (RR, 0.48; 95% CI: 0.30-0.75) and liver transplantation/death (RR, 0.36; 95% CI: 0.25-0.53) were also reduced by NA treatment and first-line NAs were superior to non-first-line NAs in regard to these outcomes (RR, 0.85; 95% CI: 0.75-0.97 and RR, 0.85; 95% CI: 0.73-0.99, respectively).

Conclusion:NA therapy lowers the risk of portal hypertension-related complications including variceal bleeding, as well as HCC, and liver transplantation/death.

❖ AA-099

Etiology Control Resulting in Hepatic Vein Pressure Gradient Reduction in Cirrhosis Patients with Portal Hypertension: A Systematic Review

Shuai Xia[1,2], Bingqiong Wang[1,2], Zhiying He[1,2], Xiaofei Tong[1,2], Wen Zhang[1,2], Ziyi Zhang[1,2], Xiaoning Wu[1,2], Jidong JIA[1,2], Hong You[1,2]
[1]Liver Research Center, Beijing Friendship Hospital, Capital Medical University, [2]National Clinical Research Center of Digestive Diseases

Background: The effect of etiology control on hepatic venous pressure gradient (HVPG) was underestimated. We aimed to assess the efficacy of etiology therapy on the change of HVPG and hemodynamic response in cirrhosis.

Method: Articles published on PubMed and Embase were systematically searched. Studies analyzing the efficacy of etiology therapy on HVPG change in cirrhosis patients were included. The data of HVPG measurement both absolute and relative change before and after treatment were collected. The pooled effect of HVPG reduction was calculated by a fixed-effect model, among them subgroup analysis was performed according to the etiological type and follow-up time. Meta-analysis was performed by STATA 16.0 software.

Result:A total of 30 studies reporting HVPG measurement in cirrhosis patients with etiological therapy were included, involving viral hepatitis-related cirrhosis and NAFLD-related cirrhosis. However, only 6 studies reported paired HVPG measurements both in treatment group and control group, which were both due to viral hepatitis-related cirrhosis. Based on these studies, the HVPG value was further decreased by 1.55 mmHg (95% CI: -2.44 to -0.66, $P < 0.05$) after antiviral therapy compared with the control group (Figure 1A). Besides, the HVPG values decreased more in studies with long-term intervals (more than 1 year) compared with studies with short-term intervals (less than 1 year) after subgroup analysis (1.61 vs. 1.41 mmHg) (Figure 1B). Another 15 studies reporting HVPG measurements in the treatment group were performed to calculate the absolute reduction of HVPG value. The HVPG value was decreased by 2.76 mmHg (95% CI: -2.89 to -2.62, $P < 0.05$) after etiology treatment (Figure 1C). Regarding the benefit of etiology therapy to hemodynamics response, a total of 26 studies were included. The proportion of patients achieving HVPG reduction by ≥ 10% in 11 studies and ≥ 20% in 9 studies were 56% (95% CI, 47-66%, $P < 0.05$) and 38% (95% CI, 31-44%, $P < 0.05$) (Figure 2A and B). Further analyzing HVPG response in different etiology, the response rate was higher in viral

hepatitis patients (viral hepatitis vs. non-viral hepatitis for a reduction ≥ 10%: 58% vs. 42%; for a reduction ≥ 20%: 40% vs. 27%). As the influence of time duration on HVPG response, the longer time of treatment, the better response (time duration > 1 year vs. < 1 year for a reduction ≥ 10%: 63% vs. 54%; for a reduction ≥ 20%: 40% vs. 35%).

Conclusion: Etiological therapy could significantly alleviate portal hypertension quantified by HVPG values in liver cirrhosis patients. Interestingly, patients with viral hepatitis treated with antiviral drugs could achieve better hemodynamics responses than that in other etiologies. The response rate enhanced with prolonged treatment duration.

Table and Figure:

Figure 1.the HVPG values was reduced in etiology treatment compared with control group

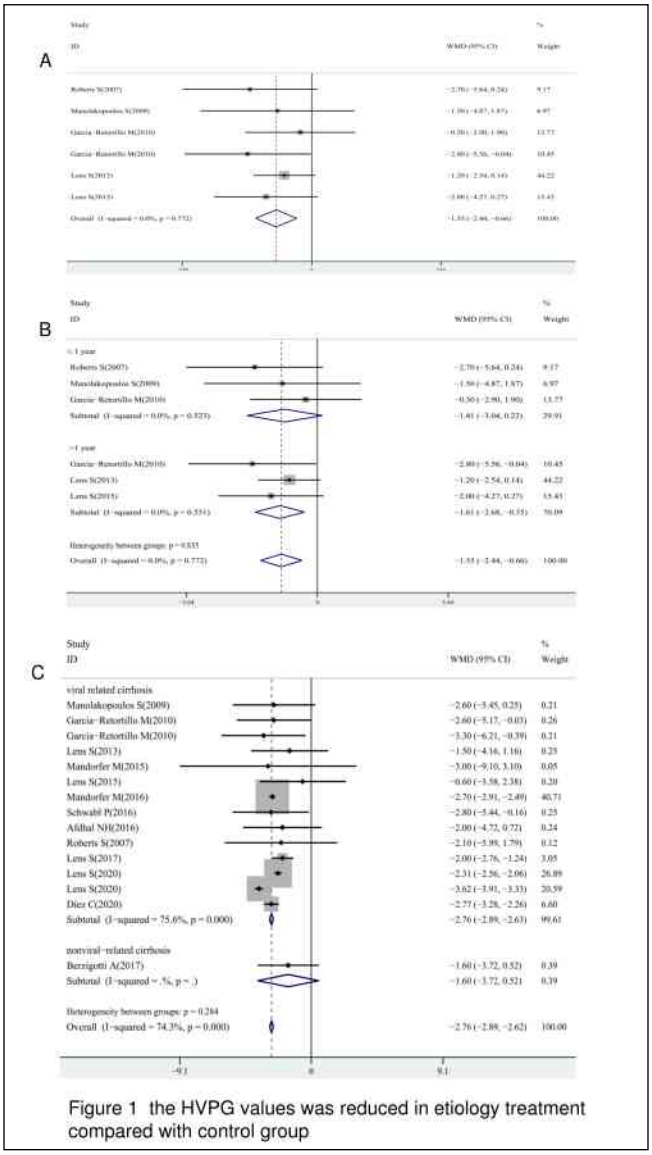

Figure 1 the HVPG values was reduced in etiology treatment compared with control group

Figure 2.the incidence of HVPG reduction after etiology treatmen

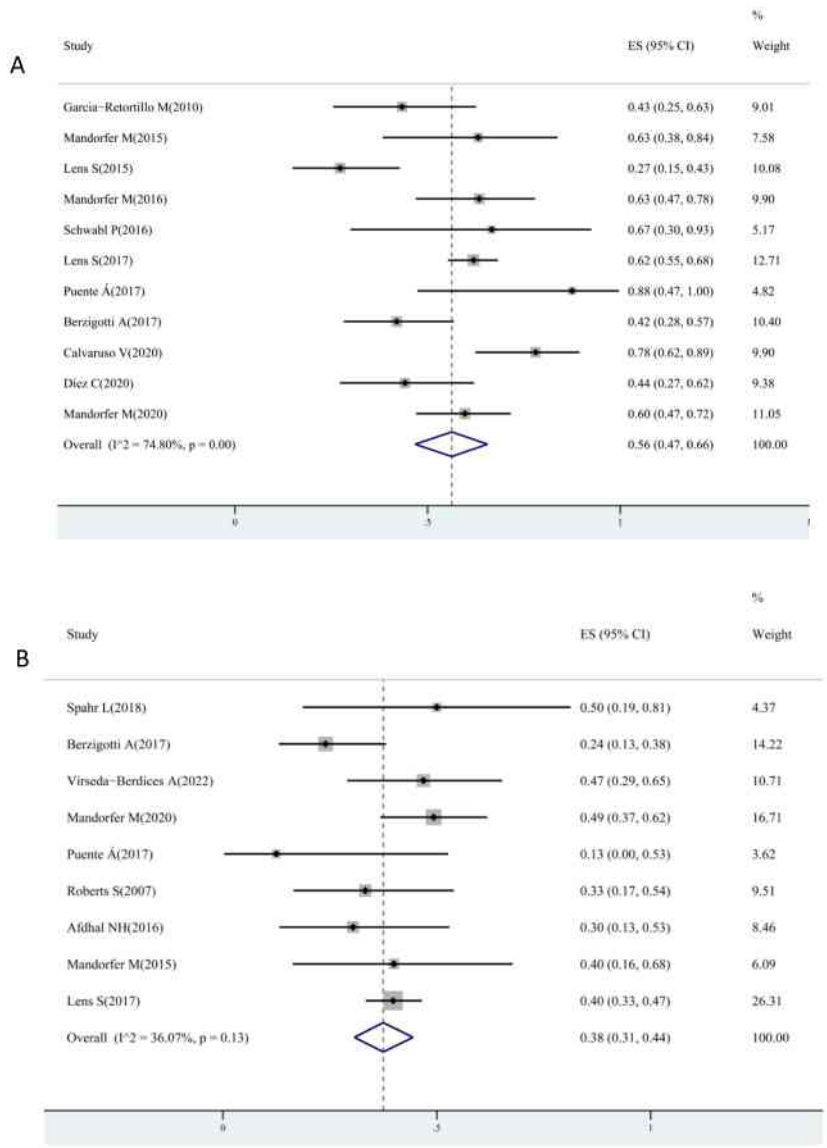

Figure 2 the incidence of HVPG reduction after etiology treatment

❖ AA-100

Analysis of the outcome and clinical features of esophageal varices during antiviral therapy for HBV related-cirrhosis

Bingqiong Wang[1,2], Xiaoning Wu[1,2], Jialing Zhou[1,2], Yameng Sun[1,2], Tongtong Meng[1,2], Shuyan Chen[1,2], Qiushuang Guan[1,2], Zhiying He[1,2], Shanshan Wu[3,2], Yuanyuan Kong[3,2], Xiaojuan Ou[1,2], Jidong Jia[1,2], Hong You[1,2]

[1]Liver Research Center, Beijing Friendship Hospital, Capital Medical University, [2]National Clinical Research Center for Digestive Diseases, [3]Clinical Epidemiology & EBM Unit, Beijing Friendship Hospital, Capital Medical University

Background: To investigate the changes of esophageal varices (EVs) and related factors in hepatitis B virus (HBV)-related cirrhosis patients during anti-HBV treatment.

Method: Patients from prospective HBV-related fibrosis/cirrhosis cohorts were screened for this study. All patients who received entecavir-based anti-HBV therapy with paired gastroscopy before and after antiviral therapy were enrolled. Changes in degree of EVs were recorded, and the clinical characteristics of patients with different outcomes were analyzed by comparison among multiple groups.

Result: After a median of 3.1 years of antiviral therapy (IQR 2.5-4.4), the proportion of patients without EVs increased from 30.8% to 51.9%, the proportion of mild EVs decreased from 40.4% to 30.8%, and the proportion of moderate-severe EVs decreased from 28.8% to 17.3% (Figure 1, P=0.001). Overall 40.4% of patients had a reversal of EVs and 13.5% had progression of EVs. The outcome of EVs differed among patients with different degrees of EVs (Figure 2, P<0.001), and a total of 60.0% of patients still maintained the moderate-severe state during antiviral therapy. In these patients, baseline and the mean change rate within 5 years of platelet were significantly lower in patients with progression than that in patients without progression (3.3% vs. 34.1%, P<0.001).

Conclusion: Overall, 40% of patients could achieve esophageal varices regression after anti-HBV treatment. A significant proportion of patients with hepatitis B cirrhosis complicated with moderate to severe esophageal varices are still at risk of progression with antiviral therapy alone, and the trend of platelet increase after antiviral therapy is a clinical sign of variceal progression.

Table and Figure:

Figure 1. Figure 1. The distribution of esophageal varices degree before and after treatment

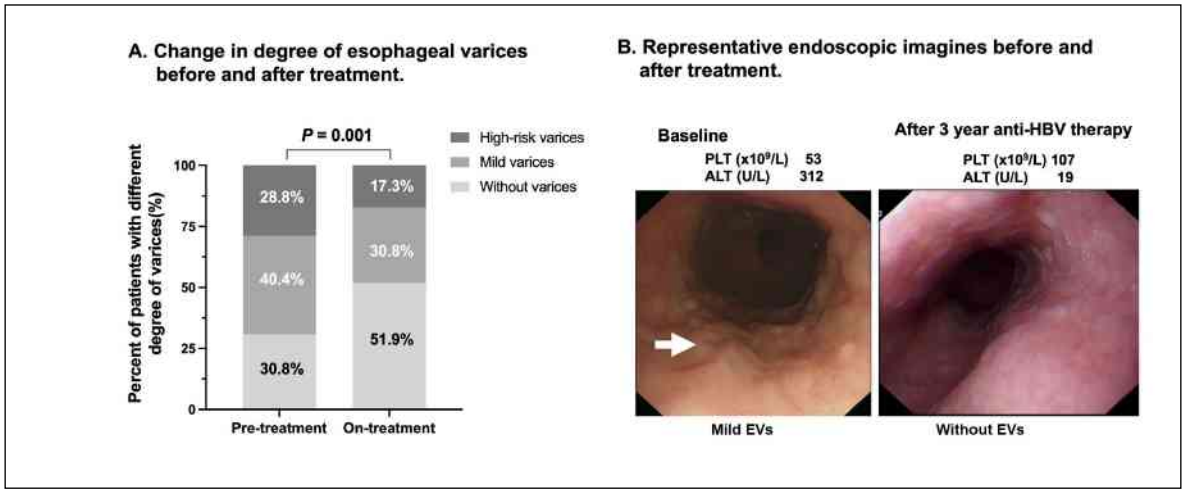

Figure 2. Figure 2. Change of esophageal varices differ from different baseline degree of varices

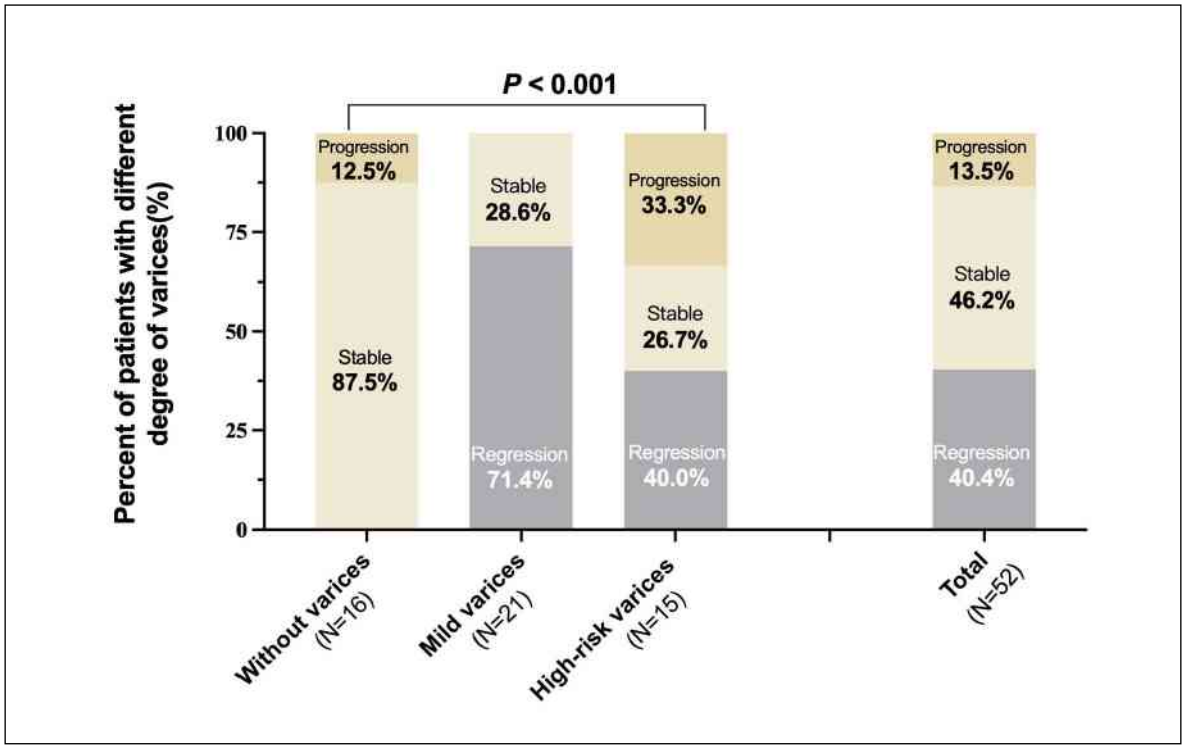

❖ AA-101

Regulating Insulin Resistance Status Could Improve Hepatic Fibrosis Progression in Chronic Hepatitis B Patients with Virological and Biochemical Response after Nucleoside/tide Analogs Treatment

Ning Yao[1], Xin Wang[2]
[1]First School of Clinical Medicine, Gansu University of Chinese Medicine, Lanzhou, Gansu Province, China, [2]School of Traditional Chinese and Western Medicine, Gansu University of Chinese Medicine, Lanzhou, Gansu Province, China

Background: Multiple studies have shown a direct proportionality between serum HBV DNA level and the risk of development of hepatic fibrosis and cirrhosis. Potent antiviral treatments with nucleoside/tide analogs (NAs) have been widely used for the treatment of chronic hepatitis B (CHB), which histologically improve HBV-related hepatic fibrosis/ cirrhosis by the suppression of HBV replication. However, it was noted that hepatic fibrosis progressed in 10-20% of patients despite receiving highly potent antiviral therapy with NAs. Metabolic factors influencing the hepatic fibrosis progression of CHB patients with NAs treatment are still unexplored. The aim of the study is to elucidate impact of insulin resistance (IR) on hepatic fibrosis in CHB patients with NAs treatment.

Method:110 CHB patients were treated with entecavir continuously for more than one year. The IR was evaluated by homeostasis model assessment of IR (HOMA-IR). Noninvasive indexes, including fibrosis index based on the four factors and AST to platelet ratio index, were applied to evaluate hepatic fibrosis. Evaluation of HOMA-IR, hepatic fibrosis, virological and biochemical parameters were measured at 24 weeks after patients having attained virological and biochemical response.

Result: Serum HOMA-IR index was proved to be the only independent correlation factor to hepatic fibrosis in CHB patients who have attained virological and biochemical response with NAs treatment. The incidence of advanced hepatic fibrosis was significantly higher in CHB patients with IR than those without IR. With increasing HOMA-IR, hepatic fibrosis progressed positively. IR increased the risk of advanced hepatic fibrosis in CHB patients.

Conclusion: Our data suggest that IR is strongly associated with hepatic fibrosis, thus reflecting the important role played by metabolic factors in hepatic fibrosis progression

during NAs treatment. These findings forebode that we could improve hepatic fibrosis progression by regulating IR level in the future.

Table and Figure:

Figure 1. Baseline Characteristic of Patients with Hepatic Fibrosis Stage by Metavir Score Predicted with FIB-4 index

Parameters	F0-F2 stage (n=24)	Indeterminate stage (n=67)	F3-F4 stage (n=19)	*P*
Male Gender [n(%)]	10 (41.7)	38 (56.7)	10 (52.6)	0.448
BMI (kg/m^2)	22.4±2.61	22.3±2.56	22.6±3.11	0.892
GGT (IU/L) *	21.0 (14.0, 27.0)	23.0 (16.0, 31.0)	27.0 (21.0, 34.0)	0.176
ALP (IU/L) *	80.5 (58.8 ,98.0)	91.0 (73.1, 114)	97.0 (90.0, 112)	0.117
TP (g/L)	71.7±7.03	70.6±8.83	74.7±7.01	0.208
ALB (g/L)	43.9±3.10	42.5±4.40	43.1±5.49	0.199
T-BIL (μmol/L)	9.59±4.48	10.2±3.97	10.9±3.79	0.601
D-BIL (μmol/L)	4.52±1.76	5.45±2.35	5.24±1.74	0.494
CHOL (mmol/L)	4.03±1.14	3.89±0.62	4.06±1.01	0.731
TG (mmol/L)	1.17±1.23	0.94±0.68	0.86±0.23	0.229
UREA (mmol/L)	4.94±0.82	5.04±1.13	5.48±1.14	0.221
CREA (μmol/L)	67.4±14.4	67.5±14.9	70.8±14.5	0.646
UA (μmol/L)	282±48.5	286±61.8	292±52.5	0.883
APTT (s)	28.6±3.15	28.3±4.16	27.8±2.84	0.647
HOMA-IR	1.12±0.18	1.54±0.36	2.35±0.34	<0.001
IR status [n(%)]	1 (4.17)	34 (50.7)	17 (89.5)	<0.001

Data presented as means ± SD.

*Median values (25% quartile, 75% quartile).

Figure 2. The Correlation between HOMA-IR and Hepatic Fibrosis Using Spearman rank Correlation Test

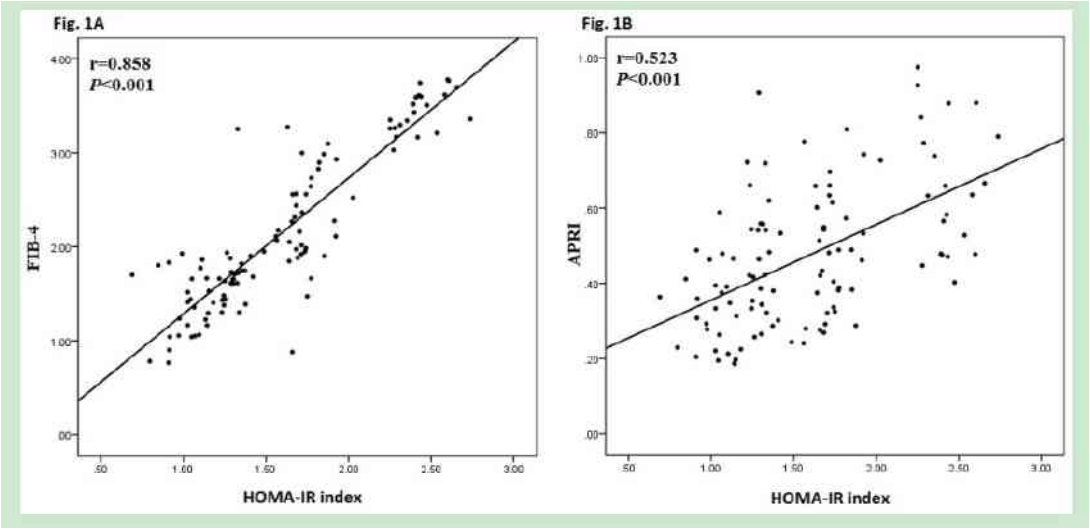

❖ AA-102

Esophageal varices regression based on etiology treatment in liver cirrhosis patients: a meta-analysis

Zhiying He[1], Bingqiong Wang[1], Shuai Xia[1], Xiaofei Tong[1], Wen Zhang[1], Ziyi Zhang[1], Xiaoning Wu[1], Jidong Jia[1], Hong You[1]
[1]Liver Research Center, Beijing Friendship Hospital, Capital Medical University; National Clinical Research Center of Digestive Diseases; Beijing, China.

Background: Esophageal varices (EVs) are the main complication of portal hypertension in liver cirrhosis, and effective etiology control could reverse liver cirrhosis and achieve esophageal varices regression. However, the efficacy of etiology treatment on EVs regression is unknown.

Method: Medline, Embase and Cochrane databases were systematically searched to identify studies analyzing the efficacy of etiology treatment on EVs regression in liver cirrhosis patients. Regression of EVs was defined as a decrease in esophageal varix size by 1 grade or more or the disappearance of red color sign with surveillance endoscopy. In addition, meta-analysis with fixed-effects model was conducted to evaluate pooled risk ratio (RR) and 95% confidence intervals (95% CI) between patients with and without etiology treatment, and the rate of EVs regression in treated patients was performed using random-effects model.

Result:A total of 12 studies comprising 876 patients with a median follow-up duration of 36.0 months were included. Of them, six studies were about hepatitis C, four studies about hepatitis B, one study about alcoholic liver disease and one study was multi-etiology. The pooled risk ratio (RR) of EVs in treated patients versus untreated patients was 1.89 (95% CI: 1.29-2.76) in 4 studies. In total of 12 studies, the rate of EVs regression was 42% (95% CI: 31%-54%) in patients with effective etiology treatment. For subgroup analysis according to baseline grade of EVs, the rate of EVs regression was 35% (95% CI: 17%-54%) in grade 1 patients, 34% (95% CI: 11%-57%) and 37% (95% CI: 3%-71%) in grade 2-3 patients with etiology treatment alone or treated simultaneously with non-selected beta-blocker, respectively.

Conclusion: Effective etiology treatment could reverse esophageal varices in liver cirrhosis patients, and about 42% of patients could achieve esophageal varices regression.

❖ AA-103

Clinical characteristics and risk factors of hepatitis B virus-related cirrhosis in Chinese adults aged 40 years or younger : a retrospective study

Jing Li[1], Yan Chun Wang[1]
[1]The second people's hospital of Tianjin

Background: Long-term clinical work has revealed that the incidence of cirrhosis in young patients is not low, and some patients initially present with serious life-threatening decompensated liver cirrhosis. So we retrospectively analyze the clinical characteristics and risk factors of young (age ≤ 40 years) patients with hepatitis B virus-related cirrhosis.

Method:163 patients with hepatitis B virus-related cirrhosis admitted to Tianjin Second People's Hospital from June 2019 to August 2020 were enrolled, and they were divided into age ≤ 40 years old group (n = 102) and age > 40 years old group (n=61). All patients were initially diagnosed as hepatitis B virus-related cirrhosis and did not receive antiviral therapy. All patients performed liver function, HBV serum markers, HBV DNA, abdominal ultrasonography,elastography,abdominal CT, and gastroscopy detections at the same period. The differences in clinical indicators between the two groups were compared, and the independent risk factors for hepatitis B cirrhosis of age ≤40 years old were further explored.

Result: Compared with patients aged > 40 years, the proportion of male with hepatitis B cirrhosis in the age ≤ 40 years group was higher (P<0.05), the proportion of patients with family history of liver disease was lower (P<0.05), the levels of ALT, GGT, ALB, CHE are higher (P<0.05), the level of TBIL is lower (P<0.05), the level of HBV DNA is higher (P<0.05); and the proportion of patients with compensatory cirrhosis is higher (P<0.001). Multivariate logistic regression analysis showed that elevated GGT levels(P=0.010,OR=1.007,95%CI:1.002-1.013), and higher HBV DNA levels(P=0.025,OR=1.353,95%CI: 1.039-1.760)are independent risk factors for hepatitis B virus-related cirrhosis in patients aged ≤40 years.

Conclusion: Young patients with hepatitis B virus-related cirrhosis have more obvious liver inflammation, better liver synthesis, and reserve function, more active replication of hepatitis B virus, and a higher proportion of patients at the compensatory stage of cirrhosis. Elevated GGT,and HBV DNA Higher level are risk factors of cirrohosis. For these

patients, liver biopsy should be actively performed, and use of antiviral drugs may be considered.

❖ AA-104

Prognosis and Risk Factors of Recurrence in HBV-related Small Hepatocellular Carcinoma after Stereotactic Body Radiation Therapy

Yifan Han[1], Jianxiang Liu[1], JIALI PAN[1], Hongyu Chen[1], Tan Ning[1], Qian Kang[1], Yuqing Yang[1], Xiaoyuan XU[1], Wengang Li[2]
[1]Peking university first hospital, [2]The Fifth Medical Center of Chinese PLA General Hospital

Background: The role of stereotactic body radiation therapy (SBRT) in the treatment of small hepatocellular carcinoma(sHCC) has gained increasing recognition. However, the prognosis and risk factors for recurrence in such patients remain unclear. This study aims to investigate the risk factors for recurrence in hepatitis B virus (HBV)-related sHCC patients after SBRT.

Method:A total of 240 HBV-related sHCC patients treated with SBRT between March 2011 and March 2020 were retrospectively analyzed. The primary endpoint is progression-free survival(PFS). The cumulative probability of recurrence was calculated according to the Kaplan–Meier method. Univariate and multivariate analyses were performed by Cox proportional hazard models.

Result: The one-, two-, three-, and five-year PFS rates were 79.1%, 55.0%, 41.7% and 19.6%, respectively. The median time to recurrence and median follow-up time were 27 and 30 months, respectively. Cox multivariate analysis indicated that age (P = 0.029, HR [1.019, 1.002-1.037]), tumor size (P = 0.012, HR [1.227, 1.045-1.440]), and aspartate aminotransferase-to-platelet (APRI) (P = 0.005, HR [1.911, 1.221-2.989]) were independent risk factors for recurrence.

Conclusion: Patients receiving SBRT for HBV-related sHCC may be at greater risk of recurrence if they have a high APRI in combination with their age and tumor size.

❖ AA-105

Early and durable fibrosis regression by shear wave elastography in chronic HBV patients during treatment with nucleotide/ nucleoside analogue

Reham Mohamed Elbasiouny[1], Mohamed Samy Kohla[1], Ali Saadeldien Nada[1], Gasser Ibrahim ElAzab[1]
[1]national liver institute , menoufiya university,Egypt

Background: Shear wave elastography (SWE) is a noninvasive ultrasound-applied technique of hepatic fibrosis not requiring a special device. Successful therapy with nucleotide/ nucleoside analogue in chronic hepatitis B patients was associated with hepatic fibrosis regression assessed by transient elastography (Fibroscan). Aim: Assessment of liver fibrosis by SWE before and after one year treatment of chronic hepatitis B (CHB).

Method: One hundred Egyptian patients with chronic hepatitis B who are positive HBsAg and HBV DNA for more than 6 months and candidate to treatment with nucleotide/ nucleoside analogue according to EASL protocol (patients with HBV DNA more than 2000 IU/ml and/or elevated ALT levels with significant fibrosis (F> 2)).Full assessment of enrolled patient was done with through history taking, laboratory investigation, HBV PCR, radiological assessment and SWE. Patients' laboratory characteristics and liver stiffness measurements (LSM) by SWE were evaluated at the beginning of treatment, 24 weeks and 48 weeks after treatment.

Result: Median age of patients was 40.5 years with (68%) males (p=0.00). 80 patients treated with Entecavir 0.5 mg, 10 treated with Entecavir 1mg and 10 treated with Tenofovir Disoproxil Fumarate 300 mg (p=0.102). Serum alanine aminotransferase (ALT) and aspartate aminotransferase (AST) levels decreased significantly after 24 week and 48 week in comparison to baseline (P value < 0.001). The mean LSM showed regression at week 24th (8.06±4.12kpa) and week 48th (7.76±4.62 kpa) in comparison to baseline (8.3±3.14kpa) (P value < 0.001).

Conclusion: SWE is a feasible, easily applicable noninvasive assessment method of liver fibrosis and treating chronically infected HBV patients with cirrhosis is a safe guard against progression of liver inflammation and fibrosis.

Table and Figure:Figure 1.

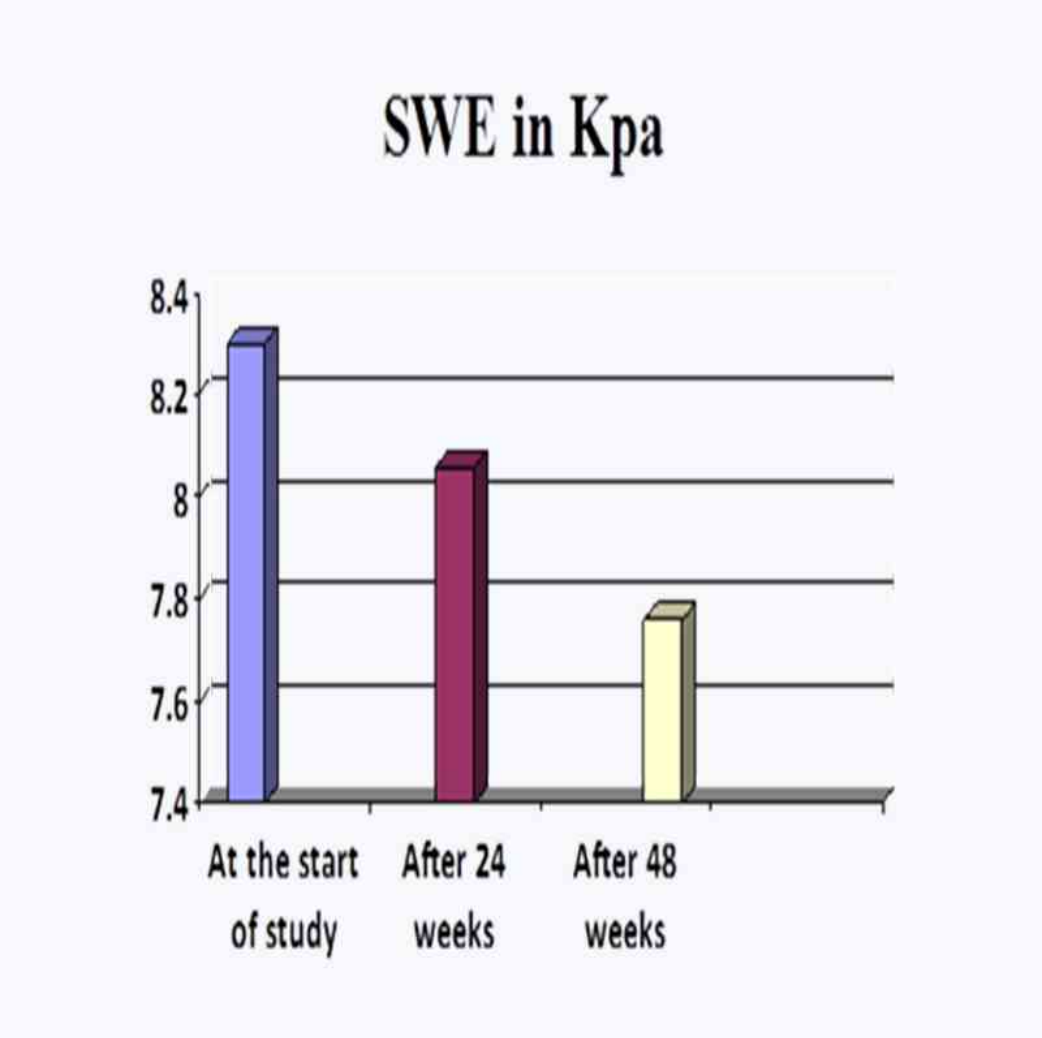

❖ AA-106

Assessment of liver fibrosis with shear wave elasticity image in patients with chronic HBV

Reham Mohamed Elbasiouny[1], Mohamed Samy Kohla[1], Ali Saadeldien Nada[1], Gasser Ibrahim El azab[1]
[1]national liver institute , menoufiya university,Egypt

Background: Shear wave elastography (SWE) is a non-invasive, easy and rapid technique that enables the direct visualization of elasticity measurements. Some patients with chronic HBV in whom the disease is not active, are not treatment candidates and antiviral therapy can be deferred, such as those with low HBV DNA, minimal or no fibrosis and persistently normal ALT levels. At National Liver Institute, Menoufiya University, patients with low HBV DNA level with normal ALT levels and without significant fibrosis (F< 2) undergo regular follow up. Aim: Assessment of liver fibrosis by SWE in chronic HBV infected patients not candidate to treatment.

Method: One hundred Egyptian patients with chronic hepatitis B who are positive HBsAg and HBV DNA for more than 6 months and scheduled for regular follow up, recruited from the outpatient clinic at National Liver Institute (NLI), Menoufia University. Patients' laboratory characteristics, fibrosis biomarkers, namely Fibrosis-4 (FIB-4) index and AST/ platelet ratio index (APRI) and liver stiffness measurements (LSM) by SWE were evaluated at baseline. SWE was performed every 6 months interval for one year to assess liver fibrosis.

Result: Median age of patients was 35.5 years (50%) males (p<0.05). Fibrosis-4 (FIB-4) index and AST/platelet ratio index (APRI) not correlate with degree of fibrosis assessed by Shear wave elastography (p value = 0.104) and (p value = 0.190) (R= - 0.166) and (R= - 0.133). Serum aspartate aminotransferase (AST) and alanine aminotransferase (ALT) levels not significantly changed at week 24th and week 48th from baseline (p value =0.701). Shear wave elastography index was (4.1±0.71kpa) at the beginning of study, (4.21±0.52 kpa) at 24th week and (4.26±0.62 kpa) at 48th week of follow up, p value = 0.035.

Conclusion: No significant fibrosis occurred in chronic hepatitis B patients, younger age with persistent normal liver enzymes, these criteria were validated by SWE. Only regular follow up is required.

Table and Figure:

Figure 1.

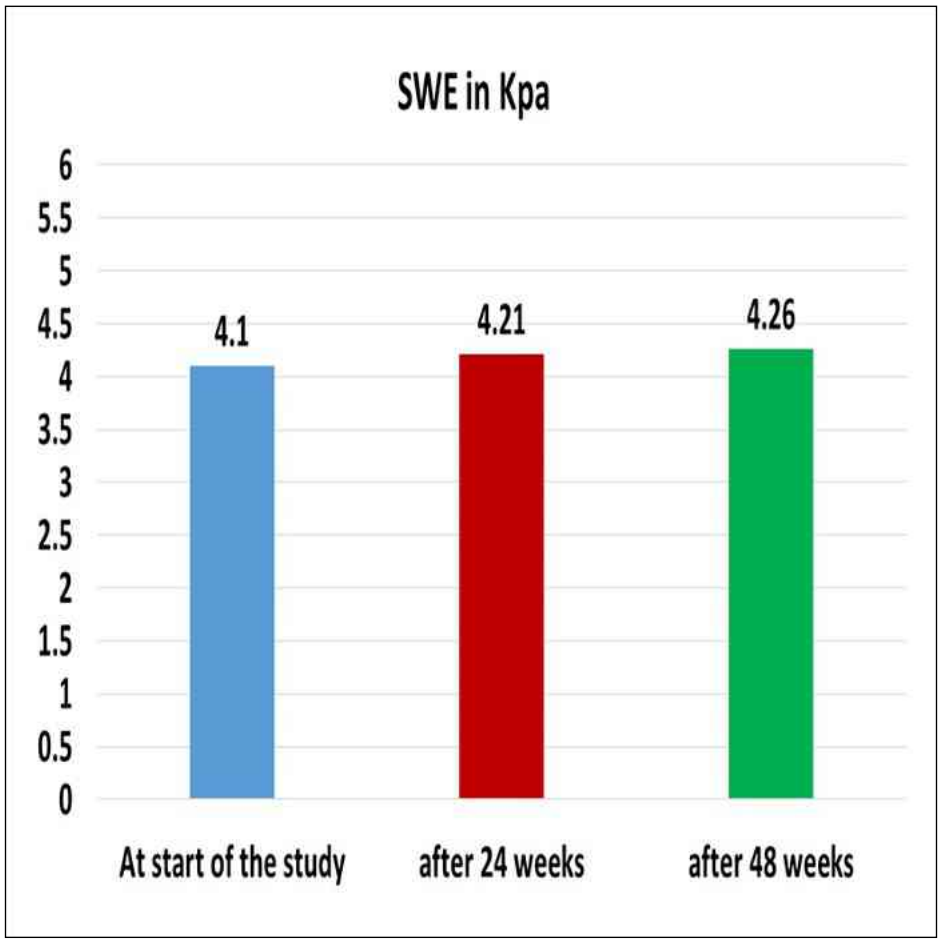

❖ AA-107

Fasting blood glucose increase the risk of significant hepatic fibrosis with U-shaped pattern in biopsy-proven non-alcoholic fatty liver disease

Jingjie Zhao[1,2], Xinyu Zhao[3,4], Min Wang[1], Xiaojuan Ou[1], Jidong Jia[1,4], Qianyi Wang[1], Hong You[1,4]

[1]Liver Research Center, Beijing Friendship Hospital, Capital Medical University, Beijing, China, [2]Clinical Center for Metabolic Associated Fatty Liver Disease, Capital Medical University, Beijing, China, [3]Clinical Epidemiology & EBM Unit, Beijing Friendship Hospital, Capital Medical University, Beijing, China, [4]National Clinical Research Center for Digestive Diseases, Beijing, China

Background: Hepatic fibrosis, especially significant fibrosis (Stage ≥ 2), is the most important prognostic factor in NAFLD and is correlated with liver-related outcomes and mortality. Abnormal fasting blood glucose (FBG) levels is crucial for the incidence of NAFLD, however, its impact on significant hepatic fibrosis is still unclear. Based on the BFH NAFLD cohort, which was proven by biopsy, the present study aimed to comprehensively investigate the association between FBG and the risk of significant hepatic fibrosis.

Method: Total of 366 biopsy-proven NAFLD patients at the Beijing Friendship Hospital, Capital Medical University (Beijing, China) between January 2016 and December 2018 were enrolled in the study. The data of FBG level were collected at the liver biopsy. Liver histology were diagnosed by two independent pathologists. The study protocol was approved by the Ethics Committee of Beijing Friendship Hospital, Capital Medical University (approval no. BJFH-EC/2018-P2-228-02). The study is registered at ClinicalTrials.gov (NCT03386890). Odds ratios (ORs) and 95% confidence intervals (CIs) were calculated by logistic regression models and restricted cubic spline (RCS) to evaluate the association between FBG and significant hepatic fibrosis.

Result: The average age of the NAFLD patients was 40.318.3, there were 107(29.2%) male, and 155(42.3%) patients with significant hepatic fibrosis. Compared to the NAFLD with normal FBG level (< 5.6 mmol/L), patients with elevated FBG (5.6-6.9 mmol/L) had a higher risk of significant hepatic fibrosis (univariate model: OR=2.19, 95% CI:1.24-3.87, p=0.007 ; Age- and gender- adjusted model: OR=1.85, 95% CI:1.01-3.38, p=0.046 ; multivariate model: OR=1.73, 95% CI: 0.91-3.26, p=0.093); and the risk of significant hepatic fibrosis was more obvious in the patients with diabetes mellitus (≥ 7.0mmol/L) (univariate model: OR=2.74, 95% CI:1.56-4.81, p=0.001; Age- and gender- adjusted

model: OR=2.87, 95% CI:1.60-5.15, p0.001; multivariate model: OR=3.21, 95% CI: 1.70-6.06, p0.001) (Table 1). RCS analysis showed a positive non-linearly association between the FBG levels and the OR of significant hepatic fibrosis (p for overall<0.001, p for non-linear =0.009). As the levels of FBG currently recommended in guidelines (7 mmol/ L) was chosen to be the reference, the ORs of significant hepatic fibrosis related to FBG levels rise sharply and then steadily when FBG levels was over 7.0 mmol/L. (Figure 1)

Conclusion: Increased FBG is an important risk factor for significant hepatic fibrosis in NAFLD patients, lower FBG levels than are currently recommended in guidelines (7.0 mmol/L) can decrease the risk of significant hepatic fibrosis.

Table and Figure:

Figure 1. The association of FBG and significant Hepatic fibrosis

Table 1. The association of FBG and significant Hepatic fibrosis

		Univariate model		Age- and gender-adjusted model		Multivariate model	
FBG	n/N	OR (95%CI)	*P* value	OR (95%CI)	*P* value	OR (95%CI)	*P* value
<5.6	63/185	1		1		1	
5.6-6.9	35/66	2.19(1.24-3.87)	0.007	1.85(1.01-3.38)	0.0464	1.73(0.91-3.26)	0.093
7.0-	41/70	2.74(1.56-4.81)	0.001	2.87(1.60-5.15)	0.0004	3.21(1.70-6.06)	<0.001

Multivariate model was adjusted age, gender, ln translated AST, ln translated PLT, and ln translated GGT

Figure 2. Cubic spline graph of the adjusted OR (represented by solid line) and 95% CI (represented by the dotted lines) for the association between FBG and risk of significant hepatic fibrosis.

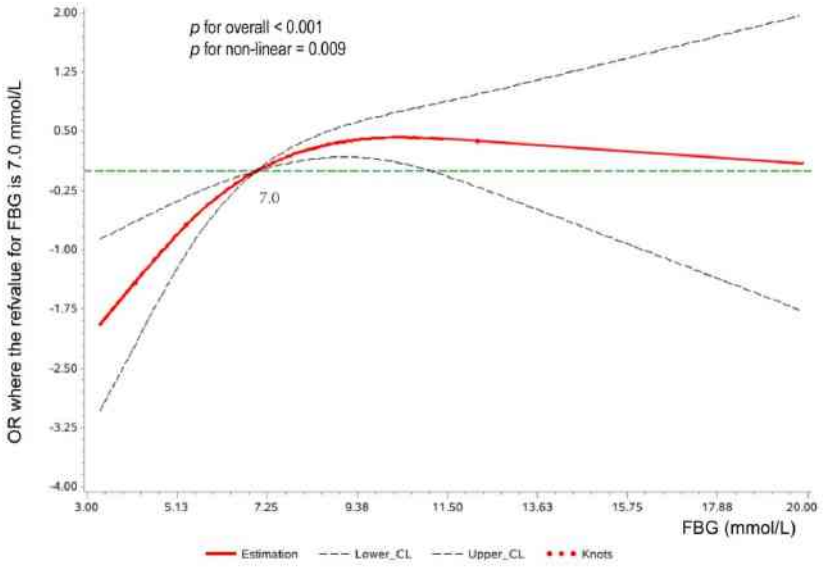

Figure 1. Cubic spline graph of the adjusted OR (represented by solid line) and 95% CI (represented by the dotted lines) for the association between FBG and risk of significant hepatic fibrosis.

Knots: 4.12 mmol/L (5th), 5.34 mmol/L (50th), and 12.20 mmol/L (95th) of the distribution of FBG (mmol/L); Reference:7.0 mmol/L.

❖ AA-108

Transjugular intrahepatic portosystemic shunt benefits for hepatic sinusoidal obstruction syndrome associated with consumption of Gynura segetum: a propensity score-matched analysis

Li Sai[1], Li Yong[2], Zhou Chunhui[1], Li Haiping[1], Chen Changyong[1], Peng Changli[1], Wang Tianming[1], Liu Fei[1], Xiao Juxiong[1], Shi Liangrong[1]
[1]Interventional Radiology Center, Department of Radiology, Xiangya Hospital Central South University, Changsha 410005, Hunan, China, [2]Department of Gastroenterology, Xiangya Hospital, Central South University, Changsha 410005, Hunan, China

Background: The pyrrolidine alkaloids related hepatic sinusoidal obstruction syndrome (PA-HSOS) has a high mortality rate without standardized therapy. The efficacy of transjugular intrahepatic portosystemic shunt (TIPS) for them remains controversial. The study aims to evaluate the efficacy of TIPS in patients with PA-HSOS related to Gynura segetum (GS).

Method: This study retrospectively enrolled patients diagnosed with PA-HSOS between January 2017 and June 2021, with a clear history of exposure to GS. Univariate and multivariate logistic regression were applied to evaluate risk factors influencing clinical response in PA-HSOS patients. A propensity score-matched analysis (PSM) was performed to compensate for differences in baseline characteristics between patients with and without TIPS. The primary endpoint was clinical response.

Result:A total of 47 patients was identified in our cohort with a clinical response rate of 51.5%. Of them, 9 patients in the TIPS group were matched with 27 in the conservative treatment group. Logistic regression analysis found the TIPS treatment (P=0.047), serum globulin levels (P=0.043), and prothrombin time (P=0.001) were independent influencing factors for the clinical response. After PSM, there was a higher long-term survival rate of patients (88.9% vs. 51.9%, P=0.048), and a shorter hospital stay (p=0.043), but a high trend in hospital costs (P=0.070) in the TIPS group.

Conclusion:TIPS therapy may be a novel treatment option for GS-related PA-HSOS patients.

Table and Figure:Figure 1. Figure 1. CT findings of a 53-year-old male patient diagnosed with PA-HSOS. (a-d) Images from plain and contrast-enhanced CT scans showed diffuse hepatomegaly, heterogeneous decreased density of the hepatic parenchyma, map-like nonhomogeneous enhancement in the venous phase and equilibrium phase. (a) Plain scan; (b) Arterial phase; (c) Portal phase; (d) Equilibrium phases. (e-f) Multiplanar reconstruction CT revealed that the inferior vena cava was compressed and thinned, and the hepatic vein was not displayed clearly. CT, Computed tomography; PA-HSOS, pyrrolidine alkaloids related hepatic sinusoidal obstruction syndrome.

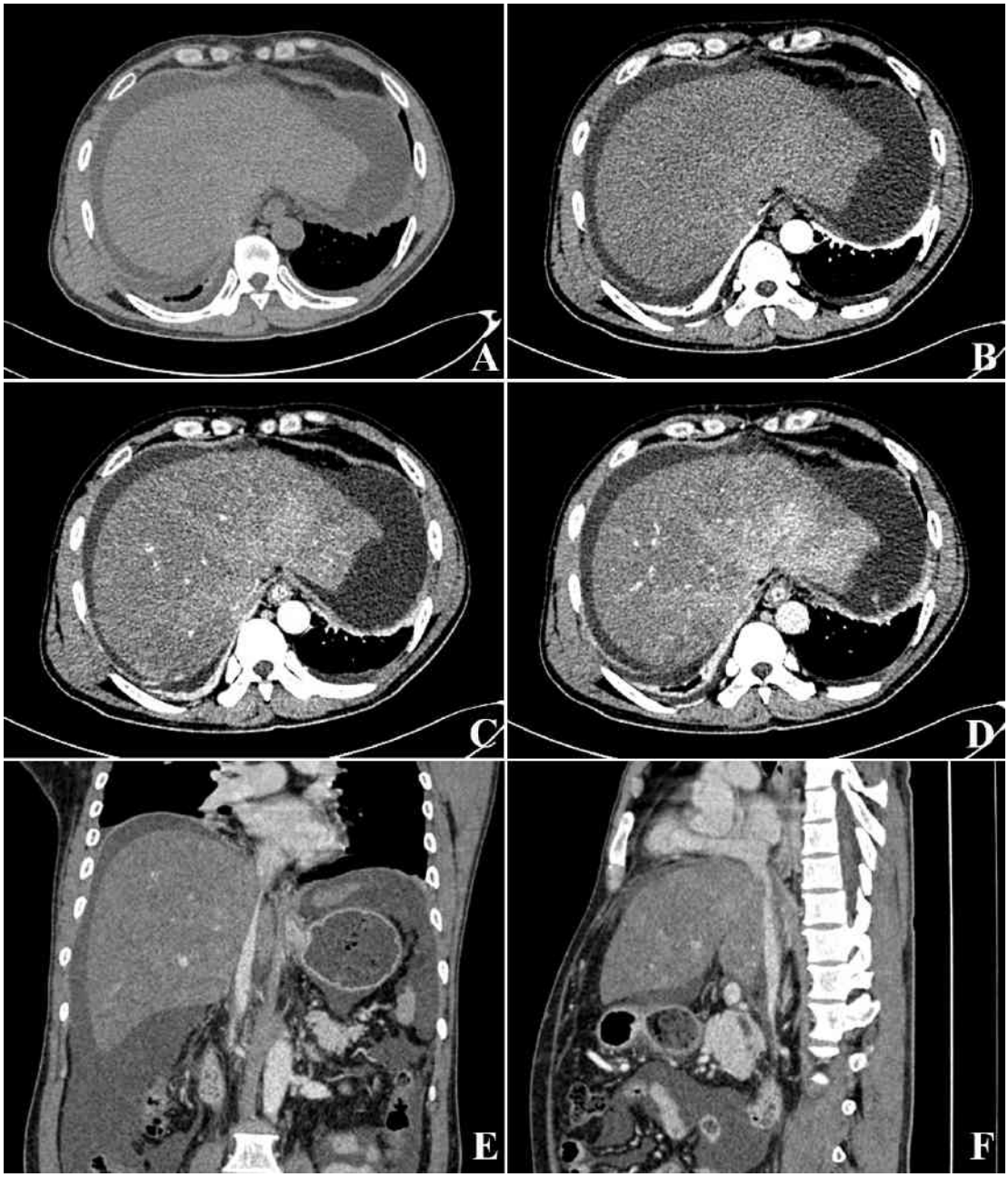

Figure 2. Figure 2. Cumulative survival rate of patients treated with two different therapies after PSM. TIPS, Transjugular intrahepatic portosystemic shunt; PSM, Propensity score-matched analysis.

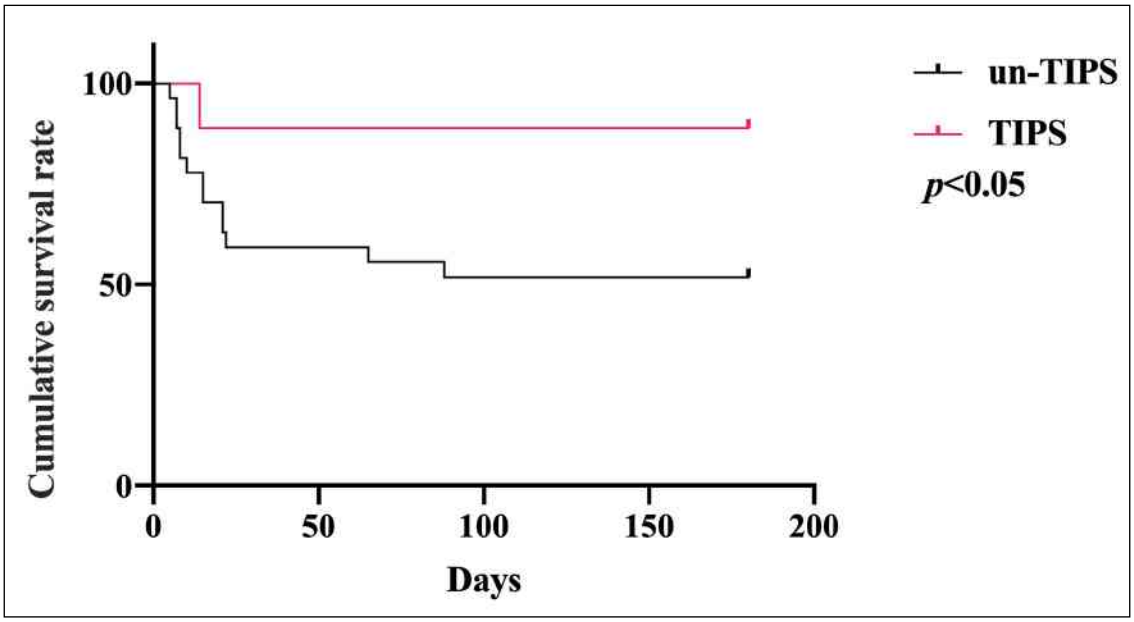

❖ AA-109

Compensated Advanced Chronic Liver Disease in MAFLD: A Prospective Cross-Sectional Study

Ling Zhou[1]
[1]*Hepatology Unit, Department of Infectious Diseases, Nanfang Hospital, Southern Medical University, Guangzhou, China*

Background: International experts have proposed changing the term non-alcoholic fatty liver disease to metabolic-associated fatty liver disease to reflect improved understanding of its complex pathophysiology. We prospectively investigated the clinical utility of the newly proposed metabolic-associated fatty liver disease criteria in unselected adults with fatty liver in southern China.

Method: We consecutively assessed the metabolic profiles of 1319 subjects with imaging-proven hepatic steatosis. Liver stiffness (LS) was measured by transient elastography. LS of ≥ 10 kPa was suggestive of compensated advanced chronic liver disease (cACLD).

Result:MAFLD diagnosis was established in 94.0% (n = 1240) of the patients, including 766 patients (61.7%) with concomitant liver diseases, and 474 (35.9%) with traditional non-alcoholic fatty liver disease. Among MAFLD patients, 227 (18.3%) patients were considered as cACLD, 92 (7.4%) patients with LS>15kPa and 47 (3.8%) patients with LS>21kPa suggesting significant portal hypertension. The risk factors associated with suggestive cACLD were older age (≥ 50 years: odds ratio 2.08; 95% confidence interval: 1.40-3.09), obesity (≥ 28 kg/m2: 2.47; 1.72-3.55), type 2 diabetes mellitus (2.41; 1.56-3.71), excessive alcohol consumption (2.41; 1.31-4.43), and hepatitis B (2.39; 1.63-3.48).

Conclusion: The new criteria dramatically expanded the fatty liver disease population. We found a high proportion of cACLD measured by TE. Our single center, prospective cross-sectional study endorsed screening of cACLD in fatty liver patients above 50 with either metabolic dysfunction (obesity and/or T2DM) or concomitant liver disease.

Table and Figure:

Figure 1. Graphic abstract

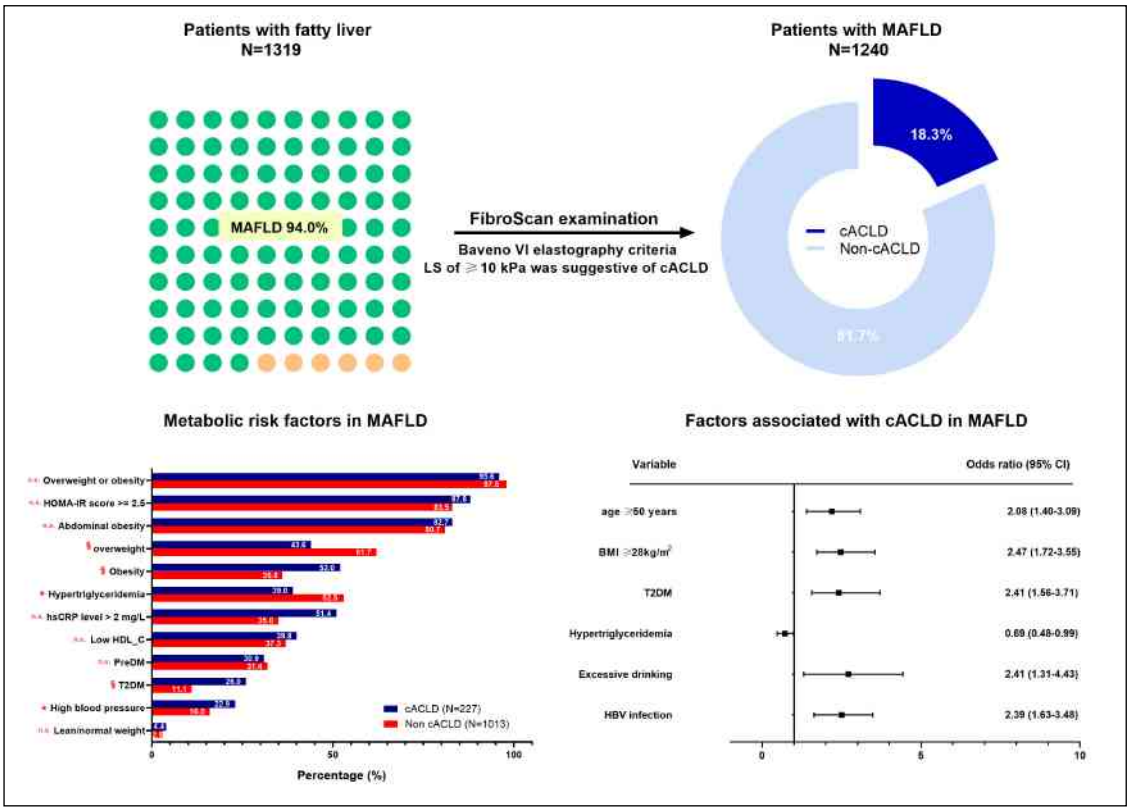

❖ AA-110

Deficiency of gluconeogenic enzyme PCK1 promotes NASH progression and fibrosis by activation of PI3K/AKT/PDGF axis

Qian Ye[1], Yi Liu[1], Guiji Zhang[1], Haijun Deng[1], Xiaojun Wang[2], Lin Tuo[3], Kai Wang[1], Ailong Huang[1], Tang Ni[1]
[1]Key Laboratory of Molecular Biology for Infectious Diseases (Ministry of Education), Institute for Viral Hepatitis, Department of Infectious Diseases, The Second Affiliated Hospital, Chongqing Medical University, Chongqing, China,
[2]Institute of Hepatobiliary Surgery, Southwest Hospital, Third Military Medical University (Army Medical University), Chongqing, China, [3]Department of Infectious Disease, Hospital of the University of Elictronic Science and Technology of China and Sichuan Provincial People's Hospital, Chengdu, China

Background: Nonalcoholic steatohepatitis (NASH) is a chronic liver disease characterized by hepatic lipid accumulation, inflammation, and progressive fibrosis. However, the pathomechanisms underlying NASH are incompletely explored. Phosphoenolpyruvate carboxykinase 1 (PCK1) catalyzes the first rate-limiting step of gluconeogenesis in the cytoplasm. This study was designed to determine the role of PCK1 in regulating NASH progression.

Method: Liver metabolism, hepatic steatosis, and fibrosis were evaluated at 24 weeks in liver-specific Pck1-knockout mice fed with NASH diet (high fat diet with ad libitum consumption of water containing glucose and fructose) or chow diet. Gain- or loss-of-function approaches were used to explore the underlying mechanism in vitro. AKT and RhoA inhibitors were evaluated for NASH treatment in vivo.

Result: Here, we found that hepatic PCK1 was downregulated in patients with NASH and mouse models of NASH. Mice with liver Pck1 deficiency displayed hepatic lipid disorder and liver injury fed with normal diet, while fibrosis and inflammation were aggravated when fed NASH diet. Transcriptome analysis revealed PCK1 deficiency upregulated genes involved in fatty acid transport and lipid droplet formation. Moreover, metabolomics analysis confirmed the accumulation of glycerol 3-phosphate, the substrate of triglyceride synthesis in the liver. Mechanistically, the loss of hepatic PCK1 activated the RhoA/PI3K/AKT pathway, which contributed to increased secretion of PDGF-AA and promoted the activation of hepatic stellate cells. Accordingly, treatment with RhoA and AKT inhibitors alleviated NASH progression in the presence of Pck1 deletion in vivo.

Conclusion:PCK1 deficiency plays a key role in the development of hepatic steatosis and fibrosis by facilitating the RhoA/PI3K/AKT/PDGF-AA axis. These findings provide a novel insight into therapeutic approaches for the treatment of NASH.

Table and Figure:

Figure 1.PCK1 is downregulated in NASH patients and mouse model, and PCK1 ablation accelerates inflammation and fibrogenesis in NASH mouse model.

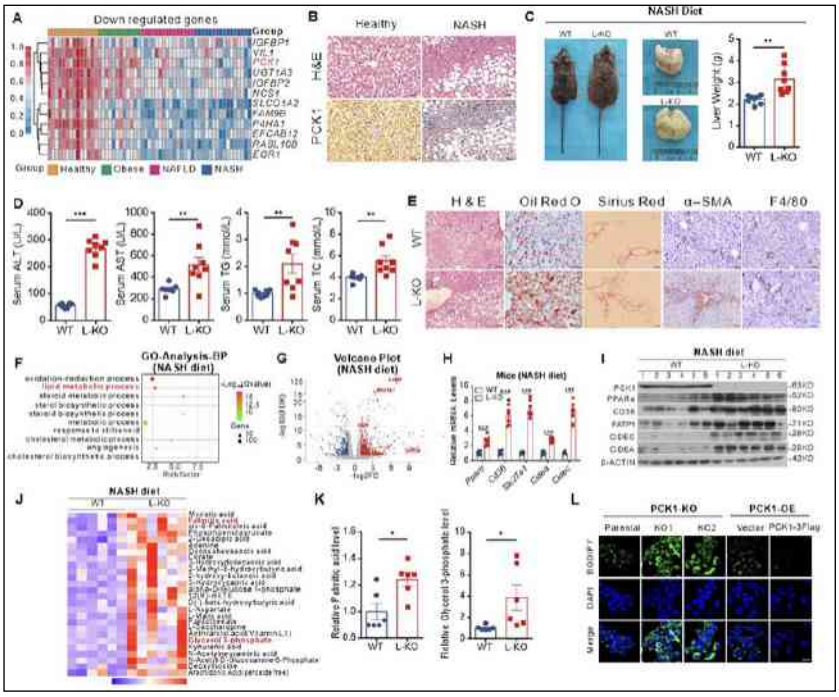

Figure 2. Hepatic PCK1 deficiency leads to HSC activation via PI3K/AKT/PDGF pathway, and AKT and RhoA inhibitors prevent the development of NASH in vivo.

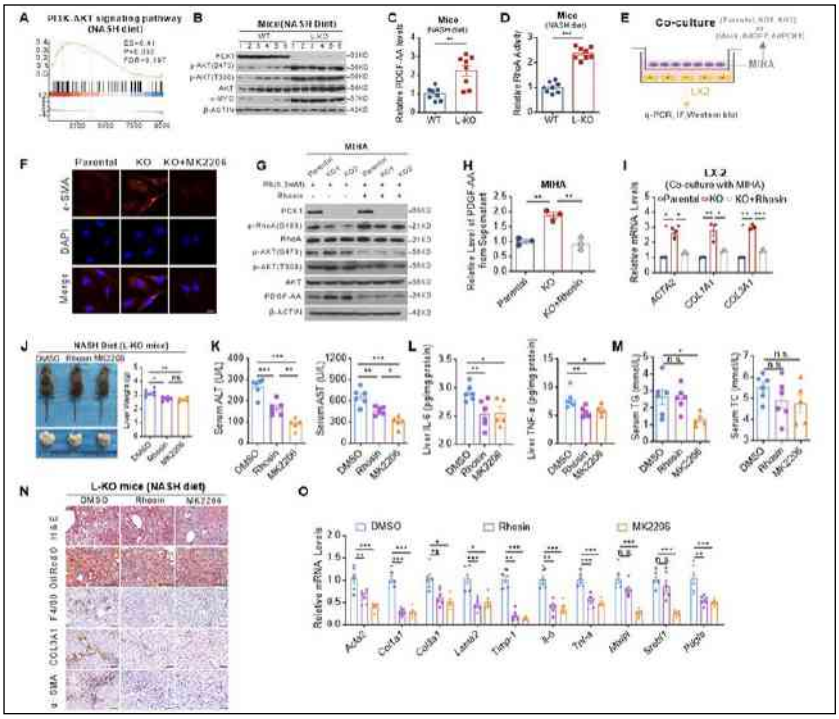

❖ AA-111

Hepatocyte-specific Mas activation enhances lipophagy and fatty acid oxidation to protect against acetaminophen-induced hepatotoxicity

Shuai Chen [1], Jing Li[1], Chang Qing Yang[1]
[1]Department of Gastroenterology and Hepatology, Tongji Hospital, School of Medicine, Tongji University, Shanghai 200092, China

Background: Acetaminophen (APAP) is the most common cause of drug-induced acute liver failure (ALF), however the treatment options are quite limited. Mas is a G protein-coupled receptor, whose role in APAP-induced hepatotoxicity has not been examined.

Method: Mas1-/-, AlbcreMas1f/f, Ppara-/-, Mas1-/-Ppara-/- and wild-type (WT) mice were challenged with APAP for the in vivo analysis of the Mas-AKT-FOXO1 axis dependent lipophagy and fatty acid oxidation (FAO), in the assistance of small-molecule inhibitors and agonists. Liver samples were collected for RNA-seq, proteomics and metabonomics analyses. Living mouse liver imaging, histological, biochemical, and molecular studies were carried out to evaluate APAP-induced hepatotoxicity in mice. Human and mouse hepatocyte cell lines were also exposed to confirm the existence of Mas-dependent lipophagy and FAO in vitro.

Result: Mice with the systemic, liver-specific or hepatocyte-specific deficiency of Mas1 were all vulnerable to APAP-induced hepatotoxicity. Meanwhile, they exhibited the substantially impaired lipophagy and downstream FAO, which was accompanied with activation of AKT and suppression of FOXO1. Besides, the systemic activation of Mas by AVE0991 showed unbelievably ideal effects to protect mice from APAP challenge, along with the remarkably enhanced lipophagy and subsequent FAO which were dependent on suppression of AKT and activation of FOXO1. Moreover, the protective effects of AVE0991 could be substantially diminished by blocking either lipophagy or FAO.

Conclusion: The activation of Mas on hepatocytes enhances the AKT-FOXO1 dependent lipophagy and downstream FAO to protect mice against APAP-induced hepatotoxicity, thus suggesting hepatocyte-specific Mas as a novel therapeutic target of drug-induced ALF.

Table and Figure:

Figure 1. Hepatocyte-specific Mas activation enhances lipophagy and fatty acid oxidation to protect against acetaminophen-induced hepatotoxicity

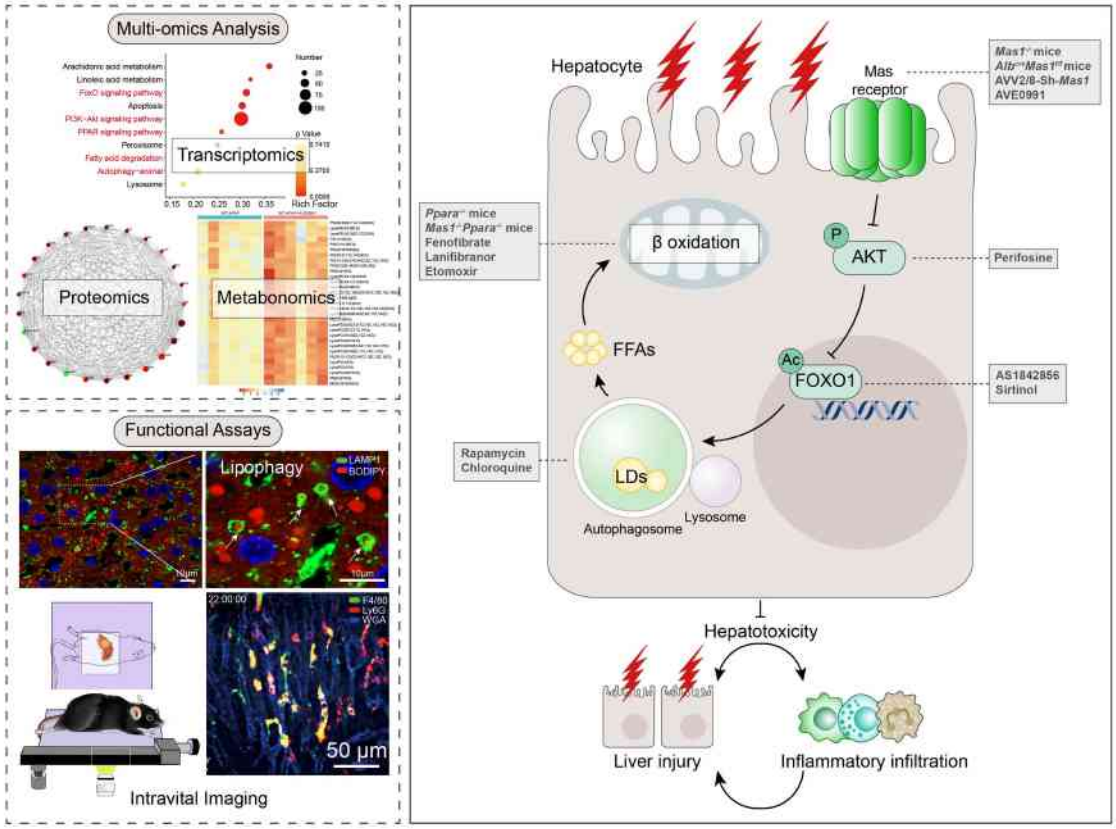

❖ AA-112

Fenofibrate improves biochemical index and long-term outcomes in UDCA-refractory primary biliary cholangitis patients with cirrhosis

Shu Xiang Li[1], Er Bu Li[1], Wei Jia Duan[1], Sha Chen[1], Ting Ting Lv[1], Xiao Ming Wang[1], Yu Wang[1], Xin Yan Zhao[1], Hong Ma[1], Xiao Juan Ou[1], Hong You[1], Ji Dong Jia[1]
[1]beijing friendship hospital

Background: Limited data are available for fenofibrate (FF) add-on ursodeoxycholic acid (UDCA) in the treatment of UDCA-refractory primary biliary cholangitis (PBC) patients with cirrhosis. Therefore, this study aimed to investigate the efficacy and safety of FF combined with UDCA in these patients.

Method: Cirrhotic PBC patients who were UDCA-refractory based on the Barcelona criteria were included in this retrospective study. Biochemical index, GLOBE and UK-PBC scores after one-year treatment, as well as the overall transplant-free survival rate and new decompensated cirrhosis development rate were compared.

Result:A total of 58 UDCA-refractory PBC patients with cirrhosis were enrolled: 26 patients received UDCA added FF (200mg/d), 32 patients received UDCA alone. Compared with the UDCA alone group, serum levels of alkaline phosphatase (ALP) and γ-glutamyl transpeptidase (GGT) at baseline in FF added-on group were significantly higher; but the proportion of patients with decompensated cirrhosis was significantly lower (Figure 1B). After 1 year of treatement, ALP and GGT were significantly decreased in both group. However, the significant decreased of aspartate aminotransferase and total bilirubin were only seen in FF added-on group (Figure 2A and 2B). And compared with the UDCA alone group, added-on group had more significant improvement in the biochemical index. FF added-on treatment significantly reduced the GLOBE score and the 5-year, 10-year and 15-year liver-related death and transplantation risk predicted by UK-PBC score (Figure 2C). The median follow-up time of FF added-on group and UDCA alone group were 3.62 and 3.21 years, respectively. Compared with the UDCA alone group, FF added-on group significantly improved the 5-year overall transplant-free survival rate (61.05% vs 79.14%, $P<0.05$), and reduced the 5-year new decompensated cirrhosis development rate (73.08% vs 32.88%, $P<0.05$) (Figure 2D). Unfortunately, serum level of creatinine was significantly

worse in the fenofibrate group (Figure 2E). In addition, four (15.4%) patients discontinued FF treatment due to liver injury.

Conclusion: In UDCA-refractory PBC patients with cirrhosis, additional fenofibrate treatment is associated with the improvements in the biochemical index, GLOBE and UK-PBC scores, overall transplant-free survival rate, and risk of decompensated cirrhosis development. However, serum level of creatinine and drug-induced liver injury should be closely monitored during treatment.

Table and Figure:

Figure 1. The flowchart of patient enrollment (A) and demographics and baseline characteristics of PBC patients with cirrhosis (B).

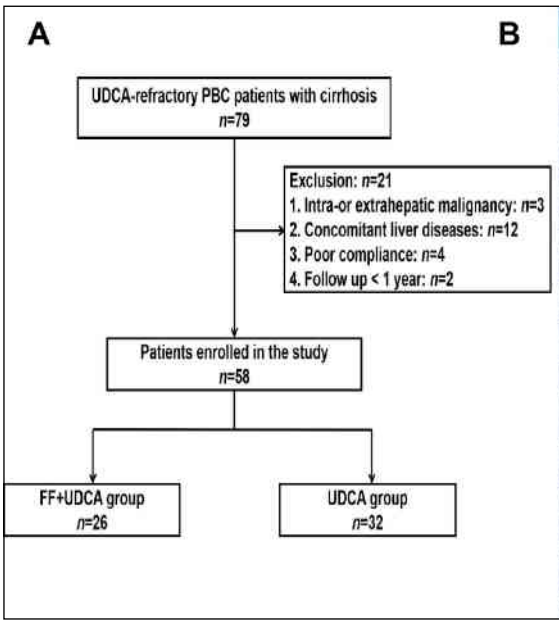

B

Characteristics	FF+UDCA (n=26)	UDCA (n=32)	*P* value
Sex, n (% female)	23 (88.5%)	28 (87.5%)	0.911
Age, years	53.8 ± 8.2	55.2 ± 7.1	0.214
Body Mass Index	22.9 ± 2.8	21.3 ± 3.1	0.010*
AMA, n (% positive)	24 (92.3%)	30 (93.7%)	0.829
ALP, U/L	345.5 (244.2-485.8)	231.5 (164.7-352.2)	0.006**
GGT, U/L	245.0 (117.0-417.0)	121.0 (74.2-186.7)	0.001**
ALT, U/L	56.0 (26.5-72.8)	40.5 (25.3-47.5)	0.106
AST, U/L	68.4 (31.9-94.5)	47.5 (32.5-58.0)	0.071
ALB, g/L	36.9 ± 4.9	34.0 ± 4.5	0.021*
GLO, g/L	34.8 ± 5.9	36.43 ± 5.15	0.331
TBIL, umol/L	23.7 (19.4-37.8)	19.2 (14.4-34.2)	0.154
TBA, umol/L	28.7 (18.2-103.1)	38.0 (21.1-81.8)	0.764
CHE, KU/L	5.5 ± 2.2	4.6 ± 1.8	0.068
CHOL, mmol/L	5.5 (4.1-6.8)	4.7 (4.2-6.7)	0.161
TG, mmol/L	1.3 (0.9-1.6)	1.1 (0.8-1.4)	0.173
HDL, mmol/L	1.7 ± 0.6	1.5 ± 0.7	0.324
LDL, mmol/L	2.8 (2.1-3.7)	2.4 (2.0-4.0)	0.521
Cr, umol/L	60.2 (49.9-71.1)	54.9 (49.9-65.0)	0.326
IgM, mg/dl	282.0 (176.0-558.2)	201.0 (161.0-601.0)	0.477
IgG, mg/dl	1553.8 ± 406.8	1736.5 ± 436.3	0.234
PLT, 10^9/L	124 (67.0-159.0)	99.0 (73.5-142.3)	0.680
Decompensation, n (%)	8 (30.8%)	18 (58.1%)	0.030*

Figure 2. Figure 2 Efficacy and safety of fenofibrate add-on therapy for UDCA-refractory PBC patients with cirrhosis.

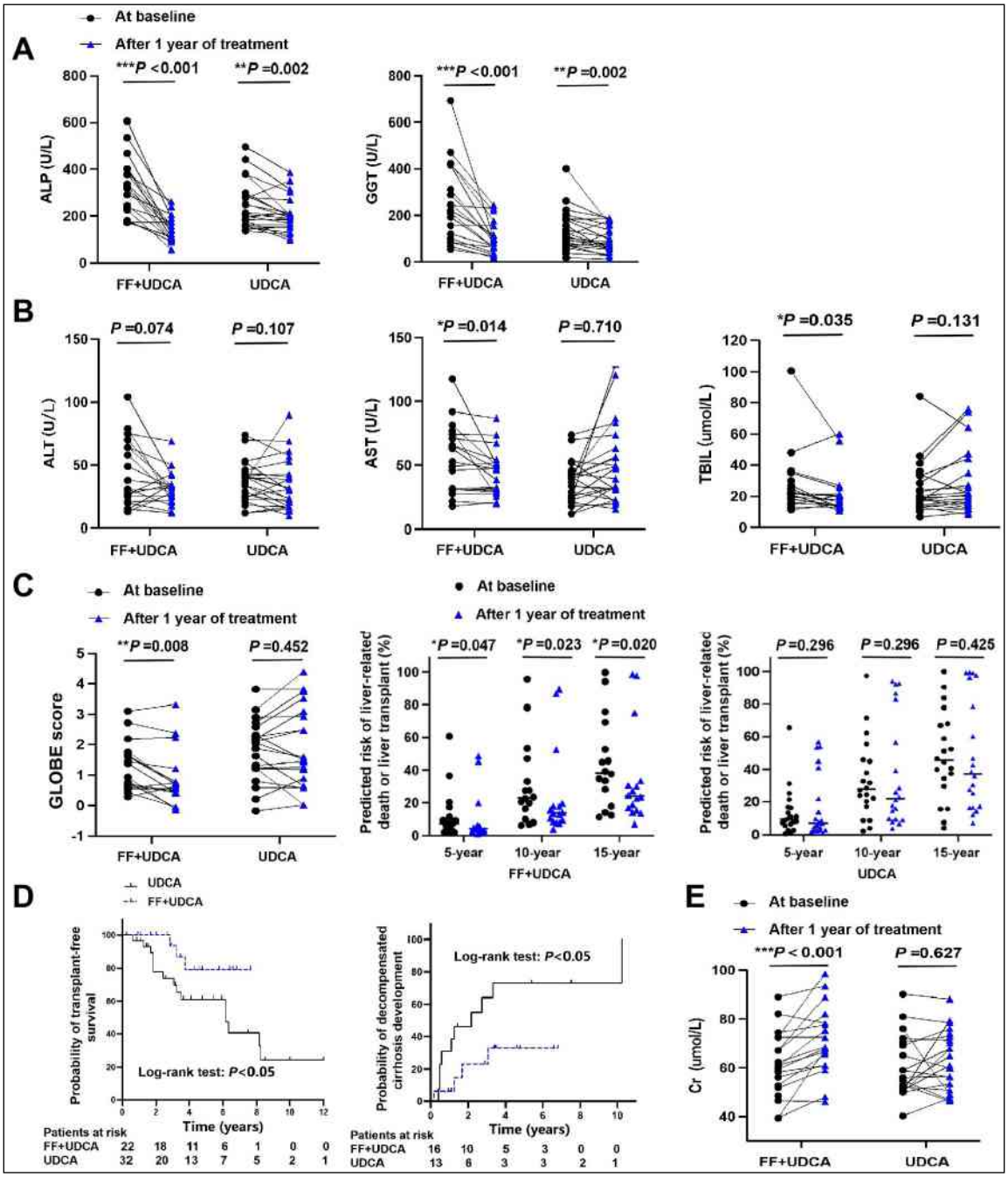

❖ AA-113

Hepatic steatosis leads to overestimation of liver stiffness measurement in both chronic hepatitis B and metabolic-associated fatty liver disease patients

Jie Liu[1,2], Ying Ma[2], Jia Li[2]
[1]Tianjin Medical University, [2]Tianjin Second People's Hospital

Background: The impact of hepatic steatosis on liver stiffness measurement (LSM) in both chronic hepatitis B(CHB) and metabolic-associated fatty liver disease (MAFLD) remains controversial. To determine whether LSM is affected by hepatic steatosis in CHB-MAFLD.

Method: Hepatic steatosis and liver fibrosis were assessed by histological and noninvasively methods. The area under the receiver operating characteristic curve (AUROC) was used to evaluate the diagnostic performance of LSM.

Result: The prevalence of MAFLD in CHB patients (n=436)was 47.5% (n=207). For patients with low amounts of fibrosis (F0-1 and F0-2), the median LSM was 8.8 kPa and 9.2 kPa in patients with moderate- severe steatosis,which was significantly higher than that in patients with none-mild steatosis ($P < 0.05$) . The positive predictive value(PPV) was lower for LSM identifying significant fibrosis ($F \geq 2$) as well as severe fibrosis ($F \geq 3$) in group which controlled attenuation parameter(CAP) ≥ 268 dB/m than its counterpart(68.2 % vs 84.6 % and 24.3% vs 45.0%). The AUROC of LSM detected F≥2 was 0.833 at a cutoff of 8.8kPa and 0.873 at a cutoff of 7.0 kPa in patients with CAP ≥ 268 and CAP < 268, respectively.

Conclusion: The presence of moderate-severe steatosis, detected by histology or CAP, should be taken into account to avoid overestimation of LSM.

Table and Figure:

Figure 1. Box plots of liver stiffness measurement (LSM) in patients without significant fibrosis (F 0−1) (A) and with significant fibrosis (F ≥2) (B) without severe fibrosis (F 0-2) (C) and with severe fibrosis (F ≥3) (D). The horizontal bar inside the box represents the median value

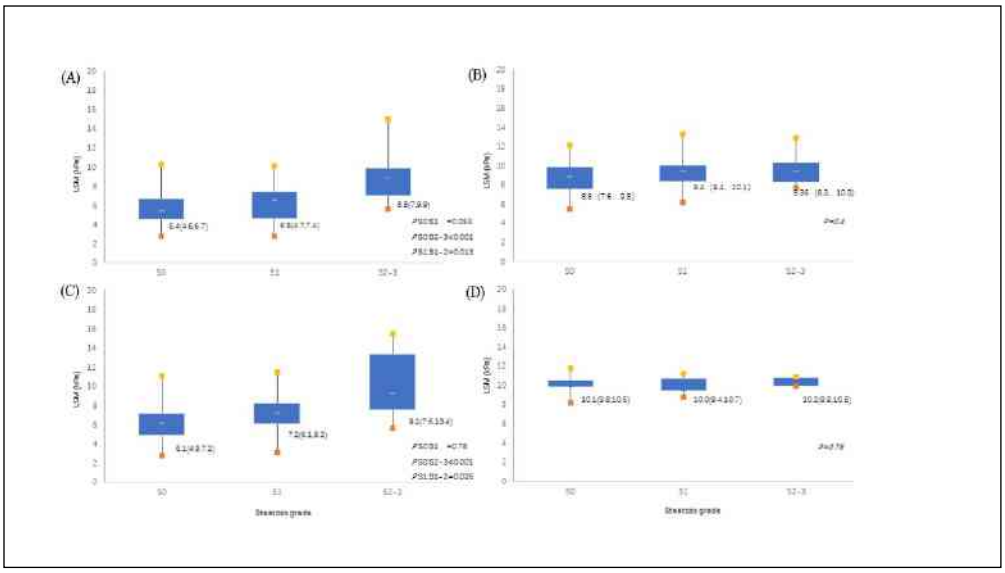

Figure 2. Proposed diagnostic flowchart for liver stiffness measurements taking into account CAP

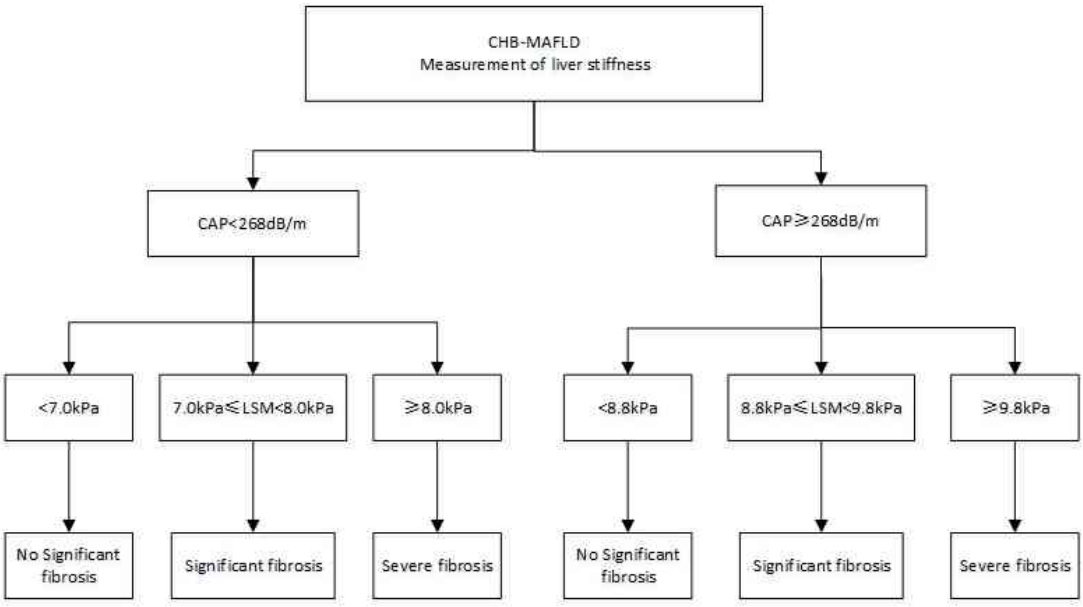

❖ AA-114

Risk factors for primary biliary cholangitis combined with Sjogren's syndrome：a cohort of Chinese patients from single center

Yu Peng[1], *Xiaowei Liu*[1]
[1]*Department of Gastroenterology, Xiangya Hospital, Central South University, 87 Xiangya Road, Changsha, 410008, Hunan, China.*

Background: Primary biliary cholangitis (PBC, formerly called primary biliary cirrhosis) is a chronic autoimmune liver disease, characterized by progressive cholestasis, which eventually leads to end-stage liver disease. Patients with PBC have at least 60% of probability to have an autoimmune extrahepatic condition. The primary objective of this study was to know about the risk factors of PBC combined with Sjogren's syndrome in the Chinese patients.

Method: Retrospective analysis of data from resident patients diagnosed with PBC at Xiangya Hospital from January 2015 to December 2020 was performed. The patients were divided into groups combined with or without Sjogren's syndrome. A total of 42 items from clinical features to laboratory tests that involving routine, biochemical, immune, coagulation and other aspects were included in the statistical analysis. Data were analyzed using Chi-squared test, Fisher exact test, Logistic regression.

Result:27 consenting PBC combined with Sjogren's syndrome patients, were compared with 27 PBC patients matched for age. Among the patients, 6(11.1%) male and 48(88.9%) female. Chi-squared test showed that PBC combined with Sjogren's syndrome was related to the following factors: 1) gender ($p<0.05$); 2) the level of extractable nuclear antigen (ENA) ($p<0.001$); 3)c. the level of total bile acid (TBA) ($p<0.05$); 4) the level of prothrombin time (PT) ($p<0.05$); 5) the level of international normalized ratio (INR) ($p<0.005$); 6) the level of activated partial thromboplastin time (APPT) ($p<0.05$). Other variables have no significant correlation with this outcome. Based on multivariate logistic regression, the independent risk factors for PBC combined with Sjogren's syndrome in Chinese patients was the level of INR (odds ratio (OR): 5.683, 95% confidence interval (CI): 1.401-31.719, $p=0.017$).

Conclusion: This pilot study suggests that the independent risk factors for PBC combined with Sjogren's syndrome in Chinese patients was the level of INR. Indeed, the pathogenic

mechanisms, clinical features, and optimal therapeutic approaches for PBC and Sjogren's syndrome are not yet fully defined. This issue should be systematically investigated to develop adapted measures.

❖ AA-115

The impact of dynamic change of insulin resistance on liver fibrosis in nonalcoholic fatty liver disease

Liling Yang[1], Xiaofei Tong[1], Xinyan Zhao[1], Xinyu Zhao[2], Yiwen Shi[1], Qianyi Wang[1], Zhengzhao Lu[1], Jingjie Zhao[1], Xiaojuan Ou[1], Jidong JIA[1], Hong YOU[1]
[1]Liver Research Center, Beijing Friendship Hospital, Capital Medical University, Beijing Key Laboratory of Translational Medicine on Liver Cirrhosis, National Clinical Research Center of Digestive Diseases, 95 Yong-An Road, Xi-Cheng District, Beijing 100050, China, [2]Epidemiology & EBM Unit, Beijing Friendship Hospital, Capital Medical University; NationClinical Research Center for Digestive Diseases, Beijing, China

Background: Insulin resistance (IR) has been considered the crucial factor in the onset of non-alcoholic fatty liver disease (NAFLD). Nevertheless, whether the dynamic change of IR contributes to fibrosis progression or regression is still unknown. We aim to evaluate the role of the change of IR in the fibrosis of NAFLD.

Method:NAFLD patients diagnosed by pathology and at least underwent twice fasting insulin (FINS) and liver stiffness measurements were enrolled. IR was assessed by HOMA-IR level with a cut-off value of 2.5. The dynamic change of liver fibrosis was assessed by non-invasive tests including LSM, FIB-4 score, and NAFLD fibrosis score (NFS). Patients were categorized into three groups according to the change of IR. (1) Increased IR group: from non-IR to IR, or HOMA-IR level increased more than 15% in the range of IR; (2) Decreased IR group: from IR to non-IR, or HOMA-IR level decreased more than 15% in the range of IR; (3) Stable IR group: maintained in the range non-IR, or HOMA-IR level increased or decreased less than 15%.

Result: There were 77 patients enrolled in the study and the median follow-up time was 30 months. At baseline, the fasting blood glucose (FBG), FINS, and HOMA-IR levels in the Decreased IR group were significantly higher than in the Stable IR and Increased IR group ($p< 0.05$). The levels of total cholesterol (TC) and low-density lipoprotein cholesterol (LDL-C) significantly increased in the Stable IR group ($p< 0.05$). There was no significant difference in LSM, FIB-4 score, and NFS score among the three groups ($p=0.227$, 0.134, 0.505 individually). For the dynamic change, the percent change of FIB-4 increased in the Increased IR group and decreased in the Decreased IR group although they had no significant difference (9.45% vs -2.01%, $p=0.623$). The BMI, FBG, FINS, and HOMA-IR levels also increased or decreased in the same direction along with the change in IR ($p< 0.05$).

Conclusion: Changes in IR by the current definition had a limited impact on liver fibrosis evaluated by non-invasive tests in NAFLD patients.

Table and Figure:Figure 1.

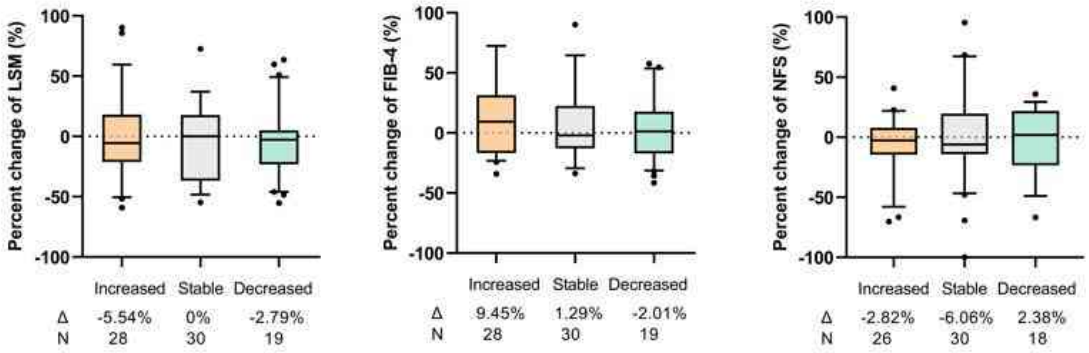

❖ AA-117

Acetaminophen promotes neutrophil extracellular traps (NETs) formation and hepatoxicity via RIPK3-MLKL-dependent necroptosis

JIALONG QI[1], HUAN LONG[2], YAO CHEN[2], LINGTING XUN[1,2]
[1]Yunnan Digestive Endoscopy Clinical Medical Center, Department of Gastroenterology, The First People's Hospital of Yunnan Province,
[2]School of Medicine, Kunming University of Science and Technology, Affiliated by The First People's Hospital of Yunnan Province.

Background: Drug-induced liver injury (DILI) is a leading cause of acute liver injury and liver failure which remains unsolved worldwide. Necroptosis has been identified as one of the most important programmed cell death during liver tissues injury by DILI, however, the physiological role of HMGB1 secreted by necroptosis in promoting the progression of DILI has not been clear.

Method: Recombinant HMGB1 protein (rhHMGB1) was expressed in BL21 E coil competent cells and purified by Ni-NTA-exclusion chromatography. Anti-HMGB1 antibody was presented for neutralized HMGB1 in vitro and in vivo. The genomic deletion of RIPK3, MLKL, and HMGB1 in mice was constructed and employed for the disease model. ELISA, RT-PCR, WB were used to identify signaling pathway change by HMGB1 regulation.

Result: Herein, we found that APAP incubation triggered hepatocytes PANoptosis including autophagy and necroptosis activation and cell cycle arrested. HMGB1 was overexpressed and secreted by hepatocytes during APAP stimulation in a time- and dose-dependent manner. Pretreatment with LPS induced more cell death, meanwhile, inhibiting autophagy by 3-MA and CQ partly rescue cell cycle arrest. Oral administration with APAP significantly reduced mice weight and promoted liver injury. In the meantime, neutrophils were recruited in liver tissues and transformed to NETs. Systemic administration of rhHMGB1 protein aggravated DILI by promoting NETs formation in the liver tissues, which was also reduced along with anti-HMGB1 antibody neutralization. Finally, RIPK3-/-, MLKL-/-, and HMGB1-/- mice suppressed APAP-induced DILI in vitro and in vivo, which was enhanced by DNase I.

Conclusion: Taken together, our results provide strong evidence that RIPK3-MLKL-dependent necroptosis secreted HMGB1 positively regulated NETs formation inducing liver injury in APAP-induced DILI.

Table and Figure:

Figure 1. Acetaminophen induced hepatocytes PANoptosis in a dose-dependent manner

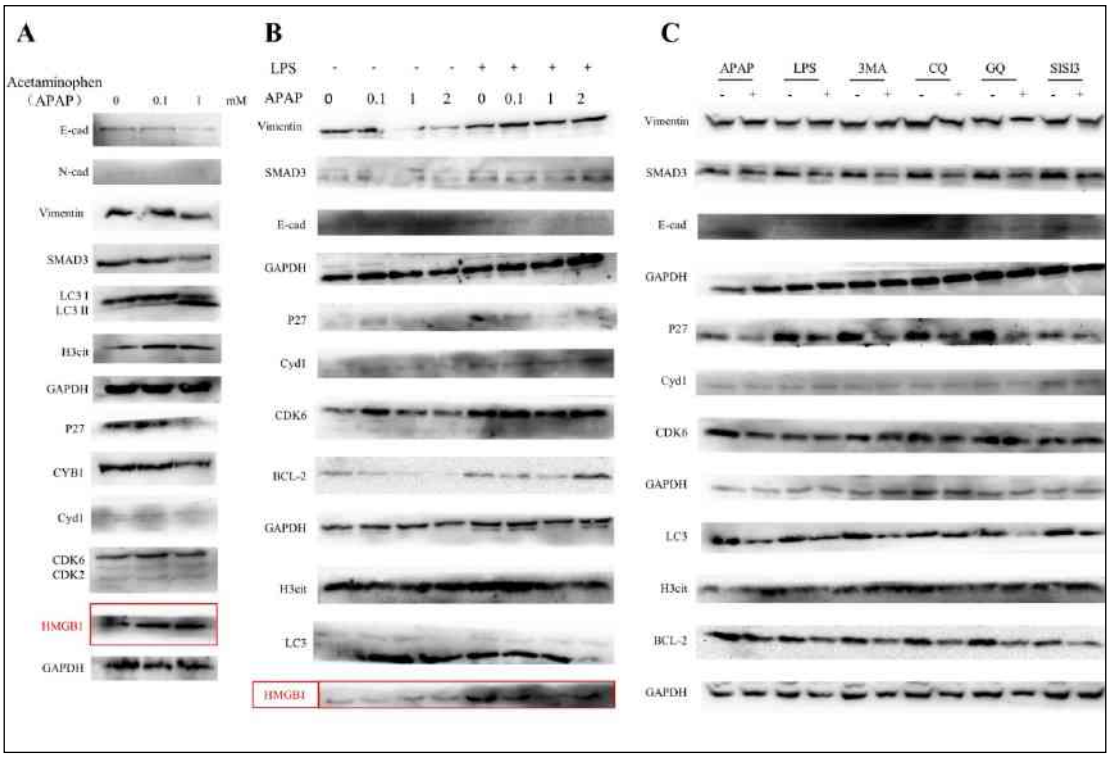

Figure 2. Acetaminophen administration triggered weight loss in vivo

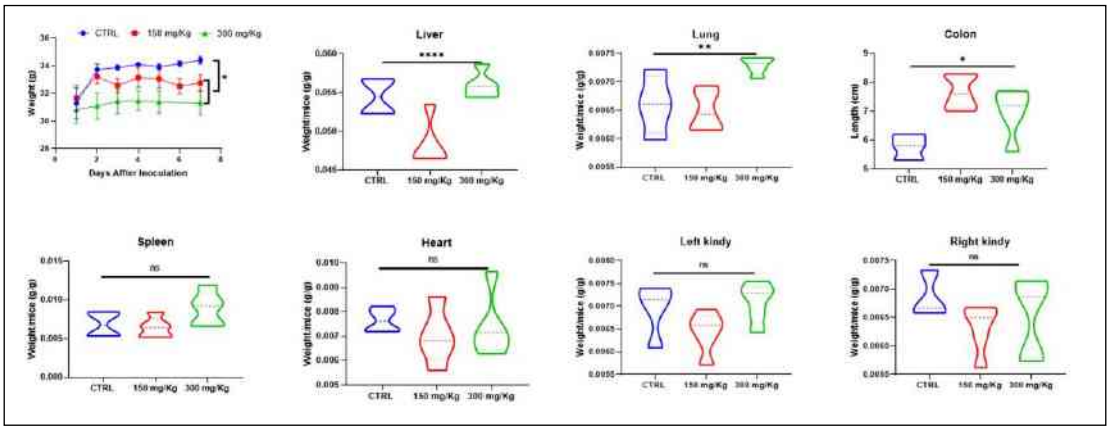

❖ AA-118

Interplay between hepatocellular ferroptosis and macrophage cGAS-STING signaling in the development of spontaneous inflammatory liver damage and progression to fibrosis and tumorigenesis

Xun Wang[1], Wantong Su[1], Haoming Zhou[1], Ling Lu[1,2,3]
[1]Hepatobiliary Center of The First Affiliated Hospital, Nanjing Medical University, Nanjing, China.,
[2]Research Unit of Liver Transplantation and Transplant Immunology, Chinese Academy of Medical Sciences, Nanjing, China.,
[3]Jiangsu Key Laboratory of Cancer Biomarkers, Prevention and Treatment, Collaborative Innovation Center for Cancer Personalized Medicine, Nanjing Medical University, Nanjing, China.

Background: Oxidative stress-mediated ferroptosis and macrophage-related inflammation plays an important role in various liver diseases. However, the precise mechanism of hepatocyte ferroptosis in regulating macrophage STING activation in the progression of liver damage, fibrosis and tumorigenesis remains unclear. Here we investigated the oxidative DNA damage from ferroptosis hepatocyte promoted macrophage cGAS-STING activation in the development of spontaneous inflammatory liver damage and progression to fibrosis and tumorigenesis.

Method: Hepatocyte-specific TAK1 deficient (TAK1ΔHEP) mice were generated to mimic inflammatory liver damage, fibrosis and tumorigenesis. Oxidative stress induced hepatocellular ferroptosis and DNA damage were measured by TEM, ROS related biomarkers and 8-OHdG. Macrophage polarization and Oxidative DNA damage STING activation were investigated by in vitro cell culture and in vivo experiment. Liver tissues from patients with ALI, fibrosis and hepatocellular carcinoma were collected to analyzed macrophage STING expression.

Result: Deletion of TAK1 in hepatocytes caused the development of spontaneous liver injury, fibrosis, and hepatocellular carcinoma. Significant liver injury and increased numbers of intrahepatic M1 macrophages were found in TAK1ΔHEP mice, peaking at 4 w and gradually decreasing at 8 w and 12 w. Meanwhile, activation of cGAS-STING-TBK1 signaling was observed in livers from TAK1ΔHEP mice at 4 w and had decreased at 8 w and 12 w. Treatment with a STING inhibitor promoted macrophage M2 polarization and alleviated liver injury and fibrosis. Moreover, TAK1ΔHEP mice demonstrated an increased oxidative response and hepatocellular ferroptosis, which could be inhibited by ROS scavenging. Suppression of ferroptosis by ferrostatin-1 inhibited activation of macrophage STING signaling, leading to attenuated liver injury and fibrosis and a reduced tumor burden. Mechanistically, increased intrahepatic and serum levels of 8-OHdG were detected in TAK1ΔHEP mice,

which was suppressed by ferroptosis inhibition. Treatment with anti 8-OHdG antibody inhibited macrophage STING activation in TAK1ΔHEP mice. Increased STING expression was found in both liver tissues and macrophages from patients with ALI, fibrosis and hepatocellular carcinoma.

Conclusion: Hepatocellular ferroptosis-derived oxidative DNA damage promoted macrophage STING activation to facilitate the development of liver injury, fibrosis, and tumorigenesis.

Table and Figure:

Figure 1. Deletion of TAK1 in hepatocytes caused the development of spontaneous liver injury, fibrosis, and hepatocellular carcinoma

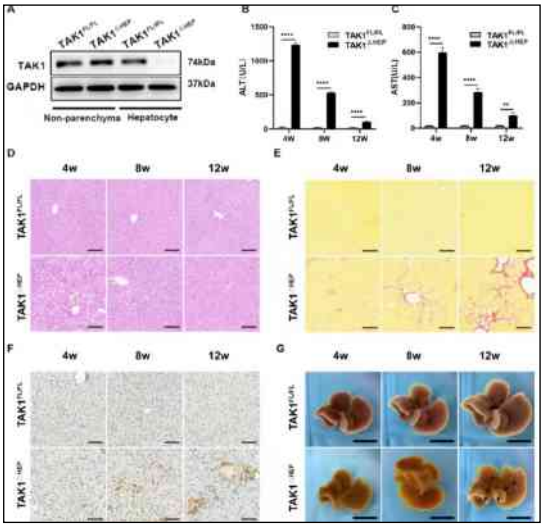

Figure 2. Hepatocyte-specific TAK1 deficiency regulated macrophage polarization at different stages

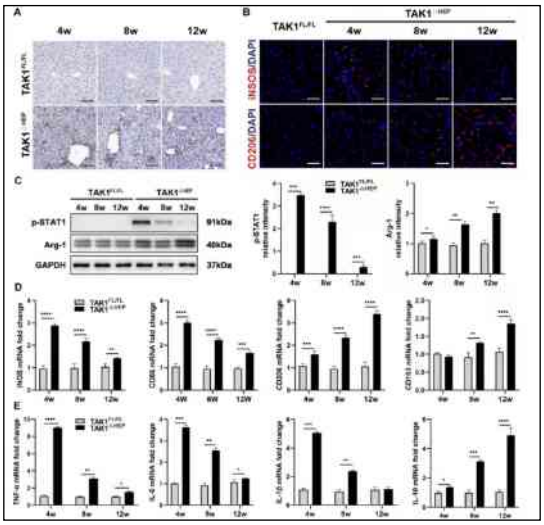

❖ AA-119

Efficacy of glucocorticoids in treating patients with severe drug-induced liver injury

Hong Li[1], Xiu Sun[2], Qiong Wang[3], Wenmin Guo[3], Yanteng Wang[3], Tian Chang[3]
[1]Shunde Hospital of Southern Medical University, [2]Ditan Hospital of Capital Medical University, [3]The First Clinical Medical College of Shanxi Medical University

Background: Current opinion on glucocorticoids (GCs) as a potential treatment option for drug-induced liver injury (DILI) is controversial. This study aimed to observe the outcomes of severe DILI patients receiving GCs in addition to symptomatic treatment.

Method: This retrospective study included severe DILI patients who were enrolled at the First Hospital of Shanxi Medical University of China from April 2014 to October2021 and received either symptomatic or symptomatic plus glucocorticoids treatment. The time when biochemical indexes dropped by 50% and 75% was observed.

Result: There were 44 patients in the steroid group and 72 patients in the non-steroid group. Cases treated with GCs were characterized by significantly higher level of bilirubin, lower levels of transaminase and albumin. Short-term use of GCs significantly reduced bilirubin recovery time, with the median time of 50% total bilirubin reduction in the steroid and non-steroid group being 8 days and 11 days respectively (p=0.025). Adverse reactions in the steroid group included 2 cases of hyperglycemia, 2 cases of secondary infection and 1 case of lower limb edema. In the non-steroid group, adverse reactions included 1 case of fever, 1 case of rash and 1 case of dizziness, all of which were controllable and improved after symptomatic treatment. Steroids did not show therapeutic efficacy for the treatment of DILI patients.

Conclusion: Short-term use of GCs in treating severe DILI that did not demonstrate remarkable improvement after the withdrawal of suspect drug might facilitate bilirubin clearance without aggravating adverse effects.

Table and Figure:

Figure 1. Patient screening chart

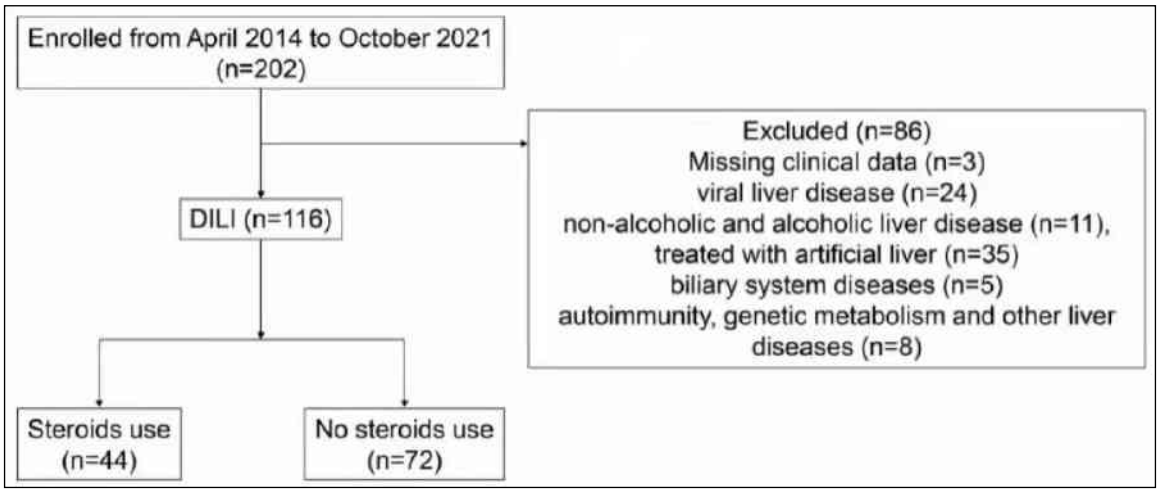

❖ AA-120

GLT25D1 Exacerbated Con A Induced Liver Injury by Promoting M1 Macrophage Polarization through MAPK-NFκB Signaling Pathway

Meixin Gao[1], Herui Wei[1], Fan Xiao[1], Hongshan Wei[1]
[1]Beijing Ditan Hospital, Capital Medical University

Background: Autoimmune hepatitis (AIH) is an immune-mediated liver injury with an increasing morbidity and mortality.However, its etiology has been still unclear. Glycosyltransferase GLT25D1 was verified to be involved in liver fibrosis and metabolic associated fatty liver disease. Here we investigated the role of GLT25D1 in AIH and mainly focused on the effect of macrophages.

Method: Con A (10mg/kg body weight) was intravenously injected to establish an immune-mediated hepatitis mouse model. WT and GLT25D1+/- mice were randomly allocated into control and Con A challenged group. Liver injury was evaluated by serum aminotransferase and histological H&E staining. M1 and M2 macrophages in liver tissues were detected by flow cytometry. And markers of M1 and M2 were detected by qRT-PCR and western blot. In vitro, We isolated bone marrow cells and used granulocyte-macrophage colony-stimulating factor (GM-CSF) for 7 days. Then lipopolysaccharide and IFNγ was used to derive M1 cells and IL-4 was used for M2 cells in vitro.

Result: We found that defect of GLT25D1 elevated the levels of ALT and AST, and aggravated liver histopathological damage in Con A mouse model. Liver kupffer cells and M2 cells had no differences between WT and GLT25D1+/- mice, while monocyte-derived macrophages and CD86+ M1 macrophage was increased in GLT25D1+/- mice after Con A challenged for 6 and 12 h. Furthermore, M1 markers such as iNOS, IL-1β and TNFα in liver tissues were increased in GLT25D1+/- mice compared with that of WT mice, especially in Con A challenged for 6 and 12 h. Besides, in consistent with the results in vivo, we found that GLT25D1 was reduced in M1 cells compared with that of M0 cells. And frequency of iNOS+ M1 cells was increased in GLT25D1+/- BMDM compared with that of WT cells. And mRNA levels of iNOS, IL-1β and IL-12 were up-regulated in GLT25D1+/- M1 cells than that of WT M1 cells. Besides, the results of western blotting showed that deficiency of GLT25D1 induced increasement of expression of iNOS, IL-1β and TNFα in M1 cells. Furthermore, we found that the levels of pp38 and p-JNK was significantly elevated in GLT25D1+/- M1 cells then that of WT M1 cells.

Conclusion: We found that defect of GLT25D1 exacerbated Con A-induced liver injury and promoted M1 macrophage polarization in vivo and in vitro, which might be related to the activation of PP38, P-JNK and NFκB signaling pathway.

Table and Figure:

Figure 1. Defect of GLT25D1 exacerbated Con A-induced liver injury and promoted M1 macrophage polarization in vivo.

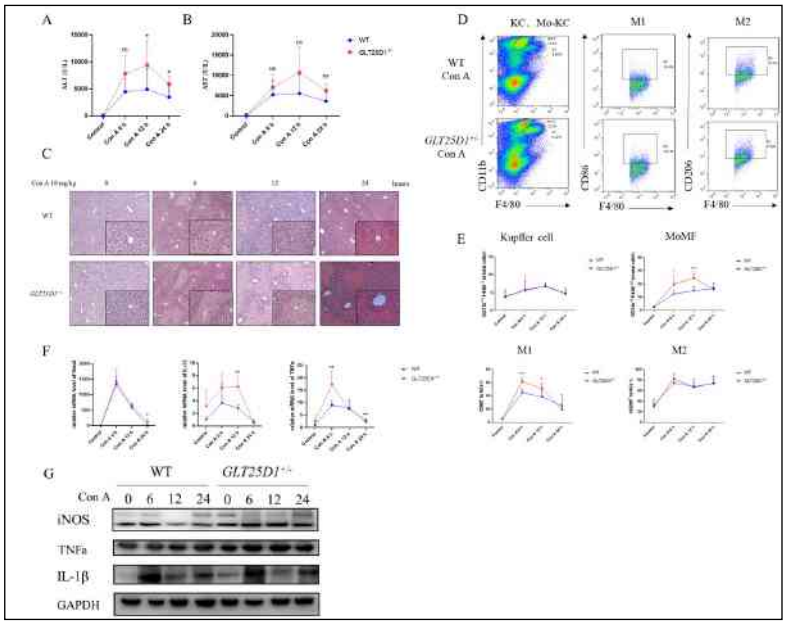

Figure 2. Defect of GLT25D1 promoted M1 macrophage polarization in vitro and facilitated the activation of MAPK-NFκB signaling pathway.

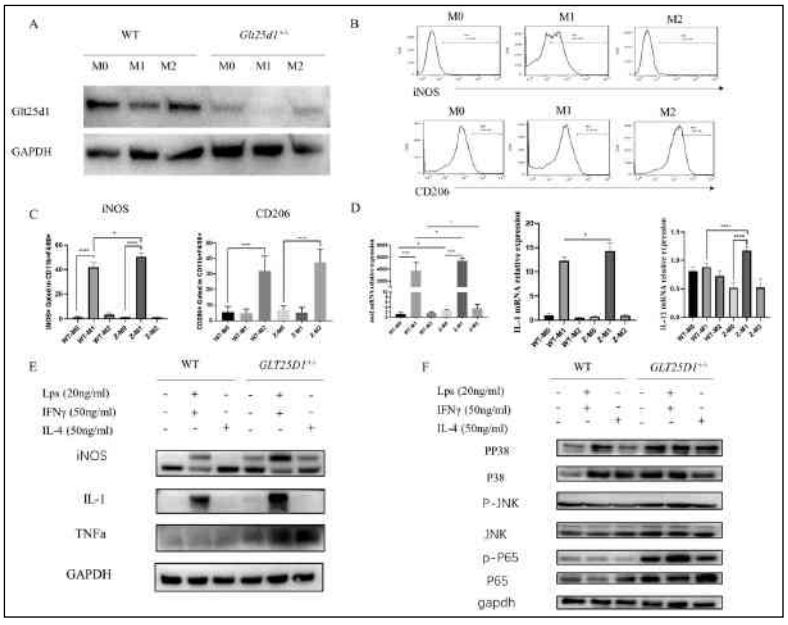

❖ AA-121

CCN6 alleviates non-alcoholic steatohepatitis through inhibition of the ASK1/MAPK signaling pathway

Yiran Song[1], Chenyang Li[1], Yuxin Luo[1], Jinbo Guo[1], Yaxing Kang[2], Fengrong Yin[1], Lihong Ye[3], Donglei Sun[1], Jun Yu[1], Xiaolan Zhang[1]
[1]Department of Gastroenterology, The Second Hospital of Hebei Medical University, [2]Department of Endocrinology, The Second Hospital of Hebei Medical University, [3]Department of Pathology, Shijiazhuang Fifth Hospital

Background: In recent years, CCNs have been found to play a regulatory role in the pathogenesis of metabolism-related diseases. CCN6 was the last CCNs member to be identified, and current studies have confirmed its role in maintaining mitochondrial structure and function and regulating redox status in different tissues and cells. Particularly, in oxidative stress-related injury, CCN6 plays a role in attenuating cellular damage, and yet, no relevant study has been reported on NASH. We investigated the role and mechanism of CCN6 in the development of NASH.

Method: Liver tissue samples from patients who had underwent clinical liver puncture biopsy were collected and used to detect hepatic CCN6 expression. High-fat-high-cholesterol (HFHC) and methionine choline-deficient (MCD) diet were applied to mice to establish NASH animal models. Liver-specific overexpression of CCN6 was induced in mice by tail vein injection of adeno-associated virus (AAV), and then the effect of CCN6 on the course of NASH was observed. Free fatty acid (FFA) was applied to HepG2 cells to construct the cell model of steatosis, and the effect of CCN6 was investigated by knocking down the expression of CCN6 through small interfering RNA (siRNA) transfection.

Result: We found that CCN6 expression was markedly reduced in NASH human liver specimens as well as in the liver of NASH mouse models of HFHC or MCD diet. We confirmed that liver-specific overexpression of CCN6 significantly attenuated hepatic steatosis, inflammation response and fibrosis in NASH mice. Based on RNA-seq analysis, we revealed that CCN6 significantly affected the MAPK pathway. Then, by interfering with apoptosis signal-regulated kinase 1 (ASK1), we identified that inhibition of ASK1 may neutralize the injury exacerbated by CCN6 deficiency in response to metabolic stimuli.

Conclusion:CCN6 protects against hepatic steatosis, inflammation response and fibrosis by inhibiting the activation of ASK1 along with its downstream MAPK signaling. CCN6 may be a potential therapeutic target for the treatment of NASH.

❖ AA-122

The utility of pentraxin 3 and platelet derived growth factor receptor beta as non-invasive biomarkers for prediction of cardiovascular risk in MAFLD patients

Hana Mostafa Badran[1], Maha Elsabawy[1], Olfat Hendy[1], Samer Ghanem[1], Hazem Omar[1], Mohamed Said Abdelgawad[1], Mai Abozeid[1], Eman Kamal El Deen[1], Mai Magdy[1], Mahmoud Magdy[1], Tamer Samir[1]
[1]National Liver Institute

Background: Metabolic associated fatty liver disease (MAFLD) has become the most common form of chronic liver disease worldwide. It's associated with increased risk of cardiovascular disease (CVD) which is the most common cause of death in these patients.

Method: This was a case control study conducted on 84 MAFLD patients with negative history of CVD (Group I) and 30 age and gender matched healthy controls (Group II). The 2 study groups were subjected to laboratory assessment (CBC, LFT, PT, INR, RFT, thyroid function test, lipid profile, uric acid, HOMA IR), radiological assessment (pelviabdominal ultrasound) and body composition was estimated by bioelectrical impedance analysis (BIA). The CVD risk was estimated by common carotid artery intima media thickness (IMT), Framingham risk score and QRISK 2 score (latter 2 predict 10 years CVD risk). The utility of two ELISA biomarkers, pentraxin 3 and PDGFRβ, were assessed in correlation with the CVD risk (CVR) in the study groups.

Result:MAFLD patients (group I) were predominantly females (71.4%) with a median age of (52.50) years. The IMT, Framingham risk score and QRISK 2 score were significantly higher in the MAFLD group than the control group (P= <0.001). Also, significantly higher serum levels of PTX 3 and PDGFRβ were observed in the MAFLD group compared to the control group (P = 0.001 and 0.016, respectively). In MAFLD group (48) patients had moderate to severe CVR as regard Framingham risk score (≥10), (34) patients had moderate to severe CVR as regard QRISK 2 score (≥10) and (11) patients with IMT (≥0.09) cm. PTX 3 was significantly correlated with IMT, visceral fat and waist hip circumference, while PDGFRβ was correlated significantly with age, IMT, visceral fat, fat mass, Framingham score, QRISK 2 score and systolic blood pressure. The ROC analysis indicated that; PTX 3 was superior to PDGFRβ in predicting moderate to severe CVR using Framingham score (≥10) in MAFLD patients with visceral fat (≤ 10) with sensitivity 85.71% and specificity 61.11% with optimal cut off value of 1.5 ng/ml, while its sensitivity was 78.57% and specificity was 47.06% in patients with visceral fat (> 10) with optimal cut

off value of 3.2 ng/ml. PDGFRβ was superior to PTX 3 in patients with systolic blood pressure (≥ 140) mm Hg; with sensitivity 76.92% and specificity 42.86% with optimal cut off value 2.9 ng/ml.

Conclusion: Serum pentraxin 3 had proved to be superior to PDGFRβ in prediction of the CVR in patients with MAFLD.

❖ AA-123

Analysis of Advanced Fibrosis in MAFLD Patients with Low-level Viremia of Chronic hepatitis B

Xue Wu[1], *Ping LI*[2]
[1]*Tianjin Medical University,* [2]*Tianjin Second People's Hospital*

Background: This study aimed to evaluate risk factors associated with advanced fibrosis in Low-level viremia of chronic hepatitis B (CHB) with metabolic dysfunction–associated fatty liver disease (MAFLD).

Method: Retrospective study of 159 MAFLD with low-level viremia patients who underwent liver biopsy involved from Tianjin Second People's Hospital during the years June 2012 to September 2019. The patients were classified into 4 MAFLD subgroups: group 1 (BMI<23kg/m2 with two or more metabolic abnormalities), group 2 (overweight, BMI23~28kg/m2), group 3 (obese, BMI>28kg/m2), and group 4 (type 2 diabetes mellitus, T2DM). Advanced fibrosis was assessed based on METAVIR scoring system in liver biopsy pathology. We investigated MAFLD subgroups' differences and determined the risk factors for advanced fibrosis.

Result: The mean age was 39.92 years, and 113 (71.1%) were male. The mean LSM value using transient elastography (FibroScan) was 27 kPa. And 25 (25.8%) patients were advanced fibrosis(F≥3). In the MAFLD subgroups, the proportion of advanced fibrosis in group1, 2, 3 and 4 was 33.3%, 20%, 22.5% and 26.7, respectively (P>0.05). Multivariable analysis indicated that the risk factors for advanced fibrosis were hypertension (OR (95%CI), 9.638(2.281-40.733); P=0.002) and LSM (OR (95%CI), 1.358(1.206-1.529); P<0.001). However, age and diabetes were not associated with advanced fibrosis in MAFLD patients.

Conclusion:MAFLD subgroups were no different in advanced fibrosis, but metabolic factors (hypertension) and LSM values were significantly associated with advanced fibrosis. In addition, LSM values can be used as an important tool for screening for liver fibrosis in patients with MAFLD.

Follow us on WeChat

Offical Minisite

APASL STC 2022 Liver Fibrosis in the Era of Translational Medicine

3 - 5 JUNE BEIJING · CHINA (HYBRID MEETING)

Host: The Asian Pacific Association for the Study of the Liver (APASL)